University of Alberta

Metalloproteinases in the Development of Hypertension and Cardiac Remodeling

by

Wang, Xiang

A thesis submitted to the Faculty of Graduate Studies and Research
in partial fulfillment of the requirements for the degree of

Doctor of Philosophy

Department of Biochemistry

©Wang, Xiang
Fall 2013
Edmonton, Alberta

Permission is hereby granted to the University of Alberta Libraries to reproduce single copies of this thesis and to lend or sell such copies for private, scholarly or scientific research purposes only. Where the thesis is converted to, or otherwise made available in digital form, the University of Alberta will advise potential users of the thesis of these terms.

The author reserves all other publication and other rights in association with the copyright in the thesis and, except as herein before provided, neither the thesis nor any substantial portion thereof may be printed or otherwise reproduced in any material form whatsoever without the author's prior written permission.

Abstract

Despite many decades of research and drug development, the diseases of the cardiovascular system remain a major health threat in the modern world. Hypertensive cardiac disease is a cardiovascular condition characterized by the co-occurrence of hypertension and pathological cardiac remodeling (hypertrophy and fibrosis).

Causative factors of hypertensive cardiac disease range from environmental stress to metabolic morbidities. However, these detrimental factors have a common effector mechanism: the sustained activation of G protein-coupled receptors (GPCRs) due to pathological levels of cognate agonists which elevate systemic blood pressure and promote pathological cardiovascular remodeling. GPCR agonists can trigger the activation of metalloproteinases, including matrix metalloproteinases (MMPs) and a disintegrin and metalloproteinases (ADAMs). These metalloproteinases are multifunctional enzymes that transactivate many intracellular signaling pathways including those leading to hypertension and cardiac remodeling. Therefore, MMPs and ADAMs have been widely speculated to be potential treatment targets for hypertensive cardiac disease.

In the current studies, we use angiotensin II and adrenoceptor ligands as prototypes of GPCR agonists to gain insights into mechanisms of hypertensive heart disease in rodent models. We determine various new roles played by MMP-2, MMP-7, ADAM-12 and ADAM-17. We demonstrate that:

1. MMP-7 mediates GPCR agonist-induced signaling with MMP-7 inhibition by pharmacological blockade, RNA interference or genetic knockout protecting against hypertensive cardiac remodeling.

2. ADAM-17 also contributes to GPCR agonist-induced cardiac hypertrophy and fibrosis. These effects of ADAM-17 are signaledby ADAM-12, a major effector metalloproteinase in cardiac hypertrophy signaling.

3. MMP-2 contributes to the development of GPCR agonist-induced hypertension such that partial blockade of MMP-2 by inhibitors and RNA interference attenuates angiotensin II-induced hypertension.

4. MMP-2 protects against hypertensive cardiac remodeling. To explain the cardioprotection rendered by MMP-2, we evoke a novel mechanism of negative regulation of the sterol-regulatory element binding protein (SREBP)-2 / 3-hydroxy-3-methyl-glutaryl-CoA reductase (HMGCR) pathway of cardiac remodeling.

These findings are a major contribution to our current understanding of the cardiovascular biology of metalloproteinases. Our data show the diverse roles of metalloproteinases in hypertensive cardiac disease and the potential and limitations of therapeutic approaches based on metalloproteinase inhibition for management of cardiovascular disease.

Acknowledgements

I would like to thank my supervisor, Dr. Carlos Fernandez-Patron, for allowing me to pursue my PhD studies in his laboratory. His guidance and advice are essential for my development as a scientist. I would also like to thank the members of my supervisory committee: Dr. James Stone, Dr. Luis Schang and Dr. Zamaneh Kassiri, for their valuable advice, support and direction.

I would like to thank the former and current members of Fernandez-Patron lab: Ana Lopez-Campistrous, Hao Li, Fung Lan Chow, Stephan Cooper, Jeffrey Odebach, Ana-Maria Bosonea, Evan Berry and Samuel Hernandez Anzaldo, for their collaboration, technical support and for creating a positive and pleasant working environment.

Certain aspects of this work would not have been possible without the help of collaborators. The technical expertise and contributions of Dr. Tatsujiro Oka, Sandra Kelly, Donna Beker, Dr. Zamaneh Kassiri and Joanne Zhao are greatly appreciated.

I would also like to thank the awards and funding agencies which supported me during my graduate studies: 75th Anniversary Scholarship, the Motyl Graduate Scholarship in Cardiac Sciences and AIHS Heritage Studentship.

Finally, I would like to thank my parents, who supported every step of my life, and my wife, who accompanied me through my highs and lows.

Table of Contents

Abstract...I

Acknowledgements...III

Table of Contents..IV

List of Tables...IX

List of Figures..XII

List of Abbreviations..XIV

Chapter 1

Introduction...1

1.1 Hypertension and hypertensive cardiovascular disease...............................1

1.1.1 Hypertension...1

- **1.1.1.1** Definition and classification of hypertension......................................1
- **1.1.1.2** Clinical complications of hypertension...1
- **1.1.1.3** Impact and financial burdens of hypertension......................................2
- **1.1.1.4** Diagnosis and measurement techniques..2
- **1.1.1.5** Contributing factors and determinants of hypertension........................3
- **1.1.1.6** Treatment strategies...5

1.1.2 Hypertensive cardiac remodeling...7

1.1.2.1 Cardiac hypertrophy..7
1.1.2.2 Cardiac fibrosis..8
1.1.2.3 Contributing factors of hypertensive cardiac remodeling....................8
1.1.2.4 Diagnosis and measurement techniques...9
1.1.2.5 Treatment strategies..10
1.1.3 Hypertensive vascular remodeling..10
1.1.4 G-protein-coupled receptor agonists in hypertension and cardiovascular remodeling...11
1.1.4.1 The renin-angiotensin-aldosterone system...11
1.1.4.2 The sympathetic nervous system..12
1.1.4.3 Endothelins..13
1.2 Cellular signaling pathways in GPCR-induced hypertension and cardiovascular remodeling...14
1.2.1 Regulation of contraction..15
1.2.2 Regulation of hypertrophic growth...16
1.2.3 Regulation of fibrosis..17
1.2.4 Molecular signals downstream of GPCRs..19
1.2.4.1 The role of PLC-β and downstream pathways in GPCR-regulated contraction and hypertrophy...19
1.2.4.1.1 Ca^{2+} in GPCR-regulated contraction and hypertrophy............19
1.2.4.1.2 PKC in GPCR-regulated contraction and hypertrophy............20
1.2.4.2 The role of PKA and downstream pathways in GPCR-regulated contraction and hypertrophy...22
1.2.4.3 Signaling pathways from GPCRs to transcription and translation.... 23
1.2.4.3.1 The Raf-MEK-ERK pathway..23
1.2.4.3.2 The PI3K-Akt pathway...25
1.2.4.4 GPCR signaling through reactive oxygen species.............................28

1.3 Metalloproteinases and transactivation pathways.....................................30

1.3.1 Metalloproteinases...30

1.3.1.1 MMPs..31

1.3.1.1.1 MMP-2..32

1.3.1.1.2 MMP-7..32

1.3.1.2 ADAMs..33

1.3.1.2.1 ADAM-12..34

1.3.1.2.2 ADAM-17..34

1.3.1.3 Activation and regulation of metalloproteinases................................34

1.3.1.4 Pathological roles and therapeutic inhibition of metalloproteinases..36

1.3.2 Transactivation pathway involving metalloproteinases................................38

1.3.2.1 GPCR agonist-induced activation of metalloproteinases....................38

1.3.2.2 Transactivation of membrane receptors by metalloproteinases and resulting downstream signaling..40

1.3.2.2.1 The EGF receptor family..40

1.3.2.2.2 Other growth factor receptors..42

1.3.2.2.3 Cytokines and their receptors...43

1.3.2.2.4 Cleavage and modulation of receptors......................................44

1.4 HMGCR, the rate-limiting enzyme in cholesterol biosynthesis.................45

1.4.1 Structure and Function...46

1.4.2 Regulation of HMGCR...47

1.4.3 HMGCR in diseases...49

1.5 Hypothesis..50

1.6 References..60

Chapter 2

MMP-7 and ADAM-12 define a signalling axis in agonist-induced hypertension and cardiac hypertrophy..91

2.1 Introduction..92

2.2 Materials and methods...93

2.3 Results..99

2.4 Discussion...103

2.5 References...132

Chapter 3

TACE is key regulator of agonist-induced cardiac hypertrophy and fibrosis..136

3.1 Introduction...137

3.2 Materials and methods..139

3.3 Results...143

3.4 Discussion...147

3.5 References...178

Chapter 4

MMP-2 Mediates Angiotensin II-induced Hypertension under the transcriptional control of MMP-7 and TACE....................................181

4.1 Introduction...182

4.2 Materials and methods..183

4.3 Results...187

4.4 Discussion..190
4.5 References..233

Chapter 5

Matrix metalloproteinase-2 is cardioprotective through a novel negative regulation of the SREBP-2 / HMGCR transcriptional pathway

Matrix metalloproteinase-2 is cardioprotective through a novel negative regulation of the SREBP-2 / HMGCR transcriptional pathway..237
5.1 Introduction..238
5.2 Materials and methods..240
5.3 Results..245
5.4 Discussion..250
5.5 References..298

Chapter 6

Discussion and Conclusions..299
6.1 Mutual regulation of metalloproteinases in the development of hypertension and cardiac remodeling..302
6.2 Differential metalloproteinase expression leads to varying physiological roles in hypertensive cardiac remodeling and other conditions...................303
6.3 Opposite roles of MMP-2 and ADAM-12 in cardiac remodeling...........306
6.4 Limitations and future directions......308
6.5 Conclusions..313
6.6 References..316

List of Tables

Table 1-1 Classification of adult blood pressure..52

Table 1-2 Human MMPs...53

Table 1-3 Human ADAMs..54

Table 2-1 Involvement of MMP-7 in the development of cardiac hypertrophy in SHR model. Morphometric, haemodynamic and echocardiographic results.......107

Table 2-2 Involvement of MMP-7 in the development of cardiac hypertrophy induced by angiotensin II (1.4 mg/kg/d for 10 days) in the mouse. Morphometric, haemodynamic and echocardiographic results..108

Table 3-1 Involvement of TACE in the development of cardiac hypertrophy in SHR model. Echocardiographic results...152

Table 3-2 The development of cardiac hypertrophy induced by angiotensin II in the mouse requires expression of TACE. Echocardiographic results.................153

Table 4-1 Nucleotide sequences of siRNAs used in experiments......................195

Table 5-1 List of peptides identified by LC-MS/MS analysis of in-gel micromave-assisted acid hydrolysis products of PSCK9 prodomain cleavage fragment...256

List of Figures

Figure 1-1 Major signal transduction pathways linking GPCR agonists to contractile processes..55

Figure 1-2 Major signal transduction pathways in GPCR agonist-induced hypertrophy and fibrosis..57

Figure 1-3 Regulation of the SREBP-2 / HMGCR pathway.................................59

Figure 2-1 MMP-7 as a mediator in rat models of acute hypertension................109

Figure 2-2 Resistance to acute hypertension in mice lacking active MMP-7.......110

Figure 2-3 Knockdown of MMP-7 by antisense oligodeoxynulceotides............113

Figure 2-4 Resistance to chronic hypertension in MMP-7$^{-/-}$ mice......................114

Figure 2-5 MMP-7 as a mediator of hypertension in spontaneously hypertensive rats...115

Figure 2-6 Targeted sequences on MMP-7 using siRNAs and antisense oligodeoxynucleotides...117

Figure 2-7 MMP-7 as a mediator of cardiac hypertrophy in spontaneously hypertensive rats..118

Figure 2-8 Assessment of off-target effects of siRNA..121

Figure 2-9 Transcriptional relationships between MMP-7, ADAM-12 and hypertrophy marker genes define novel signalling pathways under basal conditions vs. sustained agonist-stimulation..123

Figure 2-10 MMP-7$^{-/-}$ mice are protected from norepinephrine-induced cardiac PDGFR activation and hypertrophy...127

Figure 2-11 Proposed modules and network structure of the metalloproteinase signalling pathways...130

Figure 3-1 Domain structure of TACE protein and cDNA sequences (mice and rats) targeted by the siRNA...154

Figure 3-2 Effects of TACE knock-down on development of cardiac hypertrophy in spontaneously hypertensive rats..155

Figure 3-3 Knockdown of TACE decreases cardiac ERK phosphorylation…....158

Figure 3-4 Effects of TACE knock-down on blood pressure of spontaneously hypertensive rats...159

Figure 3-5 TACE, MMP-2 and ADAM-12 genes define a novel metalloproteinase signalling network...160

Figure 3-6 Knockdown of cardiac TACE in response to jugular vein injection of TACE siRNA..163

Figure 3-7 Evidence of the mediator role of TACE in agonist-induced cardiac hypertrophy...166

Figure 3-8 Luciferase siRNA has no effect on Ang II-induced cardiac hypertrophy and fibrosis..169

Figure 3-9 Knockdown of TACE blocked cardiac hypertrophy and fibrosis induced by angiotensin II infusion...172

Figure 3-10 Proposed model of TACE regulation of hypertrophy and fibrosis...177

Figure 4-1 Development of hypertension, cardiac hypertrophy and fibrosis induced by Ang II...196

Figure 4-2 Ang II induces the development of cardiac hypertrophy……………200

Figure 4-3 Ang II upregulates MMP-2 expression and enzymatic activity..........202

Figure 4-4 MMP-2 is involved in the maintenance of agonist-induced arterial constriction...205

Figure 4-5 MMP-2 mediates Ang II-induced hypertension but not cardiac hypertrophy or fibrosis..207

Figure 4-6 MMP-2 is not involved in the development of Ang II induced cardiac hypertrophy...210

Figure 4-7 Validation of MMP-2 siRNA in cultured A7R5 cells....................... 212

Figure 4-8 MMP-2 siRNA attenuates Ang II-induced hypertension but not cardiac hypertrophy or fibrosis..213
Figure 4-9 Luciferase siRNA does not attenuate Ang II-induced hypertension, cardiac hypertrophy or fibrosis..220
Figure 4-10 MMP-7 and TACE mediate the upregulation of MMP-2 induced by Ang II...226
Figure 4-11 MMP-7 and TACE mediate Ang II-induced MMP-2 upregulation..227
Figure 4-12 Simultaneous targeting of MMP-7 and TACE attenuates Ang II-induced hypertension, hypertrophy and fibrosis...228
Figure 4-13 Proposed model of metalloproteinase signaling in Ang II-induced cardiovascular disease..232
Figure 5-1 MMP-2 deficiency exacerbates agonist-induced cardiac hypertrophy in a time- and dose-dependent manner..258
Figure 5-2 MMP-2 KO exacerbates Ang II-induced cardiac hypertrophy.......... 260
Figure 5-3 MMP-2 KO exacerbates Ang II-induced cardiac hypertrophy: heart weight to tibia length ratio.. 261
Figure 5-4 Analysis of Ang II-induced LV hypertrophy and fibrosis in MMP-2 KO vs. WT mice: Time-dependence...263
Figure 5-5 Analysis of Ang II-induced LV hypertrophy and fibrosis in MMP-2 KO *vs*. WT mice: Dose-dependence...266
Figure 5-6 Echocardiographic analysis indicates a propensity to diastolic dysfunction in MMP-2 KO vs. WT mice...269
Figure 5-7 Negative regulation of the SREBP-2 / HMGCR pathway by MMP-2...270
Figure 5-8 Ang II induces changes in the cardiac SREBP-2 pathway................. 273
Figure 5-9 Negative regulation of the SREBP-2 / HMGCR pathway by MMP-2 in mouse primary cardiomyocytes...276

Figure 5-10 MMP-2 negatively regulates HMGCR and lack of MMP-2 predisposes to cardiac hypertrophy: Analysis of *in vivo* loss-of-function *vs*. gain-of-function models for a subpressor regimen of Ang II...............................278

Figure 5-11 Negative regulation of the SREBP-2 / HMGCR pathway by cholesterol in MMP-2 KO and WT mice...280

Figure 5-12 Contrasting effects of MMP-2 and MMP-7 in regulation of ADAM-12 in cardiac hypertrophy...282

Figure 5-13 MMP-2 negatively regulates the SREBP-2 / HMGCR axis: Mechanistic studies in cultured cells, *in vitro* biochemical studies and *in vivo* validation..284

Figure 5-14 MMP-2 interacts with PCSK9 and cleaves PCSK9 prodomain.......287

Figure 5-15 The proteolytic action of MMP-2 alone does not affect the ability of PCSK9 to induce LDLR degradation...290

Figure 5-16 Functional evidence that a non-proteolytic action of MMP-2 protects LDLR from degradation...292

Figure 5-17 Proposed mechanism whereby MMP-2 negatively regulates the SREBP-2 / HMGCR pathway and protects against cardiac remodeling............293

Figure 6-1 Postulated model of metalloproteinase signaling in GPCR agonist-induced hypertension and cardiac remodeling.......................................315

List of Abbreviations

5’-TOP mRNA: 5’-terminal oligopyrimidine tract mRNA,
4EBP-1: eIF4E binding protein-1,
ABC: ATP-binding cassette,
ACE: angiotensin-converting enzyme,
Ach: acetylcholine,
ACN: acetonitrile,
ADAM: a disintegrin and metalloproteinase,
Ang II: angiotensin II
ANP: atrium natriuretic peptide,
AP-1: activating protein-1,
AT1R: type-1 angiotensin II receptor,
BN-PAGE: blue native polyacrylamide gel electrophoresis,
BNP: brain-type natriuretic peptide,
BSA: bovine serum albumin,
$[Ca^{2+}]_i$: intracellular concentration of Ca^{2+},
CaM: calmodulin,
CPI-17: PKC-potentiated inhibitory protein of 17 kDa,
CREB: cAMP response element binding protein,
DAG: 1,2-diacylglycerol,
DTT: dithiotreitol,
ECM: extracellular matrix,
EDTA: Ethylenediaminetetraacetic acid,
eEF-2: eukaryotic translation elongation factor 2,
EGF: epidermal growth factor,
EGFR: EGF receptor,
eIF4E: eukaryotic translation initiation factor 4E,
eIF2B: eukaryotic translation initiation factor 2B,
ELISA: enzyme-linked immunosorbent assay,
Epac: exchange protein directly activated by cAMP,
ER: endoplasmic reticulum,
ERK: extracellular signal-regulated kinases,
ESI: electronspray ionization,
$ET_{A/B}$: endothelin receptor type A/B,
FITC: fluorescein isothiocyanate,
GAP: GTPase-activating protein,
GAPDH: glyceraldehyde 3-phosphate dehydrogenase,
GEF: guanine nucleotide exchange factor,
GPCR: G protein-coupled receptor,

GRB2: growth factor receptor-bound protein 2,
GSK-3β: glycogen synthase kinase-3β,
HAT: histone acetylase,
HB-EGF: heparin-binding EGF-like growth factor,
HDAC: histone deacetylase,
HMG-CoA: 3-hydroxy-3-methyl-glutaryl-coenzyme A,
HMGCR: HMG-CoA reductase,
HPLC: high-performance liquid chromatography
IFN: interfereon,
IGF: insulin-like growth factor,
Insig: insulin-induced gene,
IP_3: inositol 1,4,5-triphosphate,
LC: liquid chromatography,
LDL: low-density lipoprotein,
LDLR: low-density lipoprotein receptor,
L-NAME: L-nitroarginine methyl ester,
LV: left ventricle,
MAAH: microwave-assisted acid hydrolysis,
MAPK: mitogen-activated protein kinase,
MAPKAP-K1: MAPK-activated protein kinase 1,
MEF-2: myocyte enhancer factor-2,
MEK/MKK/MAPKK: MAPK kinase,
MHC: myosin heavy chain,
MLC: myosin light chain,
MMP: matrix metalloproteinase,
MS/MS: tandem mass spectrometry,
mTOR, mammalian target of rapamycin,
NFAT: nuclear factor of activated T-cell,
PBS: phosphate buffered saline,
p90RSK: p90 ribosome S6 kinase,
PCSK-9: proprotein convertase subtilisin/kexin type 9,
PDGF: platelet-derived growth factor,
PDK-1: phosphoinositide-dependent protein kinase 1,
PH: pleckstrin-homology,
PI3K: phosphatidylinositol 3-kinase,
$PI(3,4,5)P_3$: phosphatidylinositol (3,4,5)-trisphosphate,
$PI(4,5)P_2/PIP_2$: phosphatidylinositol (4,5)-bisphosphate,
PKA: cAMP-dependent protein kinase,
PKB: protein kinase B,
PKC: protein kinase C,
PKD: protein kinase D,

PCR: polymerase chain reaction,
PLC: phopholipase C,
PMA: phorbol 12-myristate 13-acetate
PMSF: phenylmethylsulfonyl fluoride,
PS: phosphatidylserine,
PTB: phosphor-tyrosine binding,
PTK: protein tyrosine kinase,
PTP: protein tyrosine phosphatase,
qRT-PCR: quantitative real-time polymerase chain reaction,
RNAi: RNA interference,
RIN-1: Ras and Rab interacter-1,
ROS: reactive oxygen species,
S1P: site-1 protease,
S2P: site-2 protease,
S6K: ribosomal protein S6 kinase,
SARA: Smad anchor for receptor activation,
Scap: SREBP-2 cleavage activating protein,
SDS: Sodium dodecylsulfate,
SDS-PAGE: SDS polyacrylamide gel electrophoresis,
SH2: Src homology 2,
SH3: Src homology 3,
SHR: spontaneously hypertensive rats,
siRNA: small interference RNA
SR: sarcoplasmic reticulum,
SRE: sterol-regulatory element,
SREBP: sterol-regulatory element binding protein,
TACE: TNF-α converting enzyme,
TAK-1: TGF-β activated kinase-1,
TβRI/II: type-I/II TGF-β receptor,
TFA: trifluoroacetic acid,
TGF: transforming growth factor,
TNF-α: tissue necrosis factor-α,
TPA: 12-O-tetradecanoylphorbol-13-acetate,
TSC-2: tuberous sclerosis protein 2,
VEGF: vascular endothelial growth factor,
VSMC: vascular smooth muscle cell,
WGA: wheat germ albumin,
WKY: Wistar Kyoto rats,

Chapter 1

Introduction

1.1Hypertension and hypertensive cardiovascular disease

1.1.1 Hypertension

1.1.1.1 Definition and classification of hypertension

Hypertension, the condition of persistently elevated arterial blood pressure (**Table 1-1**), affects over 1 billion individuals worldwide and causes approximately 7.1 million deaths per year. Whereas blood pressure <120/80 mmHg is considered as normal, the World Health Organization reports that systolic blood pressure of >115 mmHg is suboptimal and responsible for 62% of cerebrovascular disease and 49% of ischemic heart disease[1-3].

Primary (essential) hypertension, the form of hypertension which has no identifieable direct medical causes, affects account for 95% of the cases of hypertension. Less than 5% of the hypertension cases are caused by identifiable medical conditions such as tumors and kidney diseases and are known as secondary hypertension.

1.1.1.2 Clinical complications of hypertension

Hypertension is often termed as “silent killer” as it normally shows no significant early symptoms and 1/3 of the patient do not recognize their disease. However, hypertension is a predominant underlying factor for other clinical conditions, including renal diseases and other cardiovascular diseases.

Sustained high blood pressure is often accompanied by the development of cardiac remodeling, including cardiac hypertrophy and fibrosis. Hypertension and cardiac remodeling also increase the risk of myocardial ischemia, cardiac dysfunction and heart failure. Moreover, sustained hypertension leads to the remodeling of vasculature, setting up the stage for the development of atherosclerosis (hardening and thickening of vasculature), which is a main risk factor of coronary artery disease, myocardial ischemia and stroke[4]. For each increase of 20 mmHg (systolic) or 10 mmHg (diastolic) above 115/75 mmHg, the risk of other cardiovascular diseases increases by two fold[5].

Hypertension is also a risk factor of kidney injury and end stage kidney disease, often known as hypertensive nephropathy. These diseases are be related to the sustained activity of renin-angiotensin-aldosterone system (RAAS) and sympathetic nervous system, as well as the development of renal atherosclerosis.

In the brain, sustained hypertension is also suggested to contribute to cognitive impairment and dementia, in addition to cerebrovascular stroke[6].

1.1.1.3 Impact and financial burdens of hypertension

Over 40% of adults in the world are hypertensive and the prevalence of hypertension is increasing[3,7,8]. Hypertension is a substantial risk factor for renal disease and cardiovascular diseases including stroke, myocardial ischemia/infarction and congestive heart failure[1,3]. Together, cardiovascular disease is the world’s leading cause of death and disability[3,7], therefore minimizing the occurrence and severity of risk factors such as hypertension is essential.

In addition to the tremendous health burden, hypertension also imposes substantial socioeconomic concerns. Between direct costs (pharmaceuticals, medical services, etc.) and indirect costs (loss of productivity, etc.), the annual cost of hypertension in the United States was $156 billion in 2011[9]. Therefore, the development of cost-effective and efficient therapeutic strategies is required for the treatment of hypertension.

1.1.1.4 Diagnosis and measurement techniques

The pressure of blood against the arterial wall (blood pressure) is mostly measured indirectly by monitoring the presence / absence of a pulse distal to an occlusion site, instead of being directly measured by penetrating the arterial wall. In animal studies, one of the direct approaches to measuring blood pressure is radiotelemetry. A catheter is surgically placed within the femoral artery to directly measure the arterial blood pressure and transmit real-time blood pressure information in conscious, unrestrained animals[10].

In mouse and rat studies, indirect blood pressure measurement is achieved by pressure occlusion plethysmography, which works by monitoring reperfusion of blood to the tail with a pulse sensor after proximal occlusion[11]. An inflatable cuff (connected to a pump and a pressure gauge) is used to occlude the flood flow, resulting in the disappearance of the pulse signal (measured by a distally-placed pulse sensor). Then, the pressure of the occlusion cuff is slowly decreased. A pulse signal can be detected by the pulse sensor when the cuff pressure decreases to the systolic blood pressure.

Similar principles apply in the clinical setting to measure blood pressure in humans. An occlusion cuff (sphygmomanometer) is placed on the upper arm and used to occlude blood flow to the forearm. During deflation (decrease of the cuff pressure), a stethoscope is placed in the cuff to listen for a pulse. The audible pulse is heard when the cuff pressure is equal to the systolic blood pressure. The audible pulse continues to be heard until the occlusion cuff pressure decreases to the diastolic blood pressure, at which point the sounds are dampened.

1.1.1.5 Contributing factors and determinants of hypertension

Several factors, such as age, gender, stress, genetic background and obesity, increase the risk of developing hypertension.

Obesity is one of the most established risk factor of hypertension. In adults, obese individuals are 3.5-fold more likely than lean individuals to become hypertensive[12,13] and over 60% of hypertensive individuals are obese. This has been explained through the chronic activation of the sympathetic nervous system by adipocyte-derived hormones such as leptin, which promotes energy expenditure as well as systemic vasoconstriction and pathological cardiovascular remodeling[14]. Obese people also have increased levels of renin, aldosterone and angiotensin-converting enzyme (ACE), which all contribute to increased blood pressure[15]. In addition, lifestyle factors, including lack of exercise, high sodium intake, and excessive use of alcohol and tobacco products, are all associated to the development of hypertension as well as obesity[16].

Obesity predisposes patients to insulin resistance and type II diabetes with about 90% of type II diabetes being attributable to excess weight. Diabetes increases the risk of hypertension and cardiovascular disease. In USA, up to 75% of the adult patients of diabetes have hypertension[17]. Meanwhile, hypertension increases the risk of diabetes complications including retinopathy and nephropathy. Diabetes contributes to the development of hypertension by predisposing the development of vascular remodeling and atherosclerosis. Insulin resistance also triggers sympathetic nervous system activity, aldosterone secretion and sodium retention, contributing to the development of hypertension and cardiovascular remodeling. Indeed, anti-hypertensive drugs targeting Gprotein-coupled receptor (GPCR, described in 1.1.4) agonist systems such as ACE inhibitors, angiotensin receptor blockers and β-blockers are prescribed to treat and prevent cardiovascular complications (including microvascular complications of retinopathy) and progression of nephropathy in diabetic patients.

Genetic and heritable factors including sex, endocrine and ethnicity also influence the incidence rates, progression and treatment response of hypertension. For example, the prevalence of hypertension is much higher in African Americans than in Caucasians[18]. More than 50 genes, such as those encoding angiotensinogen, mineralocorticoid receptor and sodium transport proteins, have been studied in association with hypertension.

Regardless of the cause of the hypertension, increased activities of renin-angiotensin-aldosterone system and sympathetic nervous system are important contributors of high blood pressure (described in 1.1.4). These systems release GPCR agonists, such as angiotensin II (Ang II) and catecholamines, which raise arterial blood pressure by increasing cardiac output and systemic vascular resistance, two direct determinant of blood pressure. The increase of cardiac output is due to increase in either stroke volume or heart rate, whereas the increase in systemic vascular resistance is determined by increase in vascular tone (state of constriction) of systemic resistance blood vessels, increase of blood viscosity and decrease in vascular compliance.

1.1.1.6 Treatment strategies

Currently guidelines to treat hypertension utilize one or more anti-hypertensive agents that function to reduce blood pressure by: 1) antagonism of pro-hypertensive GPCR agonist receptors, 2) inhibition of pro-hypertensive GPCR agonist synthesis, 3) blockade of calcium entrance or 4) reduction of salt/water retention.

Life style modifications, including proper physical exercises, stress management, calorie restriction, low sodium intake and limited usage of tobacco and alcohol, are as efficient as antihypertensive drugs. They are often combined with other antihypertensive medications for the treatment of hypertension and are also recommended for the prevention of hypertension.

Since the significance of renin-angiotensin-aldosterone system in the regulation of blood pressure, pharmaceutical therapies have been focused on the development of drugs that: i) inhibit Ang II synthesis (i.e. ramipril, an angiotensin converting enzyme inhibitor[19]), ii) antagonize Ang II receptors (i.e. losartan, a type I Ang II receptor, or AT1R antagonist[20]) and iii) accelerate Ang II degradation (i.e. exogenous administration of recombinant ACE-2[21]). Targeting the Ang II pathway is an effective means of lowering blood pressure and is typically used as the initial pharmacological approaches in treating hypertension. In cases where hypertension remains (resistant hypertension), additional anti-hypertensive agents are used in combination until treatment goals are met[22].

Adrenoceptor antagonists are also good therapeutic candidates for anti-hypertensive therapy. alpha adrenergic antagonists (i.e. doxazosin[23]), Beta adrenergic antagonists (i.e. nebivolol[24]) and broad spectrum adrenergic antagonists (i.e. carvedilol[25]) can all be used to reduce blood pressure. However, these adrenergic antagonists are not specific to cardiovascular system. They have systemic side effects including fatigue, depression and impaired glucose tolerance[25]As such, adrenergic antagonists are mostly used in combination with other therapies in resistant hypertension, instead of being used as initial treatment lines of hypertension.

Due to the significance of calcium in the regulation of smooth muscle and cardiac contraction (as discussed below), calcium channel blockers (i.e. vascular selective dihydropyridines and cardiac selective verapamil) are often used as anti-hypertensive drugs. By blocking Ca^{2+} entry into cytosol, calcium channel blockers decrease vasoconstriction, cardiac inotropy and heart rate and therefore reduce blood pressure.

In addition to preventing systemic vasoconstriction, other approaches aim at decreasing salt and water retention in the kidney, which reduces blood volume and subsequently cardiac output and blood pressure. Thiazide diuretics (i.e. hydrochlorothiazide[26]) are typically used in combination with drugs targeting the renin-angiotensin-aldosterone system to treat hypertension. Thiazide diuretics function by inhibiting thiazide-sensitive Na^+/Cl^- symporters in the distal tubule and thus decrease Na^+ reabsorption and water retention. As a side effect of excess sodium in the kidney collecting ducts, upregulated Na^+/K^+ antiporters activity leads to increase in sodium/potassium exchange and results in hypokalemia (low blood potassium)[27]. Therefore, potassium supplements or hyperkalemic agents can be used in conjunction with thiazide diuretics to prevent its side effects[28].

In spite of the effectiveness of these antihypertensive drugs, over half of patients receiving treatment do not meet their treatment goals (of <140/90 mmHg for adults with hypertension and <130/80 mmHg for hypertension patients with diabetes or chronic renal disease)[1,14]. This is mostly due to the fact that the etiology of the hypertensive cardiac disease is complex (e.g., many GPCR agonists are involved) or unknown and that current treatment strategies are mainly based on the experience of doctors to choose a drug or drug combination until adequate blood pressure reduction and regression of cardiac remodeling are achieved. There is a strong demand for universal approaches that effectively lower blood pressure among the entire hypertensive population.

1.1.2 Hypertensive cardiac remodeling

The development of hypertension is often accompanied by the remodeling of cardiac tissues, which is characterized by the development of cardiac hypertrophy and fibrosis. These remodeling processes, in the long term, can result in cardiac dysfunction and increased risk of heart failure, both of which need to be considered for the treatment of hypertension.

1.1.2.1 Cardiac hypertrophy

In hypertensive cardiac disease, hypertrophy of the heart is revealed as an increase of cardiac mass and thickening of left ventricular walls due to the enlargement of individual cardiomyocytes. This hypertrophy of ventricular cardiomyocytes is accompanied by the expression of fetal and developmental genes (e.g., β-myosin heavy chain (β-MHC), α-skeletal actin, atrium natriuretic peptide (ANP) and brain-type natriuretic peptide (BNP)) that are normally not highly expressed in the fully-differentiated adult ventricular cardiomyocyte[29]. Although cardiac function is properly maintained during early cardiac hypertrophy, long term cardiac hypertrophy can result in cardiac dysfunction and heart failure.

1.1.2.2 Cardiac fibrosis

Pathological cardiac hypertrophy is typically accompanied by an excessive accumulation of extracellular matrix (ECM) proteins (e.g., collagen type I and type III, fibronectin) in the interstitial and perivascular regions of the heart, a process termed cardiac fibrosis. The accumulation of ECM proteins, which are mainly expressed and secreted by cardiac fibroblasts, causes mechanical stiffness and diastolic dysfunction. Excessive ECM protein deposition between layers of cardiomyocytes further disrupts cardiac electric coupling and impairs cardiac contraction. Fibrosis of perivascular areas decreases oxygen and nutrient flow from blood to myocardium, contributing to pathological remodeling of the heart[30].

1.1.2.3 Contributing factors of hypertensive cardiac remodeling

Development of hypertensive cardiac remodeling accompanies the development of hypertension. However, the mechanism of the development of hypertensive cardiac remodeling is still not completely understood. While hemodynamic overload in hypertension is suggested to induce the development cardiac hypertrophy and fibrosis, evidence has been shown that excessive GPCR signaling associated with hypertension is the mediator of hypertensive cardiac remodeling[31,32].

Cardiac hypertrophy can be a normal response to cardiovascular conditioning as occurs in athletes and enables the heart to pump more effectively[33]. Even the initial stage of cardiac hypertrophy in hypertension has been considered as adaptive to excess stress and to maintain proper cardiac function. However, prolonged hypertrophy results in cardiac dysfunction and heart failure. It has been suggested that a major factor leading to cardiac dysfunction in subjects with hypertension is the excessive deposition of extracellular matrix proteins (cardiac fibrosis) that impairs cardiac contractility[34,35]. Although developing within similar time frames and caused by common GPCR agonists, cardiac fibrosis and hypertrophy can be pharmacologically separated. It has been demonstrated that administration of recombinant human bone morphogenic protein-7 to mice with transverse aortic constriction prevents cardiac fibrosis and improves cardiac function, despite the presence of cardiac hypertrophy[36].

1.1.2.4 Diagnosis and measurement techniques

Echocardiography is the principal method to visualize anatomical features of the heart and to diagnosis cardiac hypertrophy in the clinic and in the laboratory. This ultrasound technique provides 2-dimensional imaging of the left ventricle and thus cardiac dimensions (posterior wall, ventricle chamber and interventricular septum). It also produces accurate assessment of the velocity of blood and cardiac tissue. Images taken at systole and diastole can then be used to calculate the thickness of ventricular walls, ventricle volume and ventricle mass and to access ventricle functions[37,38]. This information provides researchers and doctors with real-time data describing changes *in vivo*. *Ex vivo*, cardiac hypertrophy can also be measured by overall weight of the heart. Increases in left ventricle weight (determined by echocardiography) or whole heart weight (normalized by total body weight or tibia length) indicate the presence of cardiac hypertrophy.

In the research laboratory, histological analysis of cardiac samples can also provide insight into the pathogenesis of hypertensive cardiac remodelling. Cardiomyocyte hypertrophy can be revealed by increase of cellular cross sectional area, which can be determined by staining sections with hematoxylin and eosin. Improved contrast of cellular borders can be visualized by fluorescence using fluorescein-conjugated wheat germ agglutinin, a carbohydrate-binding leptin that recognizes N-acetylglucosamine residues of oligosaccharides on the plasma membrane[39,40]. For fibrosis, collagen deposition in heart samples can be visualized by staining heart sections with picrosirius red, a dye that binds extracellular collagen, therefore indicating the relative severity of cardiac fibrosis. The deposition of collagen in cardiac tissues can also be visualized by the blue or green colour in Masson's trichrome stain.

At the molecular level, cardiac hypertrophy and fibrosis can be assessed in the laboratory by measuring expression of hypertrophy and fibrosis marker genes by qRT-PCR. In left ventricle samples, increased expression of the fetal genes alpha-skeletal actin, ANP, BNP and β-MHC are molecular markers of cardiac hypertrophy[41,42]. Meanwhile, increased expression of extracellular matrix proteins, such as collagen type I, collagen type III and fibronectin-1 indicates the development of cardiac fibrosis[42].

1.1.2.5 Treatment strategies

As direct treatment to regress cardiac hypertrophy and fibrosis is limited, current treatment of hypertensive cardiac remodelling relies on the treatment of the underlying cause of the condition, i.e. hypertension. (i.e. ACE inhibitors, diuretics ect.)[43,44]. There are no drugs specifically targeting pathological cardiac remodeling available or clinically approved. In advanced cases of disease, surgical procedures and cardiac transplantation may be required to avoid lethal heart failure.

1.1.3 Hypertensive vascular remodeling

In addition to cardiac remodeling, hypertension is also accompanied by the remodeling of vasculature. There are two kinds of vascular remodeling: inward eutrophic remodeling (the outer and luminal diameters are decreased, media/lumen ratio is increased and cross-sectional area of the media is unaltered) and hypertrophic remodeling (the media thickens toward the lumen, which increases media cross-sectional area and media/lumen ratio). Both are associated with vascular fibrosis (i.e., the accumulation of ECM protein in the arterial wall which are promoted by growth factors and cytokines, primarily transforming growth factor (TGF)-β), hypertrophic growth (i.e. enlargement of individual cells and proliferation of vascular smooth muscle cells (VSMCs) and apoptosis[45,46].

Pathological cardiac remodelling, including cardiac hypertrophy and fibrosis, contribute to myocardial stiffness, decreased cardiac output and increased risk of heart failure[47-49]. Hypertensive vascular remodeling increases vascular resistance (by impairing vasodilatation and enhancing vasoconstriction) and arterial stiffness, which together elevate arterial blood pressure as well as providing the conditions for vascular complications (i.e., atherosclerosis) and target organ damages (i.e., kidneys and brain) [46,50-52]. All of these must be considered when devising anti-hypertensive strategies.

1.1.4 G-protein-coupled receptor agonists in hypertension and cardiovascular remodeling

Diverse conditions such as life style, stress, environmental and genetic factors and metabolic disorders all predispose to hypertension and hypertensive cardiovascular remodeling. This can be explained, at least in part, by the excessive production vasoconstrictive agonists, including Ang II, catecholamines (epinephrine and norepinepherine) and endothelins, in these conditions[19,20,53-56].

1.1.4.1 The renin-angiotensin-aldosterone system

Ang II, the major agonist molecule of the renin-angiotensin-aldosterone system, is produced by the multi-step proteolytic cleavage of the circulating pro-peptide angiotensinogen, a 452 amino acid peptide produced and released by the liver[57]. Renin, a proteolytic enzyme primarily produced in juxtaglomerular cells in the kidney, cleaves angiotensinogen and yields 10 amino acid angiotensin I (Ang I)[58,59]. Ang I then can be cleaved by circulating ACE (secreted primarily by lung, kidney and vascular endothelial cells) to remove two C-terminus residues to generate 8-amino acid Ang II[60,61]. Ang II can be further digested by enzyme ACE-2, which is mainly produced by endothelial cells in the heart and kidneys, to form angiotensin-(1-7), a far less vasoactive peptide[59]. In addition, ACE-2 can also cleave a single amino acid bond from Ang I, forming angiotensin-(1-9), which is also less active[59].

Ang II can act as a vasoconstrictive agonist in the systemic arterial vasculature by activation of AT1R, in addition to its cardiac inotropic effect and its function to stimulate water and salt re-absorption in the kidney. Ang II also stimulates the hypertrophic growth of cardiomyocytes and collagen synthesis of cardiac fibroblasts, contributing to the development of cardiac remodeling. In the adrenal gland, Ang II stimulates the synthesis of aldosterone, a mineralocorticoid hormone that acts on kidneys to increase water and salt retention[62]. This action of aldosterone increases plasma volume and contributes to blood pressure increase. Ang II also stimulates the activity of sympathetic nervous system, which also contributes to the increase of blood pressure and development of cardiovascular remodeling.

Pathological overactivation of the renin-angiotensin-aldosterone system is a common hallmark of hypertensive disorders and has led to multiple anti-hypertensive therapeutic approaches targeting mediators of the angiotensin pathway.

1.1.4.2 The sympathetic nervous system

The sympathetic nervous system is part of the autonomic (involuntary) response system that reacts to environmental stress by initiating a “fight-or-flight” response. Neuronal or hormonal stress signals the release of acetylcholine (Ach) from preganglionic neural fibres. Ach stimulates nicotinic Ach receptors[63] on the postganglionic neurons, leading to the release of catecholamines (norepinephrine and epinephrine) to innervated target organs[64]. Additionally, preganglionic release of Ach in adrenal medulla stimulates postganglionic release of catecholamines from chromaffin cells into the bloodstream, where they act systemically[65]. Catecholamines activate adrenergic receptors which, in turn, induce vasoconstriction (mainly mediated by α-adrenoceptors), increase heart rate and inotropy (mainly by β-adrenoceptors) and stimulate cardiomyocyte hypertrophic growth. Enhanced sympathetic nervous activity also leads to increased renin release and, consequently, renin-angiotensin-aldosterone system activation. Excessive adrenergic stimulation is associated with early stages of human essential hypertension, offering an additional avenue for therapeutic intervention[66,67].

1.1.4.3 Endothelins

Endothelins, including endothelin (ET)-1, -2 and -3, are a family of 21-residue peptides mainly released from endothelium. ET-1, the predominant isoform expressed in vascular system, is the most potent vasoconstrictor. Several stimuli, including vasoactive hormones, growth factors and free radicals, trigger ET-1 expression and secretion. ET-1 are first generated as a precursor peptide (proET-1) that is cleaved to big ET-1 (mainly by furin) and then to the mature 21-amino acid peptide (by endothelin-conveting enzyme) before its release from endothelial cells[68]. The overall action of endothelins is to increase blood pressure and vascular tone[68]. Endothelins can induce vasoconstriction by acting on their receptors (type A and type B endothelin receptor, or ET_A and ET_B respectively) in vascular smooth muscle cells. ET_B is also expressed in endothelium and mediates the activation of nitric oxide synthase and formation of NO, a potent vasodilator.

In the heart, endothelins have positive inotropic effect to increase cardiac output, in addition to their pro-hypertrophic effect[69]. Meanwhile, endothelins increase renin-angiotensin-aldosterone system activity, by stimulating the release of ACE and aldosterone, and sympathetic nerves system activity. Currently, ET-1 receptor blockers have been suggested for the treatment of hypertension and heart failure. A non-selective ET-1 receptor antagonist, bosentan, has been approved clinically for the treatment of pulmonary hypertension.

Despite the differences between Ang II, catecholamines and endothelins, these vasoconstrictive agonists all have cognate receptors coupled to heterotrimeric G proteins[70]. These GPCRs are connected to mechanisms that trigger and maintain contraction as well as hypertrophic and fibrotic processes in vasculature and the heart[71-73].

1.2 Cellular signaling pathways in GPCR-induced hypertension and cardiovascular remodeling

The parallel development of cardiovascular hypertrophy and fibrosis with hypertension suggests overlapping mechanisms with common inducers and mediators. Among the common inducers of hypertension, cardiovascular hypertrophy and fibrosis are vasoconstrictive GPCR agonists such as catecholamines, endothelins and Ang II. These agonists can modulate vascular tone by stimulating traditional phospholipase C (PLC) pathway and adenylyl cyclase pathway, which triggers downstream signaling molecules such as Ca^{2+}, mitogen-activated protein kinase (MAPK), phosphatidylinositol 3-kinase (PI3K) and reactive oxygen species (ROS), although novel signalling mediators (including metalloproteinases) have been identified[56,74,75]. A brief overview of each pathway is described in **1.2.4**.

GPCRs are transmembrane proteins characterized by 7 transmembrane domains. They are linked to heterotrimeric G proteins consisting of 3 subunits: Gα (active when bound to GTP and inactive when bound to GDP), Gβ and Gγ[76]. Among the receptors of vasoconstrictors, the type I Ang II receptor, the α1 adrenoceptor (the prominent catecholamine receptor in the vascular system) and the endothelin receptors ET_A and ET_B are mainly coupled to Gqα proteins which activate PLC-β. The β1-adrenoceptor (prominent cardiac catecholamine receptor) is coupled to Gsα protein that activates adenylyl cyclase.

Agonists typically bind in the pocket formed by the transmembrane domains of GPCRs, leading to conformational changes of these receptors. These GPCRs then serve as guanine nucleotide exchange factors (GEFs) to trigger the activation of their coupled G proteins by promoting the exchange of GDP to GTP on Gα. The activated Gqα protein and Gsα protein then dissociate from the βγ subunits (Gβγ). Free Gqα and Gsα interact with and activate membrane-bound PLC-β and adenylyl cyclase, respectively, to trigger downstream signaling. In addition, PLC-β and adenylyl cyclase have GTPase-activating protein (GAP) activity to increase intrinsic GTPase activity of Gα, facilitating hydrolysis of bound GTP and subsequent deactivation and reassociation with Gβγ[77]. Free Gβγ released from the active G protein can also act as signal molecules triggering the PI3K pathway and the MAPK pathway as well as regulating Ca^{2+} homeostasis[78-82].

1.2.1 Regulation of contraction

The elevation of systemic blood pressure by GPCR agonists is due to an increase in cardiac output (associated with augmented myocardial contraction) and peripheral resistance (associated with enhanced vascular tone).

The contraction of VSMCs and subsequent vasoconstriction in response to GPCR agonists rely on the contractile proteins myosin (in the thick filament in the sarcomere) and actin (in the thin filament of the sarcomere). Phosphorylation of myosin light chain (MLC) in the myosin globular head initiates the interaction between myosin and actin. This interaction leads to the activation of myosin ATPase (also in the myosin globular head) and hydrolysis of ATP, resulting in the cycling of the actin-myosin cross-bridge, subsequent VSMC contraction and vasoconstriction[83]. The phosphorylation state of MLC is primarily controlled by MLC kinases (which are activated by signaling proteins including Ca^{2+}-activated calmodulin (CaM) and PKC) and MLC phosphatase. VSMC contraction is also controlled by other regulatory proteins, such as caldesmon. Caldesmon, which is activated by CaM, inhibits myosin ATPase activity and blocks binding between myosin and actin to prohibit VSMC contraction[84].

Similar to smooth muscle cells, the contraction of cardiomyocytes is also mainly regulated by the change in the intracellular concentration of Ca^{2+}, $[Ca^{2+}]_i$. The increase in $[Ca^{2+}]_i$ triggers the association of Ca^{2+} with troponin, a protein complex composed of three subunits: TnI (which binds actin in the thin filament), TnC (which binds Ca^{2+} to induce a conformational change of TnI) and TnT (which binds tropomyosin). Binding of Ca^{2+} to troponin triggers a conformational change in tropomyosin, exposing the myosin-binding sites on actin. Actin then can bind to the myosin heads of thick filaments, leading to the process of cross-bridge cycling (which requires the energy released by myosin ATPase in the myosin head) and cardiomyocyte contraction[85]. In addition, cardiomyocyte contraction is modulated by kinases and phosphatases that phosphorylate and dephosphorylate, respectively, troponin and tropomyosin, although the exact effects of their phosphorylation are not fully understood[86,87] (**Figure 1-1**).

1.2.2 Regulation of hypertrophic growth

The development of hypertrophy, or cell enlargement, depends on an increase in protein synthesis. Although a potential decrease in protein degradation has been suggested[88], most studies on development of cardiac hypertrophy have focused on the increase in protein synthesis, at the levels of both transcription and translation (**Figure 1-2**).

One of the effects triggered by GPCR agonists to promote the development of hypertrophy in cardiomyocytes and VSMCs is the increased activity of transcription factors, such as GATA-4, myocyte enhancer factor-2 (MEF-2), nuclear factor of activated T-cell (NFAT) and activation protein-1 (AP-1). These transcription factors are activated by signal molecules including MAPKs, Ca^{2+} and calcineurin, which are activated downstream of GPCR. GPCR agonists also induce nuclear export of histone deacetylases (HDACs), facilitating chromosomal de-condensation to promote transcription[89,90]. Among the targets of these transcription factors are the genes coding for α-skeletal actin and β-MHC, which contribute to the changes in contractility of vascular smooth muscle and myocardium[91-93]. These genes, which are usually only expressed during fetal development, are induced in hypertrophic cells and are often considered markers of hypertrophy.

Increased translational activity also contributes to the development of hypertrophy. GPCR agonists promote protein translation by upregulating the synthesis and assembly of ribosomes as well as increasing the activity of eukaryotic translation initiation factors (e.g., eukaryotic translation initiation factor 4E (eIF4E)) and elongation factors (e.g., eukaryotic elongation factor 2 (eEF-2)) in cardiomyocytes and VSMCs[94,95].

1.2.3 Regulation of fibrosis

In the development of cardiac and vascular fibrosis, the excessive ECM protein synthesis depends on growth factors and cytokines (primarily TGF-β) which initiate signaling pathways invloving Smad transcription factors (**Figure**

1-2). The expression and secretion of TGF-β are induced by stimulation with GPCR agonists both *in vitro* and *in vivo*[96-98]. In addition, GPCRs facilitate TGF-β release by activating metalloproteinases, including MMP-2, MMP-9 and MT1-MMP, which can cleave and release active TGF-β. MMP-2, MMP-3 and MMP-7 can also cleave decorin, a TGF-β binding proteoglycan. Once TGF-β is free from the extracellular milieu, it binds to its membrane receptors and triggers downstream signaling[99]. Experimentally, blocking or deleting TGF-β inhibits GPCR agonist-induced development of cardiac and vascular fibrosis[71,97].

Incubation with TGF-β induces the transition of cardiac and vascular fibroblasts into myofibroblasts, which are characterized by the expression of α-smooth muscle actin and the increased release of ECM proteins, such as type I collagen, type III collagen and fibronectin. Specifically, TGF-β binds to the type-II TGF-β receptor (TβRII), which recruits the type-I TGF-β receptor (TβRI) and leads to TβRI activation (by phosphorylation) to initiate downstream signaling. Active TβRI, with the aid of the Smad anchor for receptor activation (SARA), recruits and phosphorylates the regulatory Smads (R-Smads), Smad-2 and Smad-3. Phosphorylated R-Smads subsequently bind with the cooperative Smad (C-Smad), Smad-4, and translocate to the nucleus to initiate transcription of target genes including those encoding ECM proteins. In addition, this process is inhibited by inhibitory Smads (I-Smads), Smad-6 and Smad-7, which compete with R-Smads for interaction with receptors and Smad-4, as well as facilitate the ubiquitination and degradation of R-Smad and TGF-β receptors[100](**Figure 1-2**).

In addition to fibroblasts, Ang II can induce Smad signaling and ECM protein expression in VSMCs to mediate the development of fibrosis, which is dependent on extracellular signal-regulated kinases-1/2 (ERK-1/2) or p38 MAPK activity[101,102].

1.2.4 Molecular signals downstream of GPCRs

Stimulation of GPCRs by agonists (such as Ang II) leads to activation of their coupled Gq or Gs proteins, triggering multiple signaling pathways, including PLC-PKC, protein kinase A (PKA), MAPKs, PI3K-Akt and calcineurin-NFAT, to mediate VSMC and cardiomyocyte contraction and hypertrophic growth. These signaling pathways cross-talk to promote contraction (**Figure 1-1**), hypertrophy and fibrosis (**Figure 1-2**). As **Figures 1-1** and **1-2** show, there is substantial overlap among pathways that signal contraction and those that signal remodeling.

1.2.4.1 The role of PLC-β and downstream pathways in GPCR-regulated contraction and hypertrophy

The members of the Gq_{α} protein family (including Gq_{α}, $G_{11\alpha}$, $G_{14\alpha}$ and $G_{15/16\alpha}$) are characterized by their ability to activate PLC-β[103]. In addition to Gq_{α}, $G_{\beta\gamma}$ released from active heterotrimeric G proteins can also activate PLC-β[104,105]. PLC-β cleaves phosphatidylinositol 4,5-bisphosphate ($PI(4,5)P_2$ or PIP_2) to form diacylglycerol (DAG) and inositol 1,4,5-triphosphate (IP_3)[106], leading to the respective activation of PKC and the elevation of $[Ca^{2+}]_i$, which are major regulators of VSMC and cardiomyocyte contraction. Inhibition of PLC-β activity blocks GPCR agonist-induced contraction in VSMCs and cardiomyocytes[107,108]. In addition, the significance of PLC-β in the development of cardiac hypertrophy has been confirmed by the hypertrophic growth of neonatal cardiomyocytes overexpressing PLC-β1b, one of the PLC-β isoforms[109].

1.2.4.1.1 Ca^{2+} in GPCR-regulated contraction and hypertrophy

Upon the activation of GPCRs, Gq_{α} activates PLC-β, allowing it to hydrolyze the phosphodiester bond of $PI(4,5)P_2$, one of the phospholipids in the plasma membrane. This process results in the formation of hydrophobic DAG and IP_3, two potent second messengers. DAG remains in the plasma membrane and serves as activator of PKC, as discussed later. IP_3 diffuses from the plasma membrane to the sarcoplasmic reticulum (SR), where it binds to IP_3 receptors (one of the Ca^{2+} channels on SR membrane), leading to the release of Ca^{2+} from the SR and the elevation of $[Ca^{2+}]_i$. GPCR agonists also activate plasma membrane L-type Ca^{2+} channels through $G_{\beta\gamma}$ subunits to trigger extracellular calcium entry. This process is probably mediated by the ability of $G_{\beta\gamma}$ to activate PI3K[110]. The increase in $[Ca^{2+}]_i$ (from extracellular space and intracellular stores) can induce supplementary release of Ca^{2+} from the SR by activating ryanodine receptors (Ca^{2+}-dependent Ca^{2+} channels on SR membrane), further elevating $[Ca^{2+}]_i$[111].

The Ca^{2+}-binding protein CaM is one of the primary targets of elevated $[Ca^{2+}]_i$. Ca^{2+} binding triggers the conformational change and activation of CaM. In VSMCs, activated CaM is able to bind to and activate MLC kinase, which mediates contraction as described in **1.2.1**[83]. In cardiomyocytes, elevated $[Ca^{2+}]_i$ triggers the association of Ca^{2+} with troponin, which allosterically modulates tropomyosin, exposing the myosin binding sites of thin filaments. This permits subsequent cross-bridge cycling and cardiomyocyte contraction[85]. In addition to its role in the regulation of contraction, activated CaM also promotes hypertrophic growth in cardiomyocytes and VSMCs through the activation of the calcineurin-NFAT pathway and nuclear export of HDACs[89,112].

1.2.4.1.2 PKC in GPCR-regulated contraction and hypertrophy

The activation of PLC-β and the subsequent release of DAG and IP_3 triggered by Gq protein-coupled receptor agonists also induce the activation of PKCs. The mammalian PKC family has 11 members that can be classified into conventional PKCs (cPKCs; -α, -βI, -βII, -γ, which require both Ca^{2+} and DAG for activation), novel PKCs (nPKCs; -δ, -ε, -η, -θ, which only require DAG for activation) and atypical PKCs (aPKCs; -ζ, -λ, -μ, which cannot be activated by DAG).

The elevation of $[Ca^{2+}]_i$ in response to GPCR activation results in the binding of Ca^{2+} to cPKCs in the cytoplasm, triggering cPKCs' structural changes and translocation from the cytoplasm to the inner face of the plasma membrane. On the other hand, DAG remaining in the plasma membrane cooperates with phosphatidylserine (PS) to interact with and activate membrane-bound PKCs, including both cPKCs and nPKCs[113].

PKCs, which are serine/threonine protein kinases, can activate the small G protein RAS-GTPase which in turn initiates downstream signaling pathways including the MEK-ERK pathway and the PI3K pathway, signaling the development of cardiovascular hypertrophy[114-118]. Experimentally, the overexpression of PKC-α, -β, -δ, or -ε triggers ERK and/or PI3K activation and hypertrophic growth in cultured cardiomyocytes and VSMCs as well as in the hearts of transgenic mice[119-122].

PKCs regulate smooth muscle and myocardial contraction through their ability to: 1) activate MAPKs, such as ERK-1/2, which subsequently phosphorylate the thin filament-associated protein caldesmon, reversing its inhibition of myosin ATPase activity and increasing actin-myosin interaction (cross-bridge cycling)[84], 2) phosphorylate calponin, another thin filament-associated protein, to disrupt its ability to block cross-bridge cycling[123], 3) phosphorylate Thr38 on PKC-potentiated inhibitory protein of 17 kDa (CPI-17), which in turn inhibits MLC phosphatase, increasing MLC phosphorylation and smooth muscle contraction[124].

Apart from PKC, DAG activates protein kinase D (PKD, also known as PKCμ), a serine/threonine protein kinase family that can also be activated by PKC phosphorylation[125]. Among the targets of PKD are HDACs, whose phosphorylation leads to their nuclear export, permitting pro-hypertrophic gene expression[126,127]. PKD can upregulate Ras activity and MEK/ERK signaling by phosphorylating the Ras-binding protein, Ras and Rab interacter-1 (RIN-1)[128]. The inhibition of PKD blocks HDAC nuclear export and the development of cardiomyocyte hypertrophy *in vivo* and *in vitro*[127,129].

1.2.4.2 The role of PKA and downstream pathways in GPCR-regulated contraction and hypertrophy

Stimulation of Gs protein by GPCR agonists leads to the activation of adenylyl cyclase, which generates cAMP from ATP and activates PKA. PKA is composed of two regulatory subunits and two catalytic subunits. cAMP binds to the regulatory subunits, leading to the release of the active catalytic subunits. One of the primary targets of active PKA are the L-type Ca^{2+} channels on the plasma membrane, resulting in an influx of extracellular Ca^{2+} to induce an increase in $[Ca^{2+}]_i$, promoting the contraction of VSMCs and cardiomyocytes as well as their hypertrophic growth (through the activation of CaM). PKA also phosphorylates the small G protein Rap, which in turn activates B-Raf to trigger the MEK-ERK pathway[130].

Experimentally, cardiac overexpression of β_1-adrenoceptor, which is usually coupled to Gs proteins, initially increases heart contractility in transgenic mice, but eventually results in progressive cardiomyocyte hypertrophy and fibrosis[131]. Cardiac overexpression of the catalytic subunit of PKA also induces the development of dilated cardiomyopathy associated with cardiomyocyte hypertrophy and fibrosis, supporting the pro-hypertrophic role of Gs protein-coupled receptors and their downstream signaling[132].

Other targets of PKA include transcription factors such as cAMP-response element binding protein (CREB) and cAMP-dependent transcription factor-1 (ATF-1). PKA, in addition to other kinases including ERK and CaM-dependent kinase, phosphorylates CREB on Ser133 and triggers its transcriptional activity. The target genes of CREB include those coding for the β-adrenoceptor, TGF-β and ANP, which are involved in the regulation of hypertrophic growth in cardiomyocytes. Stimulation by GPCR agonists induces the activation of CREB, the expression of its target genes and cardiomyocyte hypertrophy[133,134]. Moreover, the inhibition of CREB prevents Ang II-induced hypertrophy in VSMCs[135].

In addition to PKA, another target protein of cAMP is the exchange protein directly activated by cAMP (Epac), a small G protein GEF. The classic target of Epac is Rap, which can activate B-Raf to trigger MEK/ERK signaling[130]. Epac has been reported to mediate β-adrenergic receptor-induced cardiomyocyte hypertrophy involving the activation of Ras, Rac and calcineurin[136,137].

1.2.4.3 Signaling pathways from GPCRs to transcription and translation

Downstream of PLC, PKC and PKA, the induction of hypertrophy in VSMCs and cardiomyocytes by GPCR agonists is mainly mediated by their ability to stimulate signal pathways that regulate transcription and translation, including Raf-MEK-ERK and PI3k-Akt signaling pathways.

1.2.4.3.1 The Raf-MEK-ERK pathway

ERK-1 and -2, also known as p42- and p44-MAPKs, are members of the MAPK family of serine/threonine protein kinases and are major regulators of hypertrophic growth of VSMCs and cardiomyocytes. Their activation requires phosphorylation on threonine and tyrosine residues by the upstream MAPK kinases, MEK-1/2, which are phosphorylated and activated by Raf MAPK kinase kinase.

The significance of the Raf-MEK-ERK pathway in the development of cardiac hypertrophy has been demonstrated by the development of significant cardiac hypertrophy in mice with cardiac-specific overexpression of MEK-1[138]. In addition, mice expressing cardiac-specific dominant negative Raf-1 are resistant to the development of cardiac hypertrophy induced by transverse aortic constriction[139].

Upon stimulation by GPCR agonists, the activation of PKC through Gq_{α}-PLC signaling leads to the activation of small GTPase Ras, although the mechanism is not fully understood[114-116]. PKC can phosphorylate and inhibit Ras GAP to maintain the activity of Ras[140]. Activated Ras (i.e., in GTP-bound state) recruits Raf protein (through Raf's Ras interaction domain) to the membrane and facilitates its phosphorylation on Ser338 and Tyr341, resulting in the full activation of Raf. PKC can also activate Raf independently of Ras[141]. Additionally, cAMP generated downstream of Gs_{α} activation can activate B-Raf, one of the Raf isoforms expressed in the heart, through both PKA-dependent and -independent pathways. The serine/threonine protein kinase, Raf phosphorylates and activates MEK-1/2, which subsequently activate ERK-1/2[142]. Activated ERK-1/2 can phosphorylate and trigger transcription factors including c-myc, c-fos, Elk-1, GATA-4 and CREB to mediate gene transcription and cardiomyocyte hypertrophy[143]. The MEK-ERK pathway also regulates translation downstream of GPCR activation. In adult cardiomyocytes, phenylephrine (an α-adrenoreceptor agonist) and endothelin-1 can induce an increase in protein synthesis by activating ribosomal protein S6 kinase 1 (S6K-1) and by inducing the release of eIF4E from its inhibitory binding partner eIF4E-binding protein-1 (4EBP-1). These pro-hypertrophic processes can be blocked by inhibitors of MEK or Ras, suggesting that the MEK-ERK pathway also engages translation to mediate GPCR-induced hypertrophy[144].

Another target of ERK is MAPK-activated protein kinase 1 (MAPKAP-K1 or p90 ribosome protein S6 kinase (p90RSK)), which can phosphorylate ribosome S6 protein to promote ribosomal activity and translation. p90RSK also promotes transcription by phosphorylating and activating transcription factors like CREB and c-fos. Activation of p90RSK has been reported to mediate cardiomyocyte hypertrophy *in vivo* and *in vitro*[145,146].

The MEK-ERK pathway may also regulate the contraction of VSMCs. For example, ERK-1/2 can phosphorylate caldesmon, reverse its inhibition of myosin

ATPase activity and increase actin-myosin interaction and subsequent VSMC contraction[84].

1.2.4.3.2 The PI3K-Akt pathway

Since its discovery in the 1988, PI3K has been found to be involved in diverse cell processes including cell proliferation, differentiation and survival, mainly through the activation of its downstream serine/threonine protein kinase Akt (also known as protein kinase B (PKB))[147].

Activation of Ras downstream of GPCR-PLC-PKC can lead to the activation of class I PI3K (composed of a catalytic 110 kDa subunit and a regulatory 85 kDa or 55 kDa subunit), whose catalytic subunit contains a Ras-binding domain[117]. Moreover, free $G_{\beta\gamma,}$ upon GPCR activation, is able to activate class IB PI3K (probably through their direct interaction)[78]. Activated PI3K converts plasma membrane lipid $PI(4,5)P_2$ into phosphatidylinositol 3,4,5-trisphosphate ($PI(3,4,5)P_3$) by phosphorylation. This results in the recruitment of Akt and 3-phosphoinositide-dependent protein kinase 1 (PDK-1) to the cell membrane through the interaction between their pleckstrin-homology (PH) domains and $PI(3,4,5)P_3$. The forced colocalization of Akt and PDK-1 leads to the phosphorylation (on Thr308 and Ser473) and activation of Akt by PDK-1[148].

In transgenic mice, PI3K or Akt overexpression induces the development of cardiac hypertrophy[149,150]. Expression of a dominant negative form of PI3K results in smaller hearts compared to the wild-type mice[149,151]. Meanwhile, Akt overexpression induces VSMC hypertrophy and Akt inhibition blocks Ang II-induced VSMC hypertrophy *in vitro*[152]. These results confirm the significance of the PI3K-Akt pathway in the development of GPCR agonist-induced hypertrophy.

One of the ways that Akt contributes to the development of hypertrophy is via the activation of another protein kinase, mammalian target of rapamycin (mTOR)[94]. Inhibition of mTOR by rapamycin attenuates pathological cardiac hypertrophy and reverses myocardial dysfunction induced by cardiac Akt-1 overexpression[153,154]. Akt leads to mTOR activation through the phosphorylation of tuberous sclerosis protein 2 (TSC-2 or tuberin). Phosphorylation attenuates TSC-2's GAP activity towards small G protein Rheb, thus maintaining Rheb activity. Rheb can then bind to the N-terminal lobe of the catalytic domain of mTOR and activate mTOR[155]. Downstream of mTOR are p70/85 S6K-1 and p54/56 S6K-2. When activated by mTOR via phosphorylation, S6K-1/2 phosphorylate and activate ribosomal S6 protein, which subsequently stimulates translation of the 5'-terminal oligopyrimidine tract (5'-TOP) mRNAs (including the mRNAs of translation factors and most ribosomal proteins), promoting the synthesis of ribosomes, translation and subsequent hypertrophic growth of cardiomyocytes and VSMCs[94,156,157]. mTOR also stimulates translation by activating translation initiation factor eIF4E and translation elongation factor eEF-2. mTOR: 1) phosphorylates eIF4E-binding protein 4EBP-1, leading to the release of eIF4E and enabling it to bind 5'-capped mRNA; and 2) phosphorylates eEF-2 kinase, inhibiting its ability to phosphorylate and de-activate eEF-2[156]. In addition to Akt, ERK-1/2 also phosphorylate and inhibit TSC-2 to activate mTOR, indicating there is cross-talk between the PI3K-Akt pathway and the MEK-ERK pathway and supporting the pro-hypertrophic effect of the MEK-ERK signaling[158].

Activation of Akt via PI3K signaling also promotes cardiac hypertrophy through the phosphorylation and deactivation of glycogen synthase kinase 3β (GSK-3β). Apart from its role in metabolism, active GSK-3β phosphorylates and inhibits translation initiation factor eIF2B to block translation. The inhibition of GSK-3β by Akt facilitates translation by activating eIF2B and promotes transcription by activating transcription factors involved in hypertrophic growth, such as c-Myc, GATA-4 and NFAT[94,159]. In addition, ERK is reported to interact with GSK-3β to prime GSK-3β for inactivation[160].

PI3K has also been reported to activate membrane L-type Ca^{2+} channels to promote Ca^{2+} entry into the myocardium and smooth muscle to mediate their contraction[110,161,162]. In addition, PI3K inhibition reduces VSMC contraction and that cardiac specific expression of PI3Kα or Akt initially increases myocardial contractility, suggesting the possible involvement of the PI3K-Akt pathway in the regulation of vasoconstriction and myocardial contraction[149,163].

1.2.4.4 GPCR signaling through reactive oxygen species

Elevated levels of ROS, such as hydrogen peroxide and superoxide, damage proteins, DNA and membrane lipids via oxidation and other modifications (including oxidation of sulfhydryl groups, reduction of disulfide bonds, adduction of residues to metal ions, cross-linking and fragmentation). These damages lead to energetic deficit and cell death and contribute to the progression towards heart failure[164]. At lower levels, ROS can exert more subtle effects by regulating the activity of diverse intracellular molecules and pathways, such as the MAPK and PI3K pathways, mainly through their ability to activate kinases and inhibit tyrosine phosphatases[165,166]. These subtle effects may be more significant in the regulation of contraction and hypertrophic growth in cardiomyocytes and VSMCs[167]. Stimulation by GPCR agonists like Ang II can induce increased intracellular ROS levels to mediate contraction and hypertrophic growth in VSMCs and cardiomyocytes. Furthermore, treatment with antioxidants (such as butylated hydroxyanisole, vitamin E, and catalase) prevents the development of GPCR agonist-induced vasoconstriction and cardiovascular hypertrophy[56,168-170].

The cellular sources of ROS include mitochondria, NADPH oxidase, xanthine oxidase and nitric oxide synthase. The main sites of mitochondrial ROS generation are complex I (NADH dehydrogenase) and complex III (coenzyme Q:

cytochrome c oxidoreductase) of the electron transport chain, where single electrons are transferred to oxygen molecules (O_2) to generate superoxide radicals ($O_2^{\cdot -}$) as byproducts of respiration. Most studies suggest that mitochondrial ROS are important in models of heart failure and myocardial ischaemia-reperfusion, but less so in the process of contraction and hypertrophy[171-173]. Rather, NADPH oxidase, a membrane-associated protein complex which transfers electrons from NADPH to O_2 to generate superoxides, is considered to be the main source of ROS in acute response to GPCR activation[167,174].

Generated $O_2^{\cdot -}$ can be converted into H_2O_2 molecules (which are more stable and diffusible than radicals like $O_2^{\cdot -}$ and thus serve as better signal molecules) and hydroxyl radicals $HO^{\cdot}$ (which are highly reactive damaging molecules)[175]. $O_2^{\cdot -}$ can also react with nitric oxide to generate peroxynitrite ($ONOO^-$). This scavenging of nitric oxide, a vasodilator, contributes to the suppression of vasodilation and thus, the development of hypertension. $ONOO^-$, meanwhile, induces protein oxidation and nitration, mitochondrial membrane permeabilization and loss of mitochondrial function[176,177]. In addition, ROS generated by NADPH oxidase can further promote ROS production from nitric oxide synthase, xanthine oxidase and mitochondria as well as NADPH oxidase itself[178-181].

Stimulation by GPCR agonists like Ang II induces expression of NADPH oxidase subunits and promotes the assembly of NADPH oxidase complex on the plasma membrane, leading to its activation and subsequent ROS production in cardiomyocytes and VSMCs[182-185]. GPCR agonists also induce NADPH oxidase activation and ROS generation, which are mediated by PKC phosphorylation of p47phox, one of the subunits of NADPH oxidase required for its activation[186,187]. Treating VSMCs with phorbol-12-myristate-13-acetate (PMA, also known as 12-O-tetradecanoylphorbol-13-acetate or TPA), a DAG analogue that constitutively activates PKCs, induces an increase in intracellular ROS level. This increase can be blocked by the inhibition of PKC or NADPH oxidase, but not by inhibition of other ROS-generating enzymes including xanthine oxidase, nitric oxide synthase and the mitochondrial electron transport chain[188].

Another pathway that mediates the activation of NADPH oxidase is the PI3K-Akt pathway. Akt phosphorylates p47phox on S304 and S328 to support NADPH oxidase activation[189]. PI3K also mediates the activation of small G protein Rac, one of the regulator of NADPH oxidase, facilitating the recruitment of cytoplasmic components of the NADPH oxidase complex to the membrane[190]. Expression of constitutively active Rac increases basal and Ang II-induced levels of ROS, whereas inhibition of Rac activity can decrease Ang II–induced ROS production and VSMC contraction as well as Ang II-induced cardiomyocyte hypertrophy[184,191,192]. PI(3,4,5)P_3 produced by PI3K activates Rac-specific GEFs, such as Vav and SWAP-70[193,194], which trigger the activation of Rac. Deletion of PI3K-γ blocks Rac activation, ROS production and hypertension induced by Ang II stimulation *in vivo*[195].

The effects of ROS in signaling depend on their ability to inhibit protein tyrosine phosphatases (PTP) and to activate kinases (through the oxidation of cysteine residues)[165]. In neonatal cardiomyocytes, treatment with H_2O_2 can induce the activation of MAPKs including ERK-1/2[196,197]. ROS can activate Ras by modifying its cys-118 and increasing its GTP/GDP exchange activity [198]. Activation of Ras in turn leads to the activation of the MEK-ERK and the PI3K-Akt pathways, which promote contraction and hypertrophic growth in VSMCs and cardiomyocytes. Additionally, ROS can trigger the activation of Akt in several cell types such as VSMCs and fibroblasts[197,199]. Ang II-induced Akt activation can be inhibited by exposure to antioxidants or by overexpressing catalase, the enzyme catalyzing the decomposition of H_2O_2 to water and oxygen[199].

ROS also stimulate contraction and hypertrophic growth through the regulation of $[Ca^{2+}]_i$. ROS can oxidize a cysteine residue on the ryanodine receptor to increase Ca^{2+}-dependent Ca^{2+} release from the SR[200]. Meanwhile, NADPH oxidase-derived ROS are reported to mediate endothelin-1 and Ang II-induced activation of L-type Ca^{2+} channels[201,202].

In the hypertrophic heart, accumulation of ROS-damaged proteins, membrane lipids and DNA (including mitochondrial DNA) results in assembly defects and dysfunction of enzymes, including the mitochondrial respiration chain complexes which are essential for ATP generation. These defects also result in membrane potential abnormality, mitochondrial replication inhibition and can induce apoptosis signals to mediate death of cardiomyocytes. Furthermore, the increase in the level of ROS also mediates the proliferation of cardiac fibroblasts as well as TGF-β expression and secretion, promoting the deposition of ECM proteins and thus the development of fibrosis[203]. These pro-apoptotic and pro-fibrotic effects all contribute to the loss of heart contractility and the development of heart failure in the long term[204].

1.3 Metalloproteinases and transactivation pathways

1.3.1 Metalloproteinases

Metalloproteinases are a class of proteases belonging to the metzincin superfamily which are named for the presence of the conserved Met residue and zinc ion at the active site. This class of enzymes includes the matrix metalloproteinases (MMP) and the disintegrin metalloproteinases (ADAMs)[205,206]. The first metalloproteinase (MMP-1) was identified in 1960s as the enzyme degrading collagen triplex and contributing to the tail resorption of tadpole metamorphosis. Metalloproteinases are known for their role in the degradation of extracellular matrix proteins such as collagens and gelatin. However, over the past 20 years, our knowledge of the molecular functions of metalloproteinases has expanded. Now, metalloproteinases are known to act not only as ECM degrading enzymes but also as mediators in cell signaling pathways. Recent studies have further shown that metalloproteinases can cleave and modulate many substrates such as apoptotic ligands, cytokines, chemokines and growth factors. Tthese substrates are then released from their membrane-bound proforms (a process known as “shedding”), allowing them to “transactivate” respective receptors and induce downstream signaling[207-210]. Recent studies have also suggested that metalloproteinases can cleave membrane receptors such as insulin receptors, β2-adrenoceptors and lead to their inactivation[211,212]. Therefore, these enzymes not only regulate normal tissue remodeling, but also the processes such as cell growth and proliferation, migration, apoptosis and angiogenesis.

1.3.1.1 MMPs

MMP family contain 23 members in human and mouse (**Table 1-2**). They have similar structures that comprise of prodomain, catalytic domain and hemopexin-like domain. Although MMPs in general share structural and functional characteristics, they can be further sub-classified according to their substrate specificity and domain structure: collagenases (which can degrade collagen triple helix), gelatinases (which contain additional collagen-binding type II repeats of fibornectin and can cleave gelatin, denatured collagen), stromelysins (which can cleave broad spectrums of extracellular matrix proteins but not triple-helical fibrillar collagen), matrilysin (which lack the hemopexin-like domain) and membrane type-MMPs (MT-MMPs, which contain transmembrane domain or glycosylphosphatidylinositol anchor). Although most MMPs are thought to be secreted, intracellular function of MMPs has been reported[213,214].

1.3.1.1.1 MMP-2

MMP-2, also known as gelatinase A or 72 kDa gelatinase, is ubiquitously expressed in most tissues. It is one of the mostly studied MMP because of its constitutive expression, its dominant role in injury repair and diseases as well as ease of detection using gelatin zymography. The substrates of MMP-2 include type I, IV, V, VII and X collagens, gelatin, elastin, fibronectin and laminin. Physiologically, in coordination with other MMPs, MMP-2 regulates normal tissue remodeling events such as embryonic development, angiogenesis, ovulation, mammary gland involution and wound healing. MMP2 also triggers osteoblastic bone formation and inhibits osteoclastic bone resorption[215]. Increased expression of MMP-2, along with MMP-9 (gelatinase B, 92 kDa gelatinase), is often observed in invasive and tumorigenic cancer[216]. It also promotes tumor progress by 1) cleaving ECM, 2) cleaving and activating growth factors and, 3) promoting angiogenesis. In cardiovascular system, acute release of MMP-2 during reperfusion after ischemia contributes to cardiac mechanical dysfunction and inhibition of MMP-2 improved the recovery of mechanical function during reperfusion[217]. Increased level of circulating MMP-2 is suggested to be the marker of heart failure. MMP-2 levels above the mean serum level are associated with poor prognosis and mortality of patients with chronic heart failure[218]. Oxidative stress activates cardiac MMP-2 to cleave sarcomeric proteins (titin, troponin I and myosin light chain-1) which can impair cardiomyocyte contractility[213,219,220].

1.3.1.1.2 MMP-7

MMP-7, also known as matrilysin I, is the smallest member of MMP family. It does not have the hemopexin-like domain which is involved in protein interaction and determines the substrate specificity of MMPs. Therefore, MMP-7 has a broad spectrum of substrates, including aggrecan, fibronectin, elastin and type IV collagen. MMP-7 is highly expressed in the intestine and cleaves and activates α-defensin in intestinal mucosa, thus involved in innate immune defense[221]. In the cardiovascular system, MMP-7 has recently been reported to be the major inducing factor of endothelial dysfunction[222,223]. MMP-7 promotes GPCR agonist-induced vasoconstriction through the cleavage of heparin-binding epidermal growth factor (EGF)-like growth factor (HB-EGF) and activation of epidermal growth factor receptor (EGFR)[56].

1.3.1.2 ADAMs

The human ADAMs family has 21 members and 13 of them exhibit proteinase activity (**Table 1-3**). The typical ADAM is composed of prodomain, catalytic domain, disintegrin domain, cysteine rich domain, EGF-like domain, transmembrane domain and cytoplasmic domain. Although all ADAMs are expressed as membrane proteins, some ADAMs, such as ADAM-9, ADAM-12 and ADAM-19, have splicing isoforms lacking transmembrane and cytoplasmic domains, thus forming the secreted ADAMs[224-226].

1.3.1.2.1 ADAM-12

ADAM-12, also known as meltrin 1, is highly expressed in placenta. It is also expressed in other organs including heart and skeletal muscle. ADAM-12 is expressed as two splicing isoforms in human: the transmembrane ADAM-12L and secreted ADAM-12S, although ADAM-12S has not been observed in rodents[225]. ADAM-12 is able to cleave insulin-like growth factor (IGF)-binding protein (IGFBP) 3 and 5, which increases concentrations of bioavailable IGF and is important for foetal growth during pregnancy[227]. The expression of ADAM-12 is also highly elevated in tumors and is considered as a prognosis marker for human bladder cancer and breast cancer, although its exact role is not clear[228]. In the heart, ADAM-12 is able to cleave and release (shed) membrane-bound HB-EGF, contributing to the development of cardiac hypertrophy[229]. ADAM-12 also interacts with TGF-β receptor type II and increase the TGF-β signaling and probably fibrosis[230].

1.3.1.2.2 ADAM-17

ADAM-17 is also known as TNF-α-converting enzyme (TACE). Although ADAM-17 is a membrane metalloproteinase, only 10% of the total protein is found on the plasma membrane on the cell surface. The majority of mature, endogenous ADAM17 possessing metalloproteinase activity is localised in the endoplasmic reticulum (ER) and trans-Golgi network, suggesting possible intracellular functions[231]. As its name suggests, one of the targets of ADAM-17 is membrane-bond pro-TNF-α. The cleavage results in the release of active TNF-α[232]. ADAM-17 can also cleave and activate growth factors like TGF-α, which activate EGFR and mediate chronic kidney disease[233]. In vasculature, ADAM-17 is able to activate EGFR and mediate the proliferation and hypertrophic growth of vascular smooth muscle cells, contributing to the development of vascular remodeling[234,235]. ADAM-17 also serves as α-secretase of amyloid precursor protein, generating soluble non-amyloidogenic fragment and preventing the development of Alzheimer's disease[236].

1.3.1.3 Activation and regulation of metalloproteinases

All metalloproteinases are expressed as inactive pro-proteins which require activation to exhibit their enzymatic activity. Metalloproteinases are also regulated by a variety of other mechanisms including transcriptional regulation, posttranslational modifications (e.g. phosphorylation) and protein-protein interactions[237-240].

All metaloproteinases are synthesized as inactive zymogens with an N-terminal inhibitory prodomain. This prodomain blocks the catalytic zinc ion (via cysteine-switch mechanism, a cysteine residue in the "PKVCGY" binds to the zinc ion) and separates substrates from active site. Activation of metalloproteinases requires cleavage of the propeptide, oxidative stress or other conformational perturbations to disrupt the interaction of the cysteine residue with the zinc ion and to expose the active site[237]. The proteinases involved in the prodomain removal include furin, plasmin and other metalloproteinases. For example, MMP-3 can cleave and activate MMP-1, MMP-7, MMP-8 MMP-9 and MMP-13[241,242]. Similarly, MMP-7 activates MMP-1, MMP-2, MMP-8 and MMP-9 whereas MMP-10 activates MMP-7, MMP-8 and MMP-9[242]. In addition, pro-MMP-2 has been shown to be activated by MT1-MMP (MMP-14) after binding with tissue inhibitor of metalloproteinases (TIMP)-2[243,244].

The activation of metalloproteinase also occurs without the cleavage of the prodomain. Oxidation of the inhibitory cysteine residue by ROS can break the cysteine-switch and expose the active site. Artificially, mercury-containing compounds such as 4-aminophenylmercuric acetate (APMA) or detergent such as sodium dodecyl sulphate (SDS) can also disrupt the cysteine-switch, allowing activation of the metalloproteinase without cleavage of the prodomain[245].

Metalloproteinases are also regulated at the transcriptional level[239]. The promoters of most MMPs and ADAMs contain binding sites for transcription factors such as AP-1, activating transcription factor-2 (ATF-2), and NF-κB[246-251]. These transcription factors can be activated by MAPK and c-Jun N-terminal kinases (JNK) pathways which are triggered by growth factors (i.e. EGF), cytokines (i.e. transforming growth factor beta, TGF-β) and GPCR agonists[246,252]. PMA, which mimics DAG and constitutively activates PKC, induces the expressing of metalloproteinases, suggesting PKC pathway also regulates metalloproteinase expression[253].

Several ADAMs contain potential phosphorylation sites for serine-threonine protein kinases and tyrosine protein kinases. ADAM-17 has been shown to be activated by ERK through phosphorylation at Thr735, which is required for its maturation and trafficking[254]. Similarly, human MMP-2 activity is affected by phosphorylation at 5 different sites[240].

Metalloproteinase activation might also be mediated through protein-proteininteractions. PACSIN-3 and eve-1, two docking proteins that contain Src homology 3 (SH3) domains to interact with the proline-rich domain of ADAMs, are able to enhance ADAM-12 activation induced by PMA, suggesting their role downstream of GPCR-induced PKC-mediated ADAM activation[255,256]. Consistently, knockdown of PACSIN-3 or eve-1 inhibits ADAM-12 activation and subsequent HB-EGF shedding induced by either PMA or Ang II.

Another aspect of metalloproteinase regulation arises from their interactions with the TIMPs, which reversibly interact with metalloproteinases and inhibit their proteolytic activities in a 1:1 stoichiometric ratio[257]. TIMPs are 21-30 kDa small proteins with 4 identified isoforms (TIMP-1, 2, 3 and 4). All known MMPs and most of the ADAMs (with the exceptions of ADAM-8, 9 and 19) are inhibited by at least one of the four TIMPs[258]. In addition, TIMP-2 can form a complex involving MMP-2 and MT1-MMP[244]. In this complex, TIMP-2 interacts with MT1-MMP and recruits pro-MMP-2 for proteolytic activation by MT1-MMP. Therefore TIMP-2 is involved in the activation as well as inhibition of MMP-2.

1.3.1.4 Pathological roles and therapeutic inhibition of metalloproteinases

Due to their ability to degrade cartilage extracellular matrix (mainly composed of proteoglycans and collagens), metalloproteinases are believed to be the main player in the development of two major joint diseases: osteoarthritis and rheumatoid arthritis[259]. Metalloproteinases have also been shown to be involved in other diseases including neurodegenerative disease, cardiovascular disease and cancer[228,229,234-236].

Due to the strong upregulation and significance of metalloproteinases in these pathological conditions, metalloproteinases have been studied as potential therapeutic targets. However, despite numerous trials targeting metalloproteinases clinically, only one metalloproteinase inhibitor (doxycycline, a member of the tetracycline antibiotics group) is approved for clinical use (for periodontitis). Tetracyclines, initially identified as antibiotics, were found to inhibit metalloproteinase activity at sub-antimicrobial doses in 1983[260]. Since then, tetracyclines, including chemically modified tetracyclines (CMTs, whose antimicrobial activity is removed but metalloproteinase inhibitory activity is retained), have been studied for their metalloproteinase inhibitory activity in different disease models including diseases of the cardiovascular system[261-263]. Other metalloproteinase inhibitors, including GM6001, batimastat and marimastat have also proven effective in experimental disease models. However, success has been limited in the clinical trials[264-268]. The synthetic MMP inhibitor PG-116800 failed to improve any clinical outcomes and showed no reduction in myocardial infarction-induced ventricular remodeling in post-myocardial infarction patients, despite effective in preclinical animal studies[269]. Coronary artery disease patients receiving doxycycline for 6 month showed decreased plasma levels of high sensitivity C-reactive protein, interleukin-6 and pro-MMP-9 levels, but were not protected from cardiovascular death or myocardial infarction[270]. The lack of success in targeting metalloproteinases clinically is at least partially attributable to the presence of adverse side effects including musculoskeletal syndromeand the lack of specificity of these metalloproteinase inhibitors[257,271]. Therefore, many studies are now focusing on the design of more selective metalloproteinase inhibitors, including natural products and their derivatives as well as low molecular weight synthetic compounds incorporating different Zn^{2+}-binding groups[272,273].

1.3.2 Transactivation pathway involving metalloproteinases

In the last twenty years, studies have uncovered that stimulation by GPCR agonists can also lead to the activation of receptors of growth factors and cytokines to enhance vascular smooth muscle contraction and promote hypertrophic growth in both vascular smooth muscle and the heart[55,56,229,234]. This "transactivation" process, first described in 1996, demonstrated that activation of GPCRs leads to the phosphorylation of the EGFR and subsequent MAPK activation and c-Fos expression[274]. The significance of the transactivation process has been demonstrated in tumor cells, neurons, cardiomyocytes and VSMCs. Further studies suggested that the transactivation process is mediated at least in some cases, by MMPs and ADAMs[55,56,229,233,234,275]. These metalloproteinases, when activated, cleave and release (shed) growth factors (*e.g.*, HB-EGF) and cytokines (*e.g.*, TNF-α), leading to the activation of their receptors and downstream signaling involving MAPKs, PI3K-Akt and ROS. Studies using animal models have shown that non-specific inhibition of metalloproteinases can attenuate the development of systemic and pulmonary hypertension, cardiac hypertrophy and vascular remodeling, confirming the significance of metalloproteinases in these cardiovascular diseases[266,276-278].

1.3.2.1 Agonist-induced activation of metalloproteinases

Several studies have demonstrated that stimulation by GPCR agonists induces the activation of metalloproteinases (including MMPs and ADAMs), mediating vasoconstriction as well as the development of hypertension and cardiovascular hypertrophy[55,56,229,234].

PKC may be a key mediator of the GPCR agonist-induced activation of metalloproteinases. Treatment with the phorbol ester PMA can induce PKC activation and promote the shedding ability of metalloproteinases such as

ADAM-17[248,249]. In ADAM-17$^{-/-}$ fibroblasts, TGF-α and neuregulin shedding induced by PMA is absent[279]. PMA-induced neuregulin release is also lost in ADAM-19 deficient fibroblasts[280], and PMA-triggered HB-EGF shedding is impaired in ADAM-12 deficient cardiomyocytes[229]. Additionally, activation of the Ras-Raf-MEK-ERK pathways by GPCR agonists has been reported to activate metalloproteinases and subsequent HB-EGF shedding independent of PKC[275].

The mechanisms of GPCR agonist-induced metalloproteinase activation is at both the transcriptional and post-translational level. At the transcriptional level, GPCR activation induced by agonists such as Ang II and catecholamines increases the transcription of MMPs including MMP-1, -2, -7, -9 and -14 and ADAMs like ADAM-12[56,229,281,282]. Activation of PKC by PMA stimulation induces the expression of MMPs, suggesting PKC may mediate GPCR agonist-induced MMP expression[248,283]. GPCR agonist-induced activation of ERK-1/2 signaling and subsequent activation of transcription factors like AP-1 (consisting of c-Fos and c-Jun, whose expression and activity are triggered by ERK) may also contribute to the activation of metalloproteinases, since the *cis* element of AP-1 has been found in the promoters of almost all MMPs and some ADAMs[248-251]. Additionally, activation of NFAT has been reported to mediate upregulation of MMP-2 and MMP-9 in cardiac myocytes[284].

At the post-translation level, the activation of metalloproteinases by PKCs or MAPKs downstream of GPCRs may be mediated via phosphorylation. PKCδ interacts with ADAM-9 and ADAM-12 and mediate PMA-induced HB-EGF shedding[229,285]. ADAM-17 is activated by ERK through phosphorylation at Thr735, which is required for its maturation and trafficking[254]. Meanwhile, the activation of ADAM-17 induced by PKC is inhibited by overexpressing PTP-H1, a protein tyrosine phosphatase that is able to interact with ADAM-17 through its PDZ domain, suggesting a role for tyrosine phosphorylation in ADAM activation[286]. Increased levels of ROS downstream of GPCRs can also lead to the activation of metalloproteinases. PMA-induced activation of ADAM-17 is reported to be mediated by ROS generation in monocytic cells[287]. In COS7 cells, ADAM-17 activation downstream of AT1R is reported to signal through Ca^{2+} and ROS[288].

1.3.2.2 Transactivation of membrane receptors by metalloproteinases and resulting downstream signaling

Membrane receptor transactivation by metalloproteinases is important in the regulation of the contraction and hypertrophic growth of VSMCs and cardiomyocytes. One of the first metalloproteinases identified to mediate hypertensive cardiac disease is ADAM-12, which was found to mediate GPCR agonist-induced cardiac hypertrophy by shedding HB-EGF and transactivating EGFR[229]. In later studies, ADAM-17 was also shown to mediate VSMC hypertrophy and hyperplasia growth[234]. Previous studies from our lab suggest that MMP-7 may transactivate the EGFR to maintain GPCR agonist-induced vasoconstriction of small arteries and promote hypertension and cardiac hypertrophy[56,289].

Activated MMPs and ADAMs, downstream of GPCR agonist stimulation, can shed several growth factors and cytokines from their latent proteins located on the plasma membrane (*e.g.*, HB-EGF, TNF-α)[229,290]. They can also release some growth factors and cytokines from the ECM as well as from their inhibitory binding proteins (*e.g.*, TGF-β, IGF)[84,291-293]. These cytokines and growth factors then bind to their respective receptors to trigger downstream pathways such as MEK-ERK and PI3K-Akt to mediate contraction and hypertrophy.

1.3.2.2.1 The EGF receptor family

ErbB family receptors, including the EGFR (ErbB-1), ErbB-3 and ErbB-4, are the most studied membrane receptors that are transactivated by GPCR agonists. These receptors are single transmembrane receptors which have intracellular protein tyrosine kinase (PTK) activity[294,295]. The significance of the ErbB family receptors in hypertrophy has been demonstrated by the induction of hypertrophic growth of cardiomyocytes in response to stimulation by their ligands *in vitro*[296,297]. EGFR ligands are also known to induce vasoconstriction *in vivo* and *ex vivo*[298,299]. In addition, inhibition of the EGFR blocks the development of Ang II-induced hypertension and cardiac hypertrophy[300]. The ligands of the ErbB family receptorsinclude EGF, TGF-α, HB-EGF, amphiregulin and epiregulin (all prefer binding to the EGFR) as well as neuregulins (prefer binding to ErbB3 and ErbB4). Most of these ligands can be shed by metalloproteinases.[229,280,285,290,301].

The binding of ligands to the extracellular ligand-binding domains of ErbB family receptors leads to their homo- or hetero-dimerization, triggering their intracellular PTK activity[302]. This results in the trans-phosphorylation of multiple tyrosines on the C-terminus, which is catalyzed by the PTK sub-domains in the receptor dimer. These phospho-tyrosine residues serve as the docking sites for the binding of effector proteins, such as proteins containing SH2 domains or phospho-tyrosine binding (PTB) domains.

Activation of the ErbB family receptors triggers signaling through the MEK-ERK pathway. In brief, adaptor proteins such as growth factor receptor-bound protein 2 (GRB-2) or Shc bind to the phospho-tyrosine residues of ErbB family receptors, via their SH2 and/or PTB domains[303,304]. The PTK activity of these receptors also phosphorylates the Shc docking protein, enabling it to bind to GRB-2 or other adaptor proteins. GRB-2 then recruits the Sos protein to the plasma membrane via the interaction between two SH3 domains on the N-terminus of GRB-2 and the proline-rich domain of Sos. Sos then serves as a GEF to activate Ras and downstream Raf-MEK-ERK signaling.

The activation of Ras downstream of ErbB receptors also leads to the activation of PI3K through the interaction between Ras and the regulatory subunit of PI3K. Moreover, the phospho-tyrosine residues of active ErbB family receptors can interact with the SH2 domain of the regulatory subunit of PI3K, recruiting PI3K to the plasma membrane[304]. This binding allows PI3K to interact with its substrate PI(4,5)P_2 in the plasma membrane and convert it into PI(3,4,5)P_3, which activates Akt and initiates downstream signaling through mTOR and GSK-3β, as described above.

The activation of ErbB family receptors can also trigger the activation of NADPH oxidase to induce the production of ROS[305,306]. ErbB-triggered NADPH oxidase activation may involve PI3K, which mediates the activation of the NADPH oxidase through Rac. The induction in ROS and downstream signaling, as well as the direct activation of the PI3K-mTOR pathway and the MEK-ERK pathway downstream of ErbB receptor transactivation, promote the contraction and hypertrophy of VSMCs and cardiomyocytes.

1.3.2.2.2 Other growth factor receptors

Apart from the EGFR, transactivation of the platelet-derived growth factor (PDGF) receptor and the IGF receptor by GPCR agonists has also been reported[307-309]. Their activation triggers downstream signaling through pathways including the MEK-ERK pathway and the PI3K pathway via their own PTK activity, or via their interaction with and activation of the EGFR family receptors[310,311]. IGF alone is able to induce hypertrophic growth in cultured cardiomyocytes[312,313]. Mice overexpressing PDGF develop significant cardiac hypertrophy[314], supporting the pro-hypertrophic role of these receptors and their ligands. Although direct evidence of the shedding of IGF and PDGF by metalloproteinases in the cardiovascular system is limited, metalloproteinases including MMP-3, MMP-9, ADAM-9 and ADAM-12 have been reported to cleave IGFBPs and release active IGF[291-293]. PDGF-C and PDGF-D, new members of PDGF family, are reported to be activated by protease cleavage extracellularly[315-317].

1.3.2.2.3 Cytokines and their receptors

GPCR agonist-induced activation of metalloproteinases could also lead to the release of cytokines such as TGF-β and TNF-α to mediate the development of hypertension and cardiovascular hypertrophy and fibrosis.

TGF-β, whose expression is promoted in response to GPCR agonists, has been primarily recognized for its role in the activation of Smad signaling and the development of fibrosis (as described above). Recent studies have also shown that TGF-β mediates the development of cardiac hypertrophy. It has been reported that treatment with TGF-β1 can induce hypertrophy in cultured cardiomyocytes and that transgenic mice overexpressing TGF-β1 develop significant cardiac hypertrophy[318,319]. In addition, TGF-β1 deficient mice are protected from cardiac hypertrophy induced by Ang II infusion[71].

Several metalloproteinases have been suggested to activate TGF-β. MMP-2, MMP-3 and MMP-7 can cleave the ECM proteoglycan decorin, which sequesters TGF-β in the extracellular milieu away from its cell surface receptors[99]. In cultured cells, MMP-2 and MMP-9 have been reported to cleave and release active TGF-β from its latent form[320,321].

The role of TGF-β in hypertrophic growth has been proposed to be mediated through TGF-β activated kinase-1 (TAK-1), a member of the MAPKKK family. The activation of TAK-1 is triggered by the direct interaction between TβRII and TAK-1, or via the activation of PKCs[318,322]. TAK-1 in turn phosphorylates MKK-3 and MKK-6, which then phosphorylate and activate p38 MAPK [323]. p38 activates the transcription factors activating transcription factor-2 (ATF-2) and ATF-6[324,325]. ATF-2 promotes transcription of β-MHC, which has negative inotropic effects, mediating the development of cardiac hypertrophy and subsequent heart failure[326,327].

TNF-α is another cytokine which is activated by metalloproteinase cleavage and mediates the development of hypertension and cardiovascular hypertrophy.Treatment with TNF-α induces hypertrophy in cultured adult cardiomyocytes[328]. Cardiac overexpression of TNF-α in mice triggers the development of cardiac hypertrophy while TNF-α knockout mice show attenuated Ang II-induced hypertension and cardiac hypertrophy[329,330]. The release of TNF-α by metalloproteinases is mainly mediated by ADAM-17 (TACE), as its name suggests[331]. Moreover, several other metalloproteinases, including MMP-7 and ADAM-10, can also cleave and release active TNF-α *in vivo* and *in vitro*[332-334]. The development of cardiac hypertrophy in response to TNF-α may be mediated through the activation of Akt and ROS since expression of dominant negative Akt or use of antioxidants prevents the TNF-α-induced hypertrophic response[170,335,336].

1.3.2.2.4 Cleavage and modulation of receptors

Receptor cleavage by metalloproteianses is a novel concept that vastly expands the mechanisms of MMP and ADAM action. In addition to shedding growth factors and cytokines, MMPs and ADAMs can cleave cell surface receptors including those of growth factors, cytokines and GPCR agonists implicated in cardiovascular function and disease. ADAM-10 can cleave ErbB-2 to promote its ligand-independent activation which has been shown to lead to proliferation of breast cancer cells[337]. In spontaneously hypertensive rats, an established animal model of human essential hypertension, increased metalloproteinase activity results in the cleavage and inactivation of vascular endothelial growth factor receptor-2 (VEGFR-2) (which in turn causes endothelial apoptosis and capillary rarefaction), β_2-adrenoceptor (which mediates vascular smooth muscle relaxation to reduce peripheral resistance), insulin receptor (which leads to the increase of blood glucose level and insulin resistance) and neutrophil formyl peptide receptor (which inhibits leukocyte pseudopod retraction and thus elevates microvascular resistance) contributing to the development of hypertension and cardiac remodeling[211,212,338,339].

In cardiovasculature, previous studies from our lab demonstrate that MMP-7 can transactivate EGFR to mediate GPCR-induced vasoconstriction[56]. MMP-2 has been shown to mediate cardiac dysfunction[217,219,220]. ADAM-12 and ADAM-17 can transactivate EGFR to mediate cardiac hypertrophy and VSMC hypertrophy respectively[229,234]. However, the exact significance of these metalloproteinases in the development of hypertension and cardiac remodeling is still unclear. A better understanding of their mechanisms in animal models of hypertensive cardiac disease is crucial for the successful translation of MMP-targeted therapeutics to human hypertension and cardiac remodeling.

1.4 HMGCR, the rate-limiting enzyme in cholesterol biosynthesis

Cholesterol is a 27-carbon tetracyclic molecule which is essential for eukaryotic cell membrane fluidity and permeability as well as membrane protein functions. It also has other roles including serving as precursors for steroids and hormones. Therefore, cholesterol homeostasis is critical for normal growth and development. Disorders of cholesterol metabolism can lead to the development of diseases. The accumulation of cholesterol, particularly low-density lipoprotein (LDL)-cholesterol, in circulation is known as hypercholesterolemia and increases the risk of atherosclerosis, coronary artery disease and stroke[340]. Defects in cholesterol synthesis are associated with developmental malformations[341,342]. ATP-binding cassette (ABC) transporters family proteins mediate the delivery of cholesterol and phospholipids to apolipoproteins. Defects in ABCA1 lead to the development of Tangier disease, which induces cholesterol ester accumulation in macrophages and is also associated with increased susceptibility to atherosclerosis.

Defects in ABCG5 and ABCG9 result in the development of sitosterolaemia (increased plasma levels of plant sterols such as sitosterol), which is associated with tendon and tuberous xanthomas as well as arthritis and atherosclerosis[343].

Mammalian cells obtain cholesterol either from blood stream (through receptor-mediated endocytosis of low-density lipoprotein (LDL)) or through *de novo* synthesis from acetyl-CoA. One of the most important enzymes of cholesterol synthesis is the rate limiting enzyme, 3-hydroxy-3-methyl-glutaryl-CoA (HMG-CoA) reductase (HMGCR), which irreversibly converts HMG-CoA into mevalonate.

1.4.1 Structure and Function

HMGCR is an ER protein with an N-terminal transmembrane domain (consisting of 8 transmembrane segments) and a C-terminal catalytic domain in the cytoplasm[344]. The catalytic domain forms a dimer to comprise the active enzyme and each monomer contributes catalytic residues to form the active site[345]. Statins, the widely-used competitive inhibitors of HMGCR, directly bind to HMGCR active site and compete with HMG-CoA to inhibit HMGCR activity[346].

In addition to its role in cholesterol synthesis, HMGCR is also involved in the regulation of signaling pathways. Isopentenyl pyrophosphate, an intermediate product of cholesterol synthesis pathway, is the precursor of farnesyl pyrophosphate (which can be further converted into cholesterol) and geranylgeranyl pyrophosphate, two isoprenoids[347]. Farnesyl pyrophosphate and geranylgeranyl pyrophosphate are used in protein prenylation and are covalently attached to C-terminus of target proteins, thus regulating target protein localization, trafficking and activation. The target proteins include small GTPases such as Rho, Ras and Rac, which are involved in cardiovascular remodeling[348].

Farnesyl pyrophosphate also serves as the precursor of dolichol phosphate, and coenzyme Q (ubiquinone). In the process N-glycosylation, dolichol pyrophosphate functions as a membrane anchor for the assembly of the oligosaccharide precursor, which is next transferred to the aspargine of target proteins such as EGFR[349]. Coenzyme Q is an integral component of the mitochondrial respiratory chain. It receives electrons from complex I (from NADH) and complex II (from succinate) and transfers the electron to complex III where the electron is transported to cytochrome C. Coenzyme Q is also present in low concentrations in plasma and in cell membranes where it, in its reduced form (known as ubiquinol), functions as an antioxidant. Ubiquinol donates a hydrogen atom to carbon- and oxygen-centered radicals generated during lipid peroxidation, thereby decreasing oxidative damage to lipids, proteins, and DNA. This forms an ubisemiquinone, the semi-reduced form of coenzyme Q, which dismutates to ubiquinol and ubiquinone[350]. Coenzyme Q deficiency results in defects in mitochondrial respiratory chain and increased superoxide production in mitochondria[351]. Deficiency of coenzyme Q has thus been related to the development of hypertension, cardiomyopathy and heart failure[352]. Although having no direct vasodilation or hypotensive effect, administration of coenzyme Q can improve endothelium function and attenuate the severity of hypertension, cardiac remodeling and cardiac failure[352-355]. Therefore, coenzyme Q has been suggested to be an adjunct to standard therapies in these cardiovascular diseases where oxidative stress is a factor[355].

1.4.2 Regulation of HMGCR

HMGCR is mainly regulated by sterol-mediated feedback inhibition at transcription level by the transcription factor sterol-regulatory element binding protein (SREBP)-2[356]. SREBP-2 is also an ER transmembrane protein and forms a hairpin orientation with both N- and C-termini in the cytosol. Its N-terminal domain is a transcription factor of the helix-loop-helix leucine zipper family. Its C-terminus binds to the N-terminus of another ER membrane protein SREBP-2 cleavage activating protein (Scap).

A delicate switch-like control of SREBP-2 transport triggered by small changes in ER cholesterol regulates intracellular cholesterol synthesis. When excessive cholesterol accumulates (the ER membrane cholesterol content is above 5 mol%), cholesterol binds with Scap to promote its interaction with another ER membrane protein, insulin-induced gene (Insig) and retain the SREBP-2 / Scap complex in the ER membrane. When cholesterol is depleted (ER cholesterol is lower than 5 mol%), the SREBP-2 / Scap complex is transferred to Golgi apparatus in COP II vesicles. Then, SREBP-2 is sequentially cleaved by site-1 protease (S1P, which cleaves the luminal loop) and site-2 protease (S2P, which cleaves the N-terminal domain) to release the N-terminal transcription factor[357]. This N-terminal transcription factor then translocates to the nucleus and binds to the sterol response element (SRE) sequences to activate transcription of HMGCR and other genes involved in cholesterol supply, promoting cholesterol uptake and synthesis[358].

One of the targets of SREBP-2 is LDL receptor (LDLR), the membrane receptor mediating endocytosis of cholesterol enriched LDL. LDLR is a single-time transmembrane protein with its N-terminal LDL-binding extracellular domain and C-terminal intracellular domain. Bound to LDL, LDLR is internalized by clathrin-mediated endocytosis and transferred to endosome. Then, the cholesterol ester in LDL is hydrolyzed to release free cholesterol and LDLR is recycled back to plasma membrane[359,360]. Thus, the activity of SREBP-2 upregulates the transcription HMGCR and LDLR, both of which contribute to the increase of intracellular cholesterol levels. An excess of cholesterol inhibits SREBP-2 activation, triggering an ‘end-product negative feedback’ that maintains cellular sterol hemostasis. In accordance with this negative feedback, SREBP-2 activity also transcriptionally upregulates the expression of Insig1, which hinders SREBP-2 activation and promotes HMGCR ubiquitination and degradation[358,361].

The SREBP-2 pathway is also regulated by a positive feedback in which SREBP-2 upregulates its own activation. Proprotein convertase subtilisin/kexin type 9 (PCSK-9) is a protease transcriptionally activated by SREBP-2. In addition to its serine protease activity, PCSK-9 binds to the extracellular domain of LDLR and triggers the internalization and lysosome degradation of LDLR. Thus, PCSK-9 decreases LDLR bio-availability and downregulates cholesterol uptake. The decrease of intracellular cholesterol in turn activates the SREBP-2 pathway to increase cholesterol synthesis and uptake[362] (**Figure 1-3**).

1.4.3. HMGCR in diseases

Excessive cholesterol in the circulation or hypercholesterolemia results in significant human morbidity and mortality. Statins, the competitive inhibitors of HMGCR, have been widely used to reduce cholesterol levels for the prevention and treatment cholesterol-related diseases, including hypercholesterolemia and subsequent development of unstable atherosclerotic plaques on the lumen of arteries. Plaque rupture is strongly linked to ischemic heart attacks and cerebral strokes.

The first statin (mevastatin) was initially isolated and identified as secondary metabolites of fungi[363]. All statins, either natural or synthetic, mimic the 3-hydroxy-3-methyglutarate moiety of HMG-CoA. Thus, statins bind to the active site of HMGCR, inhibiting its activity and cholesterol synthesis[346,364]. In addition, this inhibitory effect stimulates the activation of SREBP-2 pathway, promoting the expression of LDLR. Increased LDLR level in turn enhances the clearance of plasma cholesterol levels through the uptake of LDL, thus lowering the risk of atherosclerosis, ischemic heart attack and stroke [365].

Recent studies have suggested that, in addition to their role in cholesterol clearance, statins also have pleiotropic effects: The blockade of mevalonate synthesis inhibits isoprenoids production and subsequent activation of signaling pathways downstream of Ras, Rho and Rac [366]. Statins have been shown to increase vascular endothelial function in atherosclerosis by upregulating eNOS expression through the inhibition of Rho to increase eNOS mRNA stability[367-369] and can inhibit the proliferation of VSMC[369,370]. Statins also attenuate the hypertrophy of cardiomyocytes by inhibiting Rac and NADPH oxidase activation, in both cultured cardiomyocytes and in rats models with Ang II- or pressure overload-induced cardiac hypertrophy[371,372]. Statins also inhibit the proliferation and migration of cardiac fibroblasts, their transformation into myofibroblasts and their expression of ECM proteins, thus preventing the development of cardiac fibrosis[373-376]. In addition, statins can inhibit the secretion of MMP-1, -2, -3 and -9 in VSMC, suggesting a regulation of metalloproteinase by HMGCR[377,378].

In addition to its inhibition of HMGCR activity and mevalonate synthesis, statins have been shown to bind to an allosteric site of β2 integrin leukocyte function antigen-1. This interaction inhibits leukocyte function antigen-1-mediated adhesion and costimulation of lymphocyte, thus suppressing the inflammatory response in a mouse model of peritonitis[379].

1.5 Hypothesis

Excessive stimulation of GPCR agonists induces the development of hypertension and cardiac remodeling, which accompanies the differential upregulation of metalloproteinases including MMP-2, MMP-7, ADAM-12 and ADAM-17. Previous studies have suggested that these metalloproteinases are involved in the development of hypertensive cardiac disease.

I hypothesize:

Pathologically high levels of GPCR agonists trigger the development of hypertension and cardiac remodeling, in part, through the upregulation of 4 metalloproteinases: MMP-2, MMP-7, ADAM-12 and ADAM-17. Therefore, the inhibition of these metalloproteinases by pharmacological, RNA interference or genetic means should influence the progression, development and severity of hypertensive cardiac disease.

Table 1-1 Classification of adult blood pressure

Classification	Systolic blood pressure (mmHg)	Diastolic blood pressure (mmHg)
Normal	<120	and <80
Prehypertension	120-139	or 80-89
Stage 1 hypertension	140-159	or 90-99
Stage 2 hypertension	≥160	or ≥100

Modified from: Chobanian AV, *et al.*, The seventh report of the Joint National Committee on Prevention, Detection, Evaluation and Treatment of High Blood Pressure, 2003[1]

Table 1-2 Human MMPs

Name	Human gene locus	Knockout mice phenotype
MMP-1 (Collagenase-1)	11q22	Reduced body size; reduced neovascularization; decreased primary ductal invasion in the mammary gland; reduced lung saccular development.
MMP-2 (Gelatinase A, 72kDa gelatinase)	16q22	Altered structure of neuromuscular junctions; reduced purse stringing during wound healing; altered secondary branching morphogenesis in the mammary gland.
MMP-3 (Stromelysin-1)	11q22	Abnormalities of the immune system as well as minor structural abnormalities in the neuromuscular junction
MMP-7 (Matrilysin)	11q22	Innate immunity defects; decreased re-epithelialization after lung injury.
MMP-8 (Collagenase-2)	11q22	Increased skin tumours; resistance to tumour necrosis factor (TNF)-induced lethal hepatitis.
MMP-9 (Gelatinase B, 92kDa gelatinase)	20q13	Bone-development defects; defective neuronal remyelination after nerve injury; delayed healing of bone fractures; impaired vascular remodelling; impaired angiogenesis.
MMP-10 (Stromelysin-2)	11q22	Increased inflammation and increased mortality in response to infection or wounding.
MMP-11 (Stromelysin-3)	22q11	Delayed mammary tumorigenesis.
MMP-12 (Macrophage elatase)	11q22	Diminished recovery from spinal cord crush; increased angiogenesis due to decreased angiostatin.
MMP-13 (Collagenase-3)	11q22	Bone remodelling defects; reduced hepatic fibrosis; increased collagen accumulation in atherosclerotic plaques.
MMP-14 (MT1-MMP)	14q11	Skeletal remodelling defects; angiogenesis defects; inhibition of tooth eruption and root elongation; defects in lung and submandibular gland.
MMP-15 (MT2-MMP)	16q22	Fertile and viable with no overt phenotype.
MMP-16 (MT3-MMP)	8q22	Fertile and viable with reduced skeletal growth
MMP-17 (MT4-MMP)	12q24	Fertile and viable with subtle renal developmental defects
MMP-19	12q13	Obesity.
MMP-20 (Enamelysin)	11q22	Defects in tooth enamel.
MMP-21 (XMMP)	10q26	
MMP-23B (MMP-22)	1p36	
MMP-24 (MT5-MMP)	20q11	Abnormal response to sciatic nerve injury.
MMP-25 (MT6-MMP)	16p12	
MMP-26 (Matrilysin-1)	11p15	
MMP-27	11q22	
MMP-28 (Epilysin)	17q12	Increased inflammatory response.

Table 1-3 Human ADAMs

Name	Human gene locus	Proteolytic activty	Knockout mice phenotype
Decysin	8p21	+	
ADAM2 (Fertilin-β)	8p11	-	Viable, males have severely reduced fertility
ADAM-7	8p21	-	
ADAM-8 (MS2)	10q26	+	Fertile and viable with no overt phenotype.
ADAM-9 (Meltrin-γ)	8p11	+	Fertile and viable with no overt phenotype.
ADAM-10	15q21	+	Embryonic lethal at E9.5; multiple defects in several developing organs.
ADAM-11 (Kuzbanian)	17q21	-	Fertile and viable, impaired hippocampus-dependent spatial learning and cerebellum-dependent motor coordination
ADAM-12 (Meltrin-α)	10q26	+	partial postnatal lethality, decreased brown fat, and impaired formation of neck and interscapular muscles
ADAM-15 (Metargidin)	1q21	+	Fertile and viable with no overt phenotype; decreased neovascularization in proliferative retinopathy.
ADAM-17 (TACE)	2p25	+	Perinatally lethal; Multiple defects in several organs.
ADAM-18	8p11	-	Enhanced motor coordination
ADAM-19 (Meltrin-β)	5q33	+	Perinatally lethal; Multiple heart defects.
ADAM-20	14q24	+	
ADAM-21	14q24	+	Fertile and viable with no overt phenotype.
ADAM-22	7q21	-	Die before weaning, marked hypomyelination of the peripheral nerves
ADAM-23	2q33	-	Die at p14, delayed lung development
ADAM-28	8p21	+	
ADAM-29	4q34	-	
ADAM-30	1p11	-	
ADAM-32	8p11	+	
ADAM-33	20p13	+	Fertile and viable with no overt phenotype.

Figure 1-1 Major signal transduction pathways linking GPCR agonists to contractile processes.

AC: adenylyl cyclase.
CaM: calmodulin.
DAG: 1,2-diacylglycerol.
ERK: extracellular signal-regulated kinases.
GPCR: G protein-coupled receptor.
GRB-2: growth factor receptor-bound protein 2.
GSK-3β: glycogen synthase kinase-3β.
IP_3: inositol 1,4,5-triphosphate.
MEK: mitogen-activated protein kinase kinase.
MP: metalloproteinase.
PDK-1: phosphoinositide-dependent protein kinase 1.
PI3K: phosphatidylinositol 3-kinase.
PIP_2: phosphatidylinositol (4,5)-bisphosphate.
PIP_3: phosphatidylinositol (3,4,5)-bisphosphate.
PKA: cAMP-dependent protein kinase.
PKC: protein kinase C.
PKD: protein kinase D.
PLC-β: phopholipase C isoform β.
ROS: reactive oxygen species.
Sos: son of sevenless

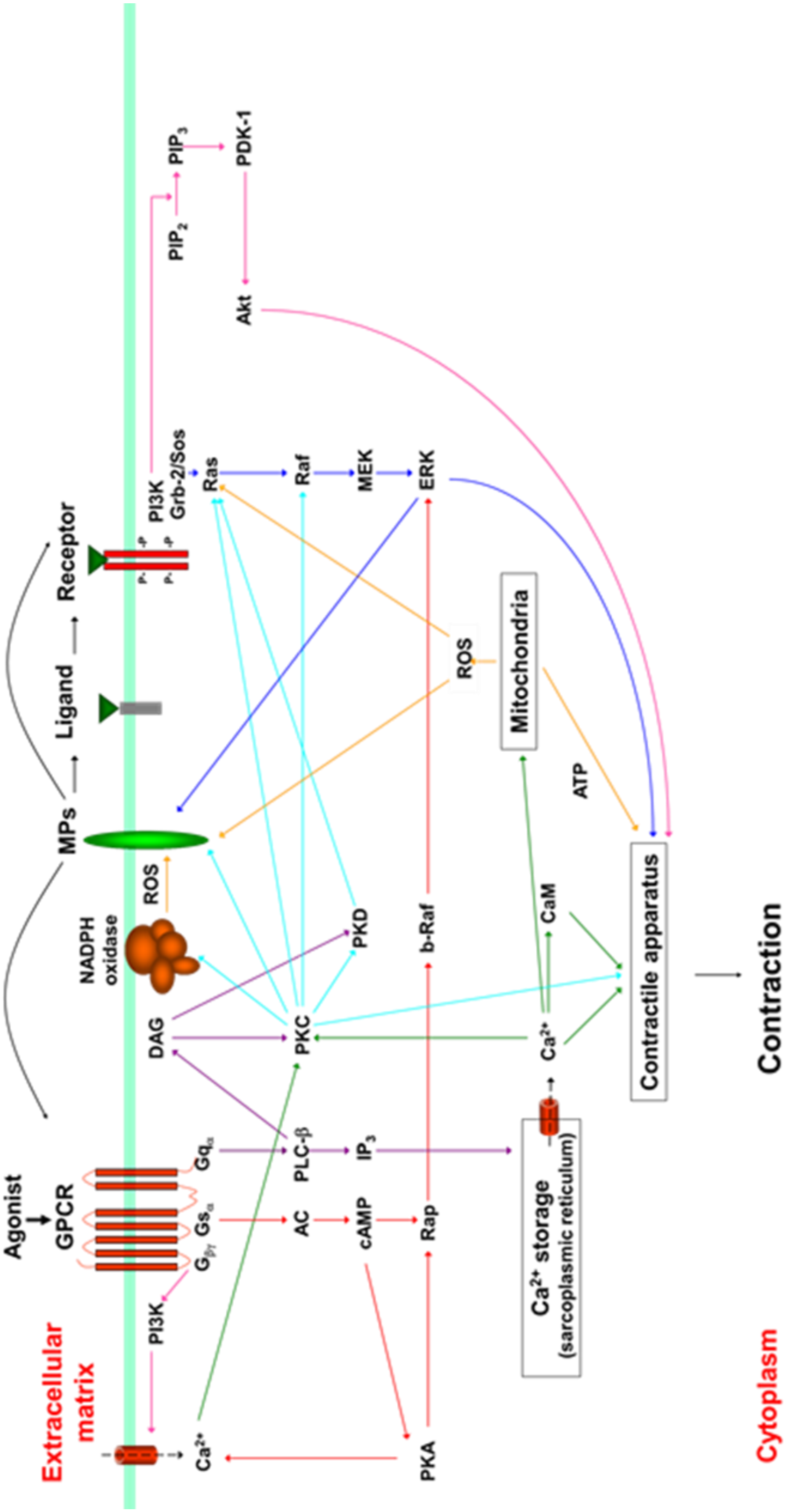
Extracellular matrix
Cytoplasm
Agonist
GPCR
$G_{\beta\gamma}$
Gs_{α}
Gq_{α}
PI3K
Ca^{2+}
AC
cAMP
PKA
PLC-β
IP_3
Rap
DAG
PKC
NADPH oxidase
ROS
MPs
PKD
b-Raf
Ca^{2+} storage
(sarcoplasmic reticulum)
Ca^{2+}
CaM
Contractile apparatus
Contraction
Ligand
Receptor
P-
-P
Mitochondria
ROS
ATP
PI3K
Grb-2/Sos
Ras
Raf
MEK
ERK
PIP_2
PIP_3
PDK-1
Akt

Figure 1-2 Major signal transduction pathways in GPCR agonist-induced hypertrophy and fibrosis.
4EBP-1: eIF4E binding protein-1.
AC: adenylyl cyclase.
AP-1: activator protein 1.
CaN: calcineurin.
CREB: cAMP response element binding protein.
DAG: 1,2-diacylglycerol.
eEF-2: eukaryotic translation elongation factor 2.
eEF2K: eEF2 kinase.
eIF4E: eukaryotic translation initiation factor 4E.
eIF2B: eukaryotic translation initiation factor 2B.
ERK: extracellular signal-regulated kinases.
GPCR: G protein-coupled receptor.
GRB-2: growth factor receptor-bound protein 2.
GSK-3β: glycogen synthase kinase-3β.
HDAC: histone deacetylase.
IP$_3$: inositol 1,4,5-triphosphate.
MEK: mitogen-activated protein kinase kinase.
MP: metalloproteinase.
mTOR: mammalian target of rapamycin.
NFAT: nuclear factor of activated T-cell.
PDK-1: phosphoinositide-dependent protein kinase 1.
PI3K: phosphatidylinositol 3-kinase.
PIP$_2$: phosphatidylinositol (4,5)-bisphosphate.
PIP$_3$: phosphatidylinositol (3,4,5)-bisphosphate.
PKA: cAMP-dependent protein kinase.
PKC: protein kinase C.
PKD: protein kinase D.
PLC-β: phopholipase C isoform β.
ROS: reactive oxygen species.
S6K: ribosomal protein S6 kinase.
Sos: son of sevenless
TSC-2: Tuberous sclerosis protein 2.

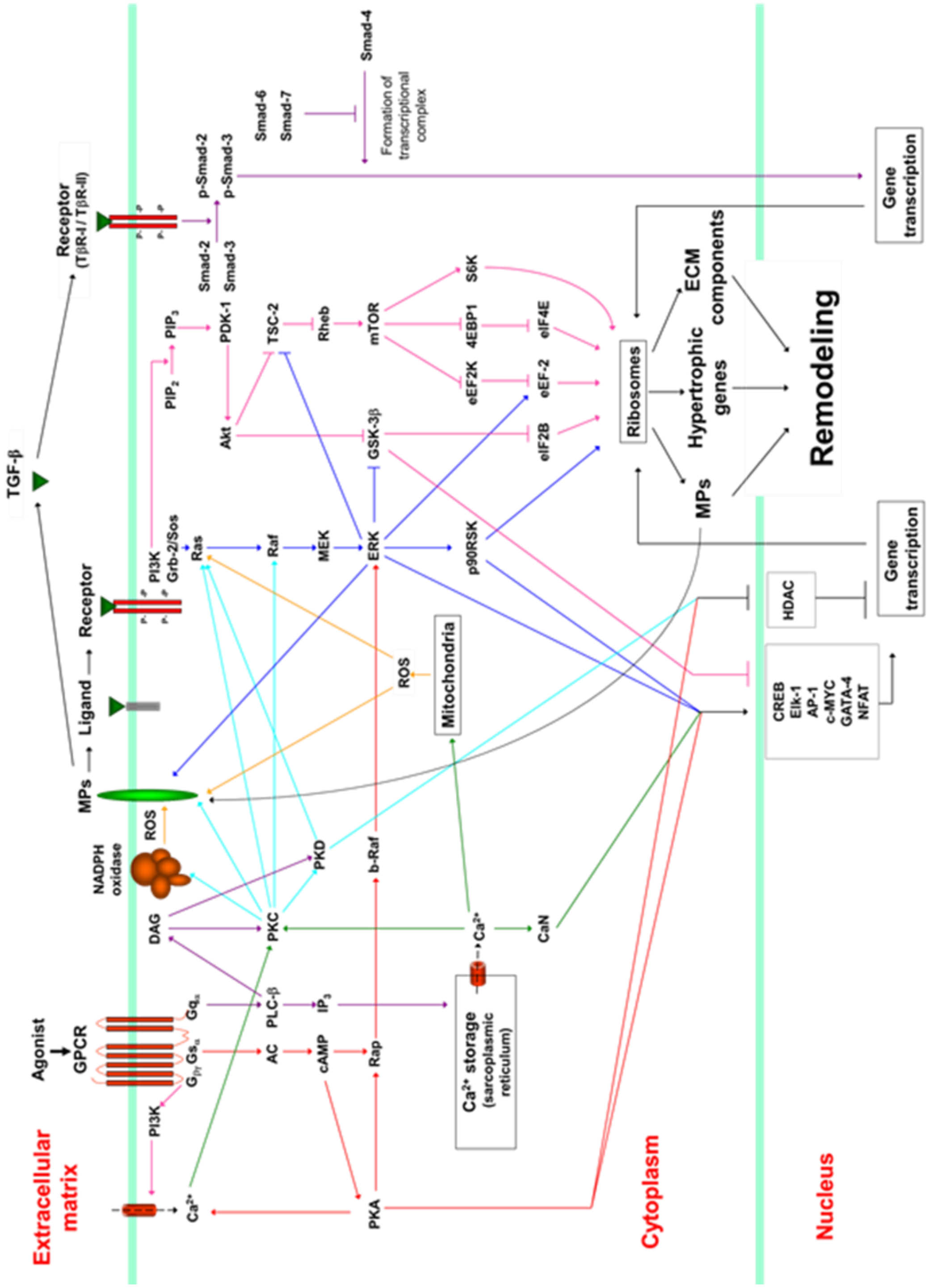
Extracellular matrix
Cytoplasm
Nucleus
Agonist
GPCR
Gq_{α}
Gs_{α}
$G_{\beta\gamma}$
PI3K
Ca^{2+}
AC
PLC-β
IP_3
cAMP
Rap
PKA
DAG
PKC
NADPH oxidase
ROS
MPs
Ligand
Receptor
TGF-β
Receptor (TβR-I / TβR-II)
PI3K
Grb-2/Sos
Ras
Raf
MEK
ERK
p90RSK
PKD
b-Raf
Ca^{2+} storage (sarcoplasmic reticulum)
Ca^{2+}
CaN
Mitochondria
ROS
PIP_2
PIP_3
PDK-1
Akt
TSC-2
Rheb
mTOR
S6K
4EBP1
eIF4E
eEF2K
eEF-2
GSK-3β
eIF2B
Smad-2
Smad-3
p-Smad-2
p-Smad-3
Smad-6
Smad-7
Smad-4
Formation of transcriptional complex
Gene transcription
Ribosomes
Hypertrophic genes
ECM components
MPs
Remodeling
HDAC
CREB
Elk-1
AP-1
c-MYC
GATA-4
NFAT
Gene transcription
Gene transcription

Figure 1-3 Regulation of the SREBP-2 / HMGCR pathway.

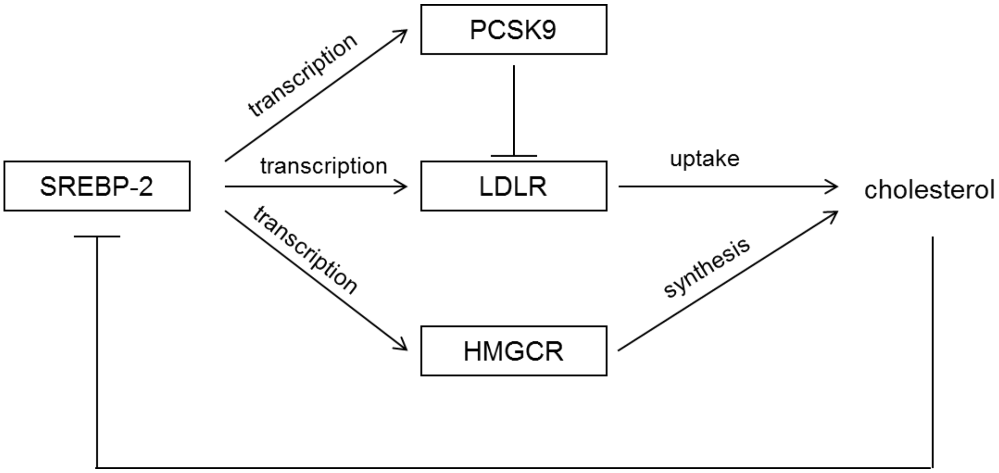
PCSK9
transcription
SREBP-2
transcription
LDLR
uptake
cholesterol
transcription
synthesis
HMGCR

1.6 References

1. Chobanian AV, Bakris GL, Black HR, Cushman WC, Green LA, Izzo JL, Jr., Jones DW, Materson BJ, Oparil S, Wright JT, Jr., Roccella EJ. Seventh report of the Joint National Committee on Prevention, Detection, Evaluation, and Treatment of High Blood Pressure. *Hypertension*. 2003;42:1206-1252
2. The World Health report 2002. *Midwifery*. 2003;19:72-73
3. WHO. *A global brief on Hypertension-Silent killer, global public health crisis*. WHO Press; 2013.
4. Renna NF, de Las Heras N, Miatello RM. Pathophysiology of vascular remodeling in hypertension. *Int J Hypertens*. 2013;2013:808353
5. Lewington S, Clarke R, Qizilbash N, Peto R, Collins R. Age-specific relevance of usual blood pressure to vascular mortality: a meta-analysis of individual data for one million adults in 61 prospective studies. *Lancet*. 2002;360:1903-1913
6. Wysocki M, Luo X, Schmeidler J, Dahlman K, Lesser GT, Grossman H, Haroutunian V, Beeri MS. Hypertension is associated with cognitive decline in elderly people at high risk for dementia. *Am J Geriatr Psychiatry*. 2012;20:179-187
7. Rosamond W, Flegal K, Friday G, Furie K, Go A, Greenlund K, Haase N, Ho M, Howard V, Kissela B, Kittner S, Lloyd-Jones D, McDermott M, Meigs J, Moy C, Nichol G, O'Donnell CJ, Roger V, Rumsfeld J, Sorlie P, Steinberger J, Thom T, Wasserthiel-Smoller S, Hong Y. Heart disease and stroke statistics--2007 update: a report from the American Heart Association Statistics Committee and Stroke Statistics Subcommittee. *Circulation*. 2007;115:e69-171
8. Flack JM. Epidemiology and unmet needs in hypertension. *J Manag Care Pharm*. 2007;13:2-8
9. HHS Secretary Sebelius statement on National High Blood Pressure Education Month. 2012;2013
10. Huetteman DA, Bogie H. Direct blood pressure monitoring in laboratory rodents via implantable radio telemetry. *Methods Mol Biol*. 2009;573:57-73
11. Van Vliet BN, Chafe LL, Antic V, Schnyder-Candrian S, Montani JP. Direct and indirect methods used to study arterial blood pressure. *J Pharmacol Toxicol Methods*. 2000;44:361-373
12. Mokdad AH, Ford ES, Bowman BA, Dietz WH, Vinicor F, Bales VS, Marks JS. Prevalence of obesity, diabetes, and obesity-related health risk factors, 2001. *Jama*. 2003;289:76-79
13. Kotchen TA. Obesity-Related Hypertension: Epidemiology, Pathophysiology, and Clinical Management. *Am J Hypertens*. 2010
14. Biaggioni I. Should we target the sympathetic nervous system in the

treatment of obesity-associated hypertension? *Hypertension*. 2008;51:168-171

15. Ruano M, Silvestre V, Castro R, Garcia-Lescun MC, Rodriguez A, Marco A, Garcia-Blanch G. Morbid obesity, hypertensive disease and the renin-angiotensin-aldosterone axis. *Obes Surg*. 2005;15:670-676
16. Reisin E. Nonpharmacologic approaches to hypertension. Weight, sodium, alcohol, exercise, and tobacco considerations. *Med Clin North Am*. 1997;81:1289-1303
17. Long AN, Dagogo-Jack S. Comorbidities of diabetes and hypertension: mechanisms and approach to target organ protection. *J Clin Hypertens (Greenwich)*. 2011;13:244-251
18. Ferdinand KC, Ferdinand DP. Race-based therapy for hypertension: possible benefits and potential pitfalls. *Expert Rev Cardiovasc Ther*. 2008;6:1357-1366
19. Muller P, Kazakov A, Jagoda P, Semenov A, Bohm M, Laufs U. ACE inhibition promotes upregulation of endothelial progenitor cells and neoangiogenesis in cardiac pressure overload. *Cardiovasc Res*. 2009;83:106-114
20. Rockman HA, Wachhorst SP, Mao L, Ross J, Jr. ANG II receptor blockade prevents ventricular hypertrophy and ANF gene expression with pressure overload in mice. *Am J Physiol*. 1994;266:H2468-2475
21. Zhong J, Basu R, Guo D, Chow FL, Byrns S, Schuster M, Loibner H, Wang XH, Penninger JM, Kassiri Z, Oudit GY. Angiotensin-converting enzyme 2 suppresses pathological hypertrophy, myocardial fibrosis, and cardiac dysfunction. *Circulation*. 2010;122:717-728, 718 p following 728
22. Kotsis V, Stabouli S, Papakatsika S, Rizos Z, Parati G. Mechanisms of obesity-induced hypertension. *Hypertens Res*. 2010;33:386-393
23. Cubeddu LX, Fuenmayor N, Caplan N, Ferry D. Clinical pharmacology of doxazosin in patients with essential hypertension. *Clin Pharmacol Ther*. 1987;41:439-449
24. Kamp O, Metra M, Bugatti S, Bettari L, Dei Cas A, Petrini N, Dei Cas L. Nebivolol: haemodynamic effects and clinical significance of combined beta-blockade and nitric oxide release. *Drugs*. 2010;70:41-56
25. Chakraborty S, Shukla D, Mishra B, Singh S. Clinical updates on carvedilol: a first choice beta-blocker in the treatment of cardiovascular diseases. *Expert Opin Drug Metab Toxicol*. 2010;6:237-250
26. Kjeldsen SE, Schmieder RE, Unger T, Mancia G. Telmisartan and hydrochlorothiazide combination therapy for the treatment of hypertension. *Curr Med Res Opin*. 2010;26:879-887
27. Maronde RF, Chan LS, Vlachakis N. Hypokalemia in thiazide-treated systemic hypertension. *Am J Cardiol*. 1986;58:18A-21A

28. Bourke E, Delaney V. Prevention of hypokalemia caused by diuretics. *Heart Dis Stroke*. 1994;3:63-67
29. Frey N, Olson EN. Cardiac hypertrophy: the good, the bad, and the ugly. *Annu Rev Physiol*. 2003;65:45-79
30. Krenning G, Zeisberg EM, Kalluri R. The origin of fibroblasts and mechanism of cardiac fibrosis. *J Cell Physiol*. 2010;225:631-637
31. Matsumoto E, Sasaki S, Kinoshita H, Kito T, Ohta H, Konishi M, Kuwahara K, Nakao K, Itoh N. Angiotensin II-induced cardiac hypertrophy and fibrosis are promoted in mice lacking Fgf16. *Genes Cells*. 2013;18:544-553
32. Levick SP, Murray DB, Janicki JS, Brower GL. Sympathetic nervous system modulation of inflammation and remodeling in the hypertensive heart. *Hypertension*. 2010;55:270-276
33. Morganroth J, Maron BJ. The athlete's heart syndrome: a new perspective. *Ann N Y Acad Sci*. 1977;301:931-941
34. Burlew BS, Weber KT. Cardiac Fibrosis as a Cause of Diastolic Dysfunction. *Herz*. 2002;27:92-98
35. Moreo A, Ambrosio G, De Chiara B, Pu M, Tran T, Mauri F, Raman SV. Influence of myocardial fibrosis on left ventricular diastolic function: noninvasive assessment by cardiac magnetic resonance and echo. *Circ Cardiovasc Imaging*. 2009;2:437-443
36. Zeisberg EM, Tarnavski O, Zeisberg M, Dorfman AL, McMullen JR, Gustafsson E, Chandraker A, Yuan X, Pu WT, Roberts AB, Neilson EG, Sayegh MH, Izumo S, Kalluri R. Endothelial-to-mesenchymal transition contributes to cardiac fibrosis. *Nat Med*. 2007;13:952-961
37. Gehrke J, Leeman S, Raphael M, Pridie RB. Non-invasive left ventricular volume determination by two-dimensional echocardiography. *Br Heart J*. 1975;37:911-916
38. Klues HG, Schiffers A, Maron BJ. Phenotypic spectrum and patterns of left ventricular hypertrophy in hypertrophic cardiomyopathy: morphologic observations and significance as assessed by two-dimensional echocardiography in 600 patients. *J Am Coll Cardiol*. 1995;26:1699-1708
39. Aubery M, Reynier M, Lopez M, Ogier-Denis E, Font J, Bardin F. WGA binding to the surface of two autologous human melanoma cell lines: different expression of sialyl and N-acetylglucosaminyl residues. *Cell Biol Int Rep*. 1990;14:275-286
40. Yamamoto K, Tsuji T, Matsumoto I, Osawa T. Structural requirements for the binding of oligosaccharides and glycopeptides to immobilized wheat germ agglutinin. *Biochemistry*. 1981;20:5894-5899
41. Yokota N, Bruneau BG, Fernandez BE, de Bold ML, Piazza LA, Eid H, de Bold AJ. Dissociation of cardiac hypertrophy, myosin heavy chain isoform

expression, and natriuretic peptide production in DOCA-salt rats. *Am J Hypertens*. 1995;8:301-310

42. Creemers EE, Pinto YM. Molecular mechanisms that control interstitial fibrosis in the pressure-overloaded heart. *Cardiovasc Res*. 2011;89:265-272
43. Dahlof B. Effect of angiotensin II blockade on cardiac hypertrophy and remodelling: a review. *J Hum Hypertens*. 1995;9 Suppl 5:S37-44
44. Heagerty AM. Functional and structural effects of ACE inhibitors on the cardiovascular system. *Cardiology*. 1991;79 Suppl 1:3-9
45. Intengan HD, Schiffrin EL. Vascular remodeling in hypertension: roles of apoptosis, inflammation, and fibrosis. *Hypertension*. 2001;38:581-587
46. Sorescu D. Smad3 mediates angiotensin II- and TGF-beta1-induced vascular fibrosis: Smad3 thickens the plot. *Circ Res*. 2006;98:988-989
47. Weber KT, Clark WA, Janicki JS, Shroff SG. Physiologic versus pathologic hypertrophy and the pressure-overloaded myocardium. *J Cardiovasc Pharmacol*. 1987;10 Suppl 6:S37-50
48. Frohlich ED. Left ventricular hypertrophy: dissociation of structural and functional effects by therapy. *Adv Exp Med Biol*. 1991;308:175-190
49. Berk BC, Fujiwara K, Lehoux S. ECM remodeling in hypertensive heart disease. *J Clin Invest*. 2007;117:568-575
50. Rizzoni D, Agabiti-Rosei E. Relationships of cardiac function and structure to blood pressure rhythms. *Ann N Y Acad Sci*. 1996;783:159-171
51. Zhang Y, Griendling KK, Dikalova A, Owens GK, Taylor WR. Vascular hypertrophy in angiotensin II-induced hypertension is mediated by vascular smooth muscle cell-derived H2O2. *Hypertension*. 2005;46:732-737
52. Schiffrin EL. Vascular stiffening and arterial compliance. Implications for systolic blood pressure. *Am J Hypertens*. 2004;17:39S-48S
53. Berk BC, Vekshtein V, Gordon HM, Tsuda T. Angiotensin II-stimulated protein synthesis in cultured vascular smooth muscle cells. *Hypertension*. 1989;13:305-314
54. Geisterfer AA, Peach MJ, Owens GK. Angiotensin II induces hypertrophy, not hyperplasia, of cultured rat aortic smooth muscle cells. *Circ Res*. 1988;62:749-756
55. Prenzel N, Zwick E, Daub H, Leserer M, Abraham R, Wallasch C, Ullrich A. EGF receptor transactivation by G-protein-coupled receptors requires metalloproteinase cleavage of proHB-EGF. *Nature*. 1999;402:884-888
56. Hao L, Du M, Lopez-Campistrous A, Fernandez-Patron C. Agonist-induced activation of matrix metalloproteinase-7 promotes vasoconstriction through the epidermal growth factor-receptor pathway. *Circ Res*. 2004;94:68-76
57. Paul M, Poyan Mehr A, Kreutz R. Physiology of local renin-angiotensin systems. *Physiol Rev*. 2006;86:747-803

58. Tewksbury DA, Dart RA, Travis J. The amino terminal amino acid sequence of human angiotensinogen. *Biochem Biophys Res Commun*. 1981;99:1311-1315
59. Siragy HM, Carey RM. Role of the intrarenal renin-angiotensin-aldosterone system in chronic kidney disease. *Am J Nephrol*. 2010;31:541-550
60. Lazartigues E, Feng Y, Lavoie JL. The two fACEs of the tissue renin-angiotensin systems: implication in cardiovascular diseases. *Curr Pharm Des*. 2007;13:1231-1245
61. Ryan US, Ryan JW. Angiotensin-converting enzyme: II. Pulmonary endothelial cells in culture. *Environ Health Perspect*. 1980;35:171-180
62. Freel EM, Connell JM. Mechanisms of hypertension: the expanding role of aldosterone. *J Am Soc Nephrol*. 2004;15:1993-2001
63. Smolen AJ. Morphology of synapses in the autonomic nervous system. *J Electron Microsc Tech*. 1988;10:187-204
64. Tsuru H, Tanimitsu N, Hirai T. Role of perivascular sympathetic nerves and regional differences in the features of sympathetic innervation of the vascular system. *Jpn J Pharmacol*. 2002;88:9-13
65. Currie G, Freel EM, Perry CG, Dominiczak AF. Disorders of blood pressure regulation-role of catecholamine biosynthesis, release, and metabolism. *Curr Hypertens Rep*. 2012;14:38-45
66. Julius S, Schork N, Schork A. Sympathetic hyperactivity in early stages of hypertension: the Ann Arbor data set. *J Cardiovasc Pharmacol*. 1988;12 Suppl 3:S121-129
67. Weber MA. The sympathetic nervous system and hypertension: mechanisms and treatment. *Clin Auton Res*. 1993;3:397-398
68. Masaki T. Historical review: Endothelin. *Trends Pharmacol Sci*. 2004;25:219-224
69. Bupha-Intr T, Haizlip KM, Janssen PM. Role of endothelin in the induction of cardiac hypertrophy in vitro. *PLoS One*. 2012;7:e43179
70. Akhter SA, Luttrell LM, Rockman HA, Iaccarino G, Lefkowitz RJ, Koch WJ. Targeting the receptor-Gq interface to inhibit in vivo pressure overload myocardial hypertrophy. *Science*. 1998;280:574-577
71. Schultz Jel J, Witt SA, Glascock BJ, Nieman ML, Reiser PJ, Nix SL, Kimball TR, Doetschman T. TGF-beta1 mediates the hypertrophic cardiomyocyte growth induced by angiotensin II. *J Clin Invest*. 2002;109:787-796
72. Lu Y, Yang S. Angiotensin II induces cardiomyocyte hypertrophy probably through histone deacetylases. *Tohoku J Exp Med*. 2009;219:17-23
73. Griffin SA, Brown WC, MacPherson F, McGrath JC, Wilson VG, Korsgaard N, Mulvany MJ, Lever AF. Angiotensin II causes vascular hypertrophy in part by a non-pressor mechanism. *Hypertension*.

1991;17:626-635
74. Schafer B, Marg B, Gschwind A, Ullrich A. Distinct ADAM metalloproteinases regulate G protein-coupled receptor-induced cell proliferation and survival. *J Biol Chem*. 2004;279:47929-47938
75. Fernandez-Patron C. Therapeutic potential of the epidermal growth factor receptor transactivation in hypertension: a convergent signaling pathway of vascular tone, oxidative stress, and hypertrophic growth downstream of vasoactive G-protein-coupled receptors? *Can J Physiol Pharmacol*. 2007;85:97-104
76. Rockman HA, Koch WJ, Lefkowitz RJ. Seven-transmembrane-spanning receptors and heart function. *Nature*. 2002;415:206-212
77. Cook B, Bar-Yaacov M, Cohen Ben-Ami H, Goldstein RE, Paroush Z, Selinger Z, Minke B. Phospholipase C and termination of G-protein-mediated signalling in vivo. *Nat Cell Biol*. 2000;2:296-301
78. Brock C, Schaefer M, Reusch HP, Czupalla C, Michalke M, Spicher K, Schultz G, Nurnberg B. Roles of G beta gamma in membrane recruitment and activation of p110 gamma/p101 phosphoinositide 3-kinase gamma. *J Cell Biol*. 2003;160:89-99
79. Crespo P, Xu N, Simonds WF, Gutkind JS. Ras-dependent activation of MAP kinase pathway mediated by G-protein beta gamma subunits. *Nature*. 1994;369:418-420
80. Inglese J, Koch WJ, Touhara K, Lefkowitz RJ. G beta gamma interactions with PH domains and Ras-MAPK signaling pathways. *Trends Biochem Sci*. 1995;20:151-156
81. Lorenz K, Schmitt JP, Schmitteckert EM, Lohse MJ. A new type of ERK1/2 autophosphorylation causes cardiac hypertrophy. *Nat Med*. 2009;15:75-83
82. Sun Y, Yamauchi J, Kaziro Y, Itoh H. Activation of c-fos promoter by Gbetagamma-mediated signaling: involvement of Rho and c-Jun N-terminal kinase. *J Biochem*. 1999;125:515-521
83. Kamm KE, Stull JT. Dedicated myosin light chain kinases with diverse cellular functions. *J Biol Chem*. 2001;276:4527-4530
84. Kordowska J, Huang R, Wang CL. Phosphorylation of caldesmon during smooth muscle contraction and cell migration or proliferation. *J Biomed Sci*. 2006;13:159-172
85. Gordon AM, Regnier M, Homsher E. Skeletal and cardiac muscle contractile activation: tropomyosin "rocks and rolls". *News Physiol Sci*. 2001;16:49-55
86. Kanaya N, Gable B, Murray PA, Damron DS. Propofol increases phosphorylation of troponin I and myosin light chain 2 via protein kinase C activation in cardiomyocytes. *Anesthesiology*. 2003;98:1363-1371
87. Monasky MM, Biesiadecki BJ, Janssen PM. Increased phosphorylation of

tropomyosin, troponin I, and myosin light chain-2 after stretch in rabbit ventricular myocardium under physiological conditions. *J Mol Cell Cardiol*. 2010;48:1023-1028

88. Magid NM, Borer JS, Young MS, Wallerson DC, DeMonteiro C. Suppression of protein degradation in progressive cardiac hypertrophy of chronic aortic regurgitation. *Circulation*. 1993;87:1249-1257
89. Lu J, McKinsey TA, Nicol RL, Olson EN. Signal-dependent activation of the MEF2 transcription factor by dissociation from histone deacetylases. *Proc Natl Acad Sci U S A*. 2000;97:4070-4075
90. Vega RB, Harrison BC, Meadows E, Roberts CR, Papst PJ, Olson EN, McKinsey TA. Protein kinases C and D mediate agonist-dependent cardiac hypertrophy through nuclear export of histone deacetylase 5. *Mol Cell Biol*. 2004;24:8374-8385
91. Tardiff JC, Hewett TE, Factor SM, Vikstrom KL, Robbins J, Leinwand LA. Expression of the beta (slow)-isoform of MHC in the adult mouse heart causes dominant-negative functional effects. *Am J Physiol Heart Circ Physiol*. 2000;278:H412-419
92. Hewett TE, Grupp IL, Grupp G, Robbins J. Alpha-skeletal actin is associated with increased contractility in the mouse heart. *Circ Res*. 1994;74:740-746
93. Krenz M, Sanbe A, Bouyer-Dalloz F, Gulick J, Klevitsky R, Hewett TE, Osinska HE, Lorenz JN, Brosseau C, Federico A, Alpert NR, Warshaw DM, Perryman MB, Helmke SM, Robbins J. Analysis of myosin heavy chain functionality in the heart. *J Biol Chem*. 2003;278:17466-17474
94. Proud CG. Ras, PI3-kinase and mTOR signaling in cardiac hypertrophy. *Cardiovasc Res*. 2004;63:403-413
95. Dorn GW, 2nd, Force T. Protein kinase cascades in the regulation of cardiac hypertrophy. *J Clin Invest*. 2005;115:527-537
96. Leask A. Potential therapeutic targets for cardiac fibrosis: TGFbeta, angiotensin, endothelin, CCN2, and PDGF, partners in fibroblast activation. *Circ Res*. 2010;106:1675-1680
97. Rosenkranz S. TGF-beta1 and angiotensin networking in cardiac remodeling. *Cardiovasc Res*. 2004;63:423-432
98. Fukuda N, Hu WY, Kubo A, Kishioka H, Satoh C, Soma M, Izumi Y, Kanmatsuse K. Angiotensin II upregulates transforming growth factor-beta type I receptor on rat vascular smooth muscle cells. *Am J Hypertens*. 2000;13:191-198
99. Imai K, Hiramatsu A, Fukushima D, Pierschbacher MD, Okada Y. Degradation of decorin by matrix metalloproteinases: identification of the cleavage sites, kinetic analyses and transforming growth factor-beta1 release. *Biochem J*. 1997;322 (Pt 3):809-814

100. Lonn P, Moren A, Raja E, Dahl M, Moustakas A. Regulating the stability of TGFbeta receptors and Smads. *Cell Res*. 2009;19:21-35

101. Rodriguez-Vita J, Sanchez-Lopez E, Esteban V, Ruperez M, Egido J, Ruiz-Ortega M. Angiotensin II activates the Smad pathway in vascular smooth muscle cells by a transforming growth factor-beta-independent mechanism. *Circulation*. 2005;111:2509-2517

102. Wang W, Huang XR, Canlas E, Oka K, Truong LD, Deng C, Bhowmick NA, Ju W, Bottinger EP, Lan HY. Essential role of Smad3 in angiotensin II-induced vascular fibrosis. *Circ Res*. 2006;98:1032-1039

103. Lee CH, Park D, Wu D, Rhee SG, Simon MI. Members of the Gq alpha subunit gene family activate phospholipase C beta isozymes. *J Biol Chem*. 1992;267:16044-16047

104. Boyer JL, Waldo GL, Harden TK. Beta gamma-subunit activation of G-protein-regulated phospholipase C. *J Biol Chem*. 1992;267:25451-25456

105. Camps M, Carozzi A, Schnabel P, Scheer A, Parker PJ, Gierschik P. Isozyme-selective stimulation of phospholipase C-beta 2 by G protein beta gamma-subunits. *Nature*. 1992;360:684-686

106. Fain JN. Regulation of phosphoinositide-specific phospholipase C. *Biochim Biophys Acta*. 1990;1053:81-88

107. Kelso EJ, McDermott BJ, Silke B, Spiers JP. Endothelin(A) receptor subtype mediates endothelin-induced contractility in left ventricular cardiomyocytes isolated from rabbit myocardium. *J Pharmacol Exp Ther*. 2000;294:1047-1052

108. Schelling JR, Nkemere N, Konieczkowski M, Martin KA, Dubyak GR. Angiotensin II activates the beta 1 isoform of phospholipase C in vascular smooth muscle cells. *Am J Physiol*. 1997;272:C1558-1566

109. Filtz TM, Grubb DR, McLeod-Dryden TJ, Luo J, Woodcock EA. Gq-initiated cardiomyocyte hypertrophy is mediated by phospholipase Cbeta1b. *Faseb J*. 2009;23:3564-3570

110. Viard P, Exner T, Maier U, Mironneau J, Nurnberg B, Macrez N. Gbetagamma dimers stimulate vascular L-type Ca2+ channels via phosphoinositide 3-kinase. *Faseb J*. 1999;13:685-694

111. Zucchi R, Ronca-Testoni S. The sarcoplasmic reticulum Ca2+ channel/ryanodine receptor: modulation by endogenous effectors, drugs and disease states. *Pharmacol Rev*. 1997;49:1-51

112. Wilkins BJ, Molkentin JD. Calcium-calcineurin signaling in the regulation of cardiac hypertrophy. *Biochem Biophys Res Commun*. 2004;322:1178-1191

113. Naruse K, King GL. Protein kinase C and myocardial biology and function. *Circ Res*. 2000;86:1104-1106

114. Rusanescu G, Gotoh T, Tian X, Feig LA. Regulation of Ras signaling

specificity by protein kinase C. *Mol Cell Biol*. 2001;21:2650-2658

115. Clerk A, Sugden PH. Signaling through the extracellular signal-regulated kinase 1/2 cascade in cardiac myocytes. *Biochem Cell Biol*. 2004;82:603-609
116. Clerk A, Bogoyevitch MA, Anderson MB, Sugden PH. Differential activation of protein kinase C isoforms by endothelin-1 and phenylephrine and subsequent stimulation of p42 and p44 mitogen-activated protein kinases in ventricular myocytes cultured from neonatal rat hearts. *J Biol Chem*. 1994;269:32848-32857
117. Pacold ME, Suire S, Perisic O, Lara-Gonzalez S, Davis CT, Walker EH, Hawkins PT, Stephens L, Eccleston JF, Williams RL. Crystal structure and functional analysis of Ras binding to its effector phosphoinositide 3-kinase gamma. *Cell*. 2000;103:931-943
118. Marais R, Light Y, Mason C, Paterson H, Olson MF, Marshall CJ. Requirement of Ras-GTP-Raf complexes for activation of Raf-1 by protein kinase C. *Science*. 1998;280:109-112
119. Nakashima H, Frank GD, Shirai H, Hinoki A, Higuchi S, Ohtsu H, Eguchi K, Sanjay A, Reyland ME, Dempsey PJ, Inagami T, Eguchi S. Novel role of protein kinase C-delta Tyr 311 phosphorylation in vascular smooth muscle cell hypertrophy by angiotensin II. *Hypertension*. 2008;51:232-238
120. Vijayan K, Szotek EL, Martin JL, Samarel AM. Protein kinase C-alpha-induced hypertrophy of neonatal rat ventricular myocytes. *Am J Physiol Heart Circ Physiol*. 2004;287:H2777-2789
121. Takeishi Y, Ping P, Bolli R, Kirkpatrick DL, Hoit BD, Walsh RA. Transgenic overexpression of constitutively active protein kinase C epsilon causes concentric cardiac hypertrophy. *Circ Res*. 2000;86:1218-1223
122. Wakasaki H, Koya D, Schoen FJ, Jirousek MR, Ways DK, Hoit BD, Walsh RA, King GL. Targeted overexpression of protein kinase C beta2 isoform in myocardium causes cardiomyopathy. *Proc Natl Acad Sci U S A*. 1997;94:9320-9325
123. Walsh MP, Horowitz A, Clement-Chomienne O, Andrea JE, Allen BG, Morgan KG. Protein kinase C mediation of Ca(2+)-independent contractions of vascular smooth muscle. *Biochem Cell Biol*. 1996;74:485-502
124. Walsh MP, Susnjar M, Deng J, Sutherland C, Kiss E, Wilson DP. Phosphorylation of the protein phosphatase type 1 inhibitor protein CPI-17 by protein kinase C. *Methods Mol Biol*. 2007;365:209-223
125. Rozengurt E. Protein kinase D signaling: multiple biological functions in health and disease. *Physiology (Bethesda)*. 2011;26:23-33
126. Xu X, Ha CH, Wong C, Wang W, Hausser A, Pfizenmaier K, Olson EN, McKinsey TA, Jin ZG. Angiotensin II stimulates protein kinase

D-dependent histone deacetylase 5 phosphorylation and nuclear export leading to vascular smooth muscle cell hypertrophy. *Arterioscler Thromb Vasc Biol*. 2007;27:2355-2362

127. Monovich L, Vega RB, Meredith E, Miranda K, Rao C, Capparelli M, Lemon DD, Phan D, Koch KA, Chapo JA, Hood DB, McKinsey TA. A novel kinase inhibitor establishes a predominant role for protein kinase D as a cardiac class IIa histone deacetylase kinase. *FEBS Lett*. 2010;584:631-637
128. Wang Y, Waldron RT, Dhaka A, Patel A, Riley MM, Rozengurt E, Colicelli J. The RAS effector RIN1 directly competes with RAF and is regulated by 14-3-3 proteins. *Mol Cell Biol*. 2002;22:916-926
129. Fielitz J, Kim MS, Shelton JM, Qi X, Hill JA, Richardson JA, Bassel-Duby R, Olson EN. Requirement of protein kinase D1 for pathological cardiac remodeling. *Proc Natl Acad Sci U S A*. 2008;105:3059-3063
130. Vuchak LA, Tsygankova OM, Prendergast GV, Meinkoth JL. Protein kinase A and B-Raf mediate extracellular signal-regulated kinase activation by thyrotropin. *Mol Pharmacol*. 2009;76:1123-1129
131. Bisognano JD, Weinberger HD, Bohlmeyer TJ, Pende A, Raynolds MV, Sastravaha A, Roden R, Asano K, Blaxall BC, Wu SC, Communal C, Singh K, Colucci W, Bristow MR, Port DJ. Myocardial-directed overexpression of the human beta(1)-adrenergic receptor in transgenic mice. *J Mol Cell Cardiol*. 2000;32:817-830
132. Antos CL, Frey N, Marx SO, Reiken S, Gaburjakova M, Richardson JA, Marks AR, Olson EN. Dilated cardiomyopathy and sudden death resulting from constitutive activation of protein kinase a. *Circ Res*. 2001;89:997-1004
133. Harrison JG, Sugden PH, Clerk A. Endothelin-1 promotes phosphorylation of CREB transcription factor in primary cultures of neonatal rat cardiac myocytes: implications for the regulation of c-jun expression. *Biochim Biophys Acta*. 2004;1644:17-25
134. Markou T, Hadzopoulou-Cladaras M, Lazou A. Phenylephrine induces activation of CREB in adult rat cardiac myocytes through MSK1 and PKA signaling pathways. *J Mol Cell Cardiol*. 2004;37:1001-1011
135. Ichiki T. Role of cAMP response element binding protein in cardiovascular remodeling: good, bad, or both? *Arterioscler Thromb Vasc Biol*. 2006;26:449-455
136. Metrich M, Lucas A, Gastineau M, Samuel JL, Heymes C, Morel E, Lezoualc'h F. Epac mediates beta-adrenergic receptor-induced cardiomyocyte hypertrophy. *Circ Res*. 2008;102:959-965
137. Morel E, Marcantoni A, Gastineau M, Birkedal R, Rochais F, Garnier A, Lompre AM, Vandecasteele G, Lezoualc'h F. cAMP-binding protein Epac induces cardiomyocyte hypertrophy. *Circ Res*. 2005;97:1296-1304

138. Bueno OF, De Windt LJ, Tymitz KM, Witt SA, Kimball TR, Klevitsky R, Hewett TE, Jones SP, Lefer DJ, Peng CF, Kitsis RN, Molkentin JD. The MEK1-ERK1/2 signaling pathway promotes compensated cardiac hypertrophy in transgenic mice. *Embo J*. 2000;19:6341-6350
139. Harris IS, Zhang S, Treskov I, Kovacs A, Weinheimer C, Muslin AJ. Raf-1 kinase is required for cardiac hypertrophy and cardiomyocyte survival in response to pressure overload. *Circulation*. 2004;110:718-723
140. Downward J, Graves JD, Warne PH, Rayter S, Cantrell DA. Stimulation of p21ras upon T-cell activation. *Nature*. 1990;346:719-723
141. Ueda Y, Hirai S, Osada S, Suzuki A, Mizuno K, Ohno S. Protein kinase C activates the MEK-ERK pathway in a manner independent of Ras and dependent on Raf. *J Biol Chem*. 1996;271:23512-23519
142. Garrington TP, Johnson GL. Organization and regulation of mitogen-activated protein kinase signaling pathways. *Curr Opin Cell Biol*. 1999;11:211-218
143. Babu GJ, Lalli MJ, Sussman MA, Sadoshima J, Periasamy M. Phosphorylation of elk-1 by MEK/ERK pathway is necessary for c-fos gene activation during cardiac myocyte hypertrophy. *J Mol Cell Cardiol*. 2000;32:1447-1457
144. Wang L, Proud CG. Ras/Erk signaling is essential for activation of protein synthesis by Gq protein-coupled receptor agonists in adult cardiomyocytes. *Circ Res*. 2002;91:821-829
145. Siddiqui RA, Shaikh SR, Kovacs R, Stillwell W, Zaloga G. Inhibition of phenylephrine-induced cardiac hypertrophy by docosahexaenoic acid. *J Cell Biochem*. 2004;92:1141-1159
146. Takeishi Y, Huang Q, Abe J, Glassman M, Che W, Lee JD, Kawakatsu H, Lawrence EG, Hoit BD, Berk BC, Walsh RA. Src and multiple MAP kinase activation in cardiac hypertrophy and congestive heart failure under chronic pressure-overload: comparison with acute mechanical stretch. *J Mol Cell Cardiol*. 2001;33:1637-1648
147. Whitman M, Downes CP, Keeler M, Keller T, Cantley L. Type I phosphatidylinositol kinase makes a novel inositol phospholipid, phosphatidylinositol-3-phosphate. *Nature*. 1988;332:644-646
148. Hemmings BA, Restuccia DF. PI3K-PKB/Akt pathway. *Cold Spring Harb Perspect Biol*. 2012;4:a011189
149. Condorelli G, Drusco A, Stassi G, Bellacosa A, Roncarati R, Iaccarino G, Russo MA, Gu Y, Dalton N, Chung C, Latronico MV, Napoli C, Sadoshima J, Croce CM, Ross J, Jr. Akt induces enhanced myocardial contractility and cell size in vivo in transgenic mice. *Proc Natl Acad Sci U S A*. 2002;99:12333-12338
150. Yano N, Tseng A, Zhao TC, Robbins J, Padbury JF, Tseng YT. Temporally

controlled overexpression of cardiac-specific PI3Kalpha induces enhanced myocardial contractility--a new transgenic model. *Am J Physiol Heart Circ Physiol*. 2008;295:H1690-1694

151. Shioi T, Kang PM, Douglas PS, Hampe J, Yballe CM, Lawitts J, Cantley LC, Izumo S. The conserved phosphoinositide 3-kinase pathway determines heart size in mice. *Embo J*. 2000;19:2537-2548
152. Hixon ML, Muro-Cacho C, Wagner MW, Obejero-Paz C, Millie E, Fujio Y, Kureishi Y, Hassold T, Walsh K, Gualberto A. Akt1/PKB upregulation leads to vascular smooth muscle cell hypertrophy and polyploidization. *J Clin Invest*. 2000;106:1011-1020
153. Shiojima I, Sato K, Izumiya Y, Schiekofer S, Ito M, Liao R, Colucci WS, Walsh K. Disruption of coordinated cardiac hypertrophy and angiogenesis contributes to the transition to heart failure. *J Clin Invest*. 2005;115:2108-2118
154. McMullen JR, Sherwood MC, Tarnavski O, Zhang L, Dorfman AL, Shioi T, Izumo S. Inhibition of mTOR signaling with rapamycin regresses established cardiac hypertrophy induced by pressure overload. *Circulation*. 2004;109:3050-3055
155. Inoki K, Li Y, Xu T, Guan KL. Rheb GTPase is a direct target of TSC2 GAP activity and regulates mTOR signaling. *Genes Dev*. 2003;17:1829-1834
156. Inoki K, Ouyang H, Li Y, Guan KL. Signaling by target of rapamycin proteins in cell growth control. *Microbiol Mol Biol Rev*. 2005;69:79-100
157. Hannan RD, Jenkins A, Jenkins AK, Brandenburger Y. Cardiac hypertrophy: a matter of translation. *Clin Exp Pharmacol Physiol*. 2003;30:517-527
158. Ma L, Chen Z, Erdjument-Bromage H, Tempst P, Pandolfi PP. Phosphorylation and functional inactivation of TSC2 by Erk implications for tuberous sclerosis and cancer pathogenesis. *Cell*. 2005;121:179-193
159. Kwon OY, Kwon IC, Song HK, Jeon H. Real-time imaging of NF-AT nucleocytoplasmic shuttling with a photoswitchable fluorescence protein in live cells. *Biochim Biophys Acta*. 2008;1780:1403-1407
160. Ding Q, Xia W, Liu JC, Yang JY, Lee DF, Xia J, Bartholomeusz G, Li Y, Pan Y, Li Z, Bargou RC, Qin J, Lai CC, Tsai FJ, Tsai CH, Hung MC. Erk associates with and primes GSK-3beta for its inactivation resulting in upregulation of beta-catenin. *Mol Cell*. 2005;19:159-170
161. Le Blanc C, Mironneau C, Barbot C, Henaff M, Bondeva T, Wetzker R, Macrez N. Regulation of vascular L-type Ca2+ channels by phosphatidylinositol 3,4,5-trisphosphate. *Circ Res*. 2004;95:300-307
162. Quignard JF, Mironneau J, Carricaburu V, Fournier B, Babich A, Nurnberg B, Mironneau C, Macrez N. Phosphoinositide 3-kinase gamma mediates

angiotensin II-induced stimulation of L-type calcium channels in vascular myocytes. *J Biol Chem*. 2001;276:32545-32551

163. Do KH, Kim MS, Kim JH, Rhim BY, Lee WS, Kim CD, Bae SS. Angiotensin II-induced aortic ring constriction is mediated by phosphatidylinositol 3-kinase/L-type calcium channel signaling pathway. *Exp Mol Med*. 2009;41:569-576
164. Giordano FJ. Oxygen, oxidative stress, hypoxia, and heart failure. *J Clin Invest*. 2005;115:500-508
165. Finkel T. Oxidant signals and oxidative stress. *Curr Opin Cell Biol*. 2003;15:247-254
166. Frank GD, Mifune M, Inagami T, Ohba M, Sasaki T, Higashiyama S, Dempsey PJ, Eguchi S. Distinct mechanisms of receptor and nonreceptor tyrosine kinase activation by reactive oxygen species in vascular smooth muscle cells: role of metalloprotease and protein kinase C-delta. *Mol Cell Biol*. 2003;23:1581-1589
167. Murdoch CE, Zhang M, Cave AC, Shah AM. NADPH oxidase-dependent redox signalling in cardiac hypertrophy, remodelling and failure. *Cardiovasc Res*. 2006;71:208-215
168. Yoshizumi M, Tsuchiya K, Suzaki Y, Kirima K, Kyaw M, Moon JH, Terao J, Tamaki T. Quercetin glucuronide prevents VSMC hypertrophy by angiotensin II via the inhibition of JNK and AP-1 signaling pathway. *Biochem Biophys Res Commun*. 2002;293:1458-1465
169. Garrido AM, Griendling KK. NADPH oxidases and angiotensin II receptor signaling. *Mol Cell Endocrinol*. 2009;302:148-158
170. Nakamura K, Fushimi K, Kouchi H, Mihara K, Miyazaki M, Ohe T, Namba M. Inhibitory effects of antioxidants on neonatal rat cardiac myocyte hypertrophy induced by tumor necrosis factor-alpha and angiotensin II. *Circulation*. 1998;98:794-799
171. Ide T, Tsutsui H, Hayashidani S, Kang D, Suematsu N, Nakamura K, Utsumi H, Hamasaki N, Takeshita A. Mitochondrial DNA damage and dysfunction associated with oxidative stress in failing hearts after myocardial infarction. *Circ Res*. 2001;88:529-535
172. Ide T, Tsutsui H, Kinugawa S, Suematsu N, Hayashidani S, Ichikawa K, Utsumi H, Machida Y, Egashira K, Takeshita A. Direct evidence for increased hydroxyl radicals originating from superoxide in the failing myocardium. *Circ Res*. 2000;86:152-157
173. Kimura S, Zhang GX, Nishiyama A, Shokoji T, Yao L, Fan YY, Rahman M, Abe Y. Mitochondria-derived reactive oxygen species and vascular MAP kinases: comparison of angiotensin II and diazoxide. *Hypertension*. 2005;45:438-444
174. Nabeebaccus A, Zhang M, Shah AM. NADPH oxidases and cardiac

remodelling. *Heart Fail Rev*. 2011;16:5-12

175. Castilho RF, Kowaltowski AJ, Meinicke AR, Bechara EJ, Vercesi AE. Permeabilization of the inner mitochondrial membrane by Ca2+ ions is stimulated by t-butyl hydroperoxide and mediated by reactive oxygen species generated by mitochondria. *Free Radic Biol Med*. 1995;18:479-486
176. Gadelha FR, Thomson L, Fagian MM, Costa AD, Radi R, Vercesi AE. Ca2+-independent permeabilization of the inner mitochondrial membrane by peroxynitrite is mediated by membrane protein thiol cross-linking and lipid peroxidation. *Arch Biochem Biophys*. 1997;345:243-250
177. Radi R, Beckman JS, Bush KM, Freeman BA. Peroxynitrite oxidation of sulfhydryls. The cytotoxic potential of superoxide and nitric oxide. *J Biol Chem*. 1991;266:4244-4250
178. Djordjevic T, Pogrebniak A, BelAiba RS, Bonello S, Wotzlaw C, Acker H, Hess J, Gorlach A. The expression of the NADPH oxidase subunit p22phox is regulated by a redox-sensitive pathway in endothelial cells. *Free Radic Biol Med*. 2005;38:616-630
179. Landmesser U, Dikalov S, Price SR, McCann L, Fukai T, Holland SM, Mitch WE, Harrison DG. Oxidation of tetrahydrobiopterin leads to uncoupling of endothelial cell nitric oxide synthase in hypertension. *J Clin Invest*. 2003;111:1201-1209
180. McNally JS, Saxena A, Cai H, Dikalov S, Harrison DG. Regulation of xanthine oxidoreductase protein expression by hydrogen peroxide and calcium. *Arterioscler Thromb Vasc Biol*. 2005;25:1623-1628
181. Zorov DB, Juhaszova M, Sollott SJ. Mitochondrial ROS-induced ROS release: an update and review. *Biochim Biophys Acta*. 2006;1757:509-517
182. Zafari AM, Ushio-Fukai M, Akers M, Yin Q, Shah A, Harrison DG, Taylor WR, Griendling KK. Role of NADH/NADPH oxidase-derived H2O2 in angiotensin II-induced vascular hypertrophy. *Hypertension*. 1998;32:488-495
183. Griendling KK, Minieri CA, Ollerenshaw JD, Alexander RW. Angiotensin II stimulates NADH and NADPH oxidase activity in cultured vascular smooth muscle cells. *Circ Res*. 1994;74:1141-1148
184. Hingtgen SD, Tian X, Yang J, Dunlay SM, Peek AS, Wu Y, Sharma RV, Engelhardt JF, Davisson RL. Nox2-containing NADPH oxidase and Akt activation play a key role in angiotensin II-induced cardiomyocyte hypertrophy. *Physiol Genomics*. 2006;26:180-191
185. Nakagami H, Takemoto M, Liao JK. NADPH oxidase-derived superoxide anion mediates angiotensin II-induced cardiac hypertrophy. *J Mol Cell Cardiol*. 2003;35:851-859
186. Reeves EP, Dekker LV, Forbes LV, Wientjes FB, Grogan A, Pappin DJ, Segal AW. Direct interaction between p47phox and protein kinase C:

evidence for targeting of protein kinase C by p47phox in neutrophils. *Biochem J*. 1999;344 Pt 3:859-866

187. Fontayne A, Dang PM, Gougerot-Pocidalo MA, El-Benna J. Phosphorylation of p47phox sites by PKC alpha, beta II, delta, and zeta: effect on binding to p22phox and on NADPH oxidase activation. *Biochemistry*. 2002;41:7743-7750
188. Inoguchi T, Li P, Umeda F, Yu HY, Kakimoto M, Imamura M, Aoki T, Etoh T, Hashimoto T, Naruse M, Sano H, Utsumi H, Nawata H. High glucose level and free fatty acid stimulate reactive oxygen species production through protein kinase C--dependent activation of NAD(P)H oxidase in cultured vascular cells. *Diabetes*. 2000;49:1939-1945
189. Hoyal CR, Gutierrez A, Young BM, Catz SD, Lin JH, Tsichlis PN, Babior BM. Modulation of p47PHOX activity by site-specific phosphorylation: Akt-dependent activation of the NADPH oxidase. *Proc Natl Acad Sci U S A*. 2003;100:5130-5135
190. Gregg D, Rauscher FM, Goldschmidt-Clermont PJ. Rac regulates cardiovascular superoxide through diverse molecular interactions: more than a binary GTP switch. *Am J Physiol Cell Physiol*. 2003;285:C723-734
191. Seshiah PN, Weber DS, Rocic P, Valppu L, Taniyama Y, Griendling KK. Angiotensin II stimulation of NAD(P)H oxidase activity: upstream mediators. *Circ Res*. 2002;91:406-413
192. Satoh M, Ogita H, Takeshita K, Mukai Y, Kwiatkowski DJ, Liao JK. Requirement of Rac1 in the development of cardiac hypertrophy. *Proc Natl Acad Sci U S A*. 2006;103:7432-7437
193. Welch HC, Coadwell WJ, Stephens LR, Hawkins PT. Phosphoinositide 3-kinase-dependent activation of Rac. *FEBS Lett*. 2003;546:93-97
194. Price MO, Atkinson SJ, Knaus UG, Dinauer MC. Rac activation induces NADPH oxidase activity in transgenic COSphox cells, and the level of superoxide production is exchange factor-dependent. *J Biol Chem*. 2002;277:19220-19228
195. Vecchione C, Patrucco E, Marino G, Barberis L, Poulet R, Aretini A, Maffei A, Gentile MT, Storto M, Azzolino O, Brancaccio M, Colussi GL, Bettarini U, Altruda F, Silengo L, Tarone G, Wymann MP, Hirsch E, Lembo G. Protection from angiotensin II-mediated vasculotoxic and hypertensive response in mice lacking PI3Kgamma. *J Exp Med*. 2005;201:1217-1228
196. Kwon SH, Pimentel DR, Remondino A, Sawyer DB, Colucci WS. H(2)O(2) regulates cardiac myocyte phenotype via concentration-dependent activation of distinct kinase pathways. *J Mol Cell Cardiol*. 2003;35:615-621
197. Blanc A, Pandey NR, Srivastava AK. Synchronous activation of ERK 1/2,

p38mapk and PKB/Akt signaling by H2O2 in vascular smooth muscle cells: potential involvement in vascular disease (review). *Int J Mol Med*. 2003;11:229-234

198. Pimentel DR, Adachi T, Ido Y, Heibeck T, Jiang B, Lee Y, Melendez JA, Cohen RA, Colucci WS. Strain-stimulated hypertrophy in cardiac myocytes is mediated by reactive oxygen species-dependent Ras S-glutathiolation. *J Mol Cell Cardiol*. 2006;41:613-622
199. Ushio-Fukai M, Alexander RW, Akers M, Yin Q, Fujio Y, Walsh K, Griendling KK. Reactive oxygen species mediate the activation of Akt/protein kinase B by angiotensin II in vascular smooth muscle cells. *J Biol Chem*. 1999;274:22699-22704
200. Kawakami M, Okabe E. Superoxide anion radical-triggered Ca2+ release from cardiac sarcoplasmic reticulum through ryanodine receptor Ca2+ channel. *Mol Pharmacol*. 1998;53:497-503
201. Zeng Q, Zhou Q, Yao F, O'Rourke ST, Sun C. Endothelin-1 regulates cardiac L-type calcium channels via NAD(P)H oxidase-derived superoxide. *J Pharmacol Exp Ther*. 2008;326:732-738
202. Amberg GC, Earley S, Glapa SA. Local regulation of arterial L-type calcium channels by reactive oxygen species. *Circ Res*. 2010;107:1002-1010
203. Li PF, Dietz R, von Harsdorf R. Superoxide induces apoptosis in cardiomyocytes, but proliferation and expression of transforming growth factor-beta1 in cardiac fibroblasts. *FEBS Lett*. 1999;448:206-210
204. Sorescu D, Griendling KK. Reactive oxygen species, mitochondria, and NAD(P)H oxidases in the development and progression of heart failure. *Congest Heart Fail*. 2002;8:132-140
205. Edwards DR, Handsley MM, Pennington CJ. The ADAM metalloproteinases. *Mol Aspects Med*. 2008;29:258-289
206. Castro MM, Tanus-Santos JE, Gerlach RF. Matrix metalloproteinases: targets for doxycycline to prevent the vascular alterations of hypertension. *Pharmacol Res*. 2011;64:567-572
207. Chow FL, Fernandez-Patron C. Many membrane proteins undergo ectodomain shedding by proteolytic cleavage. Does one sheddase do the job on all of these proteins? *IUBMB Life*. 2007;59:44-47
208. Higashiyama S, Nanba D. ADAM-mediated ectodomain shedding of HB-EGF in receptor cross-talk. *Biochim Biophys Acta*. 2005;1751:110-117
209. Hinkle CL, Sunnarborg SW, Loiselle D, Parker CE, Stevenson M, Russell WE, Lee DC. Selective roles for tumor necrosis factor alpha-converting enzyme/ADAM17 in the shedding of the epidermal growth factor receptor ligand family: the juxtamembrane stalk determines cleavage efficiency. *J Biol Chem*. 2004;279:24179-24188

210. Liao JK. Shedding growth factors in cardiac hypertrophy. *Nat Med*. 2002;8:20-21

211. DeLano FA, Schmid-Schonbein GW. Proteinase activity and receptor cleavage: mechanism for insulin resistance in the spontaneously hypertensive rat. *Hypertension*. 2008;52:415-423

212. Rodrigues SF, Tran ED, Fortes ZB, Schmid-Schonbein GW. Matrix metalloproteinases cleave the beta2-adrenergic receptor in spontaneously hypertensive rats. *Am J Physiol Heart Circ Physiol*. 2010;299:H25-35

213. Ali MA, Cho WJ, Hudson B, Kassiri Z, Granzier H, Schulz R. Titin is a target of matrix metalloproteinase-2: implications in myocardial ischemia/reperfusion injury. *Circulation*. 2010;122:2039-2047

214. Wang W, Schulze CJ, Suarez-Pinzon WL, Dyck JR, Sawicki G, Schulz R. Intracellular action of matrix metalloproteinase-2 accounts for acute myocardial ischemia and reperfusion injury. *Circulation*. 2002;106:1543-1549

215. Inoue K, Mikuni-Takagaki Y, Oikawa K, Itoh T, Inada M, Noguchi T, Park JS, Onodera T, Krane SM, Noda M, Itohara S. A crucial role for matrix metalloproteinase 2 in osteocytic canalicular formation and bone metabolism. *J Biol Chem*. 2006;281:33814-33824

216. Roomi MW, Monterrey JC, Kalinovsky T, Rath M, Niedzwiecki A. Patterns of MMP-2 and MMP-9 expression in human cancer cell lines. *Oncol Rep*. 2009;21:1323-1333

217. Cheung PY, Sawicki G, Wozniak M, Wang W, Radomski MW, Schulz R. Matrix metalloproteinase-2 contributes to ischemia-reperfusion injury in the heart. *Circulation*. 2000;101:1833-1839

218. Zile MR, Desantis SM, Baicu CF, Stroud RE, Thompson SB, McClure CD, Mehurg SM, Spinale FG. Plasma biomarkers that reflect determinants of matrix composition identify the presence of left ventricular hypertrophy and diastolic heart failure. *Circ Heart Fail*. 2011;4:246-256

219. Sawicki G, Leon H, Sawicka J, Sariahmetoglu M, Schulze CJ, Scott PG, Szczesna-Cordary D, Schulz R. Degradation of myosin light chain in isolated rat hearts subjected to ischemia-reperfusion injury: a new intracellular target for matrix metalloproteinase-2. *Circulation*. 2005;112:544-552

220. Gao CQ, Sawicki G, Suarez-Pinzon WL, Csont T, Wozniak M, Ferdinandy P, Schulz R. Matrix metalloproteinase-2 mediates cytokine-induced myocardial contractile dysfunction. *Cardiovasc Res*. 2003;57:426-433

221. Ayabe T, Satchell DP, Pesendorfer P, Tanabe H, Wilson CL, Hagen SJ, Ouellette AJ. Activation of Paneth cell alpha-defensins in mouse small intestine. *J Biol Chem*. 2002;277:5219-5228

222. Lee MY, Tse HF, Siu CW, Zhu SG, Man RY, Vanhoutte PM. Genomic

changes in regenerated porcine coronary arterial endothelial cells. *Arterioscler Thromb Vasc Biol*. 2007;27:2443-2449

223. Vanhoutte PM. MMP-7 and cardiovascular disease: not so surprising! *Basic Clin Pharmacol Toxicol*. 2013;112:2
224. Kurisaki T, Wakatsuki S, Sehara-Fujisawa A. Meltrin beta mini, a new ADAM19 isoform lacking metalloprotease and disintegrin domains, induces morphological changes in neuronal cells. *FEBS Lett*. 2002;532:419-422
225. Gilpin BJ, Loechel F, Mattei MG, Engvall E, Albrechtsen R, Wewer UM. A novel, secreted form of human ADAM 12 (meltrin alpha) provokes myogenesis in vivo. *J Biol Chem*. 1998;273:157-166
226. Mazzocca A, Coppari R, De Franco R, Cho JY, Libermann TA, Pinzani M, Toker A. A secreted form of ADAM9 promotes carcinoma invasion through tumor-stromal interactions. *Cancer Res*. 2005;65:4728-4738
227. Loechel F, Fox JW, Murphy G, Albrechtsen R, Wewer UM. ADAM 12-S cleaves IGFBP-3 and IGFBP-5 and is inhibited by TIMP-3. *Biochem Biophys Res Commun*. 2000;278:511-515
228. Peduto L, Reuter VE, Sehara-Fujisawa A, Shaffer DR, Scher HI, Blobel CP. ADAM12 is highly expressed in carcinoma-associated stroma and is required for mouse prostate tumor progression. *Oncogene*. 2006;25:5462-5466
229. Asakura M, Kitakaze M, Takashima S, Liao Y, Ishikura F, Yoshinaka T, Ohmoto H, Node K, Yoshino K, Ishiguro H, Asanuma H, Sanada S, Matsumura Y, Takeda H, Beppu S, Tada M, Hori M, Higashiyama S. Cardiac hypertrophy is inhibited by antagonism of ADAM12 processing of HB-EGF: metalloproteinase inhibitors as a new therapy. *Nat Med*. 2002;8:35-40
230. Atfi A, Dumont E, Colland F, Bonnier D, L'Helgoualc'h A, Prunier C, Ferrand N, Clement B, Wewer UM, Theret N. The disintegrin and metalloproteinase ADAM12 contributes to TGF-beta signaling through interaction with the type II receptor. *J Cell Biol*. 2007;178:201-208
231. Tellier E, Canault M, Rebsomen L, Bonardo B, Juhan-Vague I, Nalbone G, Peiretti F. The shedding activity of ADAM17 is sequestered in lipid rafts. *Exp Cell Res*. 2006;312:3969-3980
232. Black RA, Rauch CT, Kozlosky CJ, Peschon JJ, Slack JL, Wolfson MF, Castner BJ, Stocking KL, Reddy P, Srinivasan S, Nelson N, Boiani N, Schooley KA, Gerhart M, Davis R, Fitzner JN, Johnson RS, Paxton RJ, March CJ, Cerretti DP. A metalloproteinase disintegrin that releases tumour-necrosis factor-alpha from cells. *Nature*. 1997;385:729-733
233. Lautrette A, Li S, Alili R, Sunnarborg SW, Burtin M, Lee DC, Friedlander G, Terzi F. Angiotensin II and EGF receptor cross-talk in chronic kidney

diseases: a new therapeutic approach. *Nat Med*. 2005;11:867-874

234. Ohtsu H, Dempsey PJ, Frank GD, Brailoiu E, Higuchi S, Suzuki H, Nakashima H, Eguchi K, Eguchi S. ADAM17 mediates epidermal growth factor receptor transactivation and vascular smooth muscle cell hypertrophy induced by angiotensin II. *Arterioscler Thromb Vasc Biol*. 2006;26:e133-137
235. Takaguri A, Kimura K, Hinoki A, Bourne AM, Autieri MV, Eguchi S. A Disintegrin and Metalloprotease 17 Mediates Neointimal Hyperplasia in Vasculature. *Hypertension*. 2011;57:841-845
236. Asai M, Hattori C, Szabo B, Sasagawa N, Maruyama K, Tanuma S, Ishiura S. Putative function of ADAM9, ADAM10, and ADAM17 as APP alpha-secretase. *Biochem Biophys Res Commun*. 2003;301:231-235
237. Van Wart HE, Birkedal-Hansen H. The cysteine switch: a principle of regulation of metalloproteinase activity with potential applicability to the entire matrix metalloproteinase gene family. *Proc Natl Acad Sci U S A*. 1990;87:5578-5582
238. Hoyhtya M, Fridman R, Komarek D, Porter-Jordan K, Stetler-Stevenson WG, Liotta LA, Liang CM. Immunohistochemical localization of matrix metalloproteinase 2 and its specific inhibitor TIMP-2 in neoplastic tissues with monoclonal antibodies. *Int J Cancer*. 1994;56:500-505
239. Corcoran ML, Hewitt RE, Kleiner DE, Jr., Stetler-Stevenson WG. MMP-2: expression, activation and inhibition. *Enzyme Protein*. 1996;49:7-19
240. Sariahmetoglu M, Crawford BD, Leon H, Sawicka J, Li L, Ballermann BJ, Holmes C, Berthiaume LG, Holt A, Sawicki G, Schulz R. Regulation of matrix metalloproteinase-2 (MMP-2) activity by phosphorylation. *Faseb J*. 2007;21:2486-2495
241. Beklen A, Tuter G, Sorsa T, Hanemaaijer R, Virtanen I, Tervahartiala T, Konttinen YT. Gingival tissue and crevicular fluid co-operation in adult periodontitis. *J Dent Res*. 2006;85:59-63
242. Salo J, Mackiewicz Z, Indahl A, Konttinen YT, Holm AK, Sukura A, Holm S. Plasmin-matrix metalloproteinase cascades in spinal response to an experimental disc lesion in pig. *Spine (Phila Pa 1976)*. 2008;33:839-844
243. Atkinson SJ, Crabbe T, Cowell S, Ward RV, Butler MJ, Sato H, Seiki M, Reynolds JJ, Murphy G. Intermolecular autolytic cleavage can contribute to the activation of progelatinase A by cell membranes. *J Biol Chem*. 1995;270:30479-30485
244. English JL, Kassiri Z, Koskivirta I, Atkinson SJ, Di Grappa M, Soloway PD, Nagase H, Vuorio E, Murphy G, Khokha R. Individual Timp deficiencies differentially impact pro-MMP-2 activation. *J Biol Chem*. 2006;281:10337-10346
245. Weiss SJ, Peppin G, Ortiz X, Ragsdale C, Test ST. Oxidative autoactivation

of latent collagenase by human neutrophils. *Science*. 1985;227:747-749

246. Kim ES, Sohn YW, Moon A. TGF-beta-induced transcriptional activation of MMP-2 is mediated by activating transcription factor (ATF)2 in human breast epithelial cells. *Cancer Lett*. 2007;252:147-156
247. Bergman MR, Cheng S, Honbo N, Piacentini L, Karliner JS, Lovett DH. A functional activating protein 1 (AP-1) site regulates matrix metalloproteinase 2 (MMP-2) transcription by cardiac cells through interactions with JunB-Fra1 and JunB-FosB heterodimers. *Biochem J*. 2003;369:485-496
248. Benbow U, Brinckerhoff CE. The AP-1 site and MMP gene regulation: what is all the fuss about? *Matrix Biol*. 1997;15:519-526
249. Lin CW, Georgescu HI, Evans CH. The role of AP-1 in matrix metalloproteinase gene expression. *Agents Actions*. 1993;39 Spec No:C215-218
250. Moshal KS, Sen U, Tyagi N, Henderson B, Steed M, Ovechkin AV, Tyagi SC. Regulation of homocysteine-induced MMP-9 by ERK1/2 pathway. *Am J Physiol Cell Physiol*. 2006;290:C883-891
251. Taniguchi Y, Doronbekov K, Yamada T, Sasaki Y, Takano A, Sugimoto Y. Genomic organization and promoter analysis of the bovine ADAM12 gene. *Anim Biotechnol*. 2008;19:178-189
252. Jimenez E, Perez de la Blanca E, Urso L, Gonzalez I, Salas J, Montiel M. Angiotensin II induces MMP 2 activity via FAK/JNK pathway in human endothelial cells. *Biochem Biophys Res Commun*. 2009;380:769-774
253. Kim S, Han J, Lee SK, Choi MY, Kim J, Lee J, Jung SP, Kim JS, Kim JH, Choe JH, Lee JE, Nam SJ. Berberine suppresses the TPA-induced MMP-1 and MMP-9 expressions through the inhibition of PKC-alpha in breast cancer cells. *J Surg Res*. 2012;176:e21-29
254. Diaz-Rodriguez E, Montero JC, Esparis-Ogando A, Yuste L, Pandiella A. Extracellular signal-regulated kinase phosphorylates tumor necrosis factor alpha-converting enzyme at threonine 735: a potential role in regulated shedding. *Mol Biol Cell*. 2002;13:2031-2044
255. Mori S, Tanaka M, Nanba D, Nishiwaki E, Ishiguro H, Higashiyama S, Matsuura N. PACSIN3 binds ADAM12/meltrin alpha and up-regulates ectodomain shedding of heparin-binding epidermal growth factor-like growth factor. *J Biol Chem*. 2003;278:46029-46034
256. Tanaka M, Nanba D, Mori S, Shiba F, Ishiguro H, Yoshino K, Matsuura N, Higashiyama S. ADAM binding protein Eve-1 is required for ectodomain shedding of epidermal growth factor receptor ligands. *J Biol Chem*. 2004;279:41950-41959
257. Newby AC. Matrix metalloproteinase inhibition therapy for vascular diseases. *Vascul Pharmacol*. 2012;56:232-244

258. Hemmann S, Graf J, Roderfeld M, Roeb E. Expression of MMPs and TIMPs in liver fibrosis - a systematic review with special emphasis on anti-fibrotic strategies. *J Hepatol*. 2007;46:955-975

259. Murphy G, Nagase H. Reappraising metalloproteinases in rheumatoid arthritis and osteoarthritis: destruction or repair? *Nat Clin Pract Rheumatol*. 2008;4:128-135

260. Golub LM, Lee HM, Lehrer G, Nemiroff A, McNamara TF, Kaplan R, Ramamurthy NS. Minocycline reduces gingival collagenolytic activity during diabetes. Preliminary observations and a proposed new mechanism of action. *J Periodontal Res*. 1983;18:516-526

261. Maitra SR, Bhaduri S, Valane PD, Tervahartiala T, Sorsa T, Ramamurthy N. Inhibition of matrix metalloproteinases by chemically modified tetracyclines in sepsis. *Shock*. 2003;20:280-285

262. Steinberg J, Halter J, Schiller HJ, Dasilva M, Landas S, Gatto LA, Maisi P, Sorsa T, Rajamaki M, Lee HM, Nieman GF. Metalloproteinase inhibition reduces lung injury and improves survival after cecal ligation and puncture in rats. *J Surg Res*. 2003;111:185-195

263. Salo T, Soini Y, Oiva J, Kariylitalo, Nissinen A, Biancari F, Juvonen T, Satta J. Chemically modified tetracyclines (CMT-3 and CMT-8) enable control of the pathologic remodellation of human aortic valve stenosis via MMP-9 and VEGF inhibition. *Int J Cardiol*. 2006;111:358-364

264. Peterson JT. Matrix metalloproteinase inhibitor development and the remodeling of drug discovery. *Heart Fail Rev*. 2004;9:63-79

265. Sparano JA, Bernardo P, Stephenson P, Gradishar WJ, Ingle JN, Zucker S, Davidson NE. Randomized phase III trial of marimastat versus placebo in patients with metastatic breast cancer who have responding or stable disease after first-line chemotherapy: Eastern Cooperative Oncology Group trial E2196. *J Clin Oncol*. 2004;22:4683-4690

266. Guimaraes DA, Rizzi E, Ceron CS, Oliveira AM, Oliveira DM, Castro MM, Tirapelli CR, Gerlach RF, Tanus-Santos JE. Doxycycline dose-dependently Inhibits MMP-2-mediated vascular changes in 2K1C hypertension. *Basic Clin Pharmacol Toxicol*. 2011;108:318-325

267. Errami M, Galindo CL, Tassa AT, Dimaio JM, Hill JA, Garner HR. Doxycycline attenuates isoproterenol- and transverse aortic banding-induced cardiac hypertrophy in mice. *J Pharmacol Exp Ther*. 2008;324:1196-1203

268. Camp TM, Tyagi SC, Aru GM, Hayden MR, Mehta JL. Doxycycline ameliorates ischemic and border-zone remodeling and endothelial dysfunction after myocardial infarction in rats. *J Heart Lung Transplant*. 2004;23:729-736

269. Hudson MP, Armstrong PW, Ruzyllo W, Brum J, Cusmano L, Krzeski P,

Lyon R, Quinones M, Theroux P, Sydlowski D, Kim HE, Garcia MJ, Jaber WA, Weaver WD. Effects of selective matrix metalloproteinase inhibitor (PG-116800) to prevent ventricular remodeling after myocardial infarction: results of the PREMIER (Prevention of Myocardial Infarction Early Remodeling) trial. *J Am Coll Cardiol*. 2006;48:15-20

270. Brown DL, Desai KK, Vakili BA, Nouneh C, Lee HM, Golub LM. Clinical and biochemical results of the metalloproteinase inhibition with subantimicrobial doses of doxycycline to prevent acute coronary syndromes (MIDAS) pilot trial. *Arterioscler Thromb Vasc Biol*. 2004;24:733-738
271. Fingleton B. MMPs as therapeutic targets--still a viable option? *Semin Cell Dev Biol*. 2008;19:61-68
272. Sang QX, Jin Y, Newcomer RG, Monroe SC, Fang X, Hurst DR, Lee S, Cao Q, Schwartz MA. Matrix metalloproteinase inhibitors as prospective agents for the prevention and treatment of cardiovascular and neoplastic diseases. *Curr Top Med Chem*. 2006;6:289-316
273. Dorman G, Kocsis-Szommer K, Spadoni C, Ferdinandy P. MMP inhibitors in cardiac diseases: an update. *Recent Pat Cardiovasc Drug Discov*. 2007;2:186-194
274. Daub H, Weiss FU, Wallasch C, Ullrich A. Role of transactivation of the EGF receptor in signalling by G-protein-coupled receptors. *Nature*. 1996;379:557-560
275. Shah BH, Shah FB, Catt KJ. Role of metalloproteinase-dependent EGF receptor activation in alpha-adrenoceptor-stimulated MAP kinase phosphorylation in GT1-7 neurons. *J Neurochem*. 2006;96:520-532
276. Castro MM, Rizzi E, Figueiredo-Lopes L, Fernandes K, Bendhack LM, Pitol DL, Gerlach RF, Tanus-Santos JE. Metalloproteinase inhibition ameliorates hypertension and prevents vascular dysfunction and remodeling in renovascular hypertensive rats. *Atherosclerosis*. 2008;198:320-331
277. Herget J, Novotna J, Bibova J, Povysilova V, Vankova M, Hampl V. Metalloproteinase inhibition by Batimastat attenuates pulmonary hypertension in chronically hypoxic rats. *Am J Physiol Lung Cell Mol Physiol*. 2003;285:L199-208
278. Miura S, Ohno I, Suzuki J, Suzuki K, Okada S, Okuyama A, Nawata J, Ikeda J, Shirato K. Inhibition of matrix metalloproteinases prevents cardiac hypertrophy induced by beta-adrenergic stimulation in rats. *J Cardiovasc Pharmacol*. 2003;42:174-181
279. Sahin U, Weskamp G, Kelly K, Zhou HM, Higashiyama S, Peschon J, Hartmann D, Saftig P, Blobel CP. Distinct roles for ADAM10 and ADAM17 in ectodomain shedding of six EGFR ligands. *J Cell Biol*. 2004;164:769-779

280. Kurohara K, Komatsu K, Kurisaki T, Masuda A, Irie N, Asano M, Sudo K, Nabeshima Y, Iwakura Y, Sehara-Fujisawa A. Essential roles of Meltrin beta (ADAM19) in heart development. *Dev Biol*. 2004;267:14-28
281. Ancha HR, Kurella RR, Stewart CA, Damera G, Ceresa BP, Harty RF. Histamine stimulation of MMP-1(collagenase-1) secretion and gene expression in gastric epithelial cells: role of EGFR transactivation and the MAP kinase pathway. *Int J Biochem Cell Biol*. 2007;39:2143-2152
282. Coker ML, Jolly JR, Joffs C, Etoh T, Holder JR, Bond BR, Spinale FG. Matrix metalloproteinase expression and activity in isolated myocytes after neurohormonal stimulation. *Am J Physiol Heart Circ Physiol*. 2001;281:H543-551
283. Tsukioka K, Suzuki J, Fujimori M, Wada Y, Yamaura K, Ito K, Morishita R, Kaneda Y, Isobe M, Amano J. Expression of matrix metalloproteinases in cardiac allograft vasculopathy and its attenuation by anti MMP-2 ribozyme gene transfection. *Cardiovasc Res*. 2002;56:472-478
284. Saygili E, Rana OR, Meyer C, Gemein C, Andrzejewski MG, Ludwig A, Weber C, Schotten U, Kruttgen A, Weis J, Schwinger RH, Mischke K, Rassaf T, Kelm M, Schauerte P. The angiotensin-calcineurin-NFAT pathway mediates stretch-induced up-regulation of matrix metalloproteinases-2/-9 in atrial myocytes. *Basic Res Cardiol*. 2009;104:435-448
285. Izumi Y, Hirata M, Hasuwa H, Iwamoto R, Umata T, Miyado K, Tamai Y, Kurisaki T, Sehara-Fujisawa A, Ohno S, Mekada E. A metalloprotease-disintegrin, MDC9/meltrin-gamma/ADAM9 and PKCdelta are involved in TPA-induced ectodomain shedding of membrane-anchored heparin-binding EGF-like growth factor. *Embo J*. 1998;17:7260-7272
286. Zheng Y, Schlondorff J, Blobel CP. Evidence for regulation of the tumor necrosis factor alpha-convertase (TACE) by protein-tyrosine phosphatase PTPH1. *J Biol Chem*. 2002;277:42463-42470
287. Zhang Z, Oliver P, Lancaster JJ, Schwarzenberger PO, Joshi MS, Cork J, Kolls JK. Reactive oxygen species mediate tumor necrosis factor alpha-converting, enzyme-dependent ectodomain shedding induced by phorbol myristate acetate. *Faseb J*. 2001;15:303-305
288. Mifune M, Ohtsu H, Suzuki H, Nakashima H, Brailoiu E, Dun NJ, Frank GD, Inagami T, Higashiyama S, Thomas WG, Eckhart AD, Dempsey PJ, Eguchi S. G protein coupling and second messenger generation are indispensable for metalloprotease-dependent, heparin-binding epidermal growth factor shedding through angiotensin II type-1 receptor. *J Biol Chem*. 2005;280:26592-26599
289. Hao L, Nishimura T, Wo H, Fernandez-Patron C. Vascular responses to

alpha1-adrenergic receptors in small rat mesenteric arteries depend on mitochondrial reactive oxygen species. *Arterioscler Thromb Vasc Biol*. 2006;26:819-825

290. Zhan M, Jin B, Chen SE, Reecy JM, Li YP. TACE release of TNF-alpha mediates mechanotransduction-induced activation of p38 MAPK and myogenesis. *J Cell Sci*. 2007;120:692-701
291. Mohan S, Thompson GR, Amaar YG, Hathaway G, Tschesche H, Baylink DJ. ADAM-9 is an insulin-like growth factor binding protein-5 protease produced and secreted by human osteoblasts. *Biochemistry*. 2002;41:15394-15403
292. Shi Z, Xu W, Loechel F, Wewer UM, Murphy LJ. ADAM 12, a disintegrin metalloprotease, interacts with insulin-like growth factor-binding protein-3. *J Biol Chem*. 2000;275:18574-18580
293. Coppock HA, White A, Aplin JD, Westwood M. Matrix metalloprotease-3 and -9 proteolyze insulin-like growth factor-binding protein-1. *Biol Reprod*. 2004;71:438-443
294. Edwin F, Wiepz GJ, Singh R, Peet CR, Chaturvedi D, Bertics PJ, Patel TB. A historical perspective of the EGF receptor and related systems. *Methods Mol Biol*. 2006;327:1-24
295. Karunagaran D, Tzahar E, Beerli RR, Chen X, Graus-Porta D, Ratzkin BJ, Seger R, Hynes NE, Yarden Y. ErbB-2 is a common auxiliary subunit of NDF and EGF receptors: implications for breast cancer. *Embo J*. 1996;15:254-264
296. Clerk A, Aggeli IK, Stathopoulou K, Sugden PH. Peptide growth factors signal differentially through protein kinase C to extracellular signal-regulated kinases in neonatal cardiomyocytes. *Cell Signal*. 2006;18:225-235
297. Zhao YY, Sawyer DR, Baliga RR, Opel DJ, Han X, Marchionni MA, Kelly RA. Neuregulins promote survival and growth of cardiac myocytes. Persistence of ErbB2 and ErbB4 expression in neonatal and adult ventricular myocytes. *J Biol Chem*. 1998;273:10261-10269
298. Merkel LA, Rivera LM, Colussi DJ, Perrone MH. Inhibition of EGF-induced vasoconstriction in isolated rabbit aortic rings with the tyrosine kinase inhibitor RG50864. *Biochem Biophys Res Commun*. 1993;192:1319-1326
299. Florian JA, Watts SW. Epidermal growth factor: a potent vasoconstrictor in experimental hypertension. *Am J Physiol*. 1999;276:H976-983
300. Kagiyama S, Eguchi S, Frank GD, Inagami T, Zhang YC, Phillips MI. Angiotensin II-induced cardiac hypertrophy and hypertension are attenuated by epidermal growth factor receptor antisense. *Circulation*. 2002;106:909-912

301. Borrell-Pages M, Rojo F, Albanell J, Baselga J, Arribas J. TACE is required for the activation of the EGFR by TGF-alpha in tumors. *Embo J*. 2003;22:1114-1124

302. Jorissen RN, Walker F, Pouliot N, Garrett TP, Ward CW, Burgess AW. Epidermal growth factor receptor: mechanisms of activation and signalling. *Exp Cell Res*. 2003;284:31-53

303. Schlessinger J, Lemmon MA. SH2 and PTB domains in tyrosine kinase signaling. *Sci STKE*. 2003;2003:RE12

304. Olayioye MA, Neve RM, Lane HA, Hynes NE. The ErbB signaling network: receptor heterodimerization in development and cancer. *Embo J*. 2000;19:3159-3167

305. Touyz RM, Cruzado M, Tabet F, Yao G, Salomon S, Schiffrin EL. Redox-dependent MAP kinase signaling by Ang II in vascular smooth muscle cells: role of receptor tyrosine kinase transactivation. *Can J Physiol Pharmacol*. 2003;81:159-167

306. Bae YS, Kang SW, Seo MS, Baines IC, Tekle E, Chock PB, Rhee SG. Epidermal growth factor (EGF)-induced generation of hydrogen peroxide. Role in EGF receptor-mediated tyrosine phosphorylation. *J Biol Chem*. 1997;272:217-221

307. Rao GN, Delafontaine P, Runge MS. Thrombin stimulates phosphorylation of insulin-like growth factor-1 receptor, insulin receptor substrate-1, and phospholipase C-gamma 1 in rat aortic smooth muscle cells. *J Biol Chem*. 1995;270:27871-27875

308. Linseman DA, Benjamin CW, Jones DA. Convergence of angiotensin II and platelet-derived growth factor receptor signaling cascades in vascular smooth muscle cells. *J Biol Chem*. 1995;270:12563-12568

309. Kelly DJ, Cox AJ, Gow RM, Zhang Y, Kemp BE, Gilbert RE. Platelet-derived growth factor receptor transactivation mediates the trophic effects of angiotensin II in vivo. *Hypertension*. 2004;44:195-202

310. Roudabush FL, Pierce KL, Maudsley S, Khan KD, Luttrell LM. Transactivation of the EGF receptor mediates IGF-1-stimulated shc phosphorylation and ERK1/2 activation in COS-7 cells. *J Biol Chem*. 2000;275:22583-22589

311. Saito Y, Haendeler J, Hojo Y, Yamamoto K, Berk BC. Receptor heterodimerization: essential mechanism for platelet-derived growth factor-induced epidermal growth factor receptor transactivation. *Mol Cell Biol*. 2001;21:6387-6394

312. Wang KCW, Brooks DA, Botting KJ, Morrison JL. IGF-2R-Mediated Signaling Results in Hypertrophy of Cultured Cardiomyocytes from Fetal Sheep. *Biol Reprod*. 2012;86:183

313. Munoz JP, Collao A, Chiong M, Maldonado C, Adasme T, Carrasco L,

Ocaranza P, Bravo R, Gonzalez L, Diaz-Araya G, Hidalgo C, Lavandero S. The transcription factor MEF2C mediates cardiomyocyte hypertrophy induced by IGF-1 signaling. *Biochem Biophys Res Commun*. 2009;388:155-160

314. Ponten A, Li X, Thoren P, Aase K, Sjoblom T, Ostman A, Eriksson U. Transgenic overexpression of platelet-derived growth factor-C in the mouse heart induces cardiac fibrosis, hypertrophy, and dilated cardiomyopathy. *Am J Pathol*. 2003;163:673-682
315. Heeneman S, Haendeler J, Saito Y, Ishida M, Berk BC. Angiotensin II induces transactivation of two different populations of the platelet-derived growth factor beta receptor. Key role for the p66 adaptor protein Shc. *J Biol Chem*. 2000;275:15926-15932
316. LaRochelle WJ, Jeffers M, McDonald WF, Chillakuru RA, Giese NA, Lokker NA, Sullivan C, Boldog FL, Yang M, Vernet C, Burgess CE, Fernandes E, Deegler LL, Rittman B, Shimkets J, Shimkets RA, Rothberg JM, Lichenstein HS. PDGF-D, a new protease-activated growth factor. *Nat Cell Biol*. 2001;3:517-521
317. Li X, Ponten A, Aase K, Karlsson L, Abramsson A, Uutela M, Backstrom G, Hellstrom M, Bostrom H, Li H, Soriano P, Betsholtz C, Heldin CH, Alitalo K, Ostman A, Eriksson U. PDGF-C is a new protease-activated ligand for the PDGF alpha-receptor. *Nat Cell Biol*. 2000;2:302-309
318. Lim JY, Park SJ, Hwang HY, Park EJ, Nam JH, Kim J, Park SI. TGF-beta1 induces cardiac hypertrophic responses via PKC-dependent ATF-2 activation. *J Mol Cell Cardiol*. 2005;39:627-636
319. Rosenkranz S, Flesch M, Amann K, Haeuseler C, Kilter H, Seeland U, Schluter KD, Bohm M. Alterations of beta-adrenergic signaling and cardiac hypertrophy in transgenic mice overexpressing TGF-beta(1). *Am J Physiol Heart Circ Physiol*. 2002;283:H1253-1262
320. Ge G, Greenspan DS. BMP1 controls TGFbeta1 activation via cleavage of latent TGFbeta-binding protein. *J Cell Biol*. 2006;175:111-120
321. Yu Q, Stamenkovic I. Cell surface-localized matrix metalloproteinase-9 proteolytically activates TGF-beta and promotes tumor invasion and angiogenesis. *Genes Dev*. 2000;14:163-176
322. Watkins SJ, Jonker L, Arthur HM. A direct interaction between TGFbeta activated kinase 1 and the TGFbeta type II receptor: implications for TGFbeta signalling and cardiac hypertrophy. *Cardiovasc Res*. 2006;69:432-439
323. Moriguchi T, Kuroyanagi N, Yamaguchi K, Gotoh Y, Irie K, Kano T, Shirakabe K, Muro Y, Shibuya H, Matsumoto K, Nishida E, Hagiwara M. A novel kinase cascade mediated by mitogen-activated protein kinase kinase 6 and MKK3. *J Biol Chem*. 1996;271:13675-13679

324. Zhang D, Gaussin V, Taffet GE, Belaguli NS, Yamada M, Schwartz RJ, Michael LH, Overbeek PA, Schneider MD. TAK1 is activated in the myocardium after pressure overload and is sufficient to provoke heart failure in transgenic mice. *Nat Med*. 2000;6:556-563
325. Sano Y, Harada J, Tashiro S, Gotoh-Mandeville R, Maekawa T, Ishii S. ATF-2 is a common nuclear target of Smad and TAK1 pathways in transforming growth factor-beta signaling. *J Biol Chem*. 1999;274:8949-8957
326. Monzen K, Hiroi Y, Kudoh S, Akazawa H, Oka T, Takimoto E, Hayashi D, Hosoda T, Kawabata M, Miyazono K, Ishii S, Yazaki Y, Nagai R, Komuro I. Smads, TAK1, and their common target ATF-2 play a critical role in cardiomyocyte differentiation. *J Cell Biol*. 2001;153:687-698
327. Herron TJ, Vandenboom R, Fomicheva E, Mundada L, Edwards T, Metzger JM. Calcium-independent negative inotropy by beta-myosin heavy chain gene transfer in cardiac myocytes. *Circ Res*. 2007;100:1182-1190
328. Yokoyama T, Nakano M, Bednarczyk JL, McIntyre BW, Entman M, Mann DL. Tumor necrosis factor-alpha provokes a hypertrophic growth response in adult cardiac myocytes. *Circulation*. 1997;95:1247-1252
329. Dibbs ZI, Diwan A, Nemoto S, DeFreitas G, Abdellatif M, Carabello BA, Spinale FG, Feuerstein G, Sivasubramanian N, Mann DL. Targeted overexpression of transmembrane tumor necrosis factor provokes a concentric cardiac hypertrophic phenotype. *Circulation*. 2003;108:1002-1008
330. Sriramula S, Haque M, Majid DS, Francis J. Involvement of tumor necrosis factor-alpha in angiotensin II-mediated effects on salt appetite, hypertension, and cardiac hypertrophy. *Hypertension*. 2008;51:1345-1351
331. Zheng Y, Saftig P, Hartmann D, Blobel C. Evaluation of the contribution of different ADAMs to tumor necrosis factor alpha (TNFalpha) shedding and of the function of the TNFalpha ectodomain in ensuring selective stimulated shedding by the TNFalpha convertase (TACE/ADAM17). *J Biol Chem*. 2004;279:42898-42906
332. Haro H, Crawford HC, Fingleton B, Shinomiya K, Spengler DM, Matrisian LM. Matrix metalloproteinase-7-dependent release of tumor necrosis factor-alpha in a model of herniated disc resorption. *J Clin Invest*. 2000;105:143-150
333. Gearing AJ, Beckett P, Christodoulou M, Churchill M, Clements JM, Crimmin M, Davidson AH, Drummond AH, Galloway WA, Gilbert R, et al. Matrix metalloproteinases and processing of pro-TNF-alpha. *J Leukoc Biol*. 1995;57:774-777
334. Gearing AJ, Beckett P, Christodoulou M, Churchill M, Clements J, Davidson AH, Drummond AH, Galloway WA, Gilbert R, Gordon JL, et al.

Processing of tumour necrosis factor-alpha precursor by metalloproteinases. *Nature*. 1994;370:555-557

335. Condorelli G, Morisco C, Latronico MV, Claudio PP, Dent P, Tsichlis P, Frati G, Drusco A, Croce CM, Napoli C. TNF-alpha signal transduction in rat neonatal cardiac myocytes: definition of pathways generating from the TNF-alpha receptor. *Faseb J*. 2002;16:1732-1737
336. Hiraoka E, Kawashima S, Takahashi T, Rikitake Y, Kitamura T, Ogawa W, Yokoyama M. TNF-alpha induces protein synthesis through PI3-kinase-Akt/PKB pathway in cardiac myocytes. *Am J Physiol Heart Circ Physiol*. 2001;280:H1861-1868
337. Liu PC, Liu X, Li Y, Covington M, Wynn R, Huber R, Hillman M, Yang G, Ellis D, Marando C, Katiyar K, Bradley J, Abremski K, Stow M, Rupar M, Zhuo J, Li YL, Lin Q, Burns D, Xu M, Zhang C, Qian DQ, He C, Sharief V, Weng L, Agrios C, Shi E, Metcalf B, Newton R, Friedman S, Yao W, Scherle P, Hollis G, Burn TC. Identification of ADAM10 as a major source of HER2 ectodomain sheddase activity in HER2 overexpressing breast cancer cells. *Cancer Biol Ther*. 2006;5:657-664
338. Tran ED, DeLano FA, Schmid-Schonbein GW. Enhanced matrix metalloproteinase activity in the spontaneously hypertensive rat: VEGFR-2 cleavage, endothelial apoptosis, and capillary rarefaction. *J Vasc Res*. 2010;47:423-431
339. Chen AY, DeLano FA, Valdez SR, Ha JN, Shin HY, Schmid-Schonbein GW. Receptor cleavage reduces the fluid shear response in neutrophils of the spontaneously hypertensive rat. *Am J Physiol Cell Physiol*. 2010;299:C1441-1449
340. Toutouzas K, Drakopoulou M, Skoumas I, Stefanadis C. Advancing therapy for hypercholesterolemia. *Expert Opin Pharmacother*. 2010;11:1659-1672
341. Herman GE, Kratz L. Disorders of sterol synthesis: beyond Smith-Lemli-Opitz syndrome. *Am J Med Genet C Semin Med Genet*. 2012;160C:301-321
342. Porter FD, Herman GE. Malformation syndromes caused by disorders of cholesterol synthesis. *J Lipid Res*. 2011;52:6-34
343. Maxfield FR, Tabas I. Role of cholesterol and lipid organization in disease. *Nature*. 2005;438:612-621
344. Bochar DA, Stauffacher CV, Rodwell VW. Sequence comparisons reveal two classes of 3-hydroxy-3-methylglutaryl coenzyme A reductase. *Mol Genet Metab*. 1999;66:122-127
345. Istvan ES, Palnitkar M, Buchanan SK, Deisenhofer J. Crystal structure of the catalytic portion of human HMG-CoA reductase: insights into regulation of activity and catalysis. *Embo J*. 2000;19:819-830

346. Endo A, Kuroda M, Tanzawa K. Competitive inhibition of 3-hydroxy-3-methylglutaryl coenzyme A reductase by ML-236A and ML-236B fungal metabolites, having hypocholesterolemic activity. 1976. *Atheroscler Suppl*. 2004;5:39-42
347. Goldstein JL, Brown MS. Regulation of the mevalonate pathway. *Nature*. 1990;343:425-430
348. Van Aelst L, D'Souza-Schorey C. Rho GTPases and signaling networks. *Genes Dev*. 1997;11:2295-2322
349. Welti M. Regulation of dolichol-linked glycosylation. *Glycoconj J*. 2013;30:51-56
350. Maroz A, Anderson RF, Smith RA, Murphy MP. Reactivity of ubiquinone and ubiquinol with superoxide and the hydroperoxyl radical: implications for in vivo antioxidant activity. *Free Radic Biol Med*. 2009;46:105-109
351. Quinzii CM, Hirano M. Coenzyme Q and mitochondrial disease. *Dev Disabil Res Rev*. 2010;16:183-188
352. Rosenfeldt FL, Haas SJ, Krum H, Hadj A, Ng K, Leong JY, Watts GF. Coenzyme Q10 in the treatment of hypertension: a meta-analysis of the clinical trials. *J Hum Hypertens*. 2007;21:297-306
353. Huynh K, Kiriazis H, Du XJ, Love JE, Jandeleit-Dahm KA, Forbes JM, McMullen JR, Ritchie RH. Coenzyme Q10 attenuates diastolic dysfunction, cardiomyocyte hypertrophy and cardiac fibrosis in the db/db mouse model of type 2 diabetes. *Diabetologia*. 2012;55:1544-1553
354. Graham D, Huynh NN, Hamilton CA, Beattie E, Smith RA, Cocheme HM, Murphy MP, Dominiczak AF. Mitochondria-targeted antioxidant MitoQ10 improves endothelial function and attenuates cardiac hypertrophy. *Hypertension*. 2009;54:322-328
355. Pepe S, Marasco SF, Haas SJ, Sheeran FL, Krum H, Rosenfeldt FL. Coenzyme Q10 in cardiovascular disease. *Mitochondrion*. 2007;7 Suppl:S154-167
356. Goldstein JL, DeBose-Boyd RA, Brown MS. Protein sensors for membrane sterols. *Cell*. 2006;124:35-46
357. Radhakrishnan A, Goldstein JL, McDonald JG, Brown MS. Switch-like control of SREBP-2 transport triggered by small changes in ER cholesterol: a delicate balance. *Cell Metab*. 2008;8:512-521
358. Espenshade PJ, Hughes AL. Regulation of sterol synthesis in eukaryotes. *Annu Rev Genet*. 2007;41:401-427
359. Brown MS, Goldstein JL. A receptor-mediated pathway for cholesterol homeostasis. *Science*. 1986;232:34-47
360. Goldstein JL, Brown MS. The LDL receptor. *Arterioscler Thromb Vasc Biol*. 2009;29:431-438
361. DeBose-Boyd RA. Feedback regulation of cholesterol synthesis:

sterol-accelerated ubiquitination and degradation of HMG CoA reductase. *Cell Res*. 2008;18:609-621

362. Horton JD, Cohen JC, Hobbs HH. Molecular biology of PCSK9: its role in LDL metabolism. *Trends Biochem Sci*. 2007;32:71-77
363. Endo A, Kuroda M, Tsujita Y. ML-236A, ML-236B, and ML-236C, new inhibitors of cholesterogenesis produced by Penicillium citrinium. *J Antibiot (Tokyo)*. 1976;29:1346-1348
364. Istvan ES. Structural mechanism for statin inhibition of 3-hydroxy-3-methylglutaryl coenzyme A reductase. *Am Heart J*. 2002;144:S27-32
365. Pedersen TR, Kjekshus J, Berg K, Haghfelt T, Faergeman O, Faergeman G, Pyorala K, Miettinen T, Wilhelmsen L, Olsson AG, Wedel H. Randomised trial of cholesterol lowering in 4444 patients with coronary heart disease: the Scandinavian Simvastatin Survival Study (4S). 1994. *Atheroscler Suppl*. 2004;5:81-87
366. Zhou Q, Liao JK. Statins and cardiovascular diseases: from cholesterol lowering to pleiotropy. *Curr Pharm Des*. 2009;15:467-478
367. O'Driscoll G, Green D, Taylor RR. Simvastatin, an HMG-coenzyme A reductase inhibitor, improves endothelial function within 1 month. *Circulation*. 1997;95:1126-1131
368. Laufs U, Fata VL, Liao JK. Inhibition of 3-hydroxy-3-methylglutaryl (HMG)-CoA reductase blocks hypoxia-mediated down-regulation of endothelial nitric oxide synthase. *J Biol Chem*. 1997;272:31725-31729
369. Yang Z, Kozai T, van de Loo B, Viswambharan H, Lachat M, Turina MI, Malinski T, Lüscher TF. HMG-CoA reductase inhibition improves endothelial cell function and inhibits smooth muscle cell proliferation in human saphenous veins. *J Am Coll Cardiol*. 2000;36:1691-1697
370. Chandrasekar B, Mummidi S, Mahimainathan L, Patel DN, Bailey SR, Imam SZ, Greene WC, Valente AJ. Interleukin-18-induced human coronary artery smooth muscle cell migration is dependent on NF-kappaB- and AP-1-mediated matrix metalloproteinase-9 expression and is inhibited by atorvastatin. *J Biol Chem*. 2006;281:15099-15109
371. Luo JD, Xie F, Zhang WW, Ma XD, Guan JX, Chen X. Simvastatin inhibits noradrenaline-induced hypertrophy of cultured neonatal rat cardiomyocytes. *Br J Pharmacol*. 2001;132:159-164
372. Takemoto M, Node K, Nakagami H, Liao Y, Grimm M, Takemoto Y, Kitakaze M, Liao JK. Statins as antioxidant therapy for preventing cardiac myocyte hypertrophy. *J Clin Invest*. 2001;108:1429-1437
373. Shiroshita-Takeshita A, Brundel BJ, Burstein B, Leung TK, Mitamura H, Ogawa S, Nattel S. Effects of simvastatin on the development of the atrial fibrillation substrate in dogs with congestive heart failure. *Cardiovasc Res*.

2007;74:75-84

374. Moiseeva OM, Semyonova EG, Polevaya EV, Pinayev GP. Effect of pravastatin on phenotypical transformation of fibroblasts and hypertrophy of cardiomyocytes in culture. *Bull Exp Biol Med*. 2007;143:54-57
375. Chen J, Mehta JL. Angiotensin II-mediated oxidative stress and procollagen-1 expression in cardiac fibroblasts: blockade by pravastatin and pioglitazone. *Am J Physiol Heart Circ Physiol*. 2006;291:H1738-1745
376. Turner NA, Aley PK, Hall KT, Warburton P, Galloway S, Midgley L, O'Regan DJ, Wood IC, Ball SG, Porter KE. Simvastatin inhibits TNFalpha-induced invasion of human cardiac myofibroblasts via both MMP-9-dependent and -independent mechanisms. *J Mol Cell Cardiol*. 2007;43:168-176
377. Luan Z, Chase AJ, Newby AC. Statins inhibit secretion of metalloproteinases-1, -2, -3, and -9 from vascular smooth muscle cells and macrophages. *Arterioscler Thromb Vasc Biol*. 2003;23:769-775
378. Porter KE, Turner NA. Statins for the prevention of vein graft stenosis: a role for inhibition of matrix metalloproteinase-9. *Biochem Soc Trans*. 2002;30:120-126
379. Weitz-Schmidt G, Welzenbach K, Brinkmann V, Kamata T, Kallen J, Bruns C, Cottens S, Takada Y, Hommel U. Statins selectively inhibit leukocyte function antigen-1 by binding to a novel regulatory integrin site. *Nat Med*. 2001;7:687-692

Chapter 2

MMP-7 and ADAM-12 define a signalling axis in agonist-induced hypertension and cardiac hypertrophy

The data presented in this chapter is published in the following journal article:

Wang X, Chow FL, Oka T, Hao L, Lopez-Campistrous A, Kelly S, Cooper S, Odenbach J, Finegan B, Schulz R, Kassiri Z, Lopaschuk G, Fernandez-Patron C. MMP-7 and ADAM-12 define a signaling axis in agonist-induced hypertension and cardiac hypertrophy. *Circulation.* 2009 May 12;119(18):2480-9

Contribution: Designed siRNA, conducted animal studies using siRNA and antisense oligonucleotides of MMP-7, performed zymography assays, data analysis and data interpretation, contributed to the construction of the hypothesis, drafted the first version of the manuscript together with my supervisor and revised the manuscript.

2.1 Introduction

Hypertension, often termed “the silent killer”, is a systemic condition characterized by persistently elevated arterial blood pressure and is typically associated with cardiovascular hypertrophy[1]. Over 25% of the adult population in developed countries is hypertensive and, therefore, at risk of heart disease, peripheral vascular disease, end-stage renal disease and cerebrovascular stroke. The pathogenesis of most hypertensive disorders is complex. Genetic, immune and environmental factors all predispose individuals to hypertension. A difficulty faced by physicians when deciding on a therapeutic strategy is that, typically, the cause(s) of the hypertension is unknown. Thus, treatment of hypertension remains rather empirical with physicians choosing among many antihypertensive medications until a drug or drug-combination is identified that effectively lowers the blood pressure in the patient. Of those individuals treated, 65% do not meet treatment goals[2]. Therefore, treatment strategies are needed which: i) are preventative, ii) can stop pathological hypertrophy processes or induce the regression of pre-existing cardiac hypertrophy and iii) are efficacious in hypertensive disorders with multiple or unknown cause(s).

Recently, we proposed an approach to treat hypertension by blocking mediators commonly shared by many vasoconstrictors and significantly activated only in response to excessive agonist-stimulation[3]. The major vasoconstrictor systems discovered to date (catecholamines, endothelins and angiotensin II) all use Gq protein-coupled receptors (GqPCRs) as their cognate receptors. GqPCRs act through the activation of the classical phospholipase C / protein kinase C pathway and downstream matrix metalloproteinases (such as MMP-2, MMP-7 and MMP-9) and disintegrin metalloproteinases (such as ADAM-12 and ADAM-17/TACE/tumor necrosis factor-α convertase)[4-7]. Agonist-induced activation of these metalloproteinases is a rapid, post-transcriptional event mediated by protein kinase C, reactive oxygen species and other metalloproteinases (such as membrane type MMPs)[4,8,9]. Opening of the "cysteine switch" activates the pro-metalloproteinase, which sometimes results in autolysis[9]. Once activated, metalloproteinases cleave a host of common substrates including extracellular matrix proteins (e.g., collagens), pro-inflammatory mediators (e.g., TNF-α) and growth factors (e.g., TGF-α, HB-EGF). Thus, an overabundance of vasoconstrictive agonists (as occurs in hypertensive disorders) results in the activation of metalloproteinases, which next cleave and release (shed) substrates that signal through mitogen-activated protein kinases to transcriptionally activate immediate-early genes and reactivate fetal genes, including hypertrophy markers[10]. This mechanism may signal multiple processes including vascular smooth muscle and cardiomyocyte tone, cardiovascular hypertrophy and tissue injury[5,6,11].

The similar activation profile, substrates and signalling pathways of many metalloproteinases including MMP-7, MMP-2, ADAM-12 and ADAM-17/TACE[5-7,11-13] suggests a redundancy of their functions *in vivo*. However, the specific roles played by metalloproteinases, the hierarchical relationships that may coordinate their functions *in vivo*, and the therapeutic potential of these relationships remain poorly understood.

To start addressing these long-standing questions we have focused on MMP-7. Our findings suggest the existence of hierarchical and agonist-dependent relationships between MMP-7 and ADAM-12, suggesting a novel central role of MMP-7 in agonist-signalling of multiple cardiovascular processes including hypertension and hypertrophy.

2.2 Materials and methods

Animals Animal studies were conducted under the protocol approved by University of Alberta Animal Care and Use Committee. All animals were male and housed at the Animal Facility of the University of Alberta until use. MMP-7$^{-/-}$ mice and age-matched C57BL/6 (wild type) littermates (12 week old) were purchased from The Jackson Laboratory (Bar Harbor, Maine). The MMP-7$^{-/-}$ mice were generated by disrupting the MMP-7 gene through the insertion of a neomycin resistance cassette into the fragment spanning exon 3 and 4[14]. Hypertensive (22 week old) spontaneously hypertensive rats (SHR) were purchased from Charles River Laboratories Inc. (Wilmington, MA).

Acute hypertension models To induce acute hypertension in otherwise normotensive animals, we injected intraperitoneally (i.p.), as previously reported[15] one of the following pro-hypertensive agents[16]: norepinephrine or phenylephrine, angiotensin II or L-nitroarginine methyl ester (L-NAME) (Sigma-Aldrich, Canada) in 100 μL PBS. To study the significance of MMPs for the development of acute hypertension, these agents were co-administered with doxycycline (Sigma-Aldrich, 90 mg/kg, i.p.), which pharmacologically inhibits MMPs[17-19].

Chronic hypertension models We studied 3 models of chronic hypertension:

1) Angiotensin II-induced hypertension: Mice were infused Ang II (1.4 mg/kg/day) through ALZETosmotic minipumps (DURECT Corporation, Cupertino, CA) implanted subcutaneously on the back of the animals.

2) Norepinephrine-induced hypertension: Mice were injected norepinephrine (1.5 mg/kg, i.p.) once or twice daily for 9 days, as previously reported[15].

3) Spontaneously hypertensive rats.

Knockdown of MMP-7 in mice using antisense oligodeoxynucleotides Previously validated, commercially available, MMP-7 antisense and scrambled (inactive) oligodeoxynucleotides were synthesized by Integrated DNA Technologies (Toronto, Ontario)[20-22]. MMP-7 antisense sequence: 5’-GTATATGATACGATC-3’. Scrambled sequence: 5’-GTATTAGTATCGAAC-3’. These antisense oligos and their dose were previously reported to produce a knock-down of MMP-7 expression that lasts for at least 40 days in mouse[22]. To produce a sustained inhibition of MMP-7 expression in mice, we infused these antisense or scrambled oligodeoxynucleotides (1.31 μmol/kg/d, i.e., 0.6 mg/kg/d) or PBS for 14 days through osmotic minipumps subcutaneously implanted on the back right side of the mice.

Knocdown of MMP-7 using siRNA A mouse model of MMP-7 expression knock-down was generated using a siRNA designed as to overlap with the mRNA sequence targeted by the MMP-7 specific antisense oligodeoxynucleotides (for siRNA designs, please see **Figure 2-6**). MMP-7 siRNAwere synthesized by Sigma-Aldrich. The first two nucleotides of each oligo were 2'-O methylated to increase siRNA stability. The siRNAs were dissolved in PBS prior to use, a dose previously validated[23].

siRNA studies in mice As with oligodeoxynucleotides, the siRNAs (30 nmol/kg/d, i.e., 0.4 mg/kg/d) or PBS were infused for 14 days into mice through subquetaneously-implanted osmotic minipumps.

siRNA studies in rats The siRNAs (9 nmol/kg/d, i.e., 0.12 mg/kg/d) or PBS were infused for 14 days into SHR through subquetaneously-implanted osmotic minipumps.

Systolic blood pressure measurement Systolic blood pressure of conscious animals was measured indirectly using a commercially available computerized tail cuff plethysmography system (Kent Scientific Corporation, Torrington, CT).

Vascular tone studies in microperfusion bioassay system Mouse mesenteric arteries were dissected and microperfused as described earlier[6,24] using a Danish MyoTechnology arteriograph system (Aarhus, Denmark). This microperfusion system facilitates the study of vascular reactivity to luminal infusions of drugs as well as to drugs added to the bath (adventitia side). The bioassay closely mimics the *in vivo* situation in which adrenergic agonists are administered i.p. and enter the systemic circulation to act on the luminal side of arteries. The arteries were perfused at constant temperature (37°C) and flow rate (2 μL/min) with standard HEPES-PSS (142 mM sodium chloride, 4.7 mM potassium chloride, 1.17 mM magnesium sulfate, 1.56 mM calcium chloride, 1.18 mM potassium phosphate, 10 mM HEPES, 5.5 mM glucose, pH 7.4). In experiments involving the luminal administration of drugs, small volumes (5 μL) of drugs were injected into the perfusion line towards the artery. Changes in arterial outer diameter in response to drugs were monitored using a video camera and processed using VediView software (Danish MyoTechnology). The injection of drugs in the line towards the artery, without introducing flow rate change-related artifacts, was facilitated by an HPLC injection valve (Rheodyne Model 9725I, Mandel Scientific Co., ON, Canada).

Echocardiography *In vivo* assessment of anatomical structures and hemodynamic function in mice was conducted by echocardiography. The animals were first anaesthetized with 2.0 % Isoflurane, and their cardiac function was subsequently analyzed using a Vevo 770 high-resolution imaging system (ON, Canada). Three consecutive heartbeats of each frame were analyzed to measure the wall thickness and end-diastolic (EDD) and end-systolic (ESD) internal dimensions of the left ventricle (LV). Echocardiographic corrected LV mass (in mg) was calculated as: $1.05 \times 0.8 \times [(LVID;d + LVPW;d + IVS;d)^3 - (LVID;d)^3]$ on diastole (d). In the formula, ID is internal diameter (in mm), PW is the posterior wall dimension (in mm) and IVS is the interventricular septum dimension (in mm).

Sample Preparation Animal organs were washed in isotonic saline buffer, rinsed and weighed (Denver Instruments model APX-60, Colorado, USA). Proteins were extracted in 25 mM Tris, 62.5 mM NaCl, 1.25 mM PMSF, 62.5 mM Glycerol-2-phosphate, 12.5 mM sodium pyrophosphate, 125 μM NaF, 6.25 μg/ml leupeptine, 312.5 μM sodium orthovanadate, 12.5% glycerol, pH 7.4, supplemented with 5% SDS and 1% Triton X-100. To determine the protein content, the extracts were separated by 12% SDS-PAGE followed by densitometric analysis of Coomassie blue stained bands. Equal protein loads (approximately 50 μg/well) were subsequently subjected to zymography or western analysis.

Substrate zymography To determine MMP-7 and MMP-2 levels, lysates were subjected to electrophoresis on SDS-PAGE gels co-polymerized with casein (2.5 mg/mL) or gelatin (2 mg/mL), two well characterized substrates of MMP-7 and MMP-2, respectively. Following electrophoresis, the gel was washed with 2.5% Triton X-100 for 3 x 20 min. Activity was shown by incubating the gel for 16 hrs at 37°C in enzyme assay buffer (25 mM Tris, 5 mM $CaCl_2$, 142 mM NaCl, 0.5 mM NaN_3, pH 7.6) supplemented with 1 mM benzamidine and then the gel was stained with Coomassie blue.

Western immunoblotting The extracted proteins were separated using SDS-PAGE gels. The proteins were transferred to nitrocellulose membrane (BioRad) and blocked in 5% milk or 5% BSA. Blots were incubated with antibody against MMP-7 (1:250) (Calbiochem, Santa Cruz), ADAM12 (1:1000) (Chemicon) or phopho-ERK1/2 (1:1000) (Sigma-Aldrich), followed by incubation in corresponding secondary antibodies.

Cryosectioning Hearts and aortas from SHR treated with PBS, or MMP-7 siRNA (n=3) were embedded in Tissue-Tek (Sakura), frozen in dry ice and stored at -70 ºC. Sections were cut by a Leica microtome and left at room temperature overnight to dehydrate prior to fixation.

H+E Stain Protocol and Nuclei Count Cryosections of SHR hearts were fixed in acetone for 5 minutes and allowed to dry. Slides were then re-hydrated in progressively decreasing concentrations of ethanol (100%, 90%, 80%, 50% ethanol then H_20). The slides were then stained with Gill's hematoxylin for 5 minutes and washed with warm tap water. The slides were washed twice in 95% ethanol and stained in 0.5% eosin Y for 5 minutes. After staining, the slides were washed three times in 95% ethanol, two times in 100% ethanol, once in propanol followed by two 5 minute immersions in xylene. Slides were then mounted with mounting media and covered by a coverslip. The number of nuclei per unit area was determined from pictures of H+E stained longitudinal cardiac myocytes. Pictures were taken by a DCM500 digital camera on a Kyowa Medlux-12 light microscope at 400x magnification and viewed in ScopePhoto. The total nuclei number of each picture was calculated by adding the nuclei count of each grid section.

Immunofluorescence Cryosections of SHR aortae were fixed with acetone and then blocked with 2.5% BSA in TBS-T (20 mM Tris-HCl, 137 mM NaCl, 0.1% Tween-20, pH 7.6) for 30 min. Slides were then incubated with goat anti-MMP-7 antibodies (Santa Cruz Biotechnology) (1:500 dilution each in TBS-T with 2.5% BSA) for 1 hr and washed with TBS-T and 2.5% BSA in TBS-T. Finally the aortas were incubated in Cy3 conjugated rabbit anti-goat (Sigma Chemical) and fluorescein conjugated donkey anti-rabbit antibodies (Amersham Life Sciences) (1:500 dilution in TBS-T with 2.5% BSA) for 1 hr. The slides were washed with TBS-T and 2.5% BSA in TBS-T before mounted with DAPI-containing VectaShield mounting medium and viewed at 200x magnification by a Zeiss Axiovert 200M fluorescence.

Interferon γ Measurement The level of interferon γ (IFN γ) in siRNA treated mice or SHR was measured using *VeriKine*TM Mouse IFN Gamma ELISA kit (PBL biomedical laboratories).

Genotype analysis MMP-7 gene knock-out was confirmed by genotype analysis of MMP-$7^{-/-}$ vs. wild type C57BL/6 mice. For the amplification of the MMP-7 gene, specific primers were designed based on *Mus musculus* genomic sequence and synthesized by Sigma-Proligo. The sequence of the upstream primer was (5’-AGACAGCTTCCCCTTTGATG -3’). The sequences of the downstream primers were: (5’-CTGCGTCCTCACCATCAGT-3’) for wild-type genotyping and (5’-GCTATCAGGACATAGCGTTGG-3’) for MMP-$7^{-/-}$ genotyping following the recommended protocol (Jackson Lab). A 12 μL PCR reaction was performed which included 2 μL genomic DNA, 1 μL 10x High Fidelity PCR Buffer (600 mM Tris-SO_4, pH 8.9, 180 mM Ammonium Sulfate), 1 μL each gene-specific primers 0.2 mM dNTPs, 2 mM MgSO4, and 0.3 unit of Platinum Taq High Fidelity (Invitrogen). The PCR was performed for 25 cycles with temperature at 94 °C for 30 s, 68 °C for 1 min, and 72 °C for 1 min on Mastercycler ep (Eppendorf AG). PCR products were assessed on a 1% agarose/Tris-Acetate-EDTA gel, stained with ethidium bromide and visualised with UV light.

RNA expression analysis by TaqMan RT PCR Total RNA was extracted from flash-frozen organs using Trizol, and cDNA was generated from 1 µg RNA by using a random hexamer. Expression analysis of the genes was performed by TaqMan RT-PCR using ABI 7900 sequence detection system. 18S rRNA was used as an endogenous control as described previously[25].

Data analysis Results were analyzed using one-way ANOVA (between multiple groups) or *t*-test (between two groups) (Jandel SigmaStat 3.5 statistical software). In the echocardiography studies, between-group comparisons of the means were performed by one-way ANOVA followed by Scheffe’s F correction for multiple comparisons of the means.

2.3 Results

MMP-7 as a mediator in pharmacologically induced acute hypertension

To trigger an acute hypertensive response in otherwise normotensive Sprague Dawley rats and C57BL/6 mice, we injected intraperitoneally either PBS (vehicle) or: i) α-adrenergic agonists (phenylephrine and norepinephrine), ii) angiotensin II or iii) L-nitroarginine methyl ester (L-NAME), that elevates blood pressure by blocking basal nitric oxide-dependent vasodilation, thus unmasking secondary vasoconstrictor mechanisms[26,27] (**Figure 2-1 and 2-2**).

The involvement of MMPs in these experiments was suggested by effects of doxycycline, a broad-spectrum pharmacological inhibitor of MMP activity[28]. Doxycycline (60-120 mg/kg, i.p.) blocked the acute hypertensive responses to α-adrenergic agonists, angiotensin II and L-NAME in rats (**Figure 2-1**) and mice (**Figure 2-2A**). HPLC analyses indicated that doxycycline (90 mg/kg, i.p.) resulted in plasma concentrations between 10^{-4} and 10^{-5} M, at 1 and 4 hrs after i.p. injection, respectively. These doxycycline concentrations are sufficient to relax small rat mesenteric arteries in isolation[6]. When we examined arteries collected at a time point that coincided with the maximum elevation in systolic blood pressure induced by phenylephrine, angiotensin II or L-NAME (i.e., 4, 1 or 0.5 hrs, respectively), the level of vascular MMP-7, but not MMP-2, was elevated. The increase in MMP-7 was in all cases blocked by the co-administration of doxycycline (**Figure 2-1**).

We verified the link between MMP-7 expression and systemic blood pressure regulation in studies summarized in **Figure 2-2A-C**. In these studies, we examined C57BL/6 mice in which the MMP-7 gene was disrupted by a neomycin resistance cassette to render them MMP-$7^{-/-}$. We also studied wild type C57BL/6 mice receiving MMP-7-specific antisense oligodeoxynucleotides (0.6 mg/kg/d) or scrambled (inactive) oligodeoxynucleotides (0.6 mg/kg/d) or PBS for 14 days (through subcutaneous osmotic minipumps). The antisense sequence chosen for this study was previously validated *in vivo* and has anti-cancer activity through the long-lasting knock-down of MMP-7[22]. Antisense treatment resulted in a systemic down-regulation of MMP-7 expression in various organs including aorta, heart and small intestine (where MMP-7 is normally expressed at very high levels[29]) (**Figure 2-3**).

Interestingly, resting systolic blood pressure was not significantly affected by MMP-7 antisense oligodeoxynucleotides or MMP-7 gene knock-out (**Figure 2-2D**). However, mice that received MMP-7 antisense oligodeoxynucleotides displayed decreased acute hypertensive responses to norepinephrine, angiotensin II and L-NAME (vs. PBS and vs. scrambled oligodeoxynucleotides) (**Figure 2-2B, E-G**). Similarly, MMP-7$^{-/-}$ mice showed attenuated acute responses to angiotensin II and norepinephrine (**Figure 2-2C**). Moreover, MMP-7$^{-/-}$ mice (but not wild type mice) were resistant to chronic hypertension induced by repeated norepinephrine administration (**Figure 2-4A**). Isolated microperfused small mesenteric arteries from MMP-7$^{-/-}$ mice constricted less (vs. wild type mice) in response to luminally delivered boluses of the α-adrenergic agonist, phenylephrine (0, 5 or 50 pmol *per* bolus) (**Figure 2-4B**).

Together, these *in vivo* and *in vitro* functional data strongly suggested that vasoconstrictors induce hypertension, at least in part, through the post-transcriptional activation of MMP-7.

MMP-7 as a mediator of hypertension and cardiac hypertrophy in spontaneously hypertensive rats

We next examined whether blocking MMP-7 expression would decrease the systolic blood pressure of spontaneously hypertensive rats (SHR), a genetic model where hypertension is caused by multiple mechanisms including endothelial dysfunction and upregulated activities of catecholamines (i.e., sympathetic system) and angiotensin II[30-32].

Figure 2-5 illustrates results obtained in already-hypertensive 22 weeks old SHR when we targeted the MMP-7 gene by RNA interference using a small interference RNA (siRNA) against the same mRNA sequence targeted by the MMP-7 antisense oligodeoxynucleotides (for an alignment of the sequences, please see **Figure 2-6**). MMP-7 siRNA treatment significantly decreased the systolic blood pressure, producing an attenuation of the hypertension that lasted beyond the window of siRNA delivery (**Figure 2-5A**). The anti-hypertensive effects of MMP-7 siRNA treatment were associated with a significant decrease in MMP-7 in resistance arteries (**Figure 2-5B**). Interestingly, MMP-7 siRNA treatment stopped the progression of cardiac hypertrophy (**Figure 2-7A, B and Table 2-1**) in association with a down-regulation of myocardial MMP-7 (**Figure 2-7C**). Comparative gross pathology further revealed that treatment with MMP-7 siRNA resulted in approximately 50% reduction in cardiac hypertrophy vs.SHR given PBS and vs. untreated normotensive age-matched WKY rats: HW/BW (WKY) = 3.40±0.01 mg/g, HW/BW (SHR + MMP-7 siRNA) = 3.99±0.05 mg/g, HW/BW(SHR+PBS) = 4.43±0.09 mg/g; n = 3 for WKY, n = 4 for both: SHR + PBS and SHR + MMP-7 siRNA.

We excluded a major contribution of the inflammatory response in these anti-hypertensive and anti-hypertrophy effects of MMP-7 siRNA since we did not observe significantly elevated interferon γ levels in plasma or in the left ventricle of the rats (**Figure 2-8, SHR**).

The MMP-7/ADAM-12 signalling axis

Administration of MMP-7 siRNA (0.4 mg/kg/d) for 14 days resulted in a significant down-regulation in myocardial MMP-7 mRNA levels in mice (**Figure 2-9A**). Interestingly, MMP-7 siRNA inhibited ADAM-12 transcription (**Figure 2-9B**) but had otherwise insignificant effects on other genes including alpha skeletal actin, TACE, TIMP-2 and MMP-9 (**Figure 2-9C, D**) or on interferon γ levels (**Figure 2-8**). Like the MMP-7 siRNA, MMP-7 gene knock-out resulted in decreased levels of myocardial ADAM-12 mRNA (but normal levels of TACE) (**Figure 2-9E**). Mice that received MMP-7 siRNA displayed no morphometric or echocardiograhic abnormalities (**Table 2-2**).

Mice receiving angiotensin II (1.4 mg/kg/d for 10 days) displayed hypertension and left ventricular hypertrophy (**Figure 2-9F, G and Table 2-2**).Continuous angiotensin II infusion inhibited MMP-7 transcription (**Figure 2-9A**) but increased transcription of ADAM-12 and hypertrophy marker genes (β-myosin heavy chain, brain natriuretic peptide, and α-skeletal actin) (**Figure 2-9B, C**). Pre-treatment with MMP-7 siRNA attenuated angiotensin II-induced hypertension (as expected from studies in **Figures 2-1** to **2-5**), inhibited the angiotensin II-induced overexpression of both ADAM-12 and hypertrophy marker genes (**Figures 2-9B, C**) and prevented left ventricular hypertrophy (**Figure 2-9F, G and Table 2-2**). Supporting these observations, MMP-7$^{-/-}$ mice (but not age-matched wild type mice) exhibited resistance to hypertension (**Figure 2-4A**), cardiac hypertrophy (**Figure 2-10A**) and to the transactivation of cardiac growth factor receptors, which are purported mediators of agonist-activated ADAM-12[5] (**Figure 2-10B**).

2.4 Discussion

This investigation has resulted in three interrelated discoveries: 1) Our findings suggest for the first time that agonist-signalling of both hypertension and cardiac hypertrophy depends on MMP-7 gene expression and activity. 2) We revealed a novel transcriptional link between MMP-7 and ADAM-12, the major disintegrin metalloproteinase implicated in the development of cardiac hypertrophy. 3) We show that disrupting the MMP-7 / ADAM-12 axis at the level of MMP-7 protects from development of both cardiac hypertrophy and hypertension in simple models (such as mice infused angiotensin II) as well as in a complex model (spontaneously hypertensive rats). Thus, targeting the MMP-7.ADAM-12 axis (e.g., at the level of MMP-7) could have general therapeutic potential in multiple hypertensive disorders caused by multiple or unknown agonists.

Prior to this study, many characterizations of MMP-7 *in vivo* related to cancer[33] or the innate immune response[29] with the exception of a few recent studies including one showing a novel interaction between MMP-7 and connexin-43 in cardiac failure[34]. Our laboratory had proposed a role for MMP-7 in agonist-induced vasoconstriction of isolated arteries, based on broad-spectrum pharmacological inhibitor data[6]. However, none of our previous studies could establish its mediator role in agonist-induced hypertension nor its involvement in cardiac hypertrophy, a process that invariably develops subsequently to sustained vasoconstrictive agonist-stimulation. Prior to this research, MMP-7 and ADAM-12 had been studied separately[5-7,11-13]. However, these separate studies suggested their involvement in cardiovascular hypertrophy processes through a common pathway. Accordingly, high levels of vasoconstrictor agonists (as occurs in hypertensive disorders) would enhance their activity, through post-transcriptional pathways. Next, the activated MMP-7 and ADAM-12 would cleave and release substrates including growth factors and inflammatory mediators (such as HB-EGF, TGF-α and TNF-α). These mediators then trigger the mitogen-activated protein kinase cascade to promote cardiovascular hypertrophy through the transcriptional activation of immediate-early genes and fetal genes, often referred to as hypertrophy marker genes[5-7,11-13] (**Figure 2-11**, module #1).

The data suggest that MMP-7 and ADAM-12 are connected in agonist-induced post-transcriptional and transcriptional events which may ultimately result in the development of hypertension and cardiovascular hypertrophy. We have further revealed novel hierarchical relationships between these metalloproteinases and observed that these relationships are dynamic as they differ under basal conditions (**Figure 2-11**, module #2) vs. agonist-stimulation (**Figure 2-11**, module #3). Under basal conditions, MMP-7 transcriptionally controls the expression of ADAM-12 and downstream hypertrophy marker genes. However, under sustained agonist-stimulation, the MMP-7 mRNA levels and, thereby, the contribution of MMP-7 to signalling may decrease; while the expression and, thereby, the contribution of ADAM-12 to signalling may increase. We thus propose that: i) MMP-7 may mediate the early post-transcriptional events by which vasoconstrictor agonists trigger an acute elevation of blood pressure (in the short-term) and the development of cardiovascular hypertrophy (which is a long-term process). ii) Under sustained agonist-stimulation, the overexpression of ADAM-12 may act to inhibit MMP-7 transcription (in a negative feed-back loop) while increasing transcription of hypertrophy marker genes. iii) The inhibition of MMP-7 transcription by sustained agonist-stimulation may represent a novel physiological compensatory mechanism to counter hypertension and hypertrophy processes.

The therapeutic potential of disrupting the MMP-7 / ADAM-12 axis at the level of MMP-7 was evidenced by studies in both mice with agonist-induced hypertension and in spontaneously hypertensive rats, a model where hypertension has multiple or poorly understood causes[30-32]. Our data clearly showed that blocking MMP-7 expression could be valuable for attenuating hypertension as well as preventing the development of cardiac hypertrophy.

Limitations and future studies

While quantitative RT-PCR provided a reliable, highly sensitive and quantitative tool, metalloproteinase quantitation by other complementary means remains challenging for various reasons: i) MMP-7 and ADAM-12 genes have very low expression (particularly in the left ventricle), ii) commercial antibodies to these proteins have poor sensitivity or cross-react with many bands on western immunoblotting, hampering their unambiguous quantitation iii) activity-based determinations are potentially non-specific and may favour the detection of the more active forms of these metalloproteinases, thus introducing a quantitation bias.

That vasoconstrictors signal through mutually regulated metalloproteinases (and not just through isolated metalloproteinases) is a novel observation that integrates and substantially expands previous research[5-7]. This notion is in complete agreement with a previous investigation that detected a differential involvement of multiple metalloproteinases in various forms of cardiomyopathy including hypertrophic obstructive cardiomyopathy and dilated cardiopathy in humans[35]. Future studies should further dissect the dynamics of the metalloproteinase networks that may operate in various models of hypertension and cardiac hypertrophy and in different stages of the development of the disease. Such studies might enable the design of general treatments for hypertensive disorders with complex or unknown etiology such as pre-eclampsia, that complicates 5% of all pregnancies worldwide[36] and essential hypertension, which affects 25% of the adult population in developed countries[1].

Clinical Perspective

Excessive stimulation of Gq protein-coupled receptors (GqPCRs) by cognate vasoconstrictor agonists induces a variety of cardiovascular processes including hypertension and hypertrophy. Here, we observed that matrix metalloproteinase-7 (MMP-7) and a disintegrin and metalloproteinase-12 (ADAM-12) may form a novel signalling axis in these processes. We suggest further that targeting the MMP-7.ADAM-12 axis (e.g., at the level of MMP-7) using RNA interference-based approaches could have general therapeutic potential in multiple hypertensive disorders caused by multiple or unknown agonists.

Table 2-1 Involvement of MMP-7 in the development of cardiac hypertrophy in the SHR model. Morphometric, haemodynamic and echocardiographic results.

Day 40	IVS;d (mm)	LVID;d (mm)	LVPW;d (mm)
PBS	1.90 ± 0.03	8.36 ± 0.08	1.74 ± 0.04
MMP7 siRNA	1.57 ± 0.05*	8.63 ± 0.17	1.60 ± 0.03*
	EF (%)	HR (bpm)	BW (g)
PBS	65.73 ± 1.10	353.7 ± 14.8	360.0 ± 7.4
MMP7 siRNA	66.06 ± 1.13	347.7 ± 11.7	363.8 ± 9.9

PBS, phosphate buffered saline; IVS, intervetricular septum; LV, left ventricle; ID, inner diameter; PW, posterior wall dimension; d, diastoles; EF, ejection fraction; HR, heart rate; BW, body weight. Results are means ± sem. n = 4 rats per group. (*) $p < 0.01$ vs PBS. MultiANOVA with Scheffe's test.

Table 2-2 Involvement of MMP-7 in the development of the cardiac hypertrophy induced by angiotensin II (1.4 mg/kg/d for 10 days) in the mouse. Morphometric, haemodynamic and echocardiographic results.

	IVS;d (mm)	LVID;d (mm)	LVPW;d (mm)
PBS	0.68 ± 0.02	3.95 ± 0.04	0.73 ± 0.02
MMP-7 siRNA	0.67 ± 0.03	3.99 ± 0.09	0.68 ± 0.02
PBS + AngII	0.83 ± 0.01*	4.62 ± 0.09*	0.85 ± 0.03*
MMP-7 siRNA + Ang II	0.68 ± 0.04	4.07 ± 0.09	0.69 ± 0.02
	EF (%)	HR (bpm)	BW (g)
PBS	65.52 ± 2.11	524.7 ± 22.7	25.7 ± 0.2
MMP-7 siRNA	68.00 ± 2.00	521.1 ± 12.2	27.2 ± 0.5
PBS + AngII	61.99 ± 1.95	554.1 ± 23.1	24.6 ± 0.7
MMP-7 siRNA + Ang II	66.28 ± 1.76	546.0 ± 7.3	25.5 ± 0.6

PBS, phosphate buffered saline; d, diastoles; IVS, intervetricular septum; LV, left ventricle; ID, inner diameter; PW, posterior wall dimension; EF, ejection fraction; HR, heart rate; BW, body weight. Results are mean ± sem. n = 4 mice for each group. (*): $p < 0.05$ vs all groups (i.e., vs. PBS, vs. MMP-7 siRNA and vs. MMP-7 siRNA + Ang II). MultiANOVA with Scheffe's test. Note: The angiotensin II group consisted of six mice, two of which developed acute systolic dysfunction at the time of echocardiography and were excluded from the analysis. The data indicate the induction of left ventricular hypertrophy and left ventricular dilation by angiotensin II, without significantly affecting contractile function. MMP-7 siRNA treatment protected against these angiotensin II-induced alterations.

Figure 2-1 MMP-7 as a mediator in rat models of acute hypertension.

Left panels: Time course of systolic blood pressure of Sprague Dawley rats administered: angiotensin II (Ang II, 1.5 mg/kg, i.p.) either alone or together with the broad-spectrum MMP blocker, doxycycline (Dox, 90 mg/kg, i.p.).

Right panels: Representative zymograms showing the effects of vasoconstrictors on vascular MMP-7 and MMP-2 *in vivo* (n =4-5 rats in each study group). Sprague Dawley rats were administered with angiotensin II (1.5 mg/kg, i.p.) either alone or together with doxycycline (90 mg/kg, i.p.).

Vehicle was sterile phosphate buffered saline solution (PBS).

(*): $p < 0.05$ vs. PBS.

(+): $p < 0.05$ vs. agonist + Dox

Results are means ± SEM (standard error of the mean) of 4-5 rats in each study group.

(These data are obtained by Fung Lan Chow)

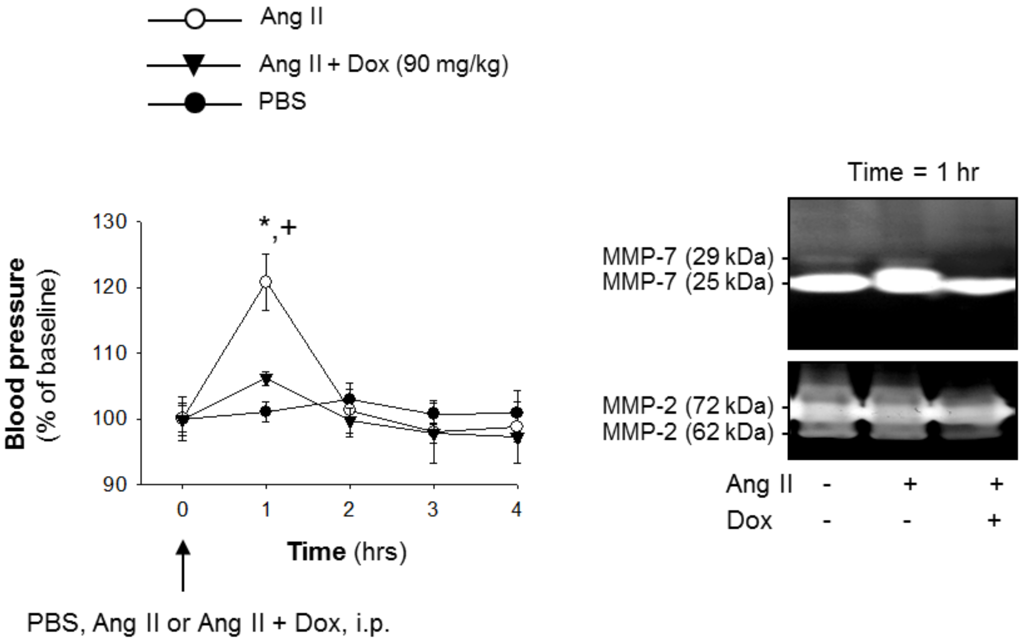

Figure 2-2 Resistance to acute hypertension in mice lacking active MMP-7.
A, Time course of systolic blood pressure on wild type mice administered norepinephrine (NE, 1.5 mg/kg, i.p.) alone or together with doxycycline (Dox, 90 mg/kg, i.p.). (*): $p < 0.05$ vs. untreated mice..
B, Protection from norepinephrine-induced acute hypertension in mice treated with MMP-7 antisense oligodeoxynucleotides (0.6 mg/kg/d for 14 days) vs. mice administered scrambled antisense oligodeoxynucleotides (0.6 mg/kg/d for 14 days). (*): $p < 0.05$ vs. untreated mice.
C, Protection from norepinephrine-induced acute hypertension in MMP-7$^{-/-}$ mice. (*): $p < 0.05$ vs. untreated wild type mice.
D, Effects of MMP-7 knock-down and MMP-7 gene knock-out on the resting blood pressure of mice. **Left panel:** Resting blood pressure of mice treated with MMP-7 antisense vs. scrambled oligodeoxynucleotides for 14 days. Blood pressure at day 15. **Right panel:** Resting blood pressure of MMP-7$^{-/-}$ mice vs. age-matched wild type mice.
E-G, Top panels: Time course of systolic blood pressure effects of norepinephrine (NE, 1.5 mg/kg, i.p.), angiotensin II (Ang II, 1.5 mg/kg, i.p.) or L-nitroargininemethylester (L-NAME, 15 mg/kg, i.p.) in mice treated with MMP-7 antisense oligodeoxynucleotides (MMP-7 antisense, 0.6 mg/kg/d for 14 days) vs. mice given PBS (PBS). **E-G, Bottom panels:** Quantitative analysis of the dose-response for each vasoconstrictor. (*): $p < 0.05$ vs. untreated mice. Results are means ± SEM of 4-5 mice in each study group.

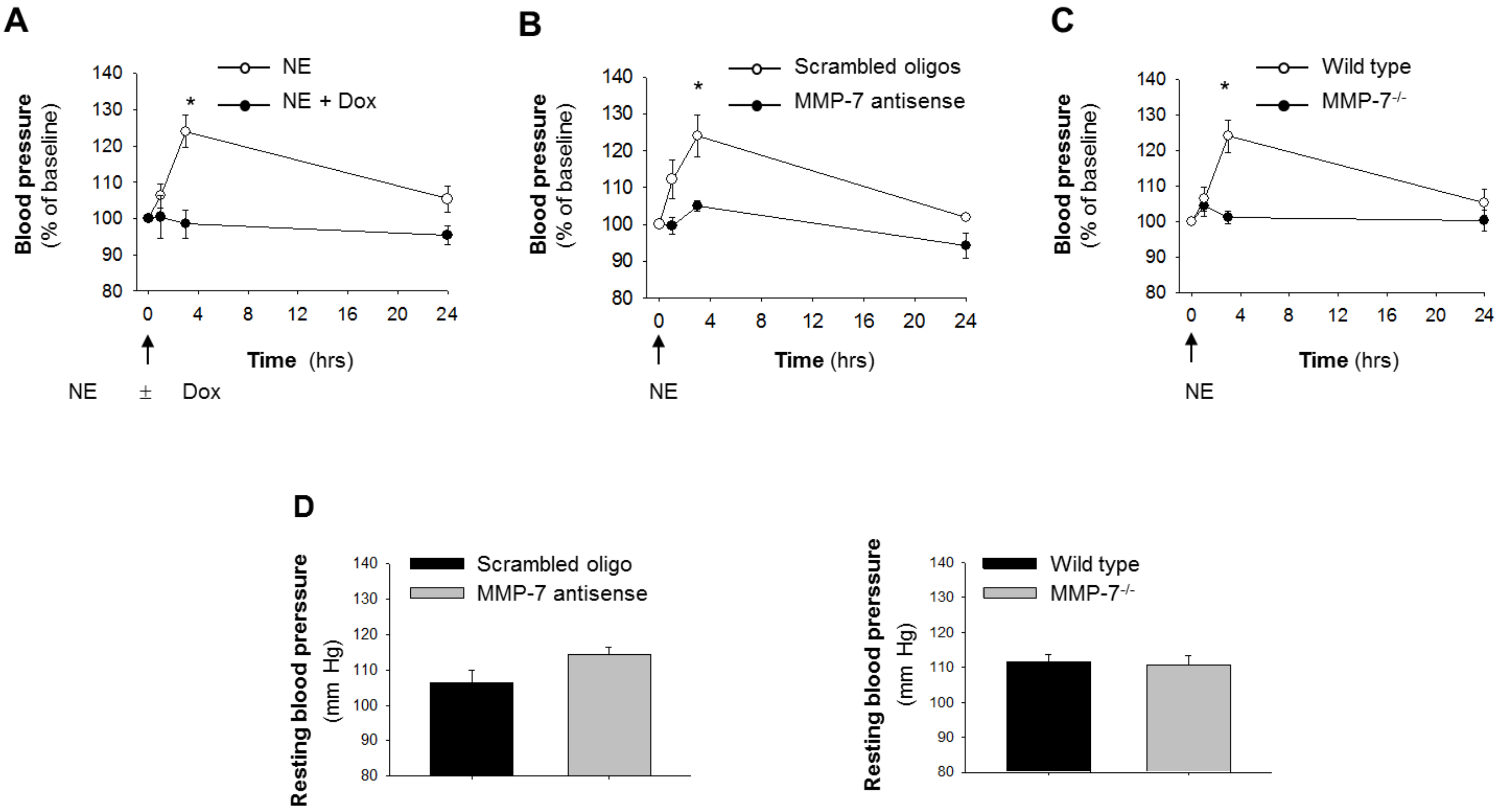
A
Blood pressure
(% of baseline)
140
130
120
110
100
90
80
0
4
8
12
16
20
24
Time (hrs)
NE ± Dox
NE
NE + Dox
*
B
Blood pressure
(% of baseline)
Time (hrs)
NE
Scrambled oligos
MMP-7 antisense
*
C
Blood pressure
(% of baseline)
Time (hrs)
NE
Wild type
MMP-7-/-
*
D
Resting blood prerssure
(mm Hg)
Scrambled oligo
MMP-7 antisense
Resting blood prerssure
(mm Hg)
Wild type
MMP-7-/-

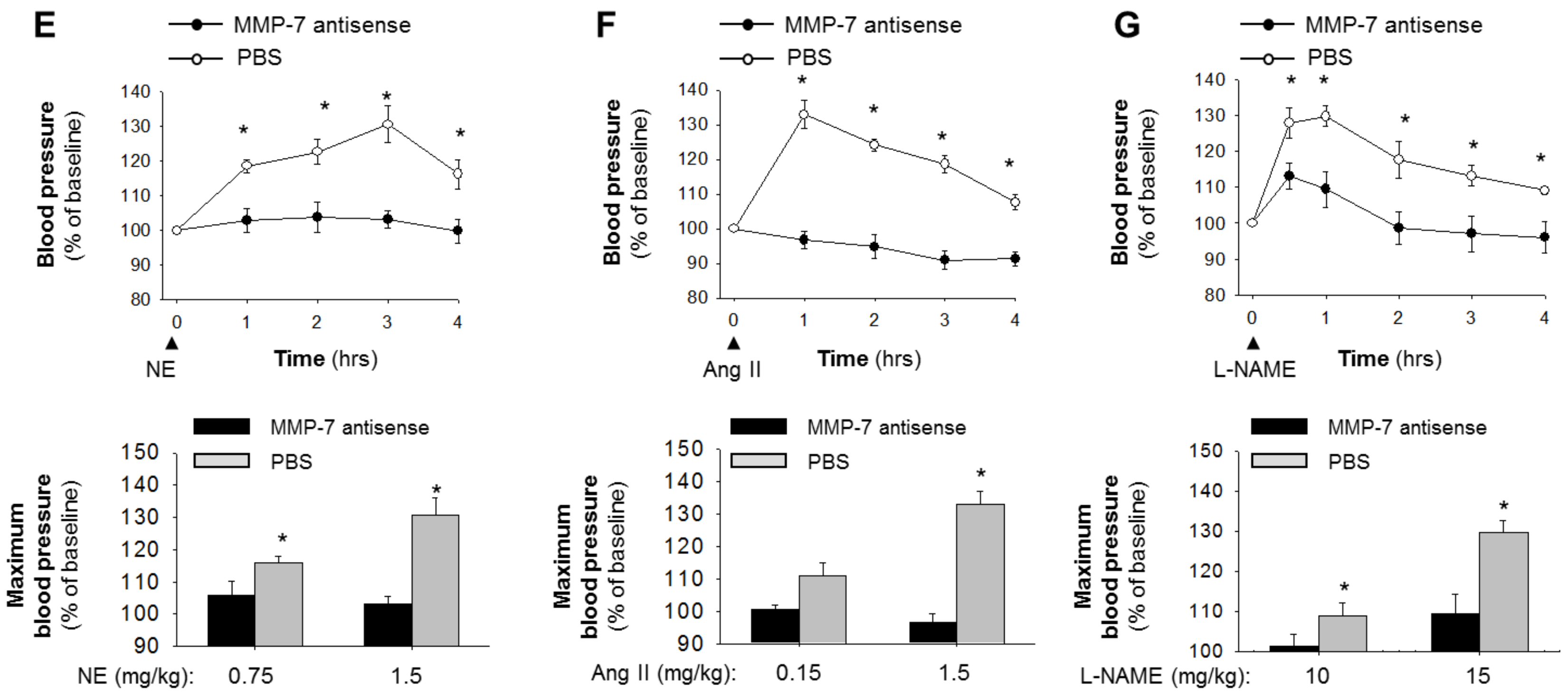
E
MMP-7 antisense
PBS
Blood pressure (% of baseline)
140
130
120
110
100
90
80
0
1
2
3
4
NE
Time (hrs)
*
Maximum blood pressure (% of baseline)
150
140
130
120
110
100
90
NE (mg/kg):
0.75
1.5
F
Ang II
Ang II (mg/kg):
0.15
1.5
G
L-NAME
L-NAME (mg/kg):
10
15

Figure 2-3 Knockdown of MMP-7 by antisense oligodeoxynulceotides. Representative casein zymograms of MMP-7 in indicated organs showing systemic MMP-7 knock-down in mice administered commercially available antisense oligodeoxynucleotides vs. mice administered vehicle (PBS) or scrambled oligodeoxynucleotides for 14 days. (*): $p < 0.05$. Results are means ± SEM of 4 mice in each group.

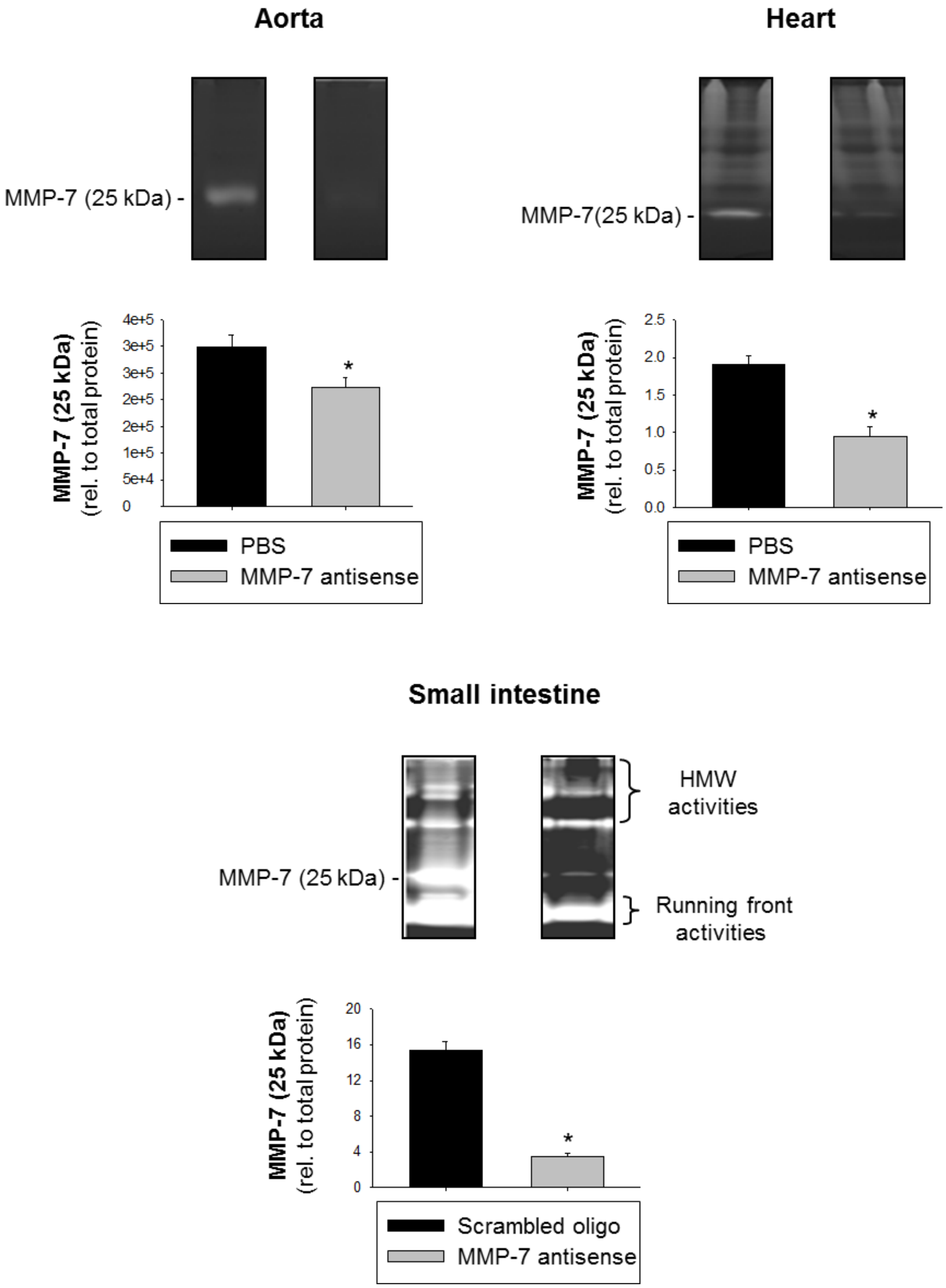

Figure 2-4 Resistance to chronic hypertension in MMP-7$^{-/-}$ mice.

A, MMP-7$^{-/-}$ and age-matched wild type mice were injected with NE (1.5 mg/kg, i.p.) once or twice daily for 9 days. Systolic blood pressure was measured on day 10 (i.e., 24 hr after the last injection of NE). (*): $p < 0.05$ vs. baseline. Results are means ± SEM of 4-5 mice in each study group.

B, Attenuation of α_1-adrenergic contractile responses in isolated small mesenteric arteries from MMP-7$^{-/-}$ vs. wild type mice. Representative traces of contractile response of small mesenteric arteries from wild type mice and MMP-7$^{-/-}$ mice to increasing doses of the α_1-adrenergic agonist, phenylephrine. Small mesenteric arteries from mice were mounted on a microperfusion arteriograph (perfusion flow rate of 1 μL/min). To induce contraction of the arteries, the indicated amounts of phenylephrine (PE, in 5 μL) were injected in the line towards the artery. Unlike wild type mice, the MMP-7$^{-/-}$ mice had attenuated responses to PE (5 pmol). Traces are representative of 3 mice in each study group.

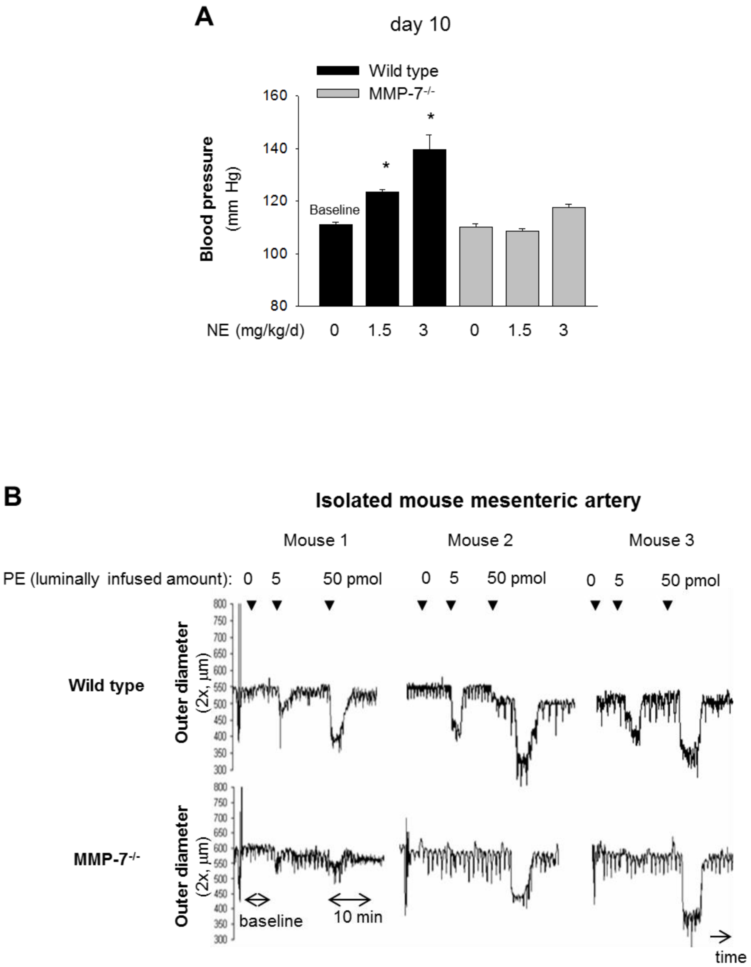

Figure 2-5 MMP-7 as a mediator of hypertension in spontaneously hypertensive rats.

A, Time course of the systolic blood pressure of already-hypertensive SHR treated with PBS or siRNA to MMP-7 (n = 4).

Treatment #1: The rats were infused with either MMP-7 siRNA or PBS through minipumps for 14 days.

Treatment #2: On day 23, treatment was restarted by implanting new minipumps containing either MMP-7 siRNA or PBS.

No treatment: Period between treatments, i.e., between day 15 and day 23 showing that protection lasted beyond the 14-day-window of siRNA delivery by the osmotic minipumps.

B, Quantitative analysis indicates that, in small (resistance) mesenteric arteries, MMP-7 expression was knocked-down by siRNAs to MMP-7, as determined using substrate zymography.

(*): $p < 0.05$ vs. PBS group. Results are means ± SEM of 3-4 rats in each group.

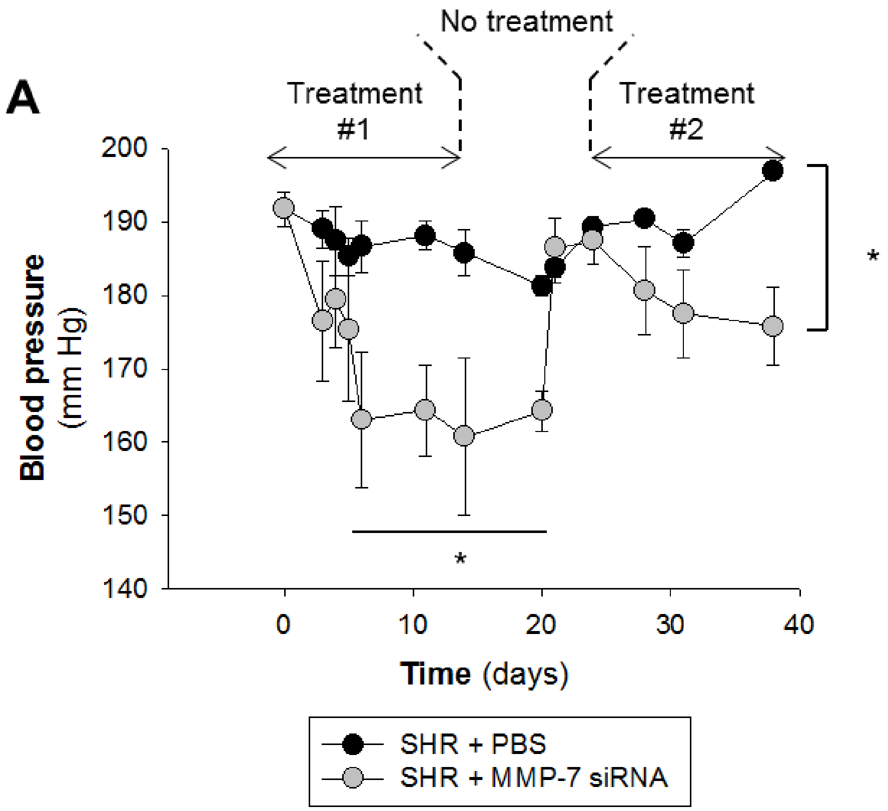

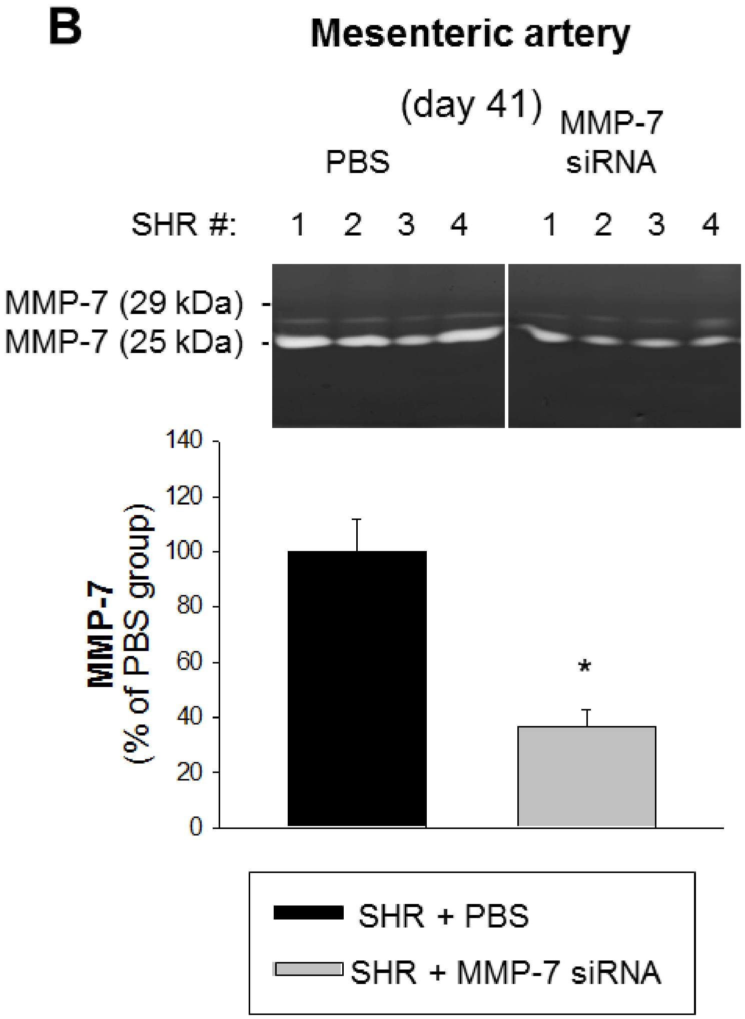
B
Mesenteric artery
(day 41)
PBS
MMP-7
siRNA
SHR #:
1
2
3
4
1
2
3
4
MMP-7 (29 kDa)
MMP-7 (25 kDa)
MMP-7
(% of PBS group)
140
120
100
80
60
40
20
0
*
SHR + PBS
SHR + MMP-7 siRNA

Figure 2-6 Targeted sequences on MMP-7 using siRNAs and antisense oligodeoxynucleotides.

Depicted are the domain structure of MMP-7 protein and the cDNA sequences targeted by the siRNA and antisense oligodeoxynucleotides.

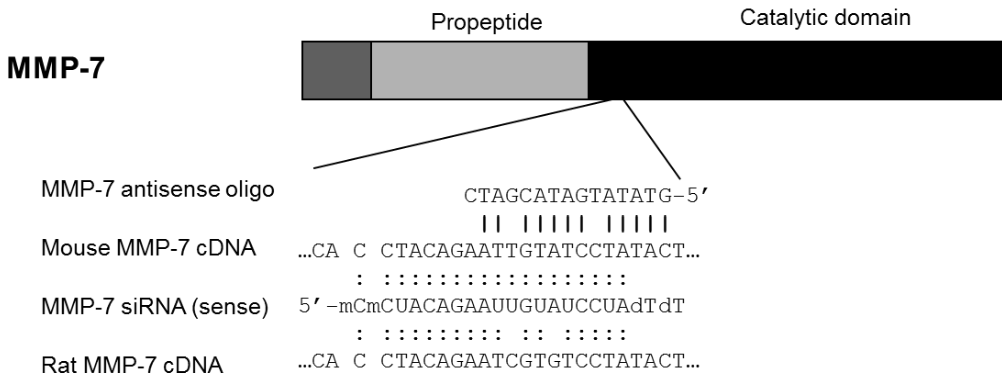
Propeptide
Catalytic domain
MMP-7
MMP-7 antisense oligo
CTAGCATAGTATATG-5′
Mouse MMP-7 cDNA
…CA C CTACAGAATTGTATCCTATACT…
MMP-7 siRNA (sense)
5′-mCmCUACAGAAUUGUAUCCUAdTdT
Rat MMP-7 cDNA
…CA C CTACAGAATCGTGTCCTATACT…

Figure 2-7 MMP-7 as a mediator of cardiac hypertrophy in spontaneously hypertensive rats.

A, Cardiac hypertrophy in SHR treated with siRNA or PBS. While the ratio of corrected left ventricle mass (corr. LV mass) to body weight (BW) increased over time in untreated rats, this ratio did not increase in rats that received siRNA. Time axis indicates when M-mode echocardiography analysis was conducted.

B, Gross pathology analysis (conducted on day 41) indicated a significantly decreased heart weight (HW) to body weight (BW) ratio.

C, Quantitative analysis and representative traces of zymography and western immunoblotting indicating knock-down of MMP-7 expression. Zymography on casein gels was relatively selective for MMP-7 active form (25 kDa). Western blots show all immunoreactive bands detected using commercially available antibodies to MMP-7.

(*): $p < 0.05$ vs. PBS group. Results are means ± SEM of 3-4 rats in each group.

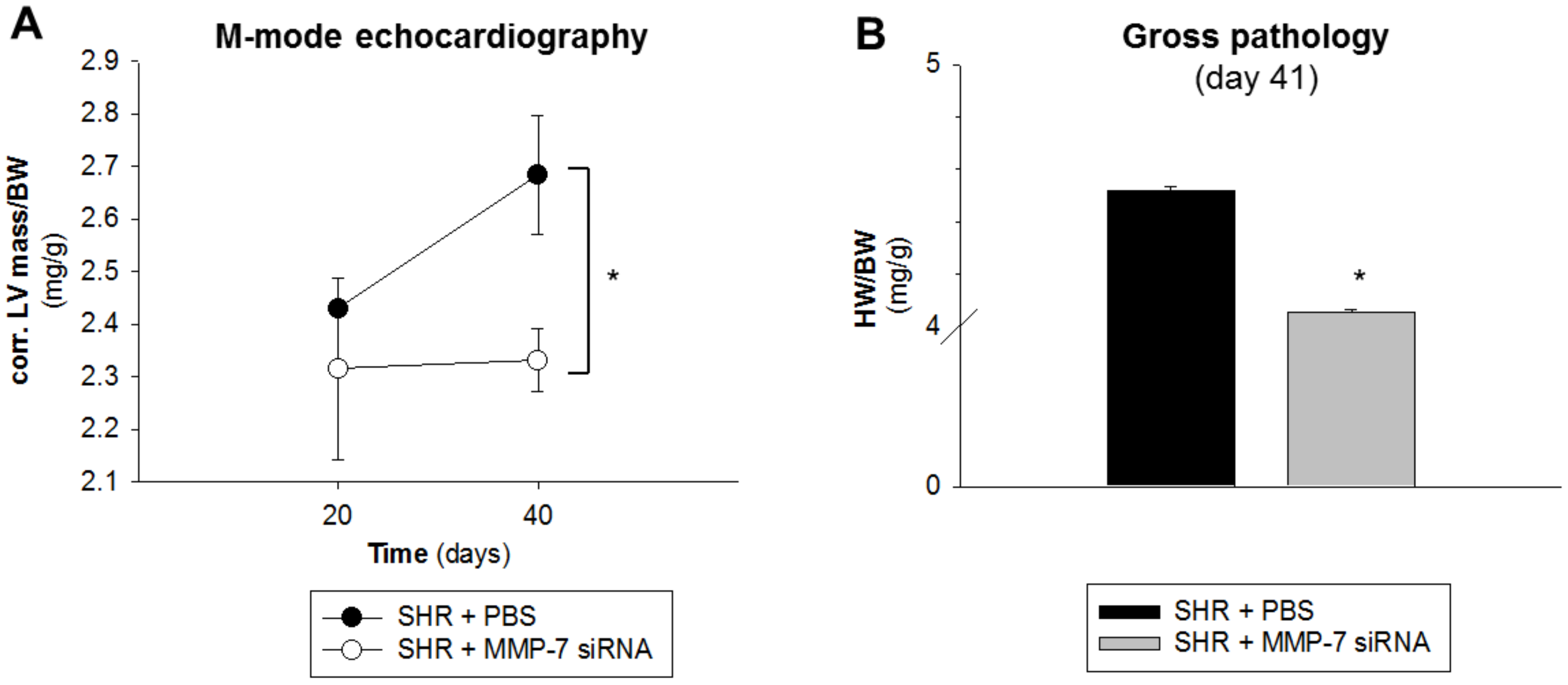
A
M-mode echocardiography
corr. LV mass/BW
(mg/g)
2.9
2.8
2.7
2.6
2.5
2.4
2.3
2.2
2.1
20
40
Time (days)
*
SHR + PBS
SHR + MMP-7 siRNA
B
Gross pathology
(day 41)
HW/BW
(mg/g)
5
4
0
*
SHR + PBS
SHR + MMP-7 siRNA

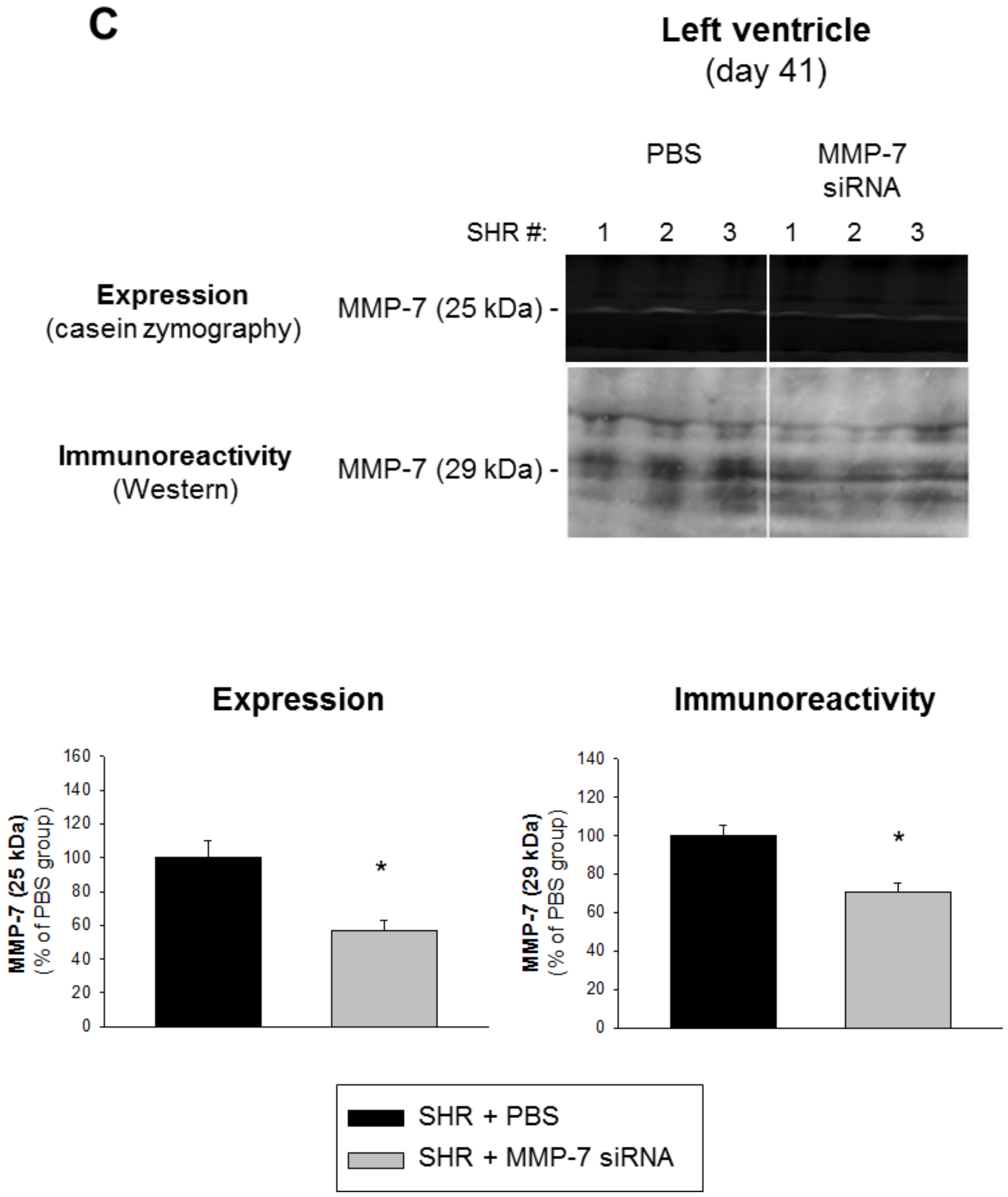
C
Left ventricle
(day 41)
PBS
MMP-7
siRNA
SHR #:
1
2
3
1
2
3
Expression
(casein zymography)
MMP-7 (25 kDa) -
Immunoreactivity
(Western)
MMP-7 (29 kDa) -
Expression
MMP-7 (25 kDa)
(% of PBS group)
0
20
40
60
80
100
120
140
160
*
Immunoreactivity
MMP-7 (29 kDa)
(% of PBS group)
0
20
40
60
80
100
120
140
*
SHR + PBS
SHR + MMP-7 siRNA

Figure 2-8 Assessment of off-target effects of siRNA.

Interferon γ (IFN-γ) levels in spontaneously hypertensive rats (SHR) and mice treated with MMP-7 siRNA or PBS. The rats were subjected to the treatment protocol illustrated in **Figure 4**; data at day 41. The mice were treated for 14 days and euthanized on day 16. IFN γ levels were measured in indicated organs by ELISA. (*): $p < 0.05$. Results are means ± SEM of 4 animals in each group.

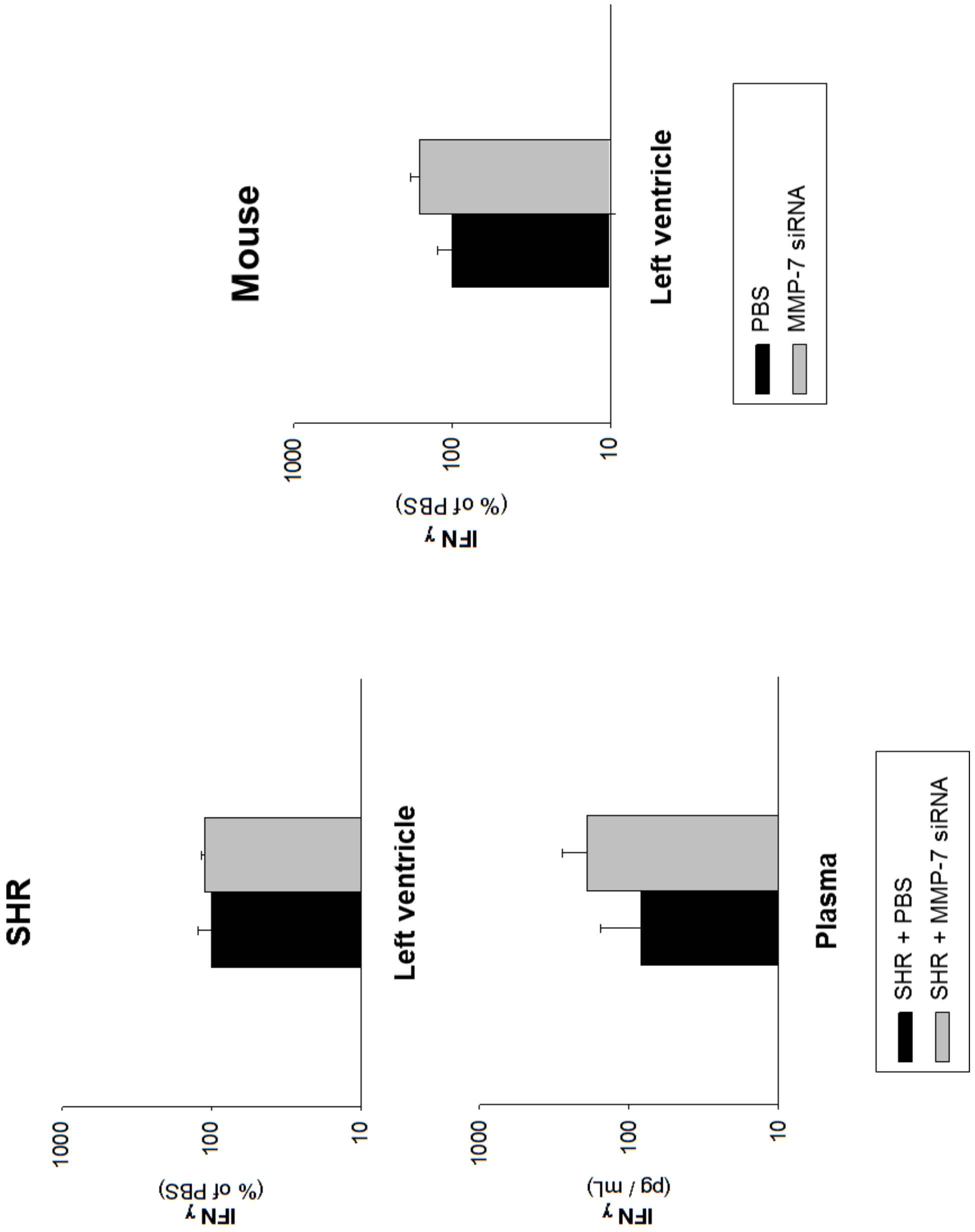
SHR
IFN γ
(% of PBS)
1000
100
10
Left ventricle
IFN γ
(pg / mL)
1000
100
10
Plasma
SHR + PBS
SHR + MMP-7 siRNA
Mouse
IFN γ
(% of PBS)
1000
100
10
Left ventricle
PBS
MMP-7 siRNA

Figure 2-9 Transcriptional relationships between MMP-7, ADAM-12 and hypertrophy marker genes define novel signalling pathways under basal conditions vs. sustained agonist-stimulation.

A-D, Quantitative analysis of mRNA expression levels of indicated genes. Mice were administered either PBS or MMP-7 siRNA (0.4 mg/kg/d for 14 days) through a 1st osmotic minipump followed by the administration of either PBS (i.e., basal conditions) or angiotensin II (1.4 mg/kg/d, for 10 days i.e., from day 5 to day 15 – i.e., sustained agonist-stimulation), through a 2nd osmotic minipump. The mice were euthanized on day 16 and mRNA levels were measured in left ventricle by quantitative RT-PCR using TaqMan probes.

A, B, Analysis of MMP-7 and ADAM-12 expression.

C, Analysis of hypertrophy marker genes: β myosin heavy chain (bMHC), brain natriuretic peptide (BNP), and α skeletal actin (alpha-sk-actin). Mice were administered either PBS or MMP-7 siRNA (0.4 mg/kg/d for 14 days) through a 1st osmotic minipump followed by the administration of either PBS (i.e., basal conditions) or angiotensin II (1.4 mg/kg/d, for 10 days i.e., from day 5 to day 15 – i.e., sustained agonist-stimulation), through a 2nd osmotic minipump. The mice were euthanized on day 16 and mRNA levels were measured in left ventricle by quantitative RT-PCR using TaqMan probes.

D, Examples of genes whose mRNA expression levels were unaltered by the administration of siRNA to MMP-7. TACE: TNF-α convertase (also known as ADAM-17). TIMP-2: tissue inhibitor of metalloproteinases-2. MMP-9: Matrix metalloproteinase-9. Mice were administered either PBS (i.e., basal conditions) or MMP-7 siRNA (0.4 mg/kg/d for 14 days). The mice were euthanized on day 16 and mRNA levels were measured in left ventricle by quantitative RT-PCR using TaqMan probes.

E, Quantitative analysis of mRNA expression levels of TACE and ADAM-12 genes in MMP-$7^{-/-}$ mice vs. age-matched wild type mice.

F, Pre-treatment with MMP-7 siRNA prior to angiotensin II infusion significantly attenuated angiotensin II-induced hypertension in mice. The mice received a 1st minipump delivering either vehicle (PBS) or siRNA (0.4 mg/kg/d for 14 days). On day 5, the mice were implanted with a 2nd minipump loaded with either PBS or angiotensin II (Ang II, 1.4 mg/kg/d).

G, Pre-treatment with MMP-7 siRNA prevents Ang II-induced left ventricular hypertrophy. **Left panel:** Ratio of corrected left ventricle mass (corr. LV mass; measured by M-mode echocardiography) to body weight (BW). Echocardiographic analysis conducted 10 days after implantation of a 2nd osmotic minipump (i.e., on day 15). **Right panel:** Heart weight (HW) to body weight (BW) ratio. The mice were euthanized on day 16.

(*): $p < 0.05$ vs. PBS. (+): $p < 0.05$ vs. (PBS + Ang II). Results are means ± SEM of 4 mice in each study group.

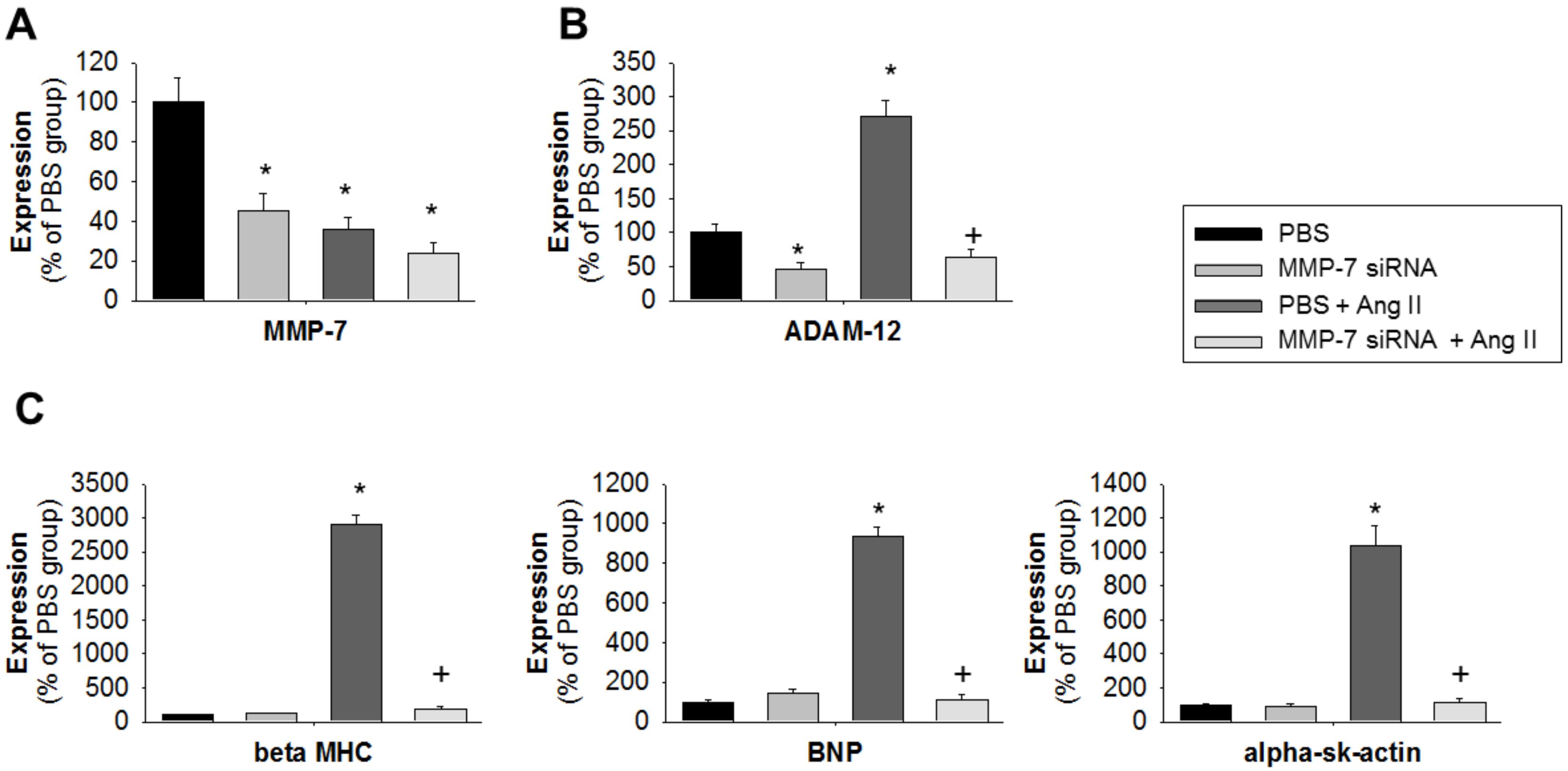
A
Expression (% of PBS group)
0
20
40
60
80
100
120
*
*
*
MMP-7
B
Expression (% of PBS group)
0
50
100
150
200
250
300
350
*
*
+
ADAM-12
PBS
MMP-7 siRNA
PBS + Ang II
MMP-7 siRNA + Ang II
C
Expression (% of PBS group)
0
500
1000
1500
2000
2500
3000
3500
*
+
beta MHC
Expression (% of PBS group)
0
200
400
600
800
1000
1200
*
+
BNP
Expression (% of PBS group)
0
200
400
600
800
1000
1200
1400
*
+
alpha-sk-actin

D

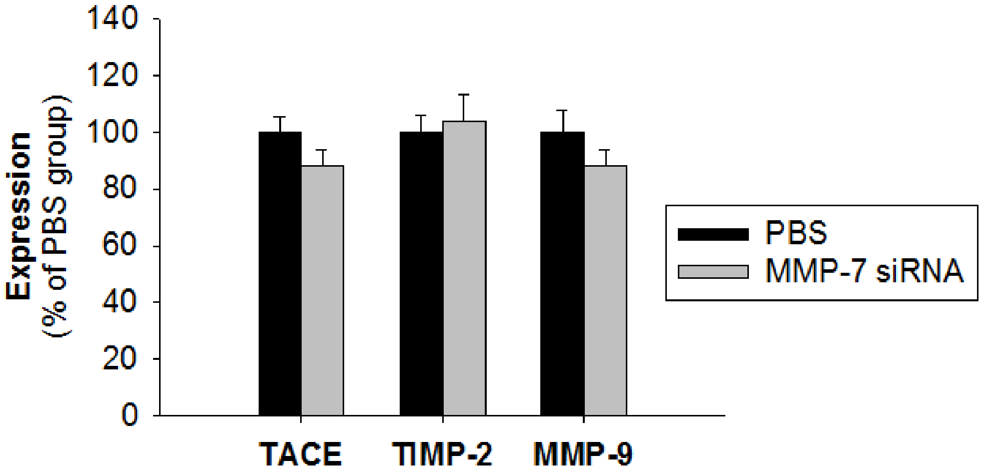
Expression
(% of PBS group)
140
120
100
80
60
40
20
0
TACE
TIMP-2
MMP-9
PBS
MMP-7 siRNA

E

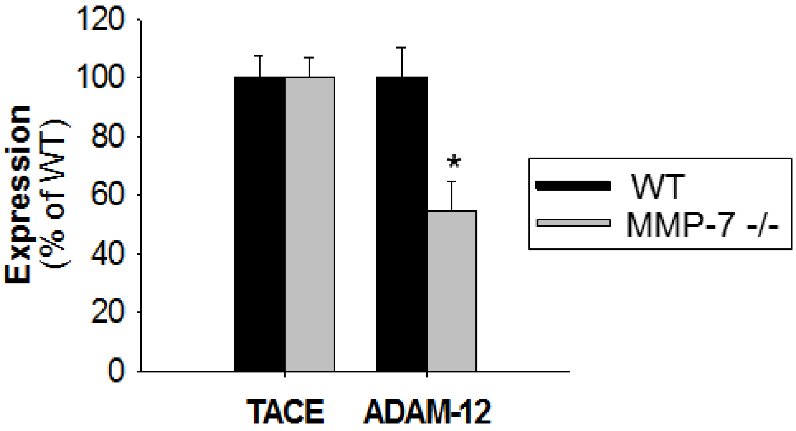
Expression
(% of WT)
120
100
80
60
40
20
0
*
TACE
ADAM-12
WT
MMP-7 -/-

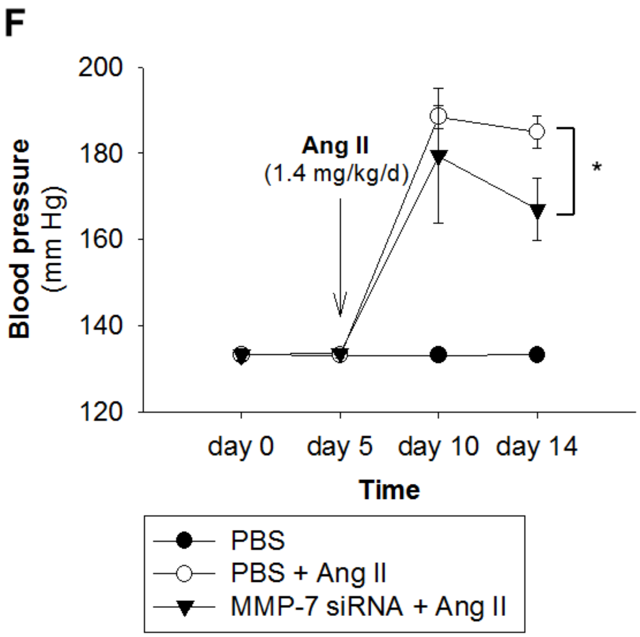
F
Blood pressure
(mm Hg)
200
180
160
140
120
Ang II
(1.4 mg/kg/d)
*
day 0
day 5
day 10
day 14
Time
PBS
PBS + Ang II
MMP-7 siRNA + Ang II

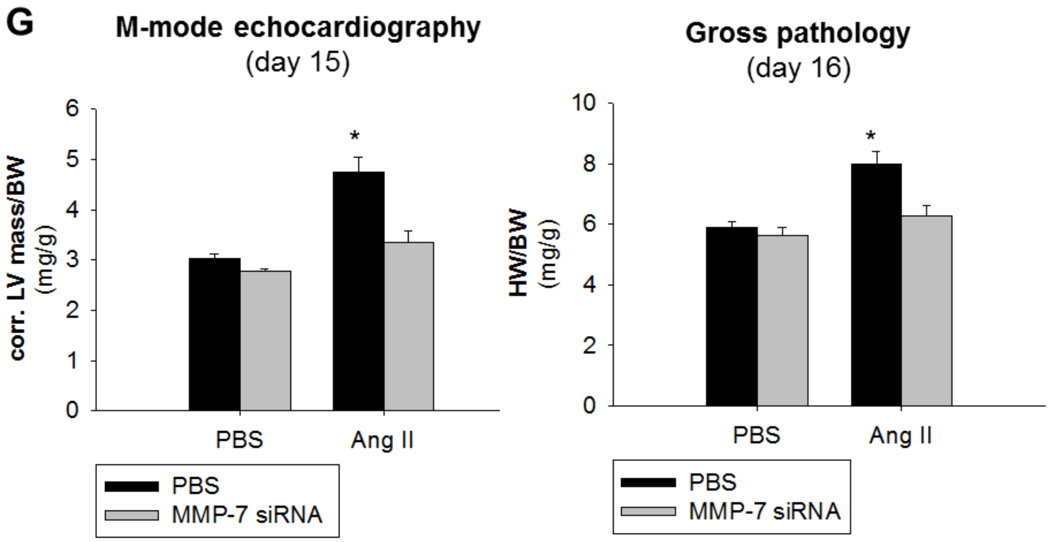
G
M-mode echocardiography
(day 15)
corr. LV mass/BW
(mg/g)
6
5
4
3
2
1
0
*
PBS
Ang II
PBS
MMP-7 siRNA
Gross pathology
(day 16)
HW/BW
(mg/g)
10
8
6
4
2
0
*
PBS
Ang II
PBS
MMP-7 siRNA

Figure 2-10 MMP-7$^{-/-}$ mice are protected from norepinephrine-induced cardiac PDGFR activation and hypertrophy.

A, Left panel: Quantitative analysis of the corrected left ventricular mass of MMP-7$^{-/-}$ mice and age-matched wild type mice challenged with norepinephrine (NE, 1.5 mg/kg/d) once or twice daily for 9 days. **Right panel:** Representative echocardiographic M-mode tracings of the left ventricle. IVS: intraventricular septum. LVID: left ventricular internal dimension. LVPW: Left ventricular posterior wall. (*): $p < 0.05$ vs. baseline. Results are means ± SEM of 4-5 mice per group.

B, Western blot analysis showing the phosphorylation of the cardiac platelet derived growth factor receptor (PDGFR) β in the heart of wild type mice vs. MMP-7$^{-/-}$ mice injected twice daily with norepinephrine (NE) for 9 days and euthanized on day 12. Results are expressed as mean ± SEM of 4 mice in each study group.

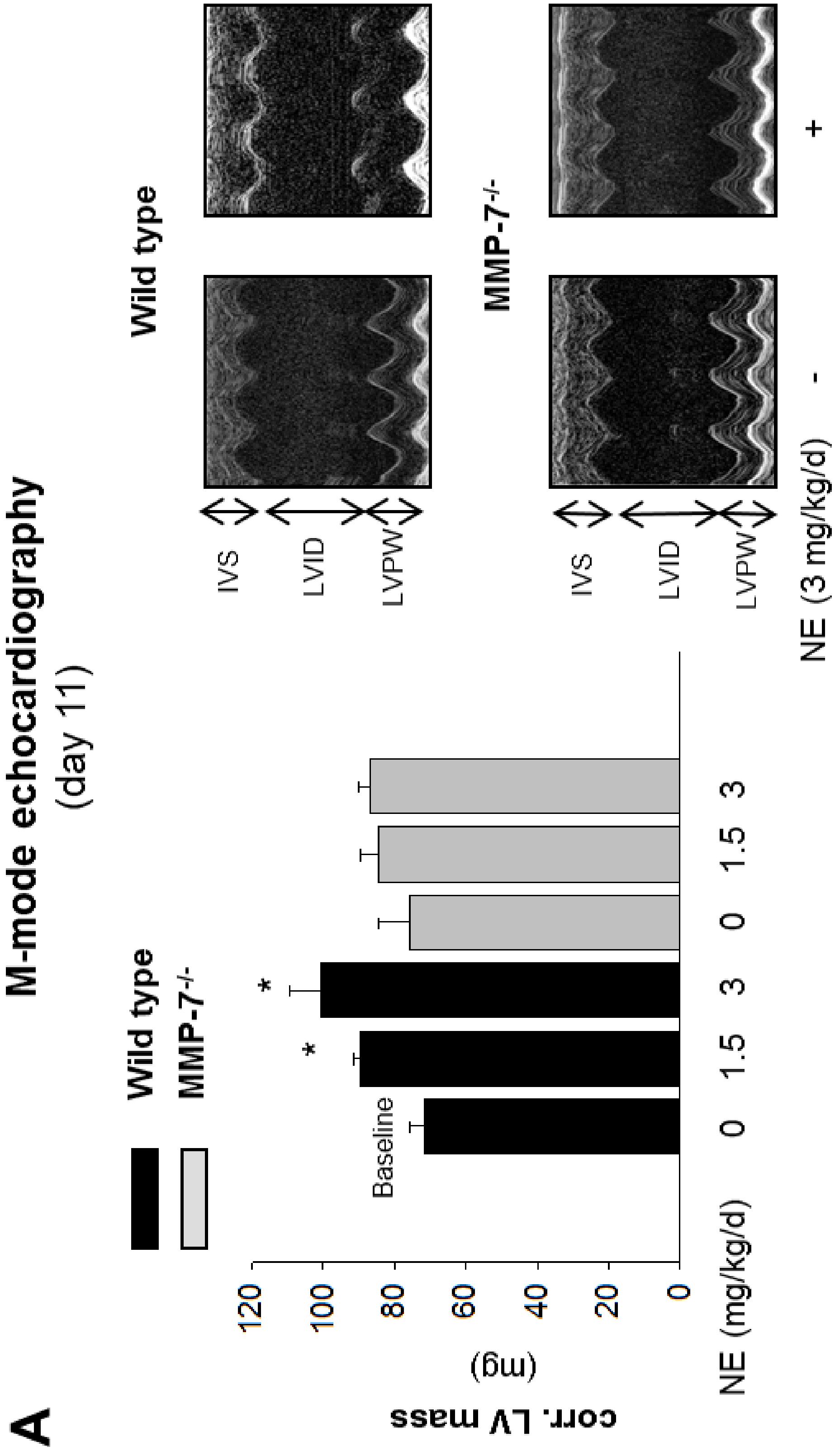
A
M-mode echocardiography
(day 11)
Wild type
MMP-7-/-
corr. LV mass (mg)
120
100
80
60
40
20
0
Baseline
*
*
NE (mg/kg/d)
0
1.5
3
0
1.5
3
Wild type
MMP-7-/-
IVS
LVID
LVPW
IVS
LVID
LVPW
NE (3 mg/kg/d)
-
+

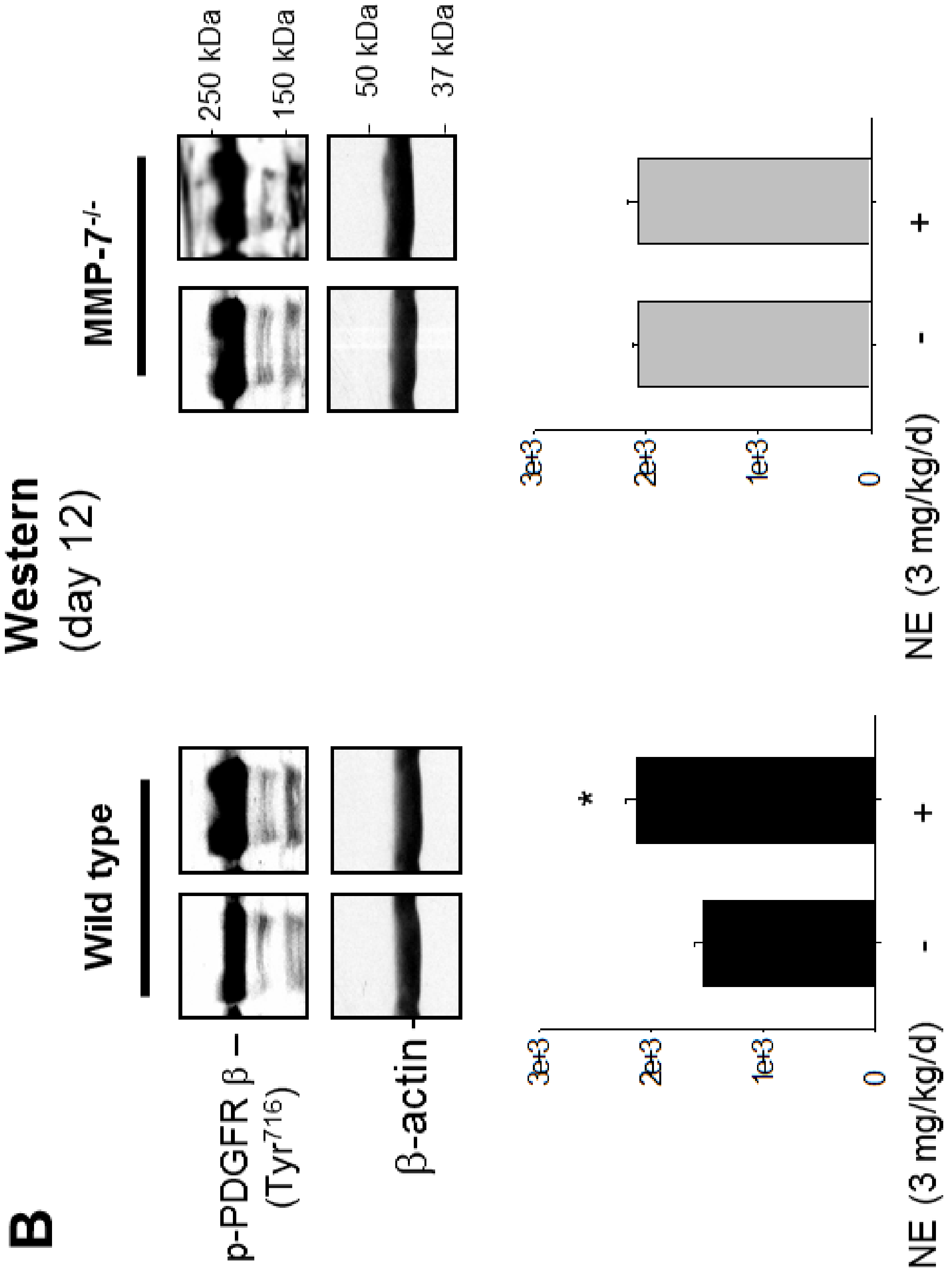
B
Western
(day 12)
Wild type
MMP-7-/-
p-PDGFR β (Tyr716)
β-actin
250 kDa
150 kDa
50 kDa
37 kDa
3e+3
2e+3
1e+3
0
*
-
+
NE (3 mg/kg/d)

Figure 2-11 Proposed modules and network structure of the metalloproteinase signalling pathways.

The diagram can explain the apparent functional redundancy of multiple metalloproteinases in the signalling of hypertension and hypertrophy processes. **Module #1** derives from previous work by many groups[5-7,11-13]. The activation of vasoconstrictive GqPCRs by cognate agonists post-transcriptionally induces the activity of metalloproteinases, such as MMP-7 and ADAM-12. The activated metalloproteinases next transactivate growth factor receptor signalling to trigger the mitogene activated protein kinase (MAPK) cascade. **Module #2** illustrates transcriptional relationships between MMP-7 and ADAM-12 under basal conditions, which is fully supported by the qRT-PCR data (**Figure 2-6**). **Module #3** is an interpretation that can explain how and why sustained GqPCR agonist-stimulation increases signalling through ADAM-12 while decreasing signalling through MMP-7. Accordingly, the high expression of ADAM-12 observed under sustained agonist-stimulation acts in a negative feed-back to inhibit MMP-7 transcription (**Figure 2-6**). The integration of the three modules can explain the complexity of metalloproteinase signalling during development of hypertension and hypertrophy processes. Accordingly, sustained agonist-stimulation regulates the development and progression of hypertension and hypertrophy processes through post-transcriptional (short-term) and transcriptional (long-term) mechanisms involving metalloproteinases, such as MMP-7 and ADAM-12[5-7,11-13]. The early signalling events by which vasoconstrictors trigger acute hypertension depend on MMP-7 but, over time, signalling becomes increasingly dependent on expression of other metalloproteinases including ADAM-12. Inhibition of MMP-7 transcription by ADAM-12 may be a compensatory mechanism to counter the development of hypertension and hypertrophy processes.

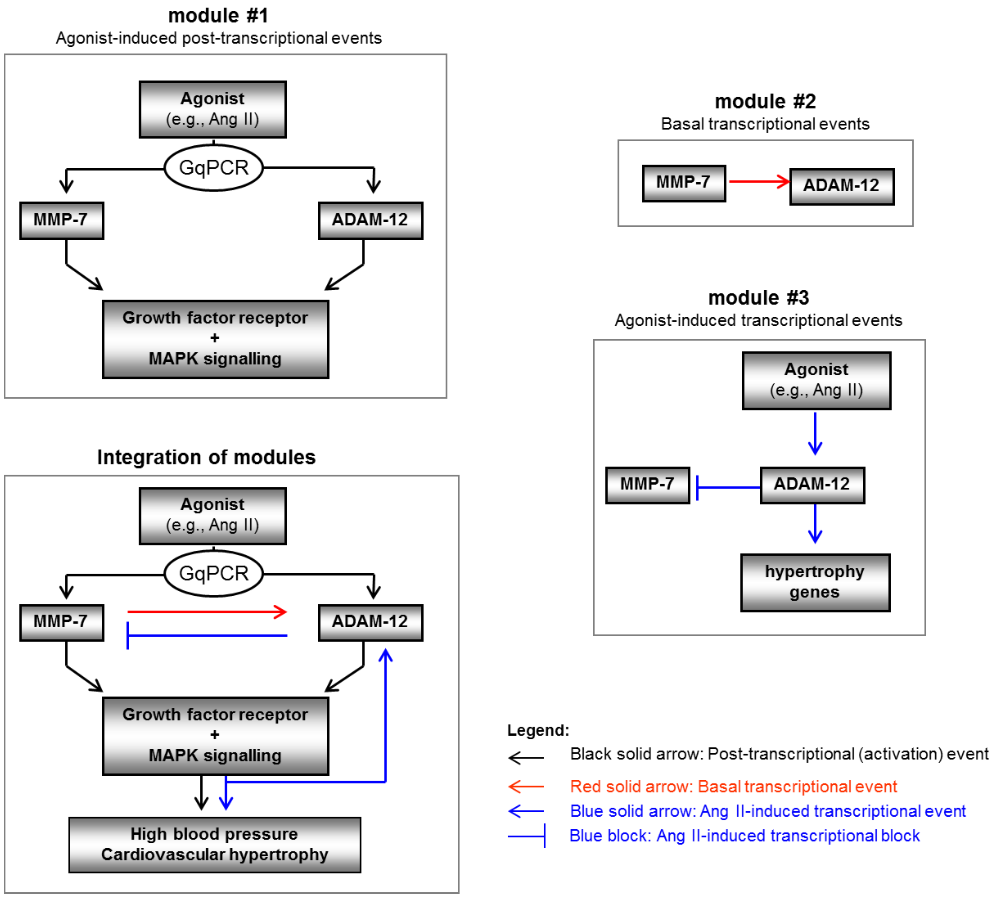
module #1
Agonist-induced post-transcriptional events
Agonist
(e.g., Ang II)
GqPCR
MMP-7
ADAM-12
Growth factor receptor
+
MAPK signalling
module #2
Basal transcriptional events
MMP-7
ADAM-12
module #3
Agonist-induced transcriptional events
Agonist
(e.g., Ang II)
MMP-7
ADAM-12
hypertrophy
genes
Integration of modules
Agonist
(e.g., Ang II)
GqPCR
MMP-7
ADAM-12
Growth factor receptor
+
MAPK signalling
High blood pressure
Cardiovascular hypertrophy
Legend:
Black solid arrow: Post-transcriptional (activation) event
Red solid arrow: Basal transcriptional event
Blue solid arrow: Ang II-induced transcriptional event
Blue block: Ang II-induced transcriptional block

2.5 References

1. Lifton RP, Gharavi AG, Geller DS. Molecular mechanisms of human hypertension. *Cell*. 2001;104:545-556
2. Biaggioni I. Should we target the sympathetic nervous system in the treatment of obesity-associated hypertension? *Hypertension*. 2008;51:168-171
3. Fernandez-Patron C. Therapeutic potential of the epidermal growth factor receptor transactivation in hypertension: a convergent signaling pathway of vascular tone, oxidative stress, and hypertrophic growth downstream of vasoactive G-protein-coupled receptors? *Can J Physiol Pharmacol*. 2007;85:97-104
4. Prenzel N, Zwick E, Daub H, Leserer M, Abraham R, Wallasch C, Ullrich A. EGF receptor transactivation by G-protein-coupled receptors requires metalloproteinase cleavage of proHB-EGF. *Nature*. 1999;402:884-888
5. Asakura M, Kitakaze M, Takashima S, Liao Y, Ishikura F, Yoshinaka T, Ohmoto H, Node K, Yoshino K, Ishiguro H, Asanuma H, Sanada S, Matsumura Y, Takeda H, Beppu S, Tada M, Hori M, Higashiyama S. Cardiac hypertrophy is inhibited by antagonism of ADAM12 processing of HB-EGF: metalloproteinase inhibitors as a new therapy. *Nat Med*. 2002;8:35-40
6. Hao L, Du M, Lopez-Campistrous A, Fernandez-Patron C. Agonist-induced activation of matrix metalloproteinase-7 promotes vasoconstriction through the epidermal growth factor-receptor pathway. *Circ Res*. 2004;94:68-76
7. Ohtsu H, Dempsey PJ, Frank GD, Brailoiu E, Higuchi S, Suzuki H, Nakashima H, Eguchi K, Eguchi S. ADAM17 mediates epidermal growth factor receptor transactivation and vascular smooth muscle cell hypertrophy induced by angiotensin II. *Arterioscler Thromb Vasc Biol*. 2006;26:e133-137
8. Rajagopalan S, Meng XP, Ramasamy S, Harrison DG, Galis ZS. Reactive oxygen species produced by macrophage-derived foam cells regulate the activity of vascular matrix metalloproteinases in vitro. Implications for atherosclerotic plaque stability. *J Clin Invest*. 1996;98:2572-2579
9. Okamoto T, Akuta T, Tamura F, van Der Vliet A, Akaike T. Molecular mechanism for activation and regulation of matrix metalloproteinases during bacterial infections and respiratory inflammation. *Biol Chem*. 2004;385:997-1006
10. Chien KR, Zhu H, Knowlton KU, Miller-Hance W, van-Bilsen M, O'Brien TX, Evans SM. Transcriptional regulation during cardiac growth and development. *Annu Rev Physiol*. 1993;55:77-95
11. Lautrette A, Li S, Alili R, Sunnarborg SW, Burtin M, Lee DC, Friedlander

G, Terzi F. Angiotensin II and EGF receptor cross-talk in chronic kidney diseases: a new therapeutic approach. *Nat Med*. 2005;11:867-874

12. Haro H, Crawford HC, Fingleton B, Shinomiya K, Spengler DM, Matrisian LM. Matrix metalloproteinase-7-dependent release of tumor necrosis factor-alpha in a model of herniated disc resorption. *J Clin Invest*. 2000;105:143-150
13. Sunnarborg SW, Hinkle CL, Stevenson M, Russell WE, Raska CS, Peschon JJ, Castner BJ, Gerhart MJ, Paxton RJ, Black RA, Lee DC. Tumor necrosis factor-alpha converting enzyme (TACE) regulates epidermal growth factor receptor ligand availability. *J Biol Chem*. 2002;277:12838-12845
14. Wilson CL, Heppner KJ, Labosky PA, Hogan BL, Matrisian LM. Intestinal tumorigenesis is suppressed in mice lacking the metalloproteinase matrilysin. *Proc Natl Acad Sci U S A*. 1997;94:1402-1407
15. Tsoporis JN, Marks A, Kahn HJ, Butany JW, Liu PP, O'Hanlon D, Parker TG. Inhibition of norepinephrine-induced cardiac hypertrophy in s100beta transgenic mice. *J Clin Invest*. 1998;102:1609-1616
16. Nava E, Rodriguez F, Moreno C, Llinas MT, Salazar FJ. Release of nitric oxide after acute hypertension. *J Cardiovasc Pharmacol*. 2000;36:444-450
17. Castro MM, Rizzi E, Figueiredo-Lopes L, Fernandes K, Bendhack LM, Pitol DL, Gerlach RF, Tanus-Santos JE. Metalloproteinase inhibition ameliorates hypertension and prevents vascular dysfunction and remodeling in renovascular hypertensive rats. *Atherosclerosis*. 2008;198:320-331
18. Brown DL, Desai KK, Vakili BA, Nouneh C, Lee HM, Golub LM. Clinical and biochemical results of the metalloproteinase inhibition with subantimicrobial doses of doxycycline to prevent acute coronary syndromes (MIDAS) pilot trial. *Arterioscler Thromb Vasc Biol*. 2004;24:733-738
19. Axisa B, Loftus IM, Naylor AR, Goodall S, Jones L, Bell PR, Thompson MM. Prospective, randomized, double-blind trial investigating the effect of doxycycline on matrix metalloproteinase expression within atherosclerotic carotid plaques. *Stroke*. 2002;33:2858-2864
20. Momiyama N, Koshikawa N, Ishikawa T, Ichikawa Y, Hasegawa S, Nagashima Y, Mitsuhashi M, Miyazaki K, Shimada H. Inhibitory effect of matrilysin antisense oligonucleotides on human colon cancer cell invasion in vitro. *Mol Carcinog*. 1998;22:57-63
21. Yonemura Y, Endo Y, Fujita H, Kimura K, Sugiyama K, Momiyama N, Shimada H, Sasaki T. Inhibition of peritoneal dissemination in human gastric cancer by MMP-7-specific antisense oligonucleotide. *J Exp Clin*

Cancer Res. 2001;20:205-212

22. Hasegawa S, Koshikawa N, Momiyama N, Moriyama K, Ichikawa Y, Ishikawa T, Mitsuhashi M, Shimada H, Miyazaki K. Matrilysin-specific antisense oligonucleotide inhibits liver metastasis of human colon cancer cells in a nude mouse model. *Int J Cancer*. 1998;76:812-816
23. Clemente CF, Tornatore TF, Theizen TH, Deckmann AC, Pereira TC, Lopes-Cendes I, Souza JR, Franchini KG. Targeting focal adhesion kinase with small interfering RNA prevents and reverses load-induced cardiac hypertrophy in mice. *Circ Res*. 2007;101:1339-1348
24. Hao L, Nishimura T, Wo H, Fernandez-Patron C. Vascular responses to alpha1-adrenergic receptors in small rat mesenteric arteries depend on mitochondrial reactive oxygen species. *Arterioscler Thromb Vasc Biol*. 2006;26:819-825
25. Kassiri Z, Oudit GY, Sanchez O, Dawood F, Mohammed FF, Nuttall RK, Edwards DR, Liu PP, Backx PH, Khokha R. Combination of tumor necrosis factor-alpha ablation and matrix metalloproteinase inhibition prevents heart failure after pressure overload in tissue inhibitor of metalloproteinase-3 knock-out mice. *Circ Res*. 2005;97:380-390
26. Rees DD, Palmer RM, Schulz R, Hodson HF, Moncada S. Characterization of three inhibitors of endothelial nitric oxide synthase in vitro and in vivo. *Br J Pharmacol*. 1990;101:746-752
27. Moncada S, Palmer RM, Higgs EA. Nitric oxide: physiology, pathophysiology, and pharmacology. *Pharmacol Rev*. 1991;43:109-142
28. Lauhio A, Konttinen YT, Salo T, Tschesche H, Nordstrom D, Lahdevirta J, Golub LM, Sorsa T. The in vivo effect of doxycycline treatment on matrix metalloproteinases in reactive arthritis. *Ann N Y Acad Sci*. 1994;732:431-432
29. Wilson CL, Ouellette AJ, Satchell DP, Ayabe T, Lopez-Boado YS, Stratman JL, Hultgren SJ, Matrisian LM, Parks WC. Regulation of intestinal alpha-defensin activation by the metalloproteinase matrilysin in innate host defense. *Science*. 1999;286:113-117
30. Zhang YC, Bui JD, Shen L, Phillips MI. Antisense inhibition of beta(1)-adrenergic receptor mRNA in a single dose produces a profound and prolonged reduction in high blood pressure in spontaneously hypertensive rats. *Circulation*. 2000;101:682-688
31. Nava E, Noll G, Luscher TF. Increased activity of constitutive nitric oxide synthase in cardiac endothelium in spontaneous hypertension. *Circulation*. 1995;91:2310-2313
32. Kawasaki H, Cline WH, Jr., Su C. Involvement of the vascular renin-angiotensin system in beta adrenergic receptor-mediated facilitation of vascular neurotransmission in spontaneously hypertensive rats. *J*

Pharmacol Exp Ther. 1984;231:23-32

33. Wang FQ, So J, Reierstad S, Fishman DA. Matrilysin (MMP-7) promotes invasion of ovarian cancer cells by activation of progelatinase. *Int J Cancer*. 2005;114:19-31
34. Lindsey ML, Escobar GP, Mukherjee R, Goshorn DK, Sheats NJ, Bruce JA, Mains IM, Hendrick JK, Hewett KW, Gourdie RG, Matrisian LM, Spinale FG. Matrix metalloproteinase-7 affects connexin-43 levels, electrical conduction, and survival after myocardial infarction. *Circulation*. 2006;113:2919-2928
35. Fedak PW, Moravec CS, McCarthy PM, Altamentova SM, Wong AP, Skrtic M, Verma S, Weisel RD, Li RK. Altered expression of disintegrin metalloproteinases and their inhibitor in human dilated cardiomyopathy. *Circulation*. 2006;113:238-245
36. Zhou CC, Zhang Y, Irani RA, Zhang H, Mi T, Popek EJ, Hicks MJ, Ramin SM, Kellems RE, Xia Y. Angiotensin receptor agonistic autoantibodies induce pre-eclampsia in pregnant mice. *Nat Med*. 2008;14:855-862

Chapter 3

TACE is key regulator of agonist-induced cardiac hypertrophy and fibrosis

The data presented in this chapter is published in the following journal article:

Wang X, Oka T, Chow FL, Cooper S, Odenbach J, Lopaschuk G, Kassiri Z, Fernandez-Patron C. TACE is a key regulator of agonist-induced cardiac hypertrophy. *Hypertension.* 2009 Sep;54(3):575-82.

Contribution: Designed siRNAs for TACE, conducted animal studies, performed zymography, western immunoblotting and proteolytic activity assays, immunofluorescent staining, data analysis and data interpretation, contributed to the construction of the hypothesis, drafted the first version of the manuscript together with my supervisor and revised the manuscript.

3.1 Introduction

Cardiac remodelling is a major hallmark of hypertensive disorders and is associated with development of cardiac hypertrophy (i.e., an increase in cell size of individual cardiomyocytes), which causes thickening of the myocardium. Although initially compensatory, sustained hypertrophic growth is pathological, in part, because of its association with the development of fibrosis (i.e., increased synthesis and deposition of extracellular matrix proteins), which disrupts the normal structure and contractile properties of the myocardium[1]. Pathological cardiac remodelling is thus detrimental for cardiac function and may cause cardiac dysfunction, myocardial stiffness and increased risk of heart failure, sudden death and stroke[2-5]. However, it remains unclear how and why such apparently distinct processes as cardiac hypertrophy and fibrosis develop with hypertension and if pressure overload in hypertension is causal.

Our laboratory is investigating the general hypothesis that cardiac remodelling may be associated with hypertension simply because high blood pressure, hypertrophy and fibrosis share common inducers, which signal through largely overlapping pathways. Among the common inducers of high blood pressure, hypertrophy and fibrosis are vasoconstrictive agonists such as catecholamines, endothelins, and angiotensin II[6-9]. These agonists all act on Gq protein-coupled receptors (GqPCRs), which in turn activate the classical phospholipase C / protein kinase C pathway and reactive oxygen species, leading to the activation of downstream matrix metalloproteinases (MMPs) and “a disintegrin and metalloproteinases” (ADAMs). Among them, ADAM-12 and ADAM-17 (TACE or tumor necrosis factor-α converting enzyme) are perhaps the best studied in the cardiovascular and endocrine systems[7-12]. ADAM-12 and TACE are synthesized and stored in the rough endoplasmic reticulum until they mature in a late Golgi compartment. Their maturation following agonist-stimulation involves the removal of the pro-domain from the precursor protein. The activated metalloproteinases from both MMP and ADAM families are able to cleave a host of common substrates including extracellular matrix (ECM) proteins (e.g., collagens), pro-inflammatory mediators (e.g., TNF-α) and growth factors (e.g., TGF-α, HB-EGF) to signal through their receptors and downstream mitogen-activated protein kinases (MAPKs), which transcriptionally activate the expression of immediate-early and fetal genes, including hypertrophy markers[13]. There is increasing evidence that different metalloproteinases including MMP-2, MMP-7, ADAM-12 and TACE may thus mediate tissue remodelling as well as injury in both cardiovascular and renal systems[7,9,12,14-18].

The similar agonist-activation profile, substrates and signalling pathways of some of the growth factor sheddases such as ADAM-12 and TACE suggest a redundancy of their functions *in vivo*, particularly in signalling of cardiovascular growth processes[7-9,12,19,20]. ADAM-12 has previously been directly implicated in cardiac hypertrophy[7]. However, the involvement of TACE in cardiac hypertrophy has been suggested[9,10] but not yet demonstrated *in vivo*. Although TACE is a key mediator of angiotensin II-induced renal injury and fibrosis[9,10,21], it is unknown whether TACE mediates the development of agonist-induced cardiac fibrosis.

If TACE plays a role in the development of cardiac hypertrophy and fibrosis, it would be important to determine whether, and if so how, TACE and ADAM-12 coordinate each other's expression and functional redundancy. Would their relationships follow a hierarchical pattern? Would such hierarchical relationships be of significance for the mechanisms and treatment of pathological cardiac remodelling?

Here, we address these important questions by focusing on the role of TACE in the development of agonist-induced cardiac hypertrophy and fibrosis processes. Our findings establish a novel central role of TACE in signalling of both processes, upstream of MMP-2 and ADAM-12.

3.2 Materials and methods

Animals Animal studies were conducted under the protocol approved by University of Alberta Animal Care and Use Committee. All animals were male and housed at the Animal Facility of the University of Alberta until use. C57BL/6 mice (12 or 20-week old) were purchased from The Jackson Laboratory (Bar Harbor, ME). Already-hypertensive (22-week old) spontaneously hypertensive rats (SHR) were purchased from Charles River Laboratories Inc. (Wilmington, MA). All animals were anesthetised by 3% isoflurane through inhalation before and during the surgical procedures.

Unless specifically indicated, 4 animals were used in each group in the experiments

Knockdown of TACE using siRNA The animal (mouse and rat) model of TACE expression knock-down was generated using a previously validated TACE siRNA[10] (for siRNA design, please see **Figure 1**) synthesized by Sigma-Aldrich (Paris). Luciferase siRNA (antisense: 5’-GUAUCUCUUCAUAGCCUUAdTdT) was used as control. The first two nucleotides of each strand were 2’-O methylated to increase siRNA stability. The siRNAs were dissolved in PBS prior to use.

siRNA studies in rats siRNAs (9 nmol/kg/d, i.e., 0.12 mg/kg/d) or PBS were infused for 14 days into spontaneously hypertensive rats (SHR) through subcutaneously implanted ALZET osmotic minipumps (DURECT Corporation, Cupertino, CA) in the back of the animals.

siRNA studies in mice siRNAs (30 nmol/kg/d, i.e., 0.4 mg/kg/d) or PBS were infused for 14 days into C57BL/6J mice through subcutaneously implanted osmotic minipumps.

Another group of mice received siRNA (15μg/mouse, i.e., 0.45mg/kg) or PBS by injection via jugular vein. The injection was conducted every 5 days to maintain the knockdown effects.

Mouse model of angiotensin II-induced hypertension Male C57BL/6 mice were infused with angiotensin II (1.4 mg/kg/d) through subcutaneously implanted osmotic minipumps implanted on the backs for 12 days.

Systolic blood pressure measurement Systolic blood pressure of conscious animals was measured indirectly using a commercially available computerized tail cuff plethysmography system (Kent Scientific Corporation, Torrington, CT). All animals were trained by being placed into the restrainer for 2-3 times before there blood pressure was measured.

Echocardiography *In vivo* assessment of anatomical structures and hemodynamic function in mice was conducted by echocardiography. The animals were first anaesthetized with 2.0% Isoflurane, and their cardiac function was subsequently analyzed using a Vevo 770 high-resolution imaging system (ON, Canada). Three consecutive heartbeats of each frame were analyzed to measure the wall thickness and end-diastolic (EDD) and end-systolic (ESD) internal dimensions of the left ventricle (LV). Echocardiographic corrected LV mass (in mg) was calculated as: $1.05 \times 0.8 \times [(LVID;d + LVPW;d + IVS;d)^3 – (LVID;d)^3]$ on diastole (d). In the formula, ID is internal diameter (in mm), PW is the posterior wall dimension (in mm) and IVS is the interventricular septum dimension (in mm).

Sample preparation Animal organs were washed in isotonic saline buffer, rinsed and weighed. Protein extraction was done in 25 mM Tris, 62.5 mM NaCl, 1.25 mM PMSF, 62.5 mM Glycerol-2-phosphate, 12.5 mM sodium pyrophosphate, 125 µM NaF, 6.25 µg/ml leupeptine, 312.5 µM sodium orthovanadate, 12.5% glycerol, pH 7.4, supplemented with 5% SDS and 1% Triton X-100. To determine the protein content, the extracts were separated by 12% SDS-PAGE followed by densitometric analysis of Coomassie blue stained bands. Equal protein loads (approximately 50 μg/well) were subsequently subjected to zymography or western analysis.

Substrate zymography To determine MMP-2 levels by quantitative substrate zymography, lysates were subjected to electrophoresis on SDS-PAGE gels co-polymerized with gelatin (2 mg/mL), respectively. Following electrophoresis, the gel was washed with 2.5% Triton X-100 for 3 x 20 min. Activity was developed by incubating the gel for 16 hrs at 37°C in enzyme assay buffer (25 mM Tris, 5 mM $CaCl_2$, 142 mM NaCl, 0.5 mM NaN_3, pH 7.6) supplemented with 1 mM benzamidine and then the gel was stained with Coomassie blue.

Western immunoblotting The extracted proteins were separated using SDS-PAGE gels. The proteins were transferred to nitrocellulose membrane (BioRad) and blocked in 5% milk or 5% BSA. Blots were incubated with antibody against TACE (1:250) (Santa Cruz), p-ERK-1/2 (1:1000) (Sigma-Aldrich), ERK-1/2 (1/1000) (Cell Signaling), MMP-2 (1/500) (Calbiochem) followed by incubation in corresponding secondary antibodies.

TACE proteolytic activity assay TACE activity was determined using a fluorogenic TACE substrate IV Abz-LAQAVRSSSR-Dpa (Calbiochem). The substrate is cleaved by TACE at the Ala-Val amide bond. The reaction was monitored by using light of 320 nm for excitation and a 420 nm filter to detect flourescence emitted by the substrate following cleavage by TACE. To further ensure selectivity, the assay was conducted in the absence and presence of a TACE pharmacological inhibitor (TAPI-2) and results were corrected by subtracting the TAPI-2 resistant activity (~40% across all samples). Equal amount of protein was used as determined by Bradford assay.

Cryosectioning Hearts and aortas from SHR treated with PBS, or TACE siRNA were embedded in Tissue-Tek (Sakura), frozen in dry ice and stored at -70 ºC.

Sections were cut with a Leica microtome and left at room temperature overnight to dehydrate prior to fixation with cold acetone.

Immunofluorescence Slides with 6μm thick sections of frozen mouse hearts were stained with commercially available antibodies for actin (Sigma) and TACE (Santa Cruz) diluted 1:250. Slides were imaged using a spinning disk laser confocal microscope (Confocal Imagine Core facility, University of Alberta) and analyzed with Improvision Velocity® software.

WGA-FITC staining and cardiomyocytes cross-sectional area quantification Slides with 10 μm thick sections of frozen mouse hearts. Slides were washed in PBS-T and incubated for 2 hrs in 50 μg/mL Wheat Germ Albumin (WGA) conjugated with FITC (Invitrogen) and DAPI solution then washed again in PBS-T and mounted with a coverslip. Confocal microscope images were taken with a spinning disk laser confocal microscope (Confocal Imagine Core facility, University of Alberta) and analyzed with ImageQuant 5.1 to determine cardiomyocyte cross-sectional area (>100 cells per heart were counted).

Collagen staining with picrosirius red Slides with 10 μm thick mouse heart frozen sections were brought back to water and stained for 1 hr in PSR staining solution (1 g/L Direct Red 80 in saturated picric acid solution), washed in acidified water and dehydrated. Slides were photographed by a DCM500 camera digital camera on a Kyowa Medlux-12 light microscope and viewed using ScopePhoto (NonLinear Dynamics). Area covered by collagen was determined by converting the image to a grayscale image showing measurement of red versus blue+green colour in Adobe Photoshop and then using ImageQuant 5.1 to measure the area of Picrosirius red staining.

Interferon-γ Measurement The level of interferon γ (IFN γ) in siRNA treated mice or SHR was measured using *VeriKine*^{TM} Mouse IFN-γ sandwich ELISA kit (Ebiosciences) as per manufactures instructions.

RNA expression analysis by TaqMan RT-PCR Total RNA was extracted from flash-frozen organs using Trizol (Invitrogen), and cDNA was generated from 1 µg RNA using the random hexamer. Expression analysis of the genes was performed by TaqMan RT-PCR using ABI 7900 sequence detection system. 18S rRNA was used as an endogenous control as described previously[22].

Data analysis Results were analyzed using one-way ANOVA (between multiple groups) or t-test (between two groups) (Jandel SigmaStat 3.5 statistical software). In the echocardiography studies, between-group comparisons of the means were performed by one-way ANOVA followed by Scheffe's F correction for multiple comparisons of the means.

3.3 Results

TACE mediates cardiac hypertrophy in genetically hypertensive rats

We examined whether blocking TACE expression in already-hypertensive 22-week old spontaneously hypertensive rats (SHR) would affect systolic blood pressure and/or development of cardiac hypertrophy. To inhibit TACE gene expression we chose an RNA interference-based approach using a previously validated siRNA[10] with the exception that we introduced a chemical modification (2'-O-methylation) on the 5' end of the double stranded RNA molecule to enhance its resistance to nucleases *in vivo* (**Figure 3-1**). The administration of TACE siRNA for 30 days through a subcutaneous osmotic minipump (protocol depicted in **Figure 3-2A**) effectively stopped the progression of cardiac hypertrophy as evidenced by M-mode echocardiography and gross pathology studies (**Figure 3-2B, C and Table 3-1**). In addition, the cross-sectional width of cardiomyocytes was decreased on average by 38% in SHR receiving TACE siRNA vs. SHR receiving vehicle (PBS) (n=3 rats in each study group, $p<0.05$ by t-test), confirming the anti-hypertrophic effects of TACE siRNA.

Rats receiving TACE siRNA had significantly lower TACE immunoreactivity (**Figures 3-2D**) and TACE proteolytic activity (100.00±6.52% (PBS) *vs.* 58.35±4.00% (TACE siRNA), *p*=0.006 by *t*-test n=3), MMP-2 activity (**Figure 3-2D**), and ERK-1/2 phosphorylation (**Figure 3-3**), compared with rats receiving an unrelated RNA or vehicle (PBS). These data indicated that the TACE siRNA effectively decreases TACE expression and activity as well as TACE downstream signalling.

However, treatment with TACE siRNA did not decrease the blood pressure in the SHR model (**Figure 3-4A**) despite TACE siRNA causing a significant inhibition of TACE proteolytic activity in resistance arteries of the rats (**Figure 3-4B**).

Taken together, these observations provide strong *in vivo* evidence that TACE expression regulates development of cardiac hypertrophy, but TACE may not play a major role in regulation of blood pressure in hypertension.

TACE and ADAM-12 form a novel signalling axis *in vivo*

To further clarify how TACE knock-down impacts the development of cardiac hypertrophy we conducted functional studies, quantitative RT-PCR and activity determinations in mice where TACE was knocked-down by *in vivo* RNA interference.

Administration of TACE siRNA (0.4 mg/kg/d) through subcutaneous osmotic minipumps for 14 days in mice resulted in a significant down-regulation in myocardial TACE mRNA levels (**Figure 3-5A**) and proteolytic activity (**Figure 3-5B**).

To substantiate the effects of TACE siRNA, we conducted a small additional study (n=2 mice per group) using a different route of siRNA administration (ie, intravenous). Mice were injected with TACE siRNA (15 μg every five days) into their jugular vein, a method that was shown to effectively knockdown the expression of cardiac target proteins[23]. TACE expression was decreased by 30±5 % in mice that received TACE siRNA by intravenous injection, vs. mice that received PBS.

Mice that received TACE siRNA did not display any echocardiographic abnormalities (**Table 3-2**).

Interestingly, knock-down of TACE resulted in the down-regulation of MMP-2 mRNA levels (**Figure 3-5C**) and activity (**Figure 3-5D**) as well as in ADAM-12 gene expression (**Figure 3-5E**). However, the siRNA had otherwise insignificant effects on other genes including MMP-9 (n=4 mice, *p*=0.488 by t-test), tissue inhibitor of metalloproteinases (TIMP)-3 – an endogenous inhibitor of TACE[20] (n=4 mice, *p*=0.223 by t-test) and interferon-γ (n=4 mice, *p*=0.45 by t-test). The unchanged level of interferon-γ demonstrated that the small RNA-induced innate immune response[24]was not activated. This further suggested that the observed down-regulation of MMP-2 or ADAM-12 was caused by a decrease in TACE expression, rather than a non-specific effect of the TACE siRNA.

As expected, the blood pressure of mice receiving angiotensin II through osmotic minipumps (1.4 mg/kg/d for 10 days) was significantly elevated vs. mice receiving PBS {BP (PBS + Ang II) = 188±1 mmHg, BP(PBS) = 133±2 mmHg, *p*<0.001 by t-test, n=4 mice per study group}. Mice receiving either TACE siRNA or luciferase (Luc) siRNA (0.4 mg/kg/d) by osmotic minipumps also developed hypertension upon infusion of angiotensin II for 10 days {BP(TACE siRNA + Ang II) = 167±13 mmHg, BP(Luc siRNA + Ang II) = 180±2 mmHg, n = 4 mice per group)}. Similarly, after 10 days of angiotensin II infusion, blood pressure was elevated in mice receiving PBS, TACE siRNA or Luc siRNA by jugular vein injection {BP(Ang II) = 179±4 mmHg, BP(TACE siRNA + Ang II) = 173±3 mmHg, BP(Luc siRNA + Ang II) = 179±3 mmHg, n=3-4 mice per study group}.

Interestingly, in mice that received TACE siRNA by intravenous injection (but not in those that received TACE siRNA by osmotic minipumps) there seemed to be a delay in the on-set of the hypertension. Indeed, after 5 days of angiotensin II infusion, blood pressure was higher in mice that received either PBS or Luc siRNA by intravenous injection vs. those that received TACE siRNA {BP(PBS + Ang II) = 150±3 mmHg , BP(Luc siRNA + Ang II) = 164±9 mmHg, BP(TACE siRNA + Ang II) = 122±11 mmHg, n=3-4 mice per study group}.

Mice that received angiotensin II (1.4 mg/kg/d) for 12 days displayed elevated expression and proteolytic activity of TACE, MMP-2 and ADAM-12 (**Figures 3-5, 3-6**) as well as left ventricular hypertrophy (**Table 3-2 and Figures 3-7A, B, 38, B, 3-9A, C**) which was associated with an overexpression of myocardial hypertrophy marker genes (brain natriuretic peptide, and α-skeletal actin and β-myosin heavy chain) (**Figures 3-7C, 3-8C, 3-9B**).

Cardiac fibrosis, the increased deposition of extracellular matrix proteins in myocardium that is typically associated with pathological cardiac hypertrophy, was also induced by angiotensin II as shown by the increased expression of the extracellular matrix proteins, collagen types I and III and fibronectin (**Figures 3-7D, 3-8D, 3-9D, E**)

Pre-treatment with TACE siRNA through osmotic minipumps decreased cardiac TACE levels and activity (**Figure 3-5A, B**) and protected the mice from angiotensin II-induced left ventricular hypertrophy (**Table 3-2 and Figure 3-7A, B**) and cardiac fibrosis (**Figure 3-7D**). The protective effect of TACE siRNA was associated with the normalization of the expression of MMP-2, ADAM-12 (**Figure 3-5C-E**), hypertrophy marker genes (**Figure 3-7C**) and ECM proteins (**Figure 3-7D**).

Unlike TACE siRNA, the treatment of mice with a siRNA against luciferase did not protect from angiotensin II-induced left ventricular hypertrophy and fibrosis, as evidenced by M-mode echocardiography, gross pathology studies and RT-PCR analysis of molecular markers of hypertrophy and fibrosis (**Figure 3-8**).

Further excluding a role of the administration route in the protective effects of TACE siRNA, in mice receiving siRNA by jugular vein injection, TACE siRNA also blocked the angiotensin II-induced expression of TACE (**Figure 3-6A**), MMP-2 (**Figure 3-6B**) and ADAM-12 (**Figure 3-6C**). TACE siRNA, but not luciferase siRNA, prevented angiotensin II-induced cardiac hypertrophy, as indicated by gross pathology (**Figure 3-9A**), cardiomyocyte cross-sectional area (**Figure 3-9c**) and expression of hypertrophic markers (**Figure 3-9B)**. Additionally, knockdown of TACE by siRNA also protected mice from angiotensin II-induced cardiac fibrosis, as determined by cardiac interstitial collagen staining with picrosirius red (**Figure 3-9D**) and expression of collagen I (**Figure 3-9E**).

These findings are the first evidence that the down-regulation of TACE expression may prevent the transcription of metalloproteinases such as MMP-2 and ADAM-12 and downstream hypertrophy markers, which together could act as effectors of TACE in agonist-induced cardiac hypertrophy.

3.4 Discussion

This investigation has resulted in several novel observations: To our knowledge our findings suggest for the first time *in vivo* that agonist-induced cardiac hypertrophy and fibrosis is signalled through ADAM-17/TACE, and decreasing TACE activity by RNA interference protects from cardiac hypertrophy and fibrosis in models of hypertension. Furthermore, our data suggest that TACE may act by promoting the transcription of metalloproteinases (such as MMP-2 and ADAM-12) and downstream genes of so-called molecular markers of hypertrophy and fibrosis. Together, these pathways likely act as effectors of cardiac remodelling, downstream of ADAM-17/TACE**.** Moreover, the findings indicate that targeting TACE disrupts signalling through MMP-2 and ADAM-12, which could have generic therapeutic value for therapeutic management of cardiac hypertrophy and fibrosis, two processes that invariably develop subsequently to sustained vasoconstrictive agonist-stimulation[5].

The data gathered in this research suggest that the protective effects of TACE siRNA in agonist-induced cardiac hypertrophy (in angiotensin II-infused mice as well as SHR models) were primarily due to the down-regulation of TACE. In all the models, the degree of TACE knock-down, albeit modest, was significant - approximately 40% from baseline measured by either immunoreactivity or proteolytic activity and 25% as measured by qRT-PCR. Potential off-target effects such as signalling through the Toll-like receptor / interferon-γ pathway[24] may not be a major mechanism of protective effects of TACE siRNA because: 1) Administration of a siRNA to a non-mammalian gene (luciferase), by two different routes of administration (i.e., infusion through minipump and injection via jugular vein) had no protective effect on angiotensin II-induced hypertension, cardiac hypertrophy and fibrosis. 2) No upregulation of interferon-γ was observed - these *in vivo* findings are in agreement with a recent report using the same siRNA sequence on myoblast cultures[10].

TACE siRNA had no long-term protective effect on hypertension in neither SHR nor angiotensin II-infused mice. However, we cannot exclude that TACE siRNA treatment could have a short-term or transient protective effect, that was nonetheless insufficient to prevent the development of hypertension in both SHR and angiotensin II-infused mice. Due to the complexity of the effects of TACE inhibition on transcription of multiple genes, dedicated studies are warranted to further dissect the mechanism of the short-term roles of TACE in regulation of blood pressure of hypertension. However, our long-term data are consistent with previous research showing that the pharmacological inhibition of TACE (with TAPI-2) does not decrease systolic blood pressure in angiotensin II-infused mice[12]. Our long-term data are also in agreement with previous research showing that pharmacological blockade (with KB-R7785) of ADAM-12 (which we found to be downstream of TACE) does not protect mice from agonist-induced hypertension[7].

Previous studies have found that TACE, ADAM-12 and MMP-2 are all upregulated in human hypertrophic cardiomyopathy[16,21], and that ADAM-12 may mediate agonist-induced cardiac hypertrophy[7]. Recently, a novel role for ADAM-12 was reported in facilitating activation of transforming growth factor-β signalling through Smads, which is the main pathway mediating the development of agonist-induced fibrosis. This action of ADAM-12 is mediated via protein-protein interactions, independent of ADAM-12 protease activity[25]. Similarly, MMP-2 has been shown to promote myocardial hypertrophy and interstitial fibrosis through activation and release of transforming growth factor-β [26], thus facilitating Smad signalling[11]. Previous work also showed that TACE knock-down by RNA interference blocks mechanotransduction-induced myogenesis in cultured myoblasts[10], and that primary cultured aortic vascular smooth muscle cells expressing dominant negative mutant of TACE do not develop hypertrophy in response to angiotensin II[9]. Although the potential involvement of TACE in cardiac hypertrophy and fibrosis is suggested by previous research[9,10,21], TACE involvement in these processes has not been demonstrated *in vivo*.

This study has identified novel and significant effects of TACE siRNA on both cardiac hypertrophy and fibrosis *in vivo*. Our observations provide the first *in vivo* evidence that TACE expression regulates development of cardiac hypertrophy and fibrosis and, as such, substantially expand previous research. Taking our findings together with previous investigations, we suggest that an overabundance of vasoconstrictive agonists (as occurs in hypertensive disorders) could post-transcriptionally enhance the activity of multiple metalloproteinases such as TACE and ADAM-12, which next signal through a common pathway. Accordingly, the activated metalloproteinases may act by shedding growth factors and cytokines (such as HB-EGF, TGF-α and TNF-α) to promote the transcription of immediate-early, fetal as well as extracellular matrix genes, which are key mediators of hypertrophy and fibrosis processes[7-9,12,19,20] (**Figure 3-10**).

Despite extensive research[7-9,12,19,20], an interaction between the pathways of TACE, ADAM-12 and MMP-2 has never been identified. Therefore, a novel finding of this research has been the observations that baseline gene expression levels of TACE and ADAM-12 are transcriptionally connected, although further research is necessary to dissect the transcriptional pathways linking these metalloproteinases. Together with previously reported agonist-induced post-transcriptional signalling events[7-9,12,19,20], the TACE/ADAM-12 signalling axis may regulate the development and progression of hypertrophy and fibrosis which are hallmarks of agonist-induced cardiovascular remodelling (**Figure 3-10**).

Furthermore, it is possible that metalloproteinases form a highly regulated signalling network (as opposed to acting in isolation). Certain metalloproteinases (such as TACE) may act like primary mediators of cardiovascular (hypertrophic) growth as well as fibrosis processes whereas other metalloproteinases (such as MMP-2 and ADAM-12) are downstream effectors. Interestingly, we recently found that MMP-7 may exert a transcriptional regulation of ADAM-12 in cardiac hypertrophy, similar to that demonstrated here for TACE[27].

Perspectives

These current findings have therapeutic potential in hypertensive heart disease. Our data suggest that TACE, MMP-2 and ADAM-12 may define a novel signalling axis in agonist-induced cardiac hypertrophy and fibrosis processes, and that these processes can be disrupted by targeting TACE. This notion is supported by our studies both in mice with agonist-induced cardiac hypertrophy and in SHR, a model where cardiac hypertrophy is likely signalled by multiple agonists[28-30]. Together with previous studies on MMP-2 and ADAM-12, it may be possible to counter different hypertensive cardiac diseases and complications thereof by targeting one or more nodes in the emerging network of interconnected metalloproteinases which includes TACE, MMP-7, MMP-2 and ADAM-12.

Future studies should investigate the emerging notion of metalloproteinase networks as mediators of agonist-induced cardiovascular hypertrophy and fibrosis processes and the dynamics of this network, in various models and stages of hypertension and cardiac remodelling.

Table 3-1 Involvement of TACE in the development of cardiac hypertrophy in the SHR model. Echocardiographic results.

Day 40	IVS;d (mm)	LVID;d (mm)	LVPW;d (mm)
PBS	1.90 ± 0.03	8.36 ± 0.08	1.74 ± 0.04
TACE siRNA	1.54 ± 0.03*	8.23 ± 0.17	1.56 ± 0.02*
	EF (%)	HR (bpm)	BW (g)
PBS	65.7 ± 1.1	354 ± 15	360.0 ± 7.4
TACE siRNA	66.6 ± 0.7	349 ± 16	350.2 ± 10.1

PBS, phosphate buffered saline; IVS, interventricular septum; LV, left ventricle; ID, inner diameter; PW, posterior wall dimension; d, diastoles; EF, ejection fraction; HR, heart rate; BW, body weight.

Results are means ± sem. n = 4 rats per group. (*) $p < 0.01$ vs PBS. MultiANOVA with Scheffe's test.

Table 3-2 The development of the cardiac hypertrophy induced by angiotensin II in the mouse requires expression of TACE. Echocardiographic results.

Day 15	IVS;d (mm)	LVID;d (mm)	LVPW;d (mm)
PBS	0.68 ± 0.02	3.95 ± 0.04	0.73 ± 0.02
TACE siRNA	0.63 ± 0.02	4.18 ± 0.10	0.67 ± 0.03
PBS + AngII	0.83 ± 0.01*	4.62 ± 0.09*	0.85 ± 0.03*
TACE siRNA + Ang II	0.71 ± 0.02	4.11 ± 0.06	0.71 ± 0.02
	EF (%)	HR (bpm)	BW (g)
PBS	65.5 ± 2.1	525 ± 23	25.8 ± 0.2
TACE siRNA	66.2 ± 2.9	500 ± 23	26.8 ± 0.7
PBS + AngII	62.0 ± 1.9	554 ± 23	24.6 ± 0.7
TACE siRNA + Ang II	62.5 ± 1.5	549 ± 20	25.9 ± 0.2

PBS, phosphate buffered saline; IVS, interventricular septum; LV, left ventricle; ID, inner diameter; PW, posterior wall dimension; d, diastoles; EF, ejection fraction; HR, heart rate; BW, body weight; (*) $p<0.05$ vs PBS. MultiANOVA with Scheffe's test.

Figure 3-1 Domain structure of TACE protein and cDNA sequences (mice and rats) targeted by the siRNA.

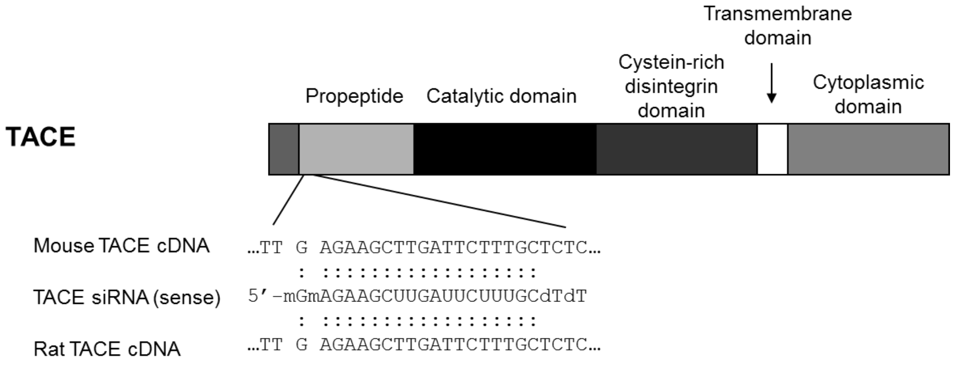
Transmembrane domain
Cystein-rich disintegrin domain
Propeptide
Catalytic domain
Cytoplasmic domain
TACE
Mouse TACE cDNA
…TT G AGAAGCTTGATTCTTTGCTCTC…
: ::::::::::::::::::
TACE siRNA (sense)
5′-mGmAGAAGCUUGAUUCUUUGCdTdT
: ::::::::::::::::::
Rat TACE cDNA
…TT G AGAAGCTTGATTCTTTGCTCTC…

Figure 3-2 Effects of TACE knock-down on development of cardiac hypertrophy in spontaneously hypertensive rats.

A, Treatment protocol: Treatment #1: The rats were infused with either TACE siRNA or PBS through minipumps for 14 days. Treatment #2: On day 23, treatment was restarted by implanting new minipumps containing either TACE siRNA or PBS. No treatment: Period between treatments, i.e., between day 15 and day 23.

B, Decreased cardiac hypertrophy in SHR treated with TACE siRNA. The ratio of corrected left ventricle mass (corr. LV mass, determined by M-mode echocardiography) to body weight (BW) increased over time in PBS-treated rats, but not in rats receiving TACE siRNA.

C, Decrease in heart weight (HW) to body weight (BW) ratio (analysis conducted on day 41) in SHR treated with siRNA vs. PBS.

D, Demonstration of the knock-down of myocardial TACE by TACE siRNA as determined by western immunoblot (110 kDa) and the decrease in myocardial MMP-2 by TACE siRNA as determined by gelatin-zymography. Signals were quantified by densitometry and normalized to SDS-PAGE gel loading controls.

(*): $p < 0.05$ vs. PBS group. Results are means ± SEM of n=4 rats in each group.

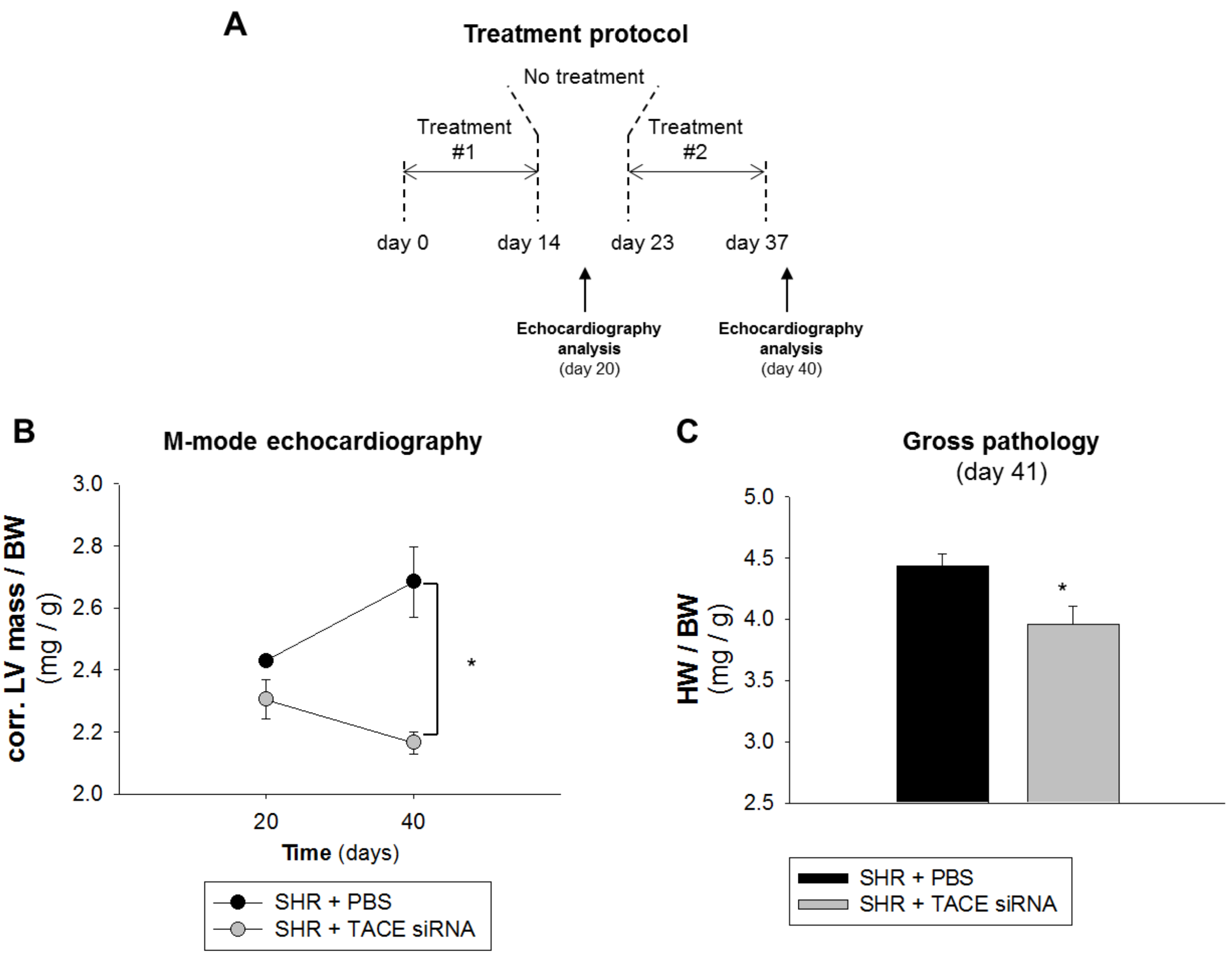
A
Treatment protocol
No treatment
Treatment #1
Treatment #2
day 0
day 14
day 23
day 37
Echocardiography analysis (day 20)
Echocardiography analysis (day 40)
B
M-mode echocardiography
corr. LV mass / BW (mg / g)
3.0
2.8
2.6
2.4
2.2
2.0
20
40
Time (days)
*
SHR + PBS
SHR + TACE siRNA
C
Gross pathology (day 41)
HW / BW (mg / g)
5.0
4.5
4.0
3.5
3.0
2.5
*
SHR + PBS
SHR + TACE siRNA

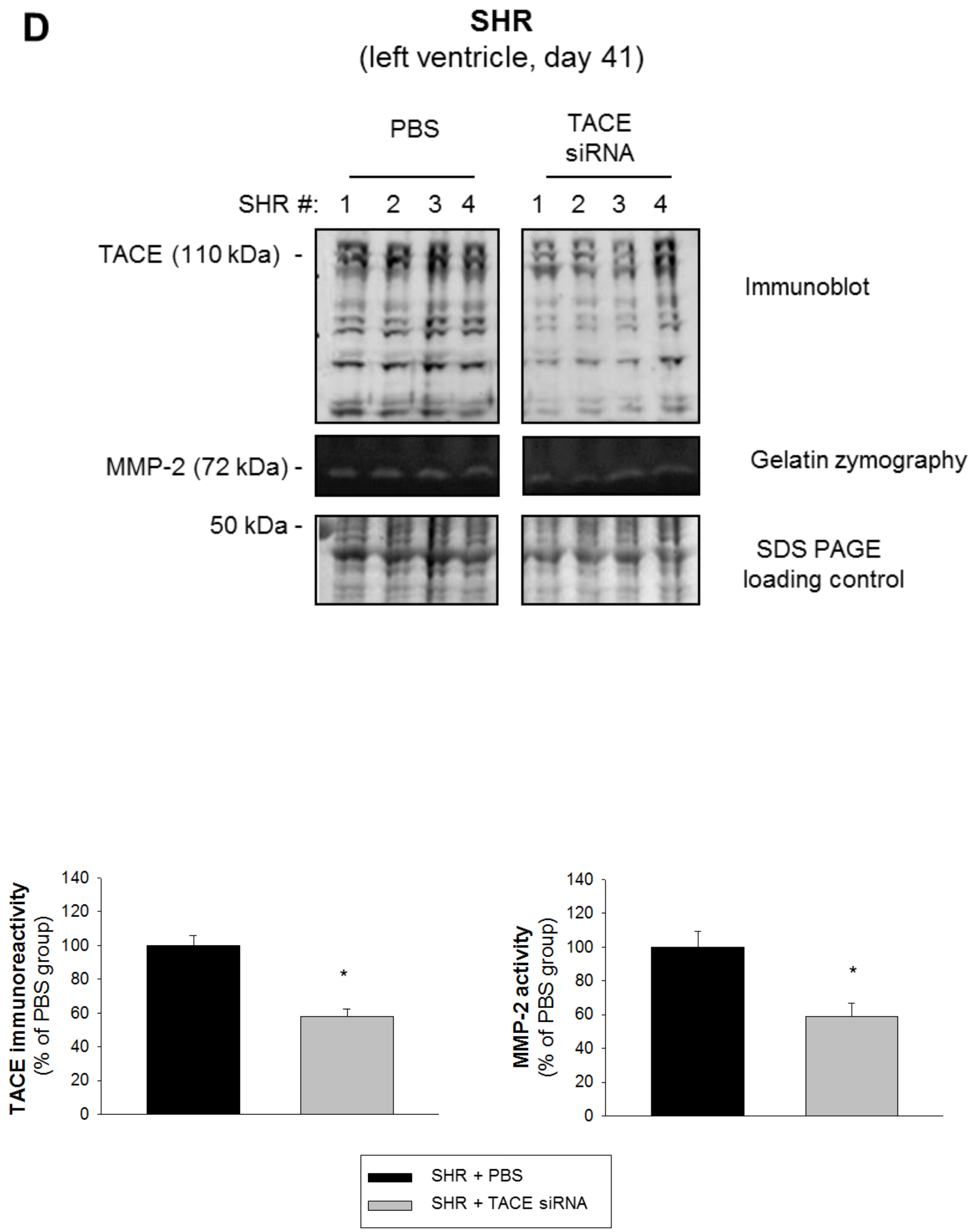
D
SHR
(left ventricle, day 41)
PBS
TACE siRNA
SHR #: 1 2 3 4 1 2 3 4
TACE (110 kDa) -
Immunoblot
MMP-2 (72 kDa) -
Gelatin zymography
50 kDa -
SDS PAGE loading control
TACE immunoreactivity (% of PBS group)
MMP-2 activity (% of PBS group)
0
20
40
60
80
100
120
140
*
SHR + PBS
SHR + TACE siRNA

Figure 3-3 Knockdown of TACE decreases cardiac ERK phosphorylation.
Western blot of phosphorylated ERK (p-ERK)-1/2 and total ERK-1/2 in the left ventricle of SHR treated with TACE siRNA vs. SHR treated with vehicle (PBS). Quantitative analysis of the ratio between p-ERK-1 and ERK-1 showed decreased phosphorylation level of ERK in the left ventricle of SHR treated with TACE siRNA. (*): $p < 0.05$ vs. PBS. Results are means ± SEM of n=4 rats in each study group.

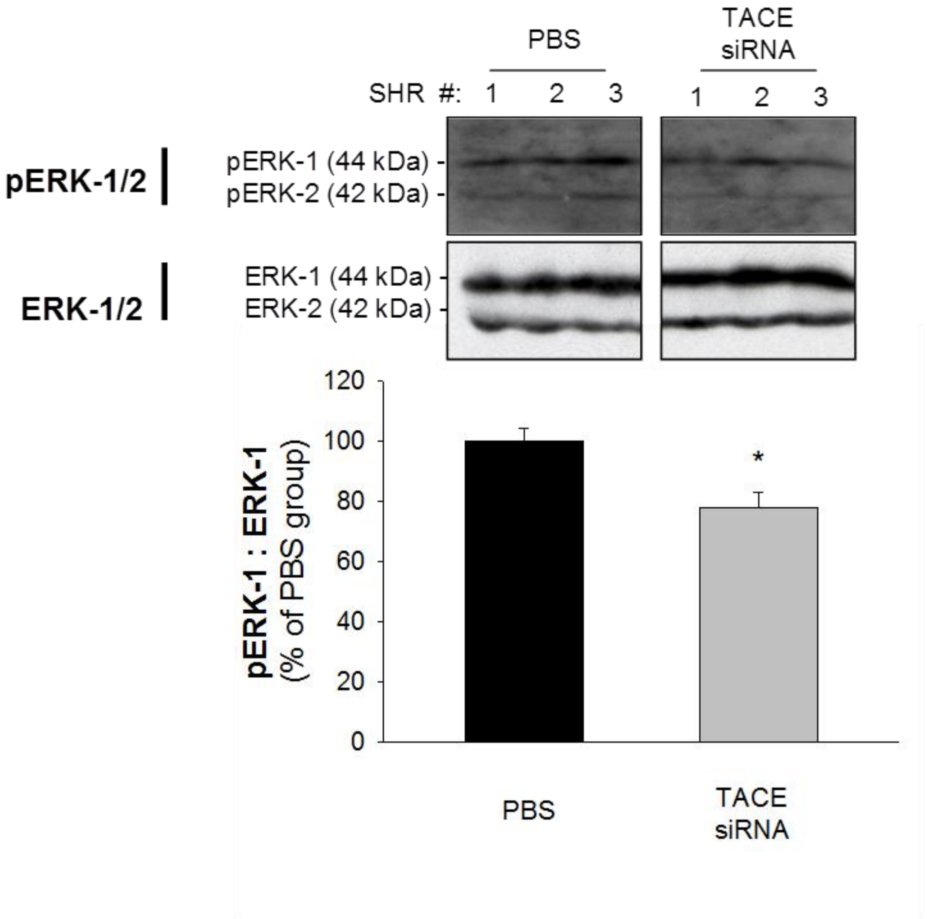

Figure 3-4 Effects of TACE knock-down on blood pressure of spontaneously hypertensive rats.

A, Time course of the systolic blood pressure of already-hypertensive SHR treated with either TACE siRNA or vehicle (PBS).

B, Demonstration of vascular TACE knock-down. Quantitative analysis indicates that, in small (resistance) mesenteric arteries, TACE proteolytic activity was significantly knocked-down by siRNAs to TACE, as determined by a commercially available fluorogenic peptide cleavage assay.

(*): $p < 0.05$ vs. PBS group. Results are means ± SEM of n=4 rats in each group.

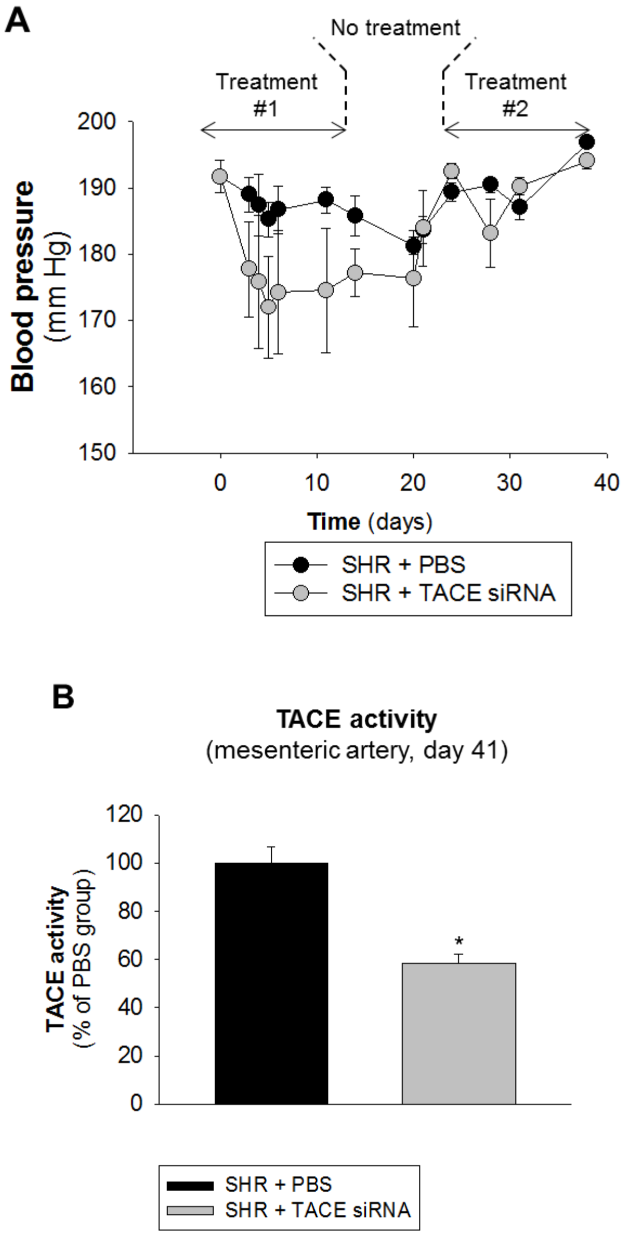

Figure 3-5 TACE, MMP-2 and ADAM-12 genes define a novel metalloproteinase signalling network.

Quantitative analysis of gene expression (i.e., mRNA levels) for: (**A, B**): TACE, (**C, D**): MMP-2, (**E**): ADAM-12. Mice (12-week old) were administered either PBS or TACE siRNA (0.4 mg/kg/d for 14 days) through a 1st osmotic minipump followed by the administration of either PBS or angiotensin II (Ang II, 1.4 mg/kg/d, for 12 days i.e., from day 5 to day 16), through a 2nd osmotic minipump. The mice were euthanized on day 16.

Expression: mRNA levels were measured in left ventricle by quantitative TaqMan RT-PCR and normalized by 18S rRNA.

Activity: TACE proteolytic activity was determined using a commercially available fluorogenic peptide. MMP-2 activity was measured by gelatin zymography. ADAM-12 antibodies were not sensitive enough to allow a reliable quantification of ADAM-12 in the left ventricle of mice.

(*): $p < 0.05$ vs. PBS. (+): $p < 0.05$ vs. (PBS + Ang II). Results are means ± SEM of n=4 mice in each study group.

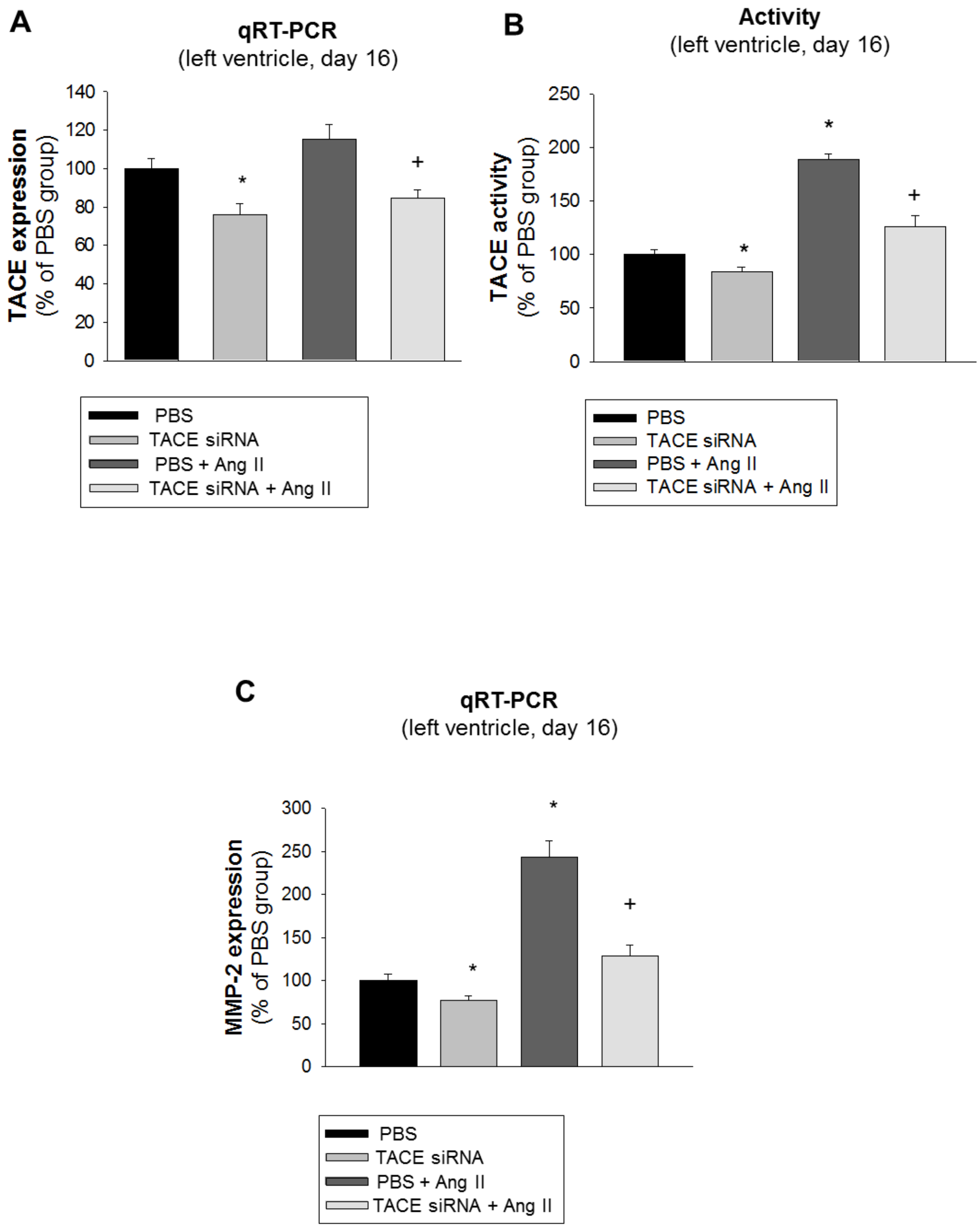
A
qRT-PCR
(left ventricle, day 16)
TACE expression
(% of PBS group)
0
20
40
60
80
100
120
140
*
+
PBS
TACE siRNA
PBS + Ang II
TACE siRNA + Ang II
B
Activity
(left ventricle, day 16)
TACE activity
(% of PBS group)
0
50
100
150
200
250
*
*
+
PBS
TACE siRNA
PBS + Ang II
TACE siRNA + Ang II
C
qRT-PCR
(left ventricle, day 16)
MMP-2 expression
(% of PBS group)
0
50
100
150
200
250
300
*
*
+
PBS
TACE siRNA
PBS + Ang II
TACE siRNA + Ang II

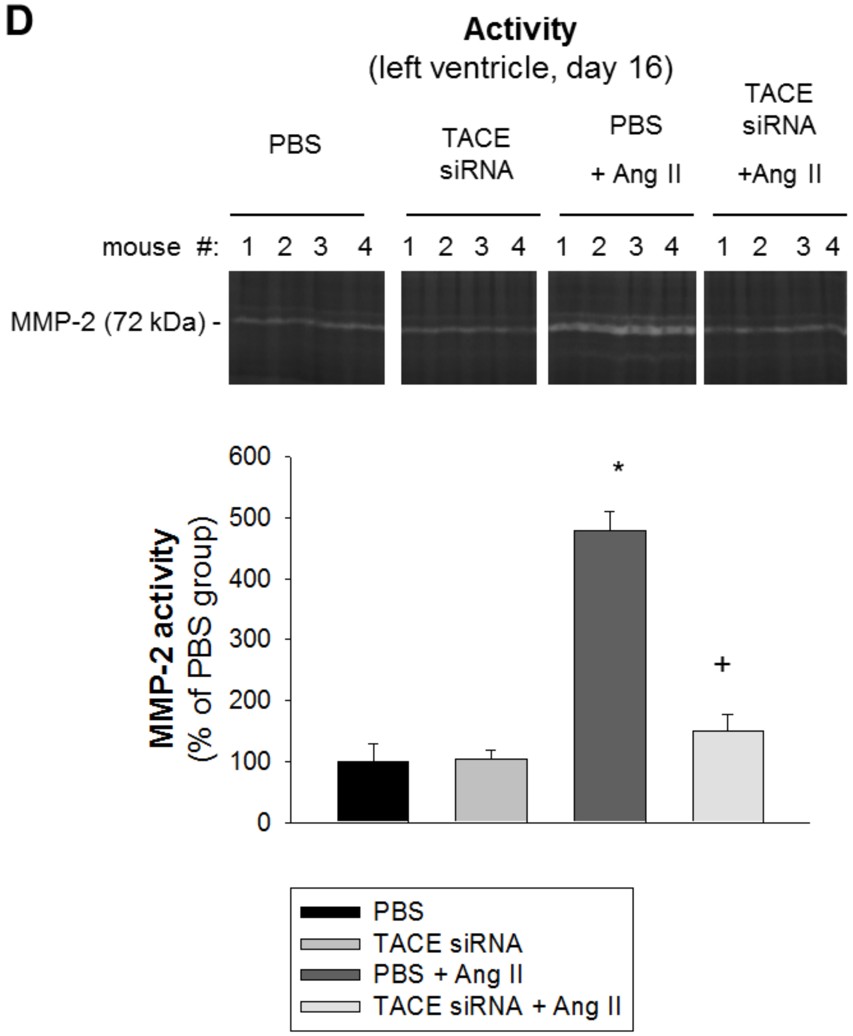
D
Activity
(left ventricle, day 16)
PBS
TACE siRNA
PBS + Ang II
TACE siRNA +Ang II
mouse #: 1 2 3 4 1 2 3 4 1 2 3 4 1 2 3 4
MMP-2 (72 kDa) -
MMP-2 activity (% of PBS group)
600
500
400
300
200
100
0
*
+
PBS
TACE siRNA
PBS + Ang II
TACE siRNA + Ang II

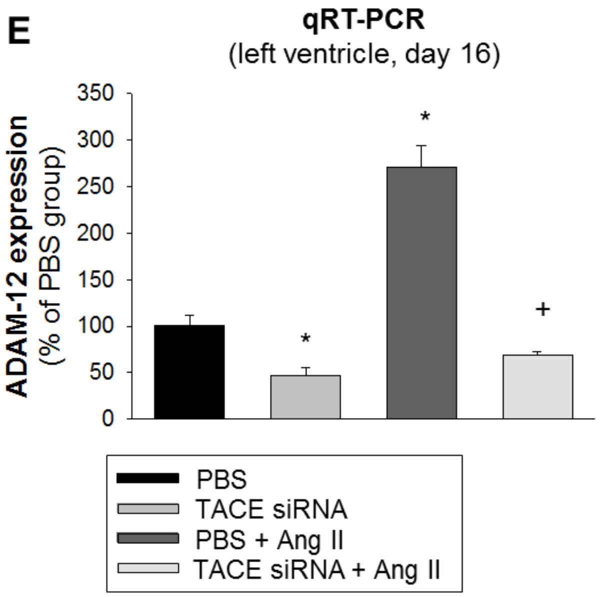
E
qRT-PCR
(left ventricle, day 16)
ADAM-12 expression (% of PBS group)
350
300
250
200
150
100
50
0
*
*
+
PBS
TACE siRNA
PBS + Ang II
TACE siRNA + Ang II

Figure 3-6 Knockdown of cardiac TACE in response to jugular vein injection of TACE siRNA.

siRNA (15 μg) or PBS was injection into mice via their jugular veins (on day 0, day 5 and day 10), angiotensin II (Ang II, 1.4 mg/kg/d) was delivered through a subcutaneously implanted osmotic minipump (from day 5 to day 16). The mice were euthanized on day 16.

A, Top panel TACE siRNA inhibited the increase in cardiac TACE expression induced by Ang II infusion as detected by immunofluorescence of TACE-FITC in representative left ventricle frozen sections (6 μm) surrounding cardiac arteries (indicated by arrows). Immunofluorescence of actin-Texas Red (TR) was also shown.

Bottom panel TACE siRNA reduced the increase in cardiac TACE activity induced by angiotensin II infusion as detected by TACE activity assay using a commercially available flourogenic TACE substrate.

B, C, Decrease in TACE expression also inhibited the increased expression of MMP-2 (**B**, detected by western blot) and ADAM-12 (**C**, measured by quantitative RT-PCR) in left ventricle induced by the angiotensin II infusion.

(*): $p < 0.05$ vs. PBS group. (+): $p < 0.05$ vs. (PBS + Ang II) group.

Results are means ± SEM of n=2-4 mice for each study group.

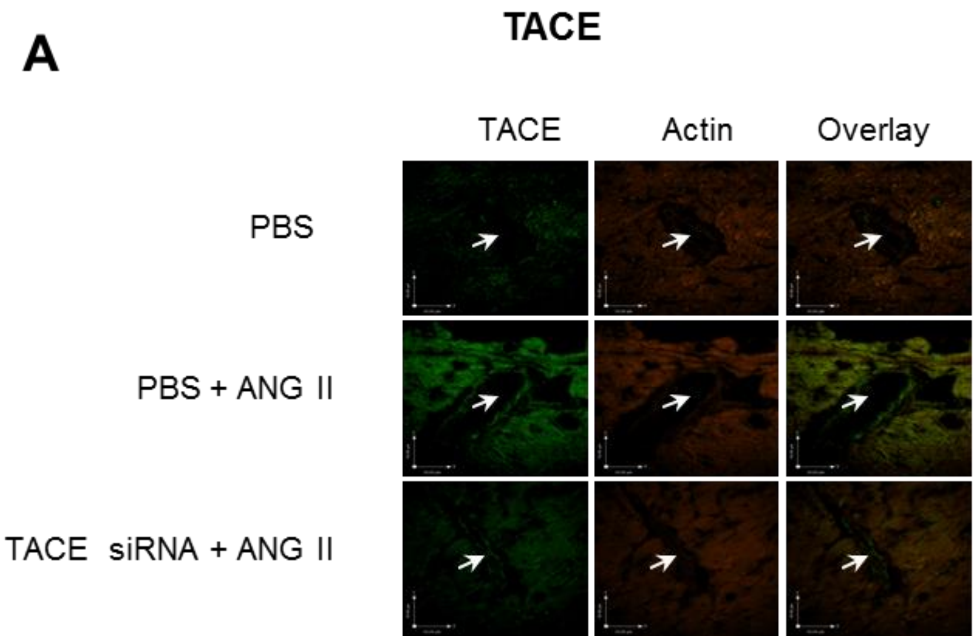
A
TACE
TACE
Actin
Overlay
PBS
PBS + ANG II
TACE siRNA + ANG II

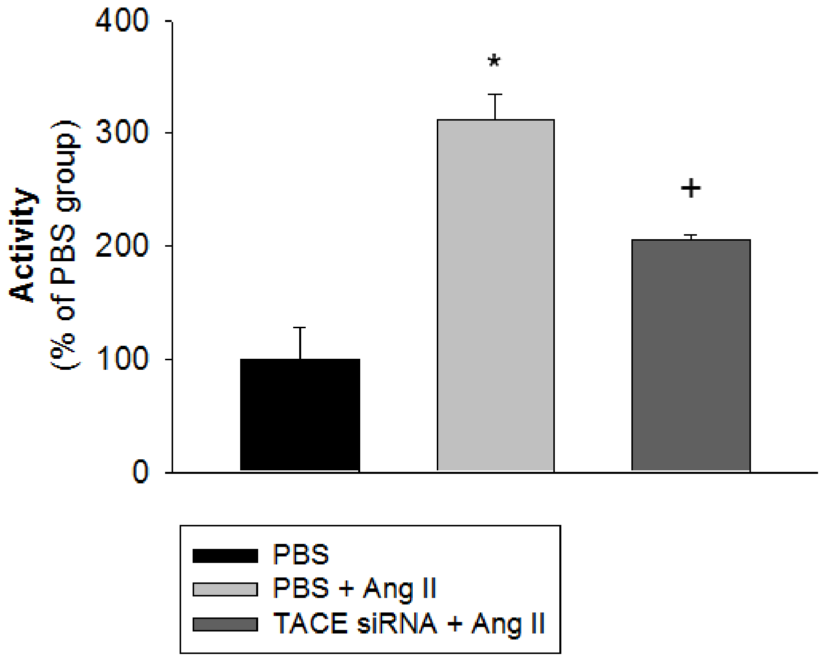
400
300
200
100
0
Activity
(% of PBS group)
*
+
PBS
PBS + Ang II
TACE siRNA + Ang II

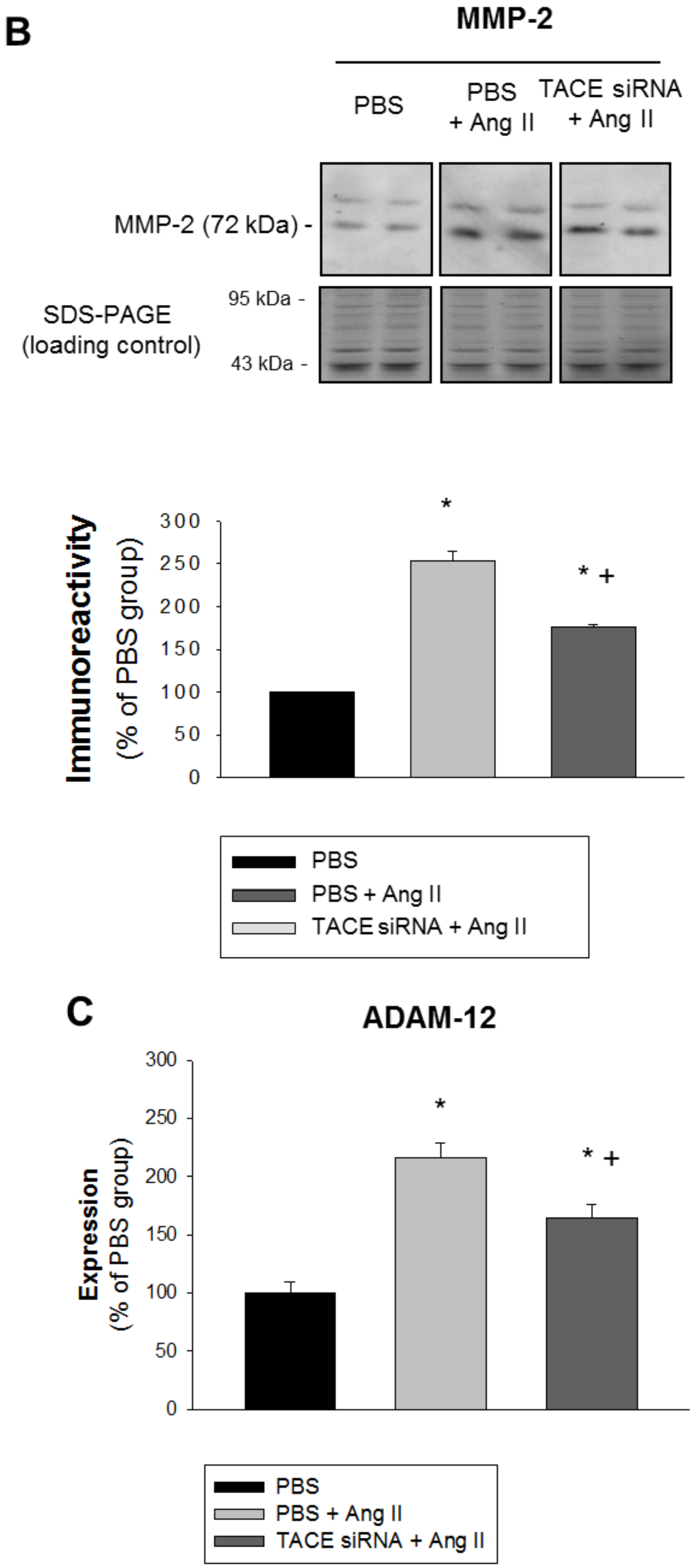
B
MMP-2
PBS
PBS + Ang II
TACE siRNA + Ang II
MMP-2 (72 kDa) -
SDS-PAGE (loading control)
95 kDa -
43 kDa -
Immunoreactivity (% of PBS group)
300
250
200
150
100
50
0
*
* +
■ PBS
▨ PBS + Ang II
□ TACE siRNA + Ang II
C
ADAM-12
Expression (% of PBS group)
300
250
200
150
100
50
0
*
* +
■ PBS
□ PBS + Ang II
▨ TACE siRNA + Ang II

Figure 3-7 Evidence of the mediator role of TACE in agonist-induced cardiac hypertrophy.

A, Pre-treatment with TACE siRNA prevented angiotensin II (Ang II)-induced left ventricular hypertrophy as evidenced by the ratio of corrected left ventricle mass (corr. LV mass) to body weight (BW) (**left panel**) detected by M-mode echocardiography. Representative M-mode echocardiographic tracings of left ventricles (**right panel**) are also shown. (IVS: intraventricular septum. LVID: left ventricular internal dimension. LVPW: Left ventricular posterior wall. See **Table 2** for quantification)

Mice (12-week old) were administered either PBS or TACE siRNA (0.4 mg/kg/d for 14 days) through a 1st osmotic minipump followed by the administration of either PBS or angiotensin II (1.4 mg/kg/d, for 12 days i.e., from day 5 to day 16), through a 2nd osmotic minipump. Echocardiographic analysis was conducted 11 days after implantation of a 2nd osmotic minipump (i.e., on day 15). The mice were euthanized on day 16.

B, Pre-treatment with TACE siRNA prevents Ang II-induced left ventricular hypertrophy as evidenced by the ratio of heart weight (HW) to body weight (BW).

C, Pre-treatment with TACE siRNA prevents Ang II-induced increase in expression of hypertrophy markers in left ventricles: brain natriuretic peptide (BNP), α-skeletal actin, and β-myosin heavy chain (β-MHC). mRNA levels were measured by quantitative TaqMan RT-PCR and normalized to 18S rRNA.

D, Pre-treatment with TACE siRNA prevents Ang II-induced increase in expression of ECM proteins in left ventricles: collagen type I, collagen type III and fibronectin. mRNA levels were measured by quantitative TaqMan RT-PCR, normalized to 18S rRNA and expressed as percent of PBS group.

(*): $p < 0.05$ vs. PBS. (+): $p < 0.05$ vs. (PBS + Ang II). Results are means ± SEM of n=4 mice in each study group.

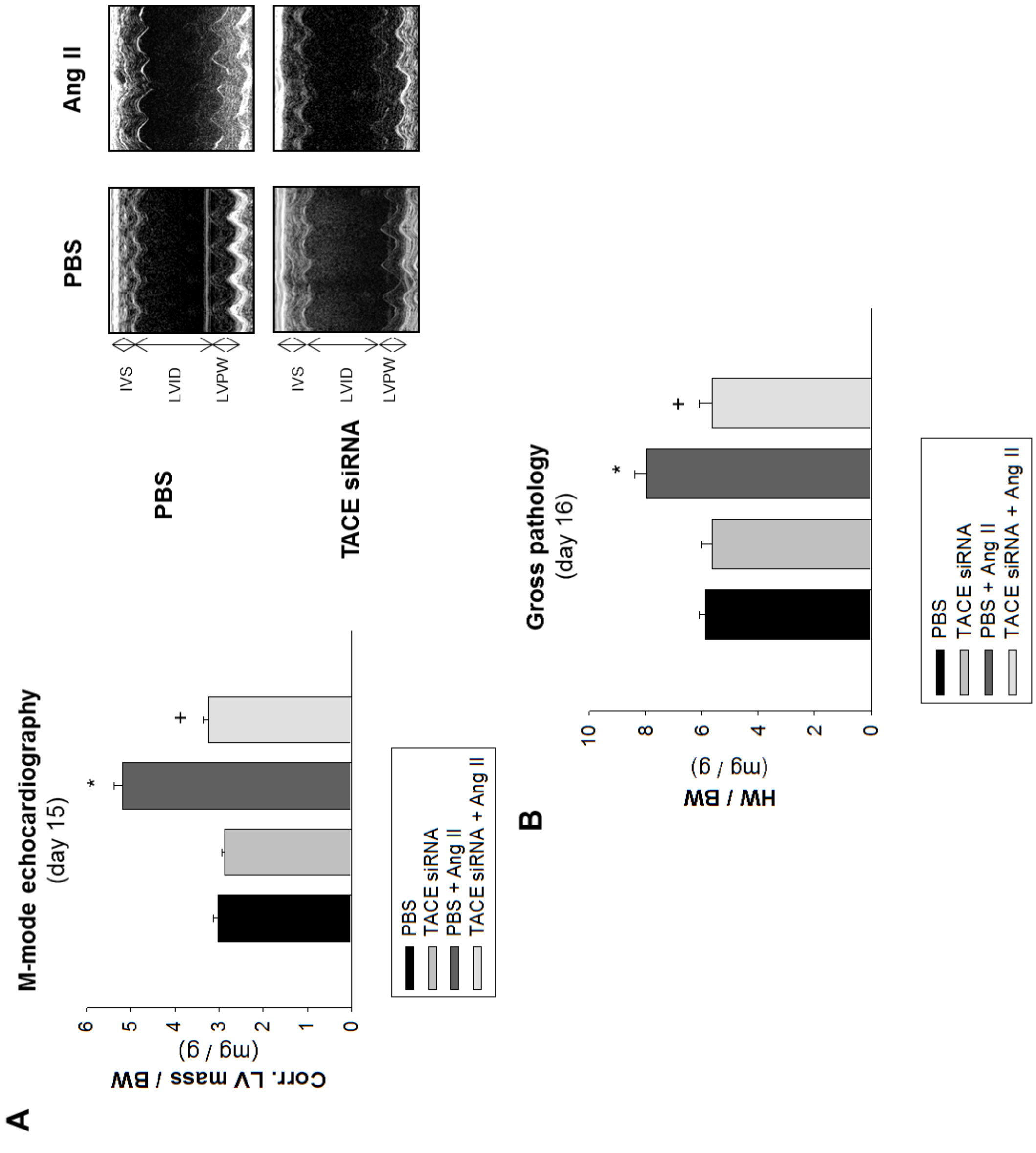
A
M-mode echocardiography
(day 15)
Corr. LV mass / BW
(mg / g)
6
5
4
3
2
1
0
*
+
PBS
TACE siRNA
PBS + Ang II
TACE siRNA + Ang II
PBS
Ang II
PBS
TACE siRNA
IVS
LVID
LVPW
IVS
LVID
LVPW
B
Gross pathology
(day 16)
HW / BW
(mg / g)
10
8
6
4
2
0
*
+
PBS
TACE siRNA
PBS + Ang II
TACE siRNA + Ang II

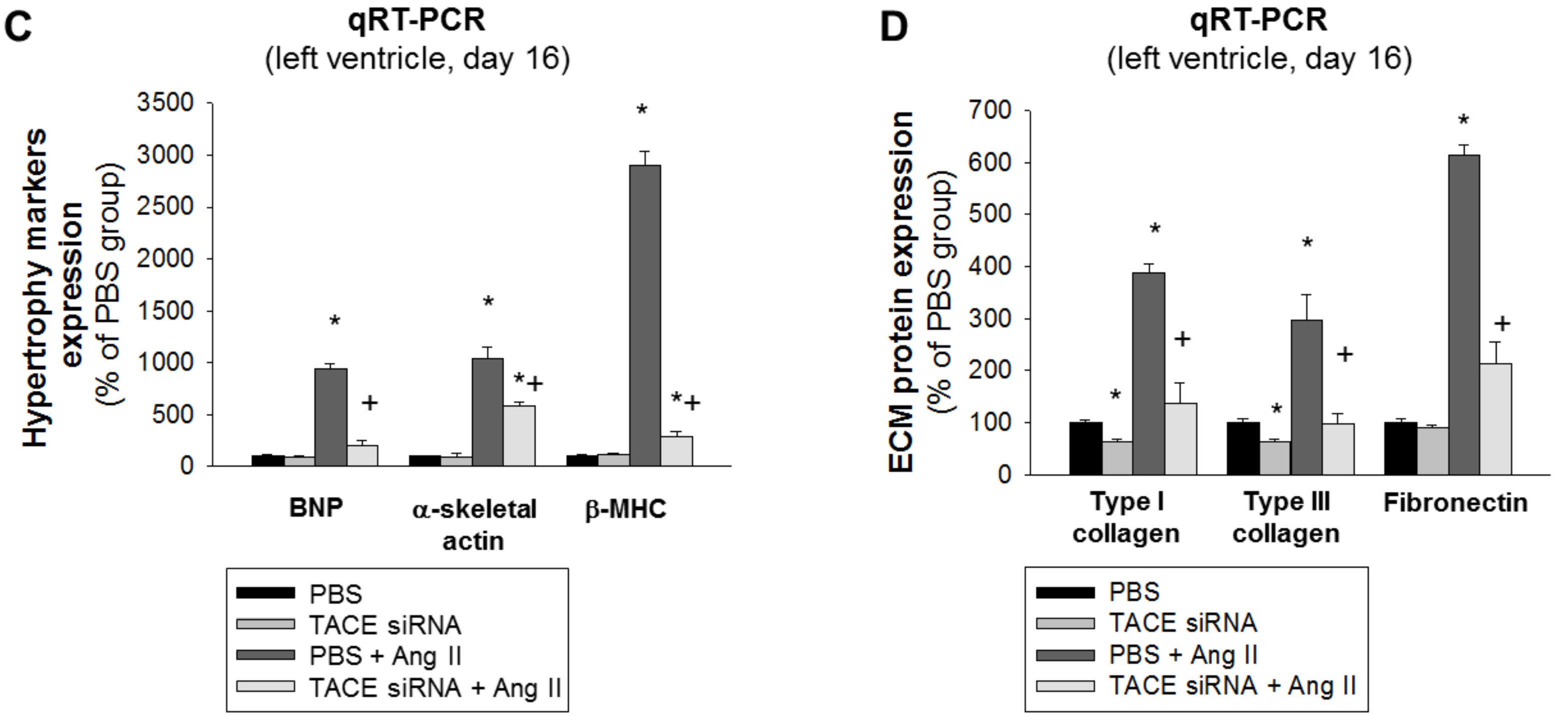
C
qRT-PCR
(left ventricle, day 16)
Hypertrophy markers expression
(% of PBS group)
3500
3000
2500
2000
1500
1000
500
0
*
+
*
*+
*
*+
BNP
α-skeletal actin
β-MHC
PBS
TACE siRNA
PBS + Ang II
TACE siRNA + Ang II
D
qRT-PCR
(left ventricle, day 16)
ECM protein expression
(% of PBS group)
700
600
500
400
300
200
100
0
*
*
+
*
*
+
*
+
Type I collagen
Type III collagen
Fibronectin
PBS
TACE siRNA
PBS + Ang II
TACE siRNA + Ang II

Figure 3-8 Luciferase siRNA has no effect on Ang II-induced cardiac hypertrophy and fibrosis.

Pre-treatment with luciferase (Luc) siRNA did not reduce angiotensin II (Ang II)-induced left ventricular hypertrophy, as evidenced by:

A, Ratio of corrected left ventricle mass (corr. LV mass, determined by M-mode echocardiography) to body weight (BW).

B, Ratio of heart weight (HW) to body weight (gross pathology analysis).

C, D, Expression of hypertrophy markers (**C**) and ECM proteins (**D**), as determined by quantitative RT-PCR using TaqMan probes. BNP: brain natriuretic peptide, β-MHC: β-myosin heavy chain.

20-week old mice were implanted with a subcutaneous osmotic minipump delivering Luc siRNA (0.4 mg/kg/d for 14 days) or sham operated, followed by the administration of either Ang II (1.4 mg/kg/d, for 12 days i.e., from day 5 to day 16) through a 2nd osmotic minipump. M-mode echocardiography was conducted 11 days after implantation of a 2nd osmotic minipump (i.e., on day 15). Mice were euthanized on day 16. Hearts were weighed out and left ventricle samples were analyzed by RT-PCR. (*): $p < 0.05$ vs. sham group.

Results are means ± SEM of n=3-4 mice in each study group.

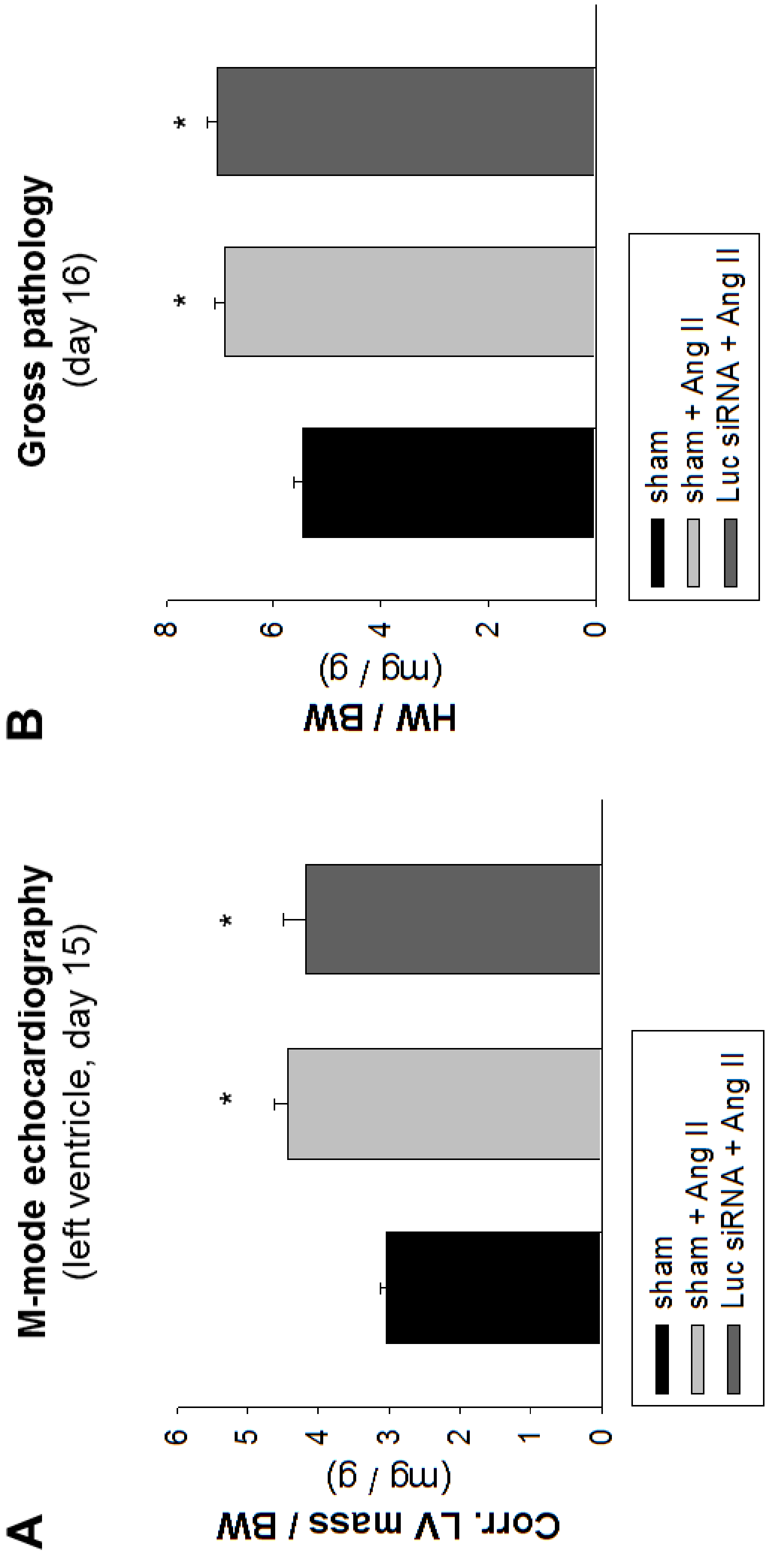
A
M-mode echocardiography
(left ventricle, day 15)
Corr. LV mass / BW
(mg / g)
0
1
2
3
4
5
6
*
*
sham
sham + Ang II
Luc siRNA + Ang II
B
Gross pathology
(day 16)
HW / BW
(mg / g)
0
2
4
6
8
*
*
sham
sham + Ang II
Luc siRNA + Ang II

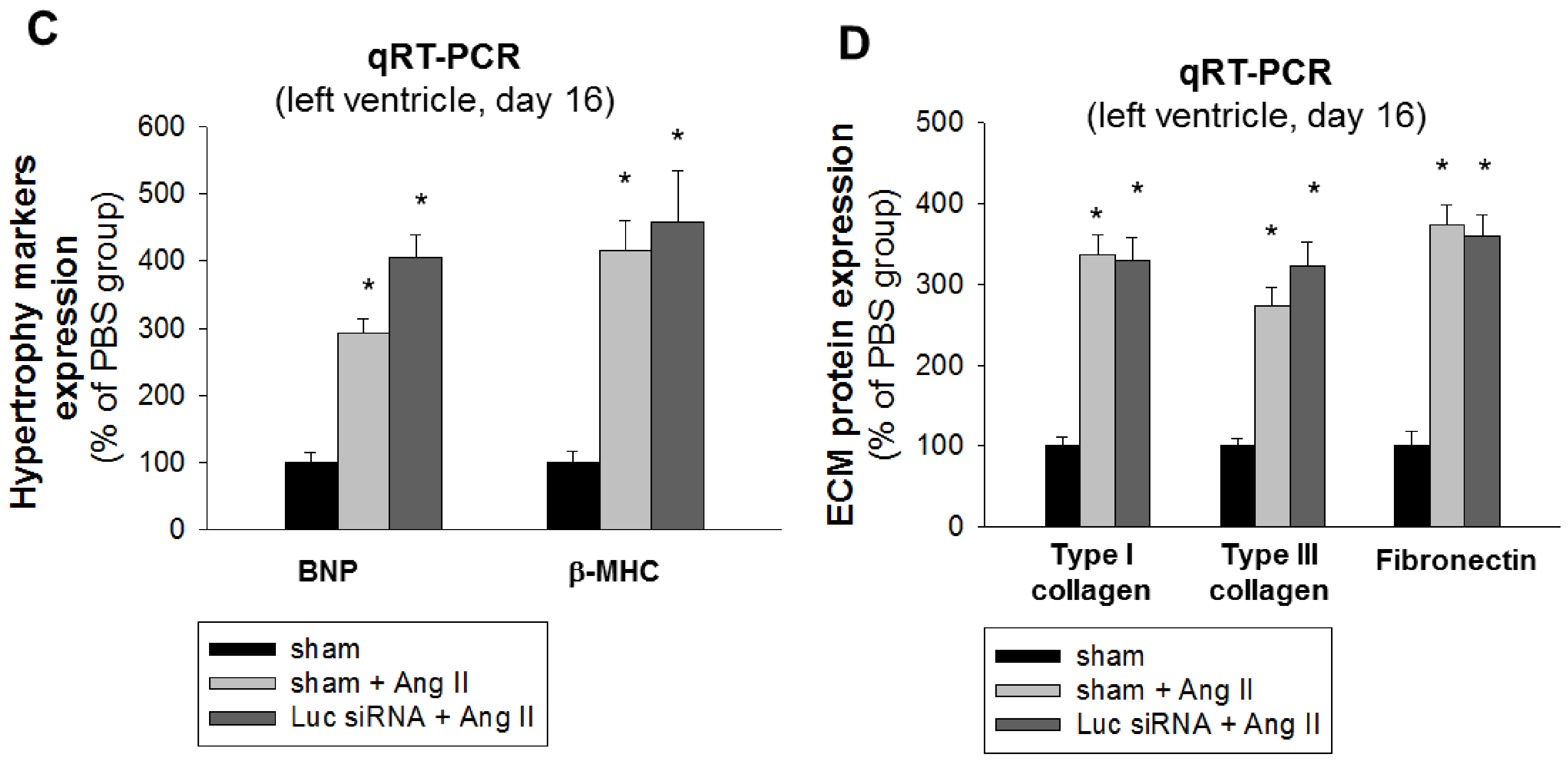
C
qRT-PCR
(left ventricle, day 16)
Hypertrophy markers expression (% of PBS group)
0
100
200
300
400
500
600
BNP
β-MHC
*
*
*
*
sham
sham + Ang II
Luc siRNA + Ang II
D
qRT-PCR
(left ventricle, day 16)
ECM protein expression (% of PBS group)
0
100
200
300
400
500
Type I collagen
Type III collagen
Fibronectin
*
*
*
*
*
*
sham
sham + Ang II
Luc siRNA + Ang II

Figure 3-9 Knockdown of TACE blocked cardiac hypertrophy and fibrosis induced by angiotensin II infusion.

siRNA (15 μg) or PBS was injection into mice via their jugular veins (on day 0, day 6 and day 10), angiotensin II (Ang II, 1.4 mg/kg/d) was delivered through a subcutaneously implanted osmotic minipump (from day 5 to day 15). The mice were euthanized on day 15.

A-C, Pre-treatment with TACE siRNA, but not luciferase (Luc) siRNA or PBS, prevented Ang II-induced left ventricular hypertrophy as evidenced by the ratio of heart weight (HW) to body weight (BW) (**A**), expression of hypertrophy markers: brain natriuretic peptide (BNP), α-skeletal actin and β-myosin heavy chain (β-MHC) (**B**, measured by quantitative RT-PCR) and size of cardiomyocytes **(C**), detected by average area of cardiomyocytes cross-section following WGA-FITC staining, >100 cells per heart were counted).

D, E, Pre-treatment with TACE siRNA, but not PBS, prevented Ang II-induced-cardiac fibrosis, as evidenced by the picrosirius red staining (**D**) and type I collagen expression (**E**, measured by quantitative RT-PCR).

(*): $p < 0.05$ vs. PBS group. (+): $p < 0.05$ vs. (PBS + Ang II) group.

Results are means ± SEM of n=2-4 mice for each study group.

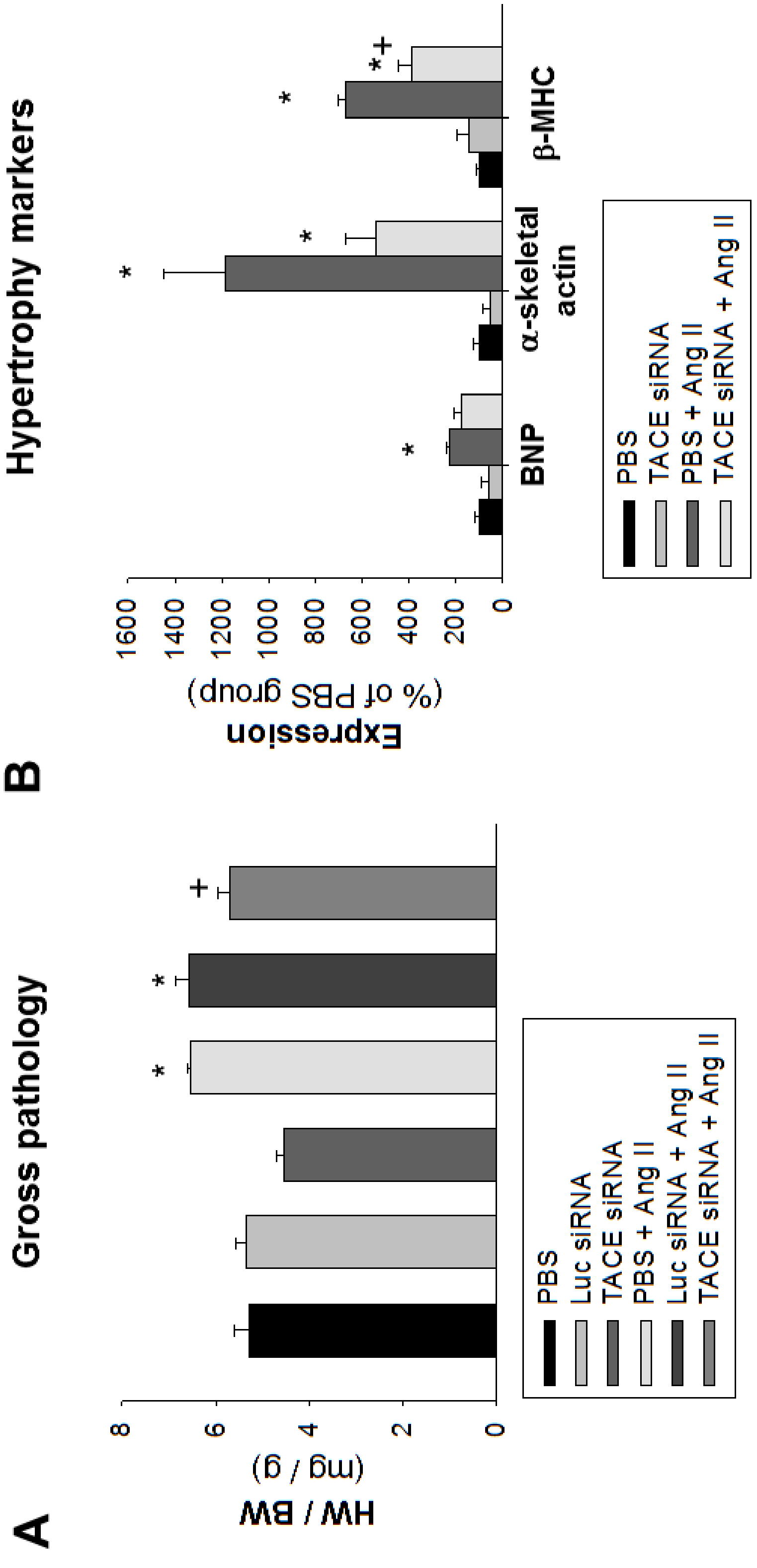
A
Gross pathology
HW / BW
(mg / g)
0
2
4
6
8
*
*
+
PBS
Luc siRNA
TACE siRNA
PBS + Ang II
Luc siRNA + Ang II
TACE siRNA + Ang II
B
Hypertrophy markers
Expression
(% of PBS group)
0
200
400
600
800
1000
1200
1400
1600
*
*
*
*
*+
BNP
α-skeletal
actin
β-MHC
PBS
TACE siRNA
PBS + Ang II
TACE siRNA + Ang II

C

WGA-FITC immunostaining

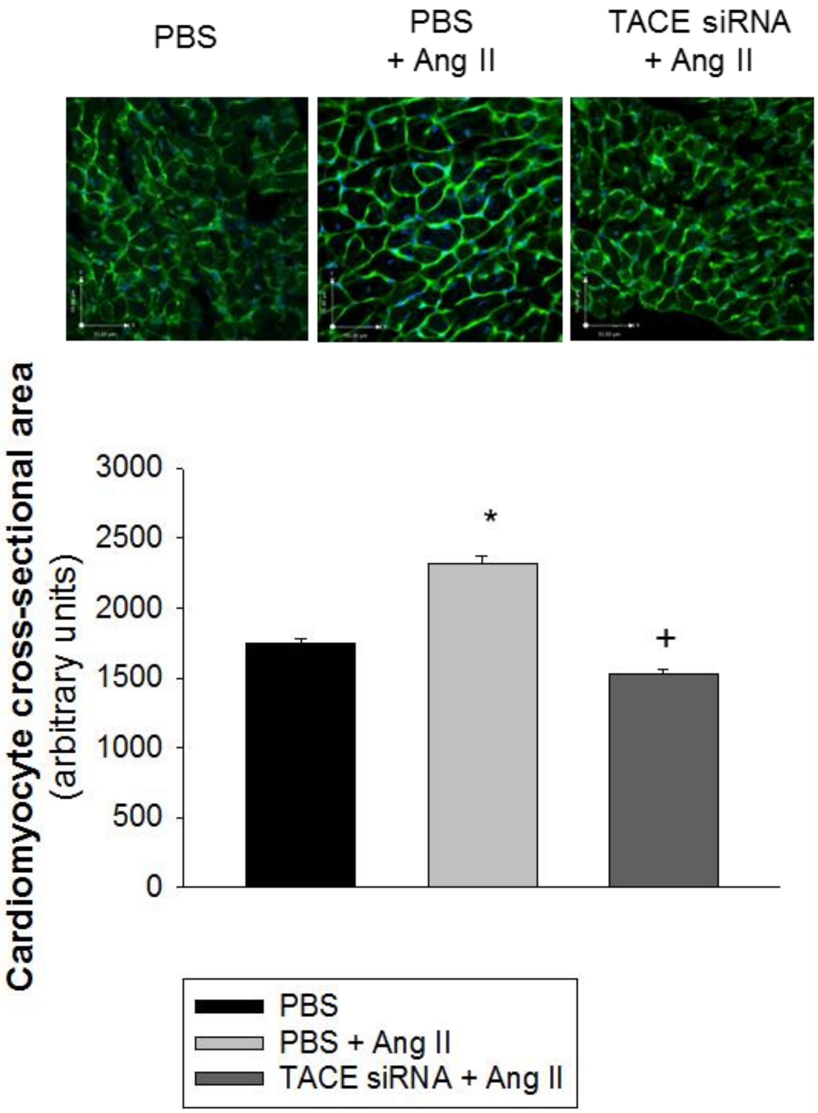

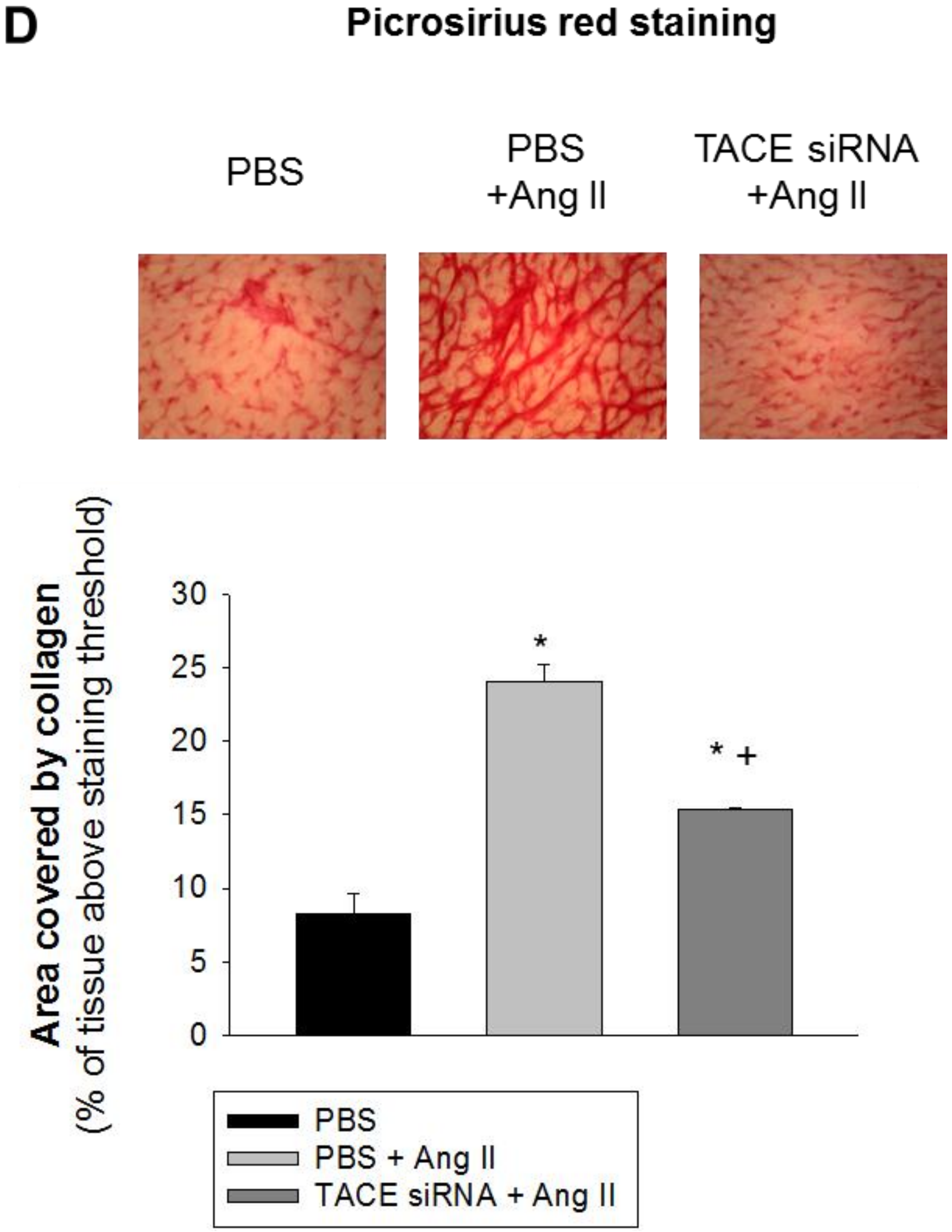
D
Picrosirius red staining
PBS
PBS +Ang II
TACE siRNA +Ang II
Area covered by collagen
(% of tissue above staining threshold)
30
25
20
15
10
5
0
*
* +
PBS
PBS + Ang II
TACE siRNA + Ang II

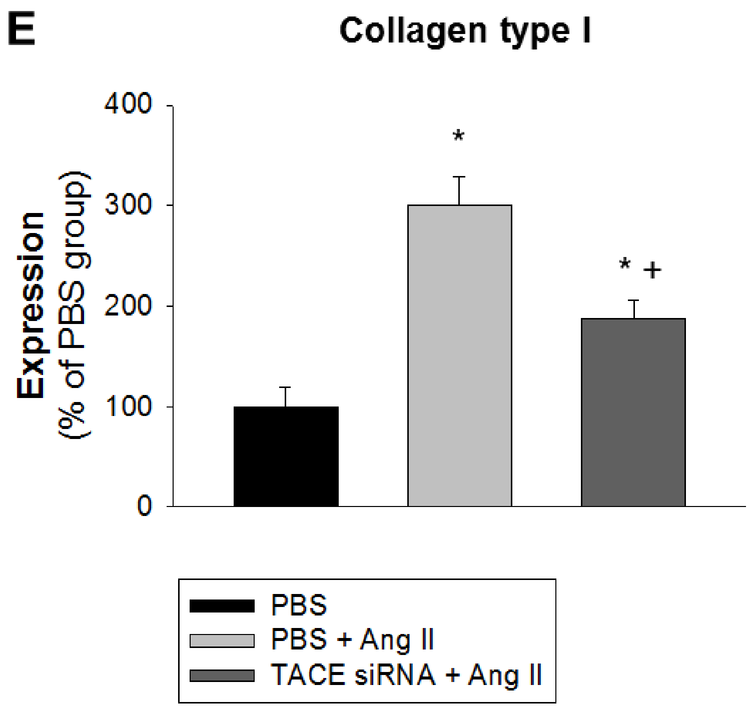
E
Collagen type I
Expression
(% of PBS group)
400
300
200
100
0
*
* +
PBS
PBS + Ang II
TACE siRNA + Ang II

Figure 3-10 Proposed model of TACE regulation of hypertrophy and fibrosis. Previous work by many groups[7,9,12,19,20] has demonstrated that vasoconstrictive GqPCR agonists trigger the post-transcriptional activation of multiple metalloproteinases, including TACE, MMP-2 and ADAM-12. The activated metalloproteinases next transactivate growth factor receptor and downstream MAPKs including ERK-1/2. Findings from this research indicate that metalloproteinases may establish novel transcriptional relationships among each other. Agonist-induced transcriptional pathways mediated by TACE may link sustained GqPCR stimulation to gene expression of other metalloproteinases including MMP-2 and ADAM-12 and developmental genes and extracellular matrix proteins. Cardiovascular hypertrophy and fibrosis processes may be signaled by a metalloproteinase network involving short-term (post-transcriptional) and long-term (transcriptional) mechanisms. The current model could explain, at least in part, the apparent functional redundancy and the concurrence of multiple metalloproteinases from the ADAM and MMP families in signaling of cardiovascular hypertrophy and fibrosis processes.

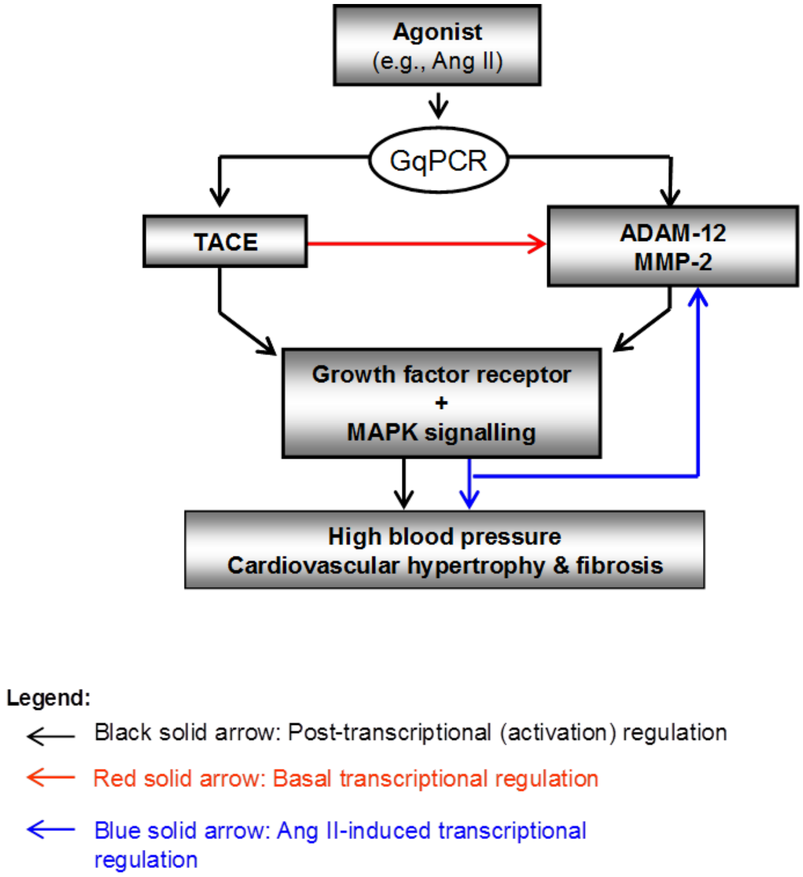
Agonist
(e.g., Ang II)
GqPCR
TACE
ADAM-12
MMP-2
Growth factor receptor
+
MAPK signalling
High blood pressure
Cardiovascular hypertrophy & fibrosis
Legend:
← Black solid arrow: Post-transcriptional (activation) regulation
← Red solid arrow: Basal transcriptional regulation
← Blue solid arrow: Ang II-induced transcriptional regulation

3.5 References

1. Lifton RP, Gharavi AG, Geller DS. Molecular mechanisms of human hypertension. *Cell*. 2001;104:545-556
2. Weber KT, Clark WA, Janicki JS, Shroff SG. Physiologic versus pathologic hypertrophy and the pressure-overloaded myocardium. *J Cardiovasc Pharmacol*. 1987;10 Suppl 6:S37-50
3. Berk BC. Vascular smooth muscle growth: autocrine growth mechanisms. *Physiol Rev*. 2001;81:999-1030
4. Frohlich ED. Left ventricular hypertrophy: dissociation of structural and functional effects by therapy. *Adv Exp Med Biol*. 1991;308:175-190
5. Berk BC, Fujiwara K, Lehoux S. ECM remodeling in hypertensive heart disease. *J Clin Invest*. 2007;117:568-575
6. Prenzel N, Zwick E, Daub H, Leserer M, Abraham R, Wallasch C, Ullrich A. EGF receptor transactivation by G-protein-coupled receptors requires metalloproteinase cleavage of proHB-EGF. *Nature*. 1999;402:884-888
7. Asakura M, Kitakaze M, Takashima S, Liao Y, Ishikura F, Yoshinaka T, Ohmoto H, Node K, Yoshino K, Ishiguro H, Asanuma H, Sanada S, Matsumura Y, Takeda H, Beppu S, Tada M, Hori M, Higashiyama S. Cardiac hypertrophy is inhibited by antagonism of ADAM12 processing of HB-EGF: metalloproteinase inhibitors as a new therapy. *Nat Med*. 2002;8:35-40
8. Hao L, Du M, Lopez-Campistrous A, Fernandez-Patron C. Agonist-induced activation of matrix metalloproteinase-7 promotes vasoconstriction through the epidermal growth factor-receptor pathway. *Circ Res*. 2004;94:68-76
9. Ohtsu H, Dempsey PJ, Frank GD, Brailoiu E, Higuchi S, Suzuki H, Nakashima H, Eguchi K, Eguchi S. ADAM17 mediates epidermal growth factor receptor transactivation and vascular smooth muscle cell hypertrophy induced by angiotensin II. *Arterioscler Thromb Vasc Biol*. 2006;26:e133-137
10. Zhan M, Jin B, Chen SE, Reecy JM, Li YP. TACE release of TNF-alpha mediates mechanotransduction-induced activation of p38 MAPK and myogenesis. *J Cell Sci*. 2007;120:692-701
11. Matsusaka H, Ide T, Matsushima S, Ikeuchi M, Kubota T, Sunagawa K, Kinugawa S, Tsutsui H. Targeted deletion of matrix metalloproteinase 2 ameliorates myocardial remodeling in mice with chronic pressure overload. *Hypertension*. 2006;47:711-717
12. Lautrette A, Li S, Alili R, Sunnarborg SW, Burtin M, Lee DC, Friedlander G, Terzi F. Angiotensin II and EGF receptor cross-talk in chronic kidney diseases: a new therapeutic approach. *Nat Med*. 2005;11:867-874
13. Chien KR, Zhu H, Knowlton KU, Miller-Hance W, van-Bilsen M, O'Brien

TX, Evans SM. Transcriptional regulation during cardiac growth and development. *Annu Rev Physiol*. 1993;55:77-95

14. Bergman MR, Teerlink JR, Mahimkar R, Li L, Zhu BQ, Nguyen A, Dahi S, Karliner JS, Lovett DH. Cardiac matrix metalloproteinase-2 expression independently induces marked ventricular remodeling and systolic dysfunction. *Am J Physiol Heart Circ Physiol*. 2007;292:H1847-1860
15. Huh JW, Kim DS, Oh YM, Shim TS, Lim CM, Lee SD, Koh Y, Kim WS, Kim WD, Kim KR. Is metalloproteinase-7 specific for idiopathic pulmonary fibrosis? *Chest*. 2008;133:1101-1106
16. Roldan V, Marin F, Gimeno JR, Ruiz-Espejo F, Gonzalez J, Feliu E, Garcia-Honrubia A, Saura D, de la Morena G, Valdes M, Vicente V. Matrix metalloproteinases and tissue remodeling in hypertrophic cardiomyopathy. *Am Heart J*. 2008;156:85-91
17. Zeisberg M, Khurana M, Rao VH, Cosgrove D, Rougier JP, Werner MC, Shield CF, 3rd, Werb Z, Kalluri R. Stage-specific action of matrix metalloproteinases influences progressive hereditary kidney disease. *PLoS Med*. 2006;3:e100
18. Zavadzkas JA, Plyler RA, Bouges S, Koval CN, Rivers WT, Beck CU, Chang EI, Stroud RE, Mukherjee R, Spinale FG. Cardiac-restricted overexpression of extracellular matrix metalloproteinase inducer causes myocardial remodeling and dysfunction in aging mice. *Am J Physiol Heart Circ Physiol*. 2008;295:H1394-1402
19. Haro H, Crawford HC, Fingleton B, Shinomiya K, Spengler DM, Matrisian LM. Matrix metalloproteinase-7-dependent release of tumor necrosis factor-alpha in a model of herniated disc resorption. *J Clin Invest*. 2000;105:143-150
20. Sunnarborg SW, Hinkle CL, Stevenson M, Russell WE, Raska CS, Peschon JJ, Castner BJ, Gerhart MJ, Paxton RJ, Black RA, Lee DC. Tumor necrosis factor-alpha converting enzyme (TACE) regulates epidermal growth factor receptor ligand availability. *J Biol Chem*. 2002;277:12838-12845
21. Fedak PW, Moravec CS, McCarthy PM, Altamentova SM, Wong AP, Skrtic M, Verma S, Weisel RD, Li RK. Altered expression of disintegrin metalloproteinases and their inhibitor in human dilated cardiomyopathy. *Circulation*. 2006;113:238-245
22. Kassiri Z, Oudit GY, Sanchez O, Dawood F, Mohammed FF, Nuttall RK, Edwards DR, Liu PP, Backx PH, Khokha R. Combination of tumor necrosis factor-alpha ablation and matrix metalloproteinase inhibition prevents heart failure after pressure overload in tissue inhibitor of metalloproteinase-3 knock-out mice. *Circ Res*. 2005;97:380-390
23. Clemente CF, Tornatore TF, Theizen TH, Deckmann AC, Pereira TC,

Lopes-Cendes I, Souza JR, Franchini KG. Targeting focal adhesion kinase with small interfering RNA prevents and reverses load-induced cardiac hypertrophy in mice. *Circ Res*. 2007;101:1339-1348

24. Kleinman ME, Yamada K, Takeda A, Chandrasekaran V, Nozaki M, Baffi JZ, Albuquerque RJ, Yamasaki S, Itaya M, Pan Y, Appukuttan B, Gibbs D, Yang Z, Kariko K, Ambati BK, Wilgus TA, DiPietro LA, Sakurai E, Zhang K, Smith JR, Taylor EW, Ambati J. Sequence- and target-independent angiogenesis suppression by siRNA via TLR3. *Nature*. 2008;452:591-597
25. Atfi A, Dumont E, Colland F, Bonnier D, L'Helgoualc'h A, Prunier C, Ferrand N, Clement B, Wewer UM, Theret N. The disintegrin and metalloproteinase ADAM12 contributes to TGF-beta signaling through interaction with the type II receptor. *J Cell Biol*. 2007;178:201-208
26. Imai K, Hiramatsu A, Fukushima D, Pierschbacher MD, Okada Y. Degradation of decorin by matrix metalloproteinases: identification of the cleavage sites, kinetic analyses and transforming growth factor-beta1 release. *Biochem J*. 1997;322 (Pt 3):809-814
27. Wang X, Chow FL, Oka T, Hao L, Lopez-Campistrous A, Kelly S, Cooper S, Odenbach J, Finegan BA, Schulz R, Kassiri Z, Lopaschuk GD, Fernandez-Patron C. Matrix metalloproteinase-7 and ADAM-12 (a disintegrin and metalloproteinase-12) define a signaling axis in agonist-induced hypertension and cardiac hypertrophy. *Circulation*. 2009;119:2480-2489
28. Zhang YC, Bui JD, Shen L, Phillips MI. Antisense inhibition of beta(1)-adrenergic receptor mRNA in a single dose produces a profound and prolonged reduction in high blood pressure in spontaneously hypertensive rats. *Circulation*. 2000;101:682-688
29. Nava E, Noll G, Luscher TF. Increased activity of constitutive nitric oxide synthase in cardiac endothelium in spontaneous hypertension. *Circulation*. 1995;91:2310-2313
30. Kawasaki H, Cline WH, Jr., Su C. Involvement of the vascular renin-angiotensin system in beta adrenergic receptor-mediated facilitation of vascular neurotransmission in spontaneously hypertensive rats. *J Pharmacol Exp Ther*. 1984;231:23-32

Chapter 4

MMP-2 Mediates Angiotensin II-induced Hypertension under the transcriptional control of MMP-7 and TACE

The data presented in this chapter is published in the following journal article:

Odenbach J, **Wang X**, Cooper S, Chow FL, Oka T, Lopaschuk G, Kassiri Z, Fernandez-Patron C. MMP-2 mediates angiotensin II-induced hypertension under the transcriptional control of MMP-7 and TACE. *Hypertension*. 2011 Jan;57(1):123-30.

Contribution: Designed siRNAs to MMP-2, MMP-7 and TACE, conducted animal studies, performed qRT-PCR, zymography assays, data analysis and data interpretation, contributed to the construction of the hypothesis, drafted the manuscript together with Jeffery Odenbach and our supervisor and revised the manuscript.

4.1 Introduction

Hypertension is a systemic condition characterized by persistently elevated arterial blood pressure and the concurrent development of pathological cardiac remodelling due to the development of cellular hypertrophy and fibrosis[1-3]. Pathological cardiac remodelling leads to myocardial stiffness, decreased cardiac output and increased risk of heart failure[4,5].

The parallel development of cardiac hypertrophy and fibrosis with hypertension suggests overlapping mechanisms with common inducers and mediators. Among the common inducers of hypertension, cardiac hypertrophy and fibrosis are vasoconstrictive Gq protein-coupled receptor (GqPCR) agonists such as catecholamines, endothelins, and angiotensin II (Ang II). Common downstream mediators of GqPCR agonists include the matrix metalloproteinases (such as MMP-2 and MMP-7) and "a disintegrin and metalloproteinases" (such as ADAM-17 / TACE -tumour necrosis factor-α converting enzyme). These metalloproteinases can, in turn, regulate vascular tone and cardiac remodelling by cleavage of vasoactive peptides, growth factor shedding and degradation of extracellular matrix (ECM) protein components[6-13].

We have suggested that MMPs and ADAMs are transcriptionally networked to mediate pro-hypertensive, pro-hypertrophic and pro-fibrotic signalling in response to GqPCR agonists. However, the exact roles of individual metalloproteinases in the development of cardiovascular disease remain unclear. Of these metalloproteinases, MMP-2 has been shown to regulate vascular function by cleavage of vasoactive peptides (such as big endothelin, calcitonin-gene related peptide and adrenomedullin[11-13]) and cell signalling receptors (such as vascular endothelial growth factor and insulin receptors[16-18]).

Here, we hypothesize that, being a major gelatinase in cardiac and vascular tissue, MMP-2 is likely to play a key role in cardiovascular homeostasis. To examine the role of MMP-2 in the development of agonist-induced cardiovascular disease, we used a mouse model of Ang II-induced hypertension and complementary approaches targeting MMP-2 by pharmacological inhibition and RNA interference (RNAi). We report that MMP-2 mediates Ang II-induced hypertension and is transcriptionally controlled by two other metalloproteinases, MMP-7 and TACE.

4.2 Materials and methods

Materials All siRNAs were synthesized by Sigma-Aldrich (Paris, France) and dissolved in PBS prior to use. The first two nucleotides of each strand were 2'-O methylated and the final two nucleotides were deoxy nucleotides to increase siRNA stability. Sequences of siRNAs are shown in Table 1 are were used as previously described[19,20]. MMP-2 inhibitors (MMP-2i I / MMP-2i III) and Ang II were obtained from Calbiochem (Gibbstown, NJ, USA). Phenylephrine was obtained from Sigma (Oakville, ON, Canada).

Cell Culture A7R5 rat aorta smooth muscle cells (ATCC, Manassas, VA, USA) were cultured in Dulbecco's modified eagle medium supplemented with 10% FBS at 37ºC and 5% CO_2. Cells were passaged using 0.05% trypsin-EDTA solution and seeded in 6 well plates. Cells were transfected with siRNA using DharmaFECT 2 transfection reagent as per manufacturer's protocol (Thermo Scientific, Rockford, IL, USA). Briefly, serum-starved cells were treated with a pre-mixed solution 100 nmol/L siRNA and 0.4% DharmaFECT 2 transfection reagent in serum-free media for 24 hours and MMP-2 activity was measured by gelatin zymography in conditioned media and cell lysates.

Animals Animal studies were conducted under the protocol approved by University of Alberta Animal Care and Use Committee. All animals were housed at the Animal Facility of the University of Alberta until use. Male C57BL/6 mice and Sprague Dawley Rats were purchased from The Jackson Laboratory (Bar Harbor, ME, USA). All animals were anesthetised using 2.0% Isoflurane by inhalation before and during surgical procedures. MMP-2 inhibitor I was given orally at a per diem dose of 40 mg/kg/d. Angiotensin II (1.4 mg/kg/d) and siRNA (0.4 mg/kg/d) were delivered by subcutaneously implanted ALZET osmotic minipumps (DURECT Corporation, Cupertino, CA, USA) on the posterior midsection, as described in previous chapters. Control mice received minipumps containing PBS (vehicle), a sham operation or were left intact. All animals were euthanized by pentobarbital overdose using Euthanyl (Bimeda-MTC, Cambridge, ON, Canada).

Blood pressure measurement Systolic blood pressure was measured indirectly using computerized tail cuff plethysmography system (Kent Scientific Corporation, Torrington, CT, USA). Conscious mice were maintained at 32-35ºC using a heating pad and restrained during measurements. Averages of 10 inflation/deflation cycles were conducted to obtain mean systolic blood pressure.

Echocardiography *In vivo* assessment of anatomical structures and hemodynamic function in mice was conducted by M-mode echocardiography. The animals were first anaesthetized with 2.0% Isoflurane and their cardiac function was subsequently analyzed using a Vevo 770 high-resolution imaging system (Visualsonics, Toronto, ON, Canada). Three consecutive heartbeats of each frame were analyzed to measure the wall thickness and end-diastolic internal dimension (EDD) and end-systolic internal dimension (ESD) of the left ventricle (LV). Echocardiographic corrected LV mass (in mg) was calculated as: 1.05 x 0.8 x $[(LVID;d + LVPW;d + IVS;d)^3 – (LVID;d)^3]$ on diastole (d). ID- internal diameter (in mm). PW- posterior wall thickness (in mm). IVS- interventricular septum thickness (in mm).

Cryosectioning Mouse hearts were embedded in Tissue-Tek (Sakura, Torrance, CA, USA), frozen on dry ice and stored at -70 ºC. Sections (10 μm) were cut on a Leica microtome and fixed with ice-cold acetone.

WGA-FITC staining and cardiomyocytes cross-sectional area quantification Sections of heart were washed in PBS-T and incubated for 2 hrs in 50 µg/mL wheat germ agglutinin-fluorescein isothiocyanate (WGA-FITC, Invitrogen, Burlington, ON, Canada), washed and mounted. Confocal microscope images were taken with a spinning disk laser confocal microscope (Confocal Imagine Core facility, University of Alberta) and cardiomyocyte cross-sectional area was determined by averaging the sizes of at least 100 cells per section.

Collagen staining with picrosirius red Sections of heart were brought back to water and stained for 1 hr in picrosirius red staining solution (1 g/L Direct Red 80 in saturated picric acid solution), washed in acidified water and dehydrated. Slides were photographed using a DCM500 camera and ScopePhoto software (Madell Technology, Beijing, China).

Homogenization Heart and aorta were washed in isotonic saline buffer, rinsed and weighed. Protein extraction was done in 50 mM Tris, 50 mM NaCl, 1.25 mM PMSF, 62.5 mM Glycerol-2-phosphate, 12.5 mM sodium pyrophosphate, 125 µM NaF, 6.25 µg/ml leupeptine, 312.5 µM sodium orthovanadate, 12.5% glycerol, 1% SDS, 0.1% Triton X-100 at pH 7.4. To determine the protein content, homogenates were separated by 10% SDS-PAGE followed by densitometric analysis of Coomassie blue stained bands. Equal protein loads were loaded for subsequent gelatin zymography analysis.

Gelatin zymography MMP-2 enzymatic activity was determined in heart and aorta homogenates using gelatin zymography. Homogenates were subjected to electrophoresis on SDS-PAGE gels co-polymerized with gelatin (2 mg/mL). Following electrophoresis, gels were washed thrice with 2.5% Triton X-100 for 20 min. Enzymatic reaction was carried out for 16 hrs at 37°C in enzyme assay buffer (25 mM Tris, 5 mM $CaCl_2$, 142 mM NaCl, 0.5 mM NaN_3, pH 7.6) and gels were stained with coomassie blue. Enzymatic activity was visualized as clear bands against a blue background in the gel.

RNA expression analysis by TaqMan RT PCR Total RNA was extracted from flash-frozen heart using Trizol reagent (Invitrogen, Burlington, ON, Canada) and cDNA was generated from 1 µg RNA using a random hexamer. Expression analysis of the reported genes was performed by TaqMan RT-PCR using ABI 7900 sequence detection system (Applied Biosystems, Carlsbad, CA, USA). 18S rRNA was used as an internal standard as previously described[21].

Microperfusion arteriography Mesenteric arteries of adult Sprague Dawley Rats (6-month old, male) were dissected and mounted on a Danish MyoTechnology arteriograph system (Aarhus, Denmark). Arteries were perfused at constant temperature (37°C) and flow rate (2 µL/min) with standard HEPES-PSS (142 mM sodium chloride, 4.7 mM potassium chloride, 1.17 mM magnesium sulfate, 1.56 mM calcium chloride, 1.18 mM potassium phosphate, 10 mM HEPES, 5.5 mM glucose, pH 7.4). Phenylephrine (10 µmol/L) was added to the bath (adventitia side) to constrict arteries for 5 min. Following constriction, MMP-2 inhibitor III (100 µmol/L) or DMSO (1%) was added to the bath for an additional 5 min. Changes in arterial diameter were recorded using Vediview acquisition software (Danish MyoTechnology, Aarhus, Denmark).

Statistical analysis Results were analyzed using one-way ANOVA (between multiple groups) or t-test (between two groups) (Jandel SigmaStat 3.5 statistical software). In the echocardiography studies, between-group comparisons of the means were performed by one-way ANOVA followed by Scheffe's F correction for multiple comparisons between means. All data are reported as means +/- SEM.

4.3 Results

MMP-2 is upregulated in Ang II-induced hypertension, cardiac hypertrophy and fibrosis

Ang II infusion (1.4 mg/kg/d, **Figure 4-1A**) resulted in a time-dependent elevation in blood pressure (**Figure 4-1B**) as well as development of left ventricular hypertrophy and fibrosis over 16 days. Hypertrophy was confirmed by increased left ventricle mass (by M-mode echocardiography, **Figure 4-1C**), heart weight to body weight ratio (**Figure 4-2A),** cardiomyocyte cross sectional area (WGA-FITC staining, **Figure 4-2B)** and expression of the hypertrophy marker genes α-skeletal actin (a-sk-actin) and brain natriuretic peptide (BNP) by qRT-PCR (**Figure 4-1D)**. Similarly, development of cardiac fibrosis was demonstrated by increased collagen deposition (picrosirius red staining, **Figure 4-1E)** and expression of the fibrosis marker genes collagen types I and III (Col I, Col III, respectively) and fibronectin-1 (Fn-1) by qRT-PCR **(Figure 4-1F).** Analysis of MMP-2 mRNA (by qRT-PCR, **Figure 4-3A, B**) and enzymatic activity (by gelatin zymography, **Figure 4-3C, D**) of heart and aorta homogenates revealed that MMP-2 was upregulated during Ang II infusion. In contrast to MMP-2, Ang II downregulated another major gelatinase, MMP-9. We therefore hypothesized that upregulation of MMP-2 may be a contributing factor in Ang II-induced cardiovascular disease.

MMP-2 selectively mediates hypertension, but not cardiac hypertrophy or fibrosis

Studies in isolated mesenteric arteries. Previous evidence indicates that MMP inhibition is a possible approach to decrease blood pressure by modulating vascular tone[8,14,22]. Our group has shown that broad-spectrum MMP inhibitors such as doxycycline, phenanthroline and GM 6001 induce a dose-dependent relaxation of microperfused small mesenteric arteries constricted with phenylephrine[23]. The cyclic peptide inhibitor, CTT, which inhibits gelatinases (MMP-2 and MMP-9), also produces similar results[11,12]. Here, we confirm these results using a biphenylsulfonamido-hydroxamate inhibitor selective for MMP-2 (MMP-2 inhibitor III, Calbiochem) in isolated small rat mesenteric arteries mounted on a microperfusion arteriograph. Treatment with MMP-2 inhibitor III (100 µmol/L), but not vehicle (DMSO, 1%), caused relaxation of arteries pre-constricted with 10 µmol/L phenylephrine (**Figure 4-4**). Taken together with our earlier studies, these results strongly suggest that agonists engage MMP-2 to maintain arterial tone.

Studies of hypertension, cardiac hypertrophy and fibrosis in mice receiving Ang II. To determine whether targeting MMP-2 could attenuate Ang II-induced cardiovascular disease *in vivo*, mice receiving Ang II were treated with either a pharmacological inhibitor or small interference RNA (siRNA) against MMP-2.

Pharmacological inhibition of MMP-2 using the lipid analogue MMP-2 inhibitor I (Calbiochem) given orally at a daily dose of 40 mg/kg/d (beginning the day before Ang II infusion) attenuated Ang II-induced hypertension over a 12 day time course (**Figure 4-5A**).

Despite the protective effects of MMP-2 inhibition on blood pressure, no protection from either cardiac hypertrophy (by M-mode echocardiography, qRT-PCR analysis of hypertrophy marker genes, heart weight to body weight ratio and cellular cross sectional area, **Figures 4-5B, 4-6**) or fibrosis (by picrosirius red staining and qRT-PCR analysis of fibrosis marker genes, **Figure 4-5C**) was observed. These results indicate that MMP-2 mediates Ang II-induced hypertension, but not cardiac hypertrophy or fibrosis.

Supplemental studies were conducted to validate these pharmacological results. We used an RNA interference approach with a siRNA (**Table 4-1**) shown to knock down MMP-2 in cultures of aortic smooth muscle cells (**Figure 4-7).** To determine if the effects of Ang II could be prevented by targeting MMP-2, we designed an experiment where MMP-2 siRNA treatment (0.4 mg/kg/d) started 5 days prior to

Ang II infusion (pre-treatment protocol, **Figure 4-8A**).To assess if the effects of Ang II could be reversed in already-hypertensive mice, we designed a rescue experiment where MMP-2 siRNA treatment started 5 days after Ang II infusion began (rescue protocol, **Figure 4-8B**). In both protocols, MMP-2 siRNA attenuated the Ang II-induced upregulation of cardiac and aortic MMP-2 enzymatic activity (**Figure 4-8A, B**). We also examined MMP-2 at two distal sites (i.e., the kidney and liver). In these organs, MMP-2 was not upregulated by Ang II and we were unable to detect any attenuation of MMP-2 activity using siRNA (**Figure 4-8C, D**). Moreover, in both protocols, administration of MMP-2 siRNA also decreased the severity of Ang II-induced hypertension (**Figure 4-8E, F**). MMP-2 siRNA treatment did not attenuate the development of cardiac hypertrophy or fibrosis by either protocol (pre-treatment, **Figure 4-8G, I, K** or rescue, **Figure 4-8H, J, L**). Therefore, MMP-2 siRNA had similar anti-hypertensive (but not anti-hypertrophic or anti-fibrotic) effects whether given before or after hypertension was initiated (pre-treatment or rescue protocols, respectively).

Confirming the target-specific effects of MMP-2 siRNA, siRNA against the non-mammalian gene Luciferase did not prevent Ang II-induced hypertension or MMP-2 upregulation (**Figure 4-9**).

MMP-7 and TACE mediate Ang II-induced MMP-2 upregulation

We next investigated how and why Ang II induces MMP-2 upregulation with a focus on metalloproteinases upstream of MMP-2. Previously, we showed that TACE is a key mediator in cardiac hypertrophy and fibrosis and that knockdown of TACE partially attenuates Ang-II induced MMP-2 upregulation. We have also shown that MMP-7 is involved in early stages of agonist-induced hypertension, but whether this role of MMP-7 is dependent on MMP-2 remains unclear[14,15]. We therefore revisited the effects of siRNAs targeting MMP-7 and

TACE either individually or together on expression of MMP-2 using validated siRNAs and treatment protocols.

In mice receiving MMP-7 siRNA, TACE siRNA or both siRNAs together, the upregulation of MMP-2 by Ang II was prevented at both the mRNA (**Figure 4-10A, B**) and enzymatic activity (**Figure 4-11**) levels. Similar to the results obtained by targeting MMP-2 directly, simultaneous knockdown of MMP-7 and TACE attenuated Ang II-induced hypertension (**Figure 4-12A, B**). In contrast to siRNA against MMP-2, siRNAs against MMP-7 and TACE attenuated the development of cardiac hypertrophy (by echocardiography and qRT-PCR analysis of hypertrophy marker genes, **Figure 4-12C**) and fibrosis (by picrosirius red staining of heart sections and qRT-PCR analysis of fibrosis marker genes, **Figure 4-12D**). These findings indicate that Ang II upregulates MMP-2 through MMP-7 and TACE.

4.4 Discussion

This research provides new evidence that agonist-induced cardiovascular disease is signalled by multiple, non-redundant metalloproteinases that play unique physiological roles. We demonstrate that MMP-2 inhibition (by pharmacological means) and gene knockdown (by RNA interference) attenuate Ang II-induced hypertension. However, these manipulations did not prevent any of the following pro-hypertrophic and pro-fibrotic responses: i) increases in left ventricle mass, ii) increases in cardiomyocyte cross sectional area, iii) increases in collagen deposition or, iv) increases in expression of hypertrophy and fibrosis marker genes. Importantly, we observed a novel transcriptional regulation of MMP-2 by two other metalloproteinases, MMP-7 and TACE. Paradoxically, while direct blockade of MMP-2 only attenuated Ang II-induced hypertension, indirect blockade of MMP-2 (by knocking down MMP-7 and TACE) attenuated Ang II-induced hypertension as well as the development of cardiac hypertrophy and fibrosis. These findings suggest a signaling bifurcation where Ang II-induced hypertension diverges from development of cardiac hypertrophy and fibrosis. Therefore, we propose a model where Ang II signals through MMP-7 and TACE to induce: i) hypertension mediated by MMP-2 and, ii) cardiac hypertrophy and fibrosis independent of MMP-2 (**Figure 4-13**).

Pathological cardiac remodelling is a clinically significant complication in hypertensive disorders. However, the causal relationship between hypertension and cardiac remodelling is poorly understood. In models of hypertension, the development of hypertensive cardiac remodelling is thought to be caused by: i) excessive systemic agonists (as done in this study) and, ii) hemodynamic pressure overload on the heart (as done in transverse aortic constriction, TAC)[24-26]. Strong evidence indicates that endogenous agonist production is required for TAC-induced remodelling. Indeed, cardiac hypertrophy is attenuated by blockade of Ang II production (ie., ACE inhibitors, ramipril[27]) or receptor antagonism (ie., AT1R antagonist, losartan[28]). Further supporting this claim, hypertrophic growth can be induced in cultured cardiomyocytes stimulated by GqPCR agonists in the absence of pressure overload[29,30]. Therefore, these data suggest that endogenous agonist signaling is necessary and sufficient for the development of hypertensive cardiac remodelling. We propose that agonist-induced cardiovascular disease depends on metalloproteinases, which regulate the expression of genes involved in pathological cardiac remodelling (e.g., brain natriuretic peptide, alpha-skeletal actin, beta-myosin heavy chain, fibronectin-1 and collagen types I and III), as well as the expression of MMP-2. Moreover, our data show that targeting MMP-2 effectively uncouples Ang II-induced hypertension from the development of cardiac hypertrophy and fibrosis. If agonist signaling is sustained, pathological cardiac remodelling can proceed in the absence of hypertension.

Our data strongly suggest that targeting MMP-2 attenuates Ang II-induced hypertension, without affecting the development of cardiac hypertrophy or fibrosis. Although we were able to attenuate Ang II-induced hypertension by targeting MMP-2, we cannot exclude the possibility that the residual increase in blood pressure of these mice contributed to the development of cardiac hypertrophy and fibrosis. However, mice challenged with Ang II and mice challenged with Ang II and MMP-2 inhibitor/siRNA developed cardiac hypertrophy and fibrosis to the same extent, suggesting that agonist signaling, and not residual hypertension, was ultimately responsible for cardiac remodelling in these mice.

Despite the detrimental effects of cardiac remodelling in Ang II-induced hypertension, other instances of cardiac hypertrophy exist in nature which can be beneficial to the heart (e.g., the heart of a well-trained athlete[31]). A major factor leading to cardiac failure in subjects with hypertension is the excessive deposition of extracellular matrix proteins (cardiac fibrosis) that impairs cardiac contractility. This process of hypertension-associated cardiac fibrosis occurs in parallel to the hypertrophy process. However, despite developing within similar time frames and having common agonists, cardiac fibrosis and hypertrophy can be pharmacologically separated. Zeisberg et al.[32] have demonstrated that administration of recombinant human bone morphogenic protein-7 to mice with aortic constriction prevents cardiac fibrosis and improves cardiac function, despite the presence of cardiac hypertrophy. Our study suggests that sustained stimulation by agonists, such as Ang II, leads to pathological cardiac remodelling characterized by increased myocardial stiffness through temporally overlapping pro-hypertrophic and pro-fibrotic mechanisms, neither of which can be attenuated by targeting MMP-2.

Although we provide new insight into the regulation of MMP-2 gene transcription by MMP-7 and TACE, the pathways by which MMP-2 regulates vascular tone are complex and arise from a multitude of MMP-2 proteolysis substrates. Previous studies have suggested that MMP-2 can cleave vasoactive peptides (such as big endothelin, calcitonin gene related peptide and adrenomedullin)[11-13] as well as extracellular receptors (such as vascular endothelial growth factor receptor-2, and insulin receptor)[16,18]. Future research should establish the specific contribution of these MMP-2 signaling mechanisms in agonist-induced hypertension.

A fascinating question in regards to development of hypertensive cardiac disease is the role played by organs distal to the heart such as the kidneys[33]. Based on our studies, we believe that elevated levels of pro-hypertensive agonists are ultimately causal of the development of hypertensive cardiac disease. In addition to acting directly on the heart and vasculature, agonists such as Ang II can stimulate secondary messaging systems (e.g., the sympathetic nervous system) by acting at sites distal to the heart. These secondary messaging systems can contribute to the development of cardiac remodelling (by acting on the heart) and hypertension (by acting on the vasculature where they could stimulate MMP-2 dependent vasoconstriction)[34].

Interestingly, we did not observe any induction of MMP-2 in the kidney. Similar to our findings, MMP-2 is not elevated in the renal medulla of the spontaneous hypertensive rat, whereas MMP-7 is[35]. There is also evidence that TACE plays a role in chronic renal disease induced by Ang II[9]. Based on these findings, renal MMP-7 and TACE may be effectors of Ang II, but might not act by upregulating MMP-2 in the kidney.

The concept that MMP-7 and TACE are upstream regulators of MMP-2 in Ang II-induced cardiovascular disease is supported by several unrelated lines of research. MMP-7 regulates MMP-2 activation *in vitro* (by direct proteolysis) and in myeloma cells to facilitate bone destruction and tumour spreading[36,37]. MMP-7 and

TACE may also facilitate MMP-2 activation by releasing TNF-α to transcriptionally upregulate MT1-MMP[38]. Further, MMP-7 and TACE can shed growth factor receptor ligands such as HB-EGF[39] which have been involved in the transcriptional upregulation of MMP-2[40].

Clinical Perspective

Pathological cardiac remodelling occurs concurrently with the development of hypertension and must be considered when devising therapeutic strategies to treat hypertension. Our findings indicate that metalloproteinases are signaling mediators and candidate therapeutic targets in hypertensive cardiac remodelling. Metalloproteinases could also be therapeutic targets in other diseases where they are strongly upregulated such as chronic renal disease, pre-eclampsia and cancer[9,41]. Paradoxically, metalloproteinase inhibitors have had very little clinical success in the cancer field. Secondary effects such as the development of musculoskeletal syndrome have further hindered the development of metalloproteinase-based therapeutics[42,43].

Although targeting MMP-2 shows promise to lower high blood pressure, our inability to prevent the development of cardiac hypertrophy and fibrosis by blocking MMP-2 (both pharmacologically and through RNA interference) indicates the need for comprehensive therapeutic strategies. One such strategy is suggested by novel findings made in this research. Targeting MMP-2 together with metalloproteinases upstream of MMP-2 (such as MMP-7 and TACE) should lower blood pressure with the added therapeutic benefits of preventing the development of cardiac hypertrophy and fibrosis. Further research is warranted to determine the biological roles and therapeutic potential of specific metalloproteinases in hypertensive cardiac disease.

Table 4-1 Nucleotide sequences of siRNAs used in experiments.

Gene	siRNA oligonucleotide sequences	
MMP-2	Sense:	5'-mCmAUACAGGAUCAUUGGUUAdTdT
	Antisense:	5'-mUmAACCAAUGAUCCUGUAUGdTdT
MMP-7	Sense:	5'-mCmCUACAGAAUUGUAUCCUAdTdT
	Antisense:	5'-mUmAGGAUACAAUUCUGUAGGdTdG
TACE	Sense:	5'-mGmAGAAGCUUGAUUCUUUGCdTdT
	Antisense:	5'-mGmCAAAGAAUCAAGCUUCUCdAdA
Luciferase	Sense:	5'-mUmAAGGCUAUGAAGAGAUACdTdT
	Antisense:	5'-mGmUAUCUCUUCAUAGCCUUAdTdT

"m" denotes O-methylation of following nucleotide. "d" indicates deoxynucleotide.

Figure 4-1 Development of hypertension, cardiac hypertrophy and fibrosis induced by Ang II.

A) Experimental protocol of Ang II delivery (1.4 mg/kg/d) in male C57BL/6 mice by subcutaneous osmotic minipumps. **B)** Time course of systolic blood pressure in control mice and mice treated with Ang II. Echocardiographic analysis of left ventricle weight to body weight ratio (**C**), qRT-PCR analysis of hypertrophy marker genes (**D**), histological analysis of heart sections (10 µm) stained with picrosirius red (**E**) and qRT-PCR analysis of fibrosis marker genes (**F**) in mice receiving Ang II for the times indicated. Scale bar indicates 250 µm. n=4 mice for each time point. * indicates $p<0.05$ vs. day 0.

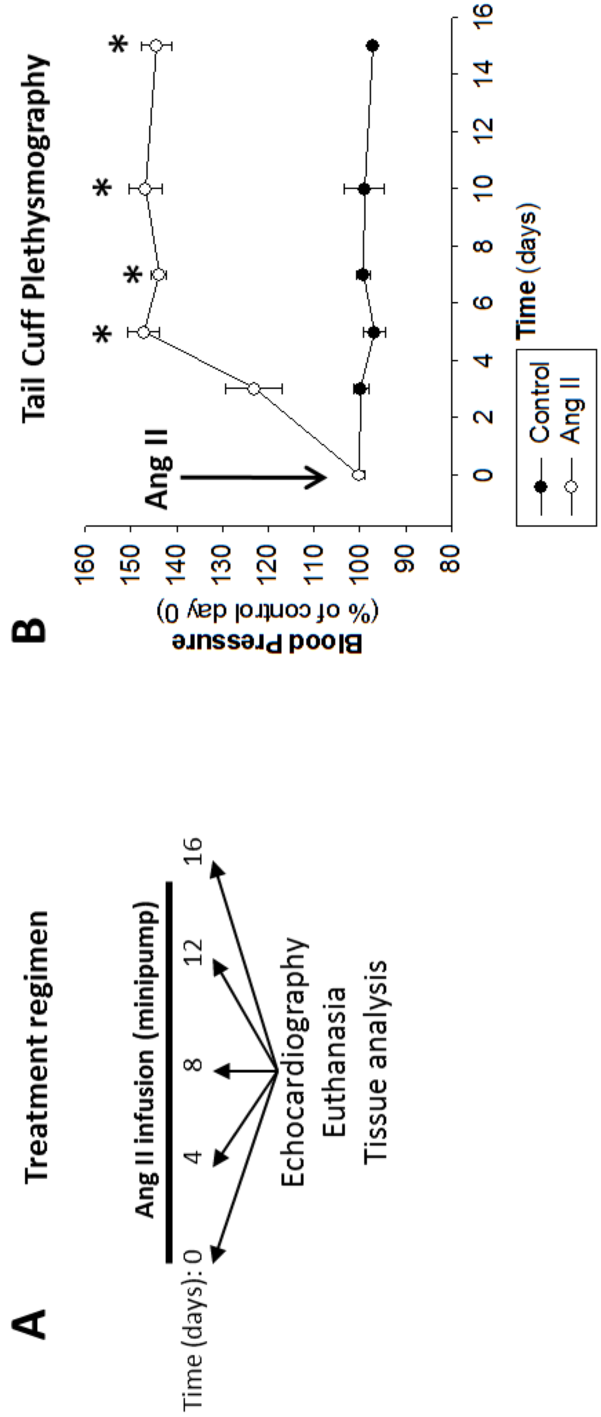
A
Treatment regimen
Time (days): 0
4
8
12
16
Ang II infusion (minipump)
Echocardiography
Euthanasia
Tissue analysis
B
Tail Cuff Plethysmography
Blood Pressure
(% of control day 0)
160
150
140
130
120
110
100
90
80
Ang II
*
Time (days)
0
2
4
6
8
10
12
14
16
Control
Ang II

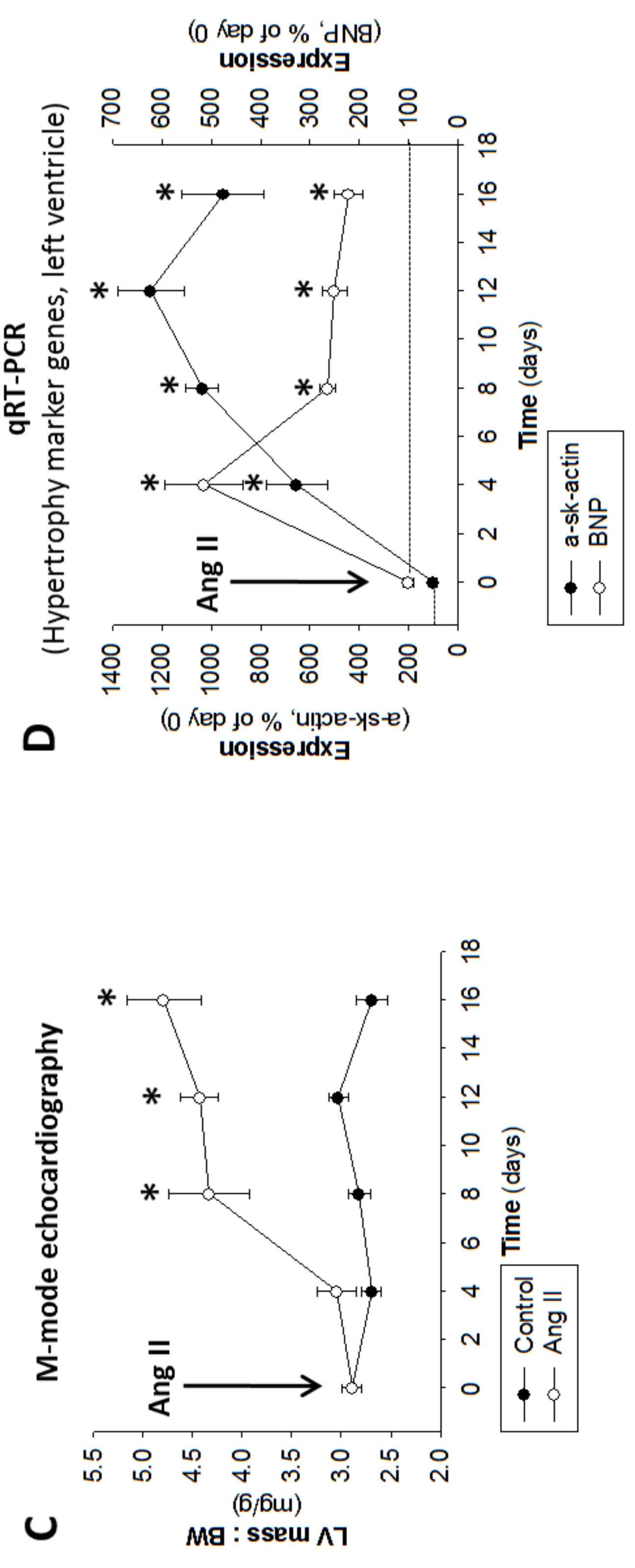
C
M-mode echocardiography
LV mass : BW (mg/g)
5.5
5.0
4.5
4.0
3.5
3.0
2.5
2.0
Ang II
*
*
*
0
2
4
6
8
10
12
14
16
18
Time (days)
Control
Ang II
D
qRT-PCR
(Hypertrophy marker genes, left ventricle)
Expression (a-sk-actin, % of day 0)
1400
1200
1000
800
600
400
200
0
Expression (BNP, % of day 0)
700
600
500
400
300
200
100
0
Ang II
*
*
*
*
*
*
*
*
0
2
4
6
8
10
12
14
16
18
Time (days)
a-sk-actin
BNP

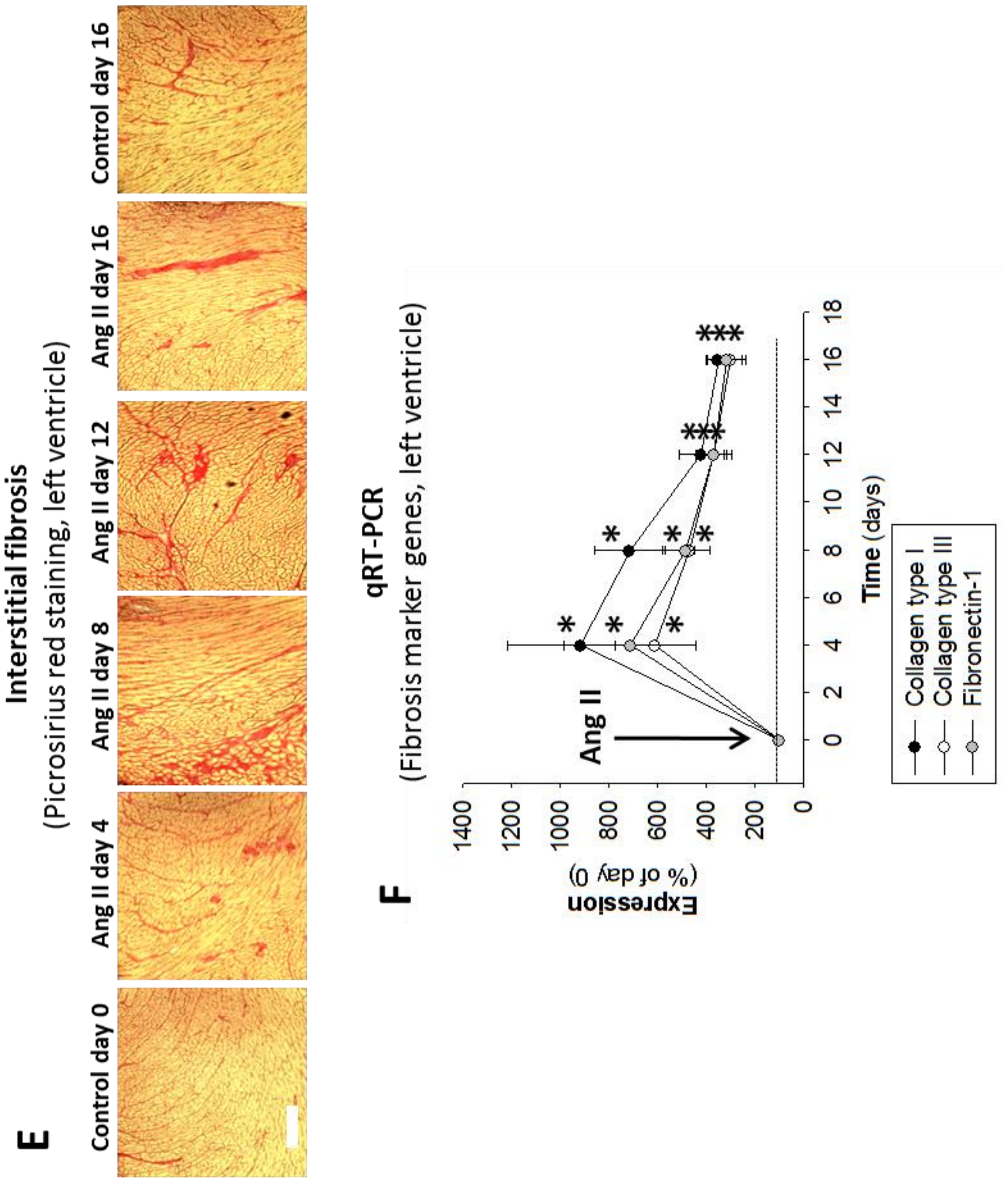
E
Interstitial fibrosis
(Picrosirius red staining, left ventricle)
Control day 0
Ang II day 4
Ang II day 8
Ang II day 12
Ang II day 16
Control day 16
F
qRT-PCR
(Fibrosis marker genes, left ventricle)
Expression
(% of day 0)
0
200
400
600
800
1000
1200
1400
Ang II
*
0
2
4
6
8
10
12
14
16
18
Time (days)
Collagen type I
Collagen type III
Fibronectin-1

Figure 4-2 Ang II induces the development of cardiac hypertrophy.
Quantification of increases in **A**) heart weight/body weight ratio and **B**) cardiomyocyte cross sectional area (WGA-FITC staining) in the development of cardiac hypertrophy in mice receiving Ang II (1.4 mg/kg/d) by subcutaneous osmotic minipumps. Scale bar indicates 100 µm. n=4 mice for each time point. * indicates p<0.05 vs. day 0.

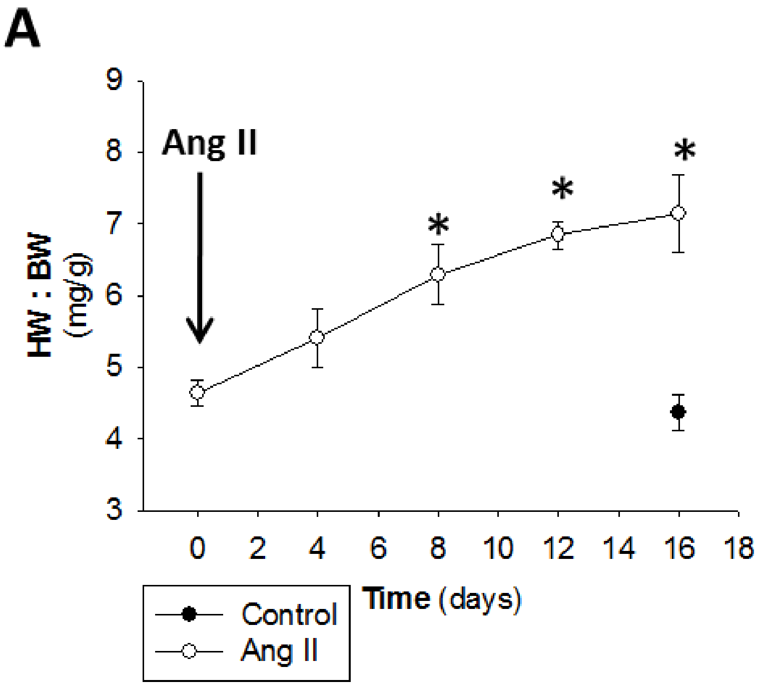

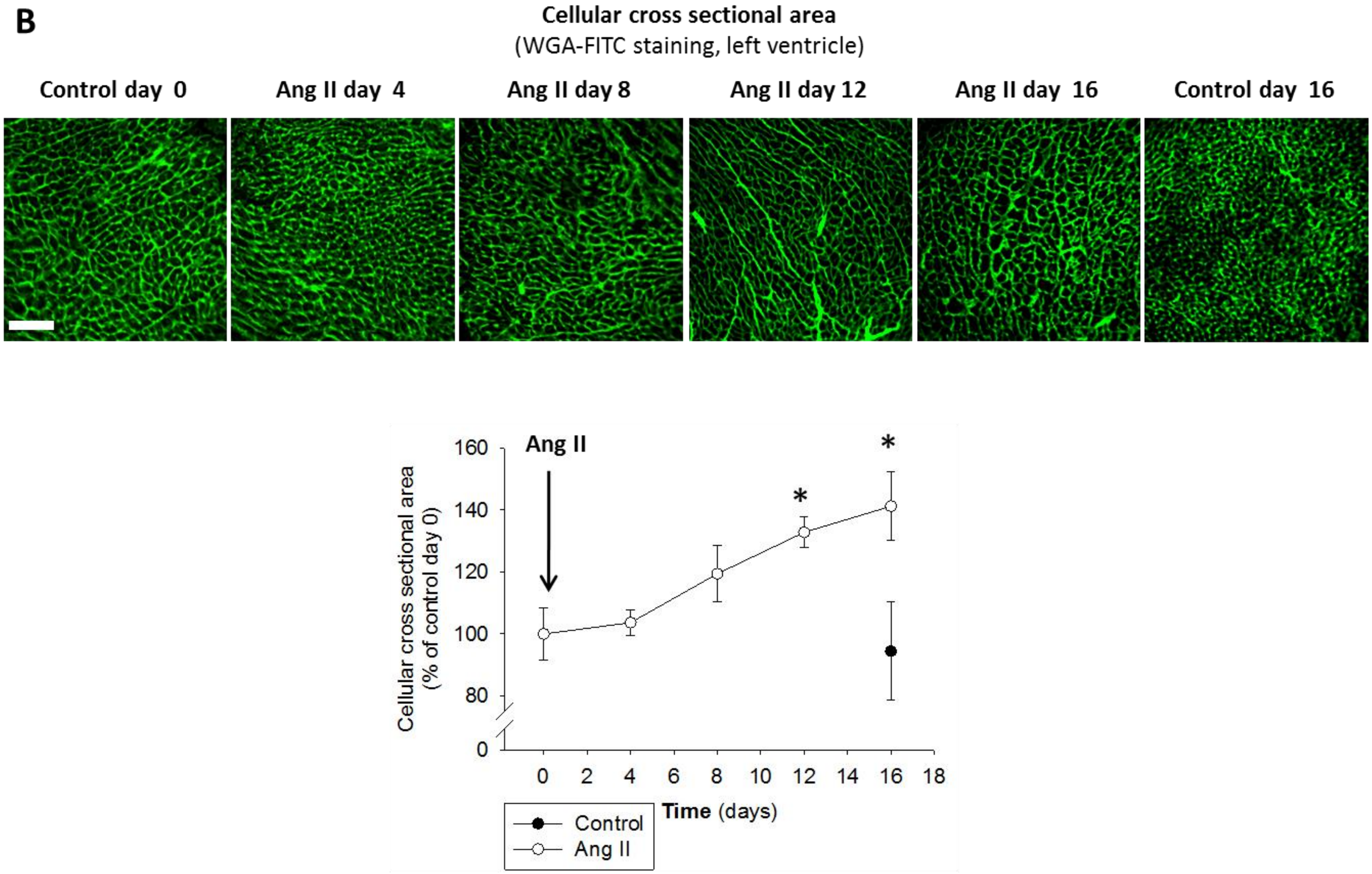
B
Cellular cross sectional area
(WGA-FITC staining, left ventricle)
Control day 0
Ang II day 4
Ang II day 8
Ang II day 12
Ang II day 16
Control day 16
Ang II
*
*
Cellular cross sectional area
(% of control day 0)
160
140
120
100
80
0
0
2
4
6
8
10
12
14
16
18
Time (days)
Control
Ang II

Figure 4-3 Ang II upregulates MMP-2 expression and enzymatic activity.
A, B) qRT-PCR analysis of MMPs in left ventricle samples over a time course of Ang II treatment (1.4 mg/kg/d). Gelatin Zymography analysis of MMP-2 enzymatic activity in left ventricle (**C**) and Aorta (**D**) samples from mice treated with Ang II over a 16 day time course. Quantification of band intensity normalized to loading control shown in lower panels. n=4 mice for time point. * indicates p<0.05 vs day 0.

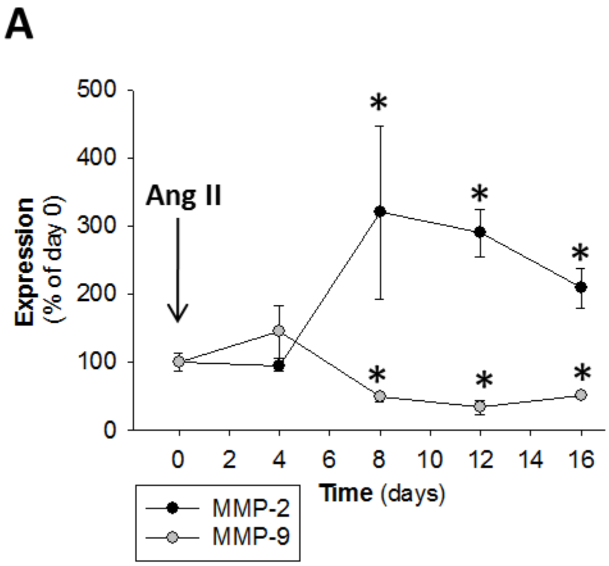

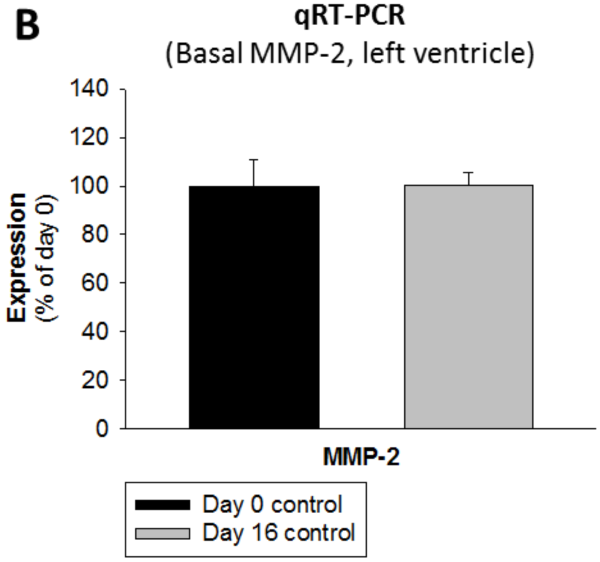

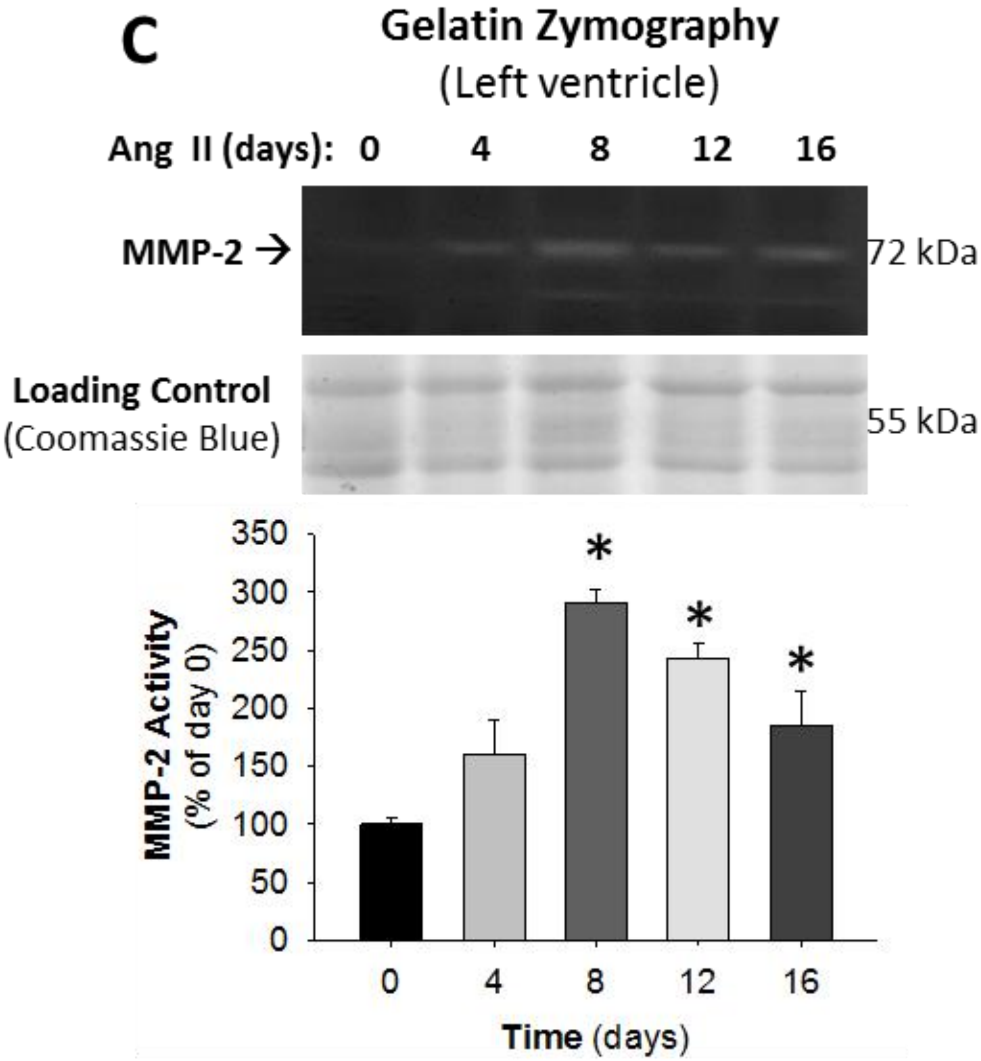
C
Gelatin Zymography
(Left ventricle)
Ang II (days): 0 4 8 12 16
MMP-2 →
72 kDa
Loading Control
(Coomassie Blue)
55 kDa
MMP-2 Activity
(% of day 0)
350
300
250
200
150
100
50
0
*
*
*
0
4
8
12
16
Time (days)

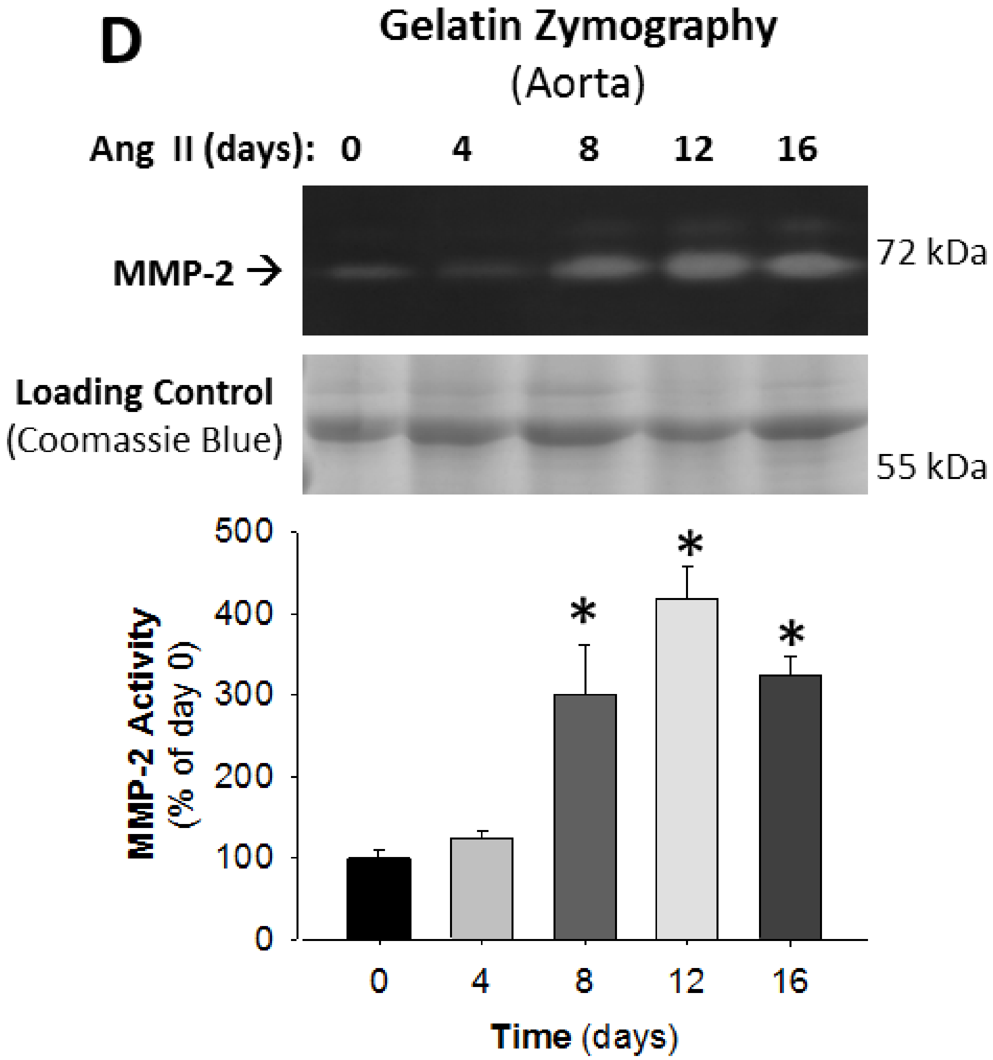
D
Gelatin Zymography
(Aorta)
Ang II (days): 0 4 8 12 16
MMP-2 →
72 kDa
Loading Control
(Coomassie Blue)
55 kDa
500
400
300
200
100
0
MMP-2 Activity
(% of day 0)
*
*
*
0
4
8
12
16
Time (days)

Figure 4-4 MMP-2 is involved in the maintenance of agonist-induced arterial constriction.

Small rat mesenteric arteries were isolated and mounted on a microperfusion arteriograph system. Top panel- Light micrograph images of arteries at baseline (0 min), constricted with phenylephrine (PE, 10 µmol/L, 5 min), treated with either MMP-2 inhibitor III (100 µmol/L) or vehicle (1% DMSO, 10 min) and washed in triplicate (washout, 15 min). Bottom panel- Quantitative analysis of artery inner diameter from acquired images. Images are representative of triplicate trials. Scale bar indicates 100 µm. * indicates $p<0.05$ vs baseline.

(These data were obtained by Jeffrey Odenbach)

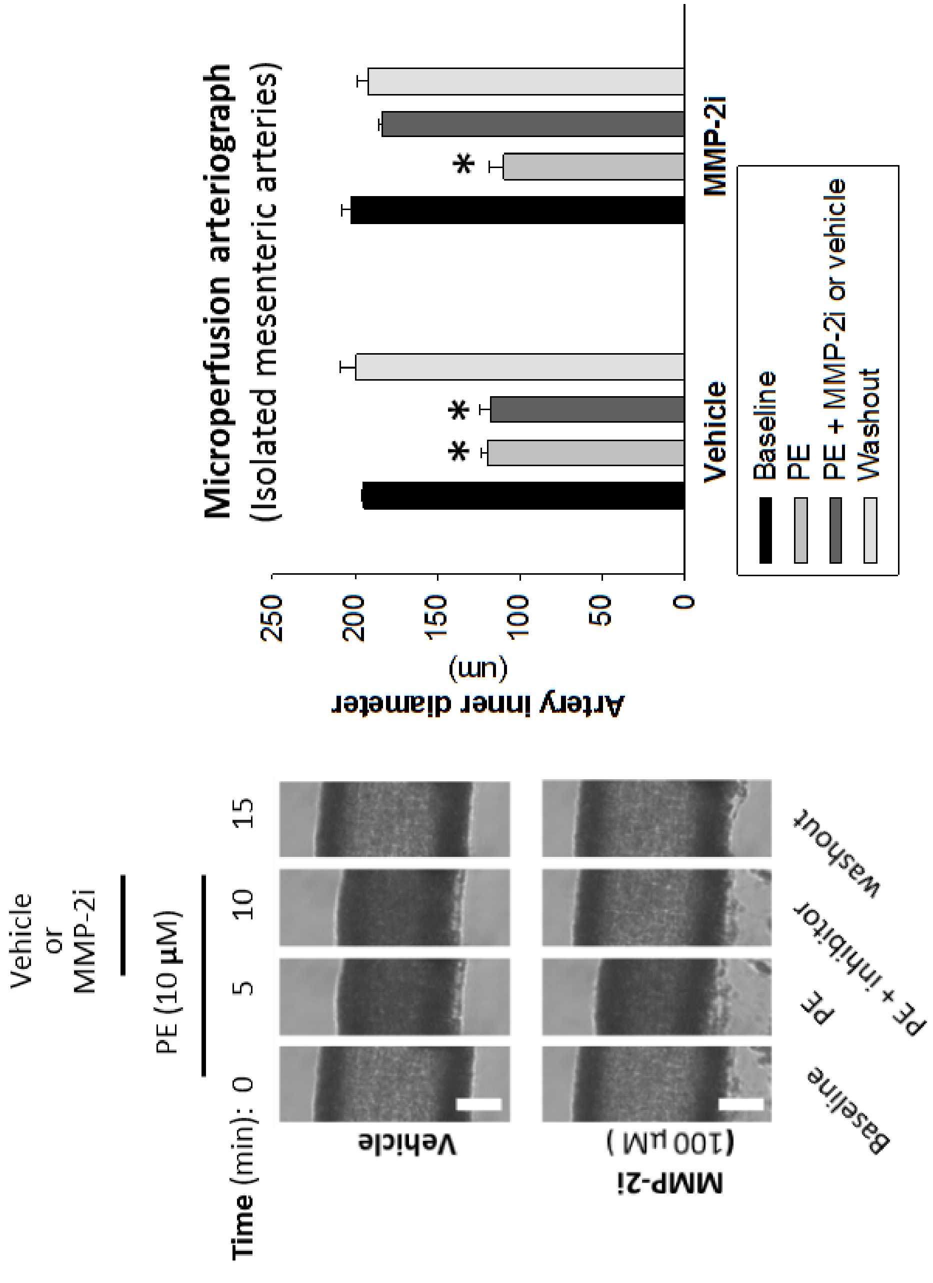
Microperfusion arteriograph
(Isolated mesenteric arteries)
Artery inner diameter (um)
0
50
100
150
200
250
*
*
*
Vehicle
MMP-2i
Baseline
PE
PE + MMP-2i or vehicle
Washout
Time (min): 0
5
10
15
PE (10 µM)
Vehicle or MMP-2i
Vehicle
MMP-2i (100 µM)
Baseline
PE
PE + inhibitor
Washout

Figure 4-5 MMP-2 mediates Ang II-induced hypertension but not cardiac hypertrophy or fibrosis.

A) Upper panel- Experimental treatment protocol of mice with MMP-2 inhibitor I (MMP-2i, 40 mg/kg/d) and Ang II (1.4 mg/kg/d) by daily oral administration and subcutaneous osmotic minipumps, respectively. Lower panel- Tail cuff plethysmography analysis of systolic blood pressure in mice treated as per above protocol. **B)** Echocardiographic analysis of left ventricle mass normalized to body weight (left panel) and qRT-PCR analysis of hypertrophy marker genes (right panel) in left ventricle samples. **C)** Collagen staining of heart sections (10 µm) stained with picrosirius red (left panel) and qRT-PCR analysis of fibrosis markers (right panel) in left ventricle samples. Scale bar indicates 250 µm. n=4 mice for each group. * indicates p<0.05 vs. control. ‡ Indicates p<0.05 vs Ang II.

(These data were obtained by Jeffrey Odenbach)

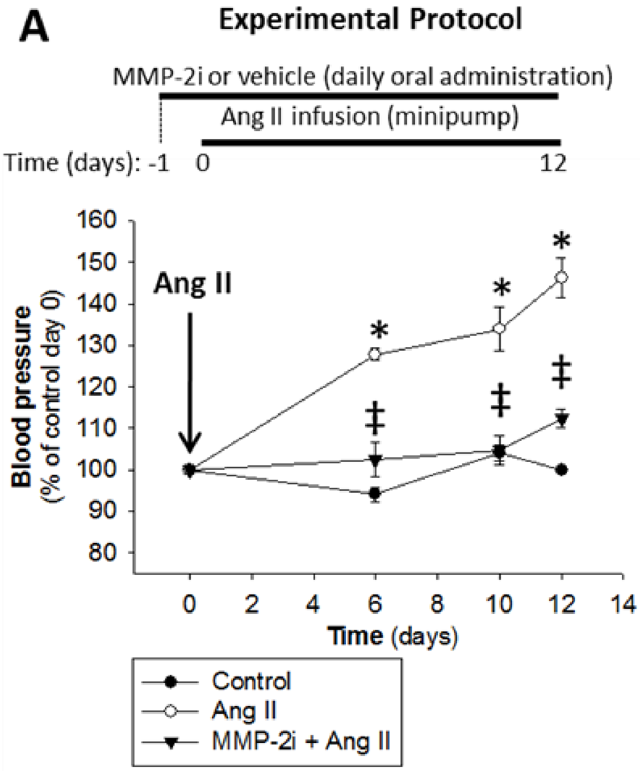

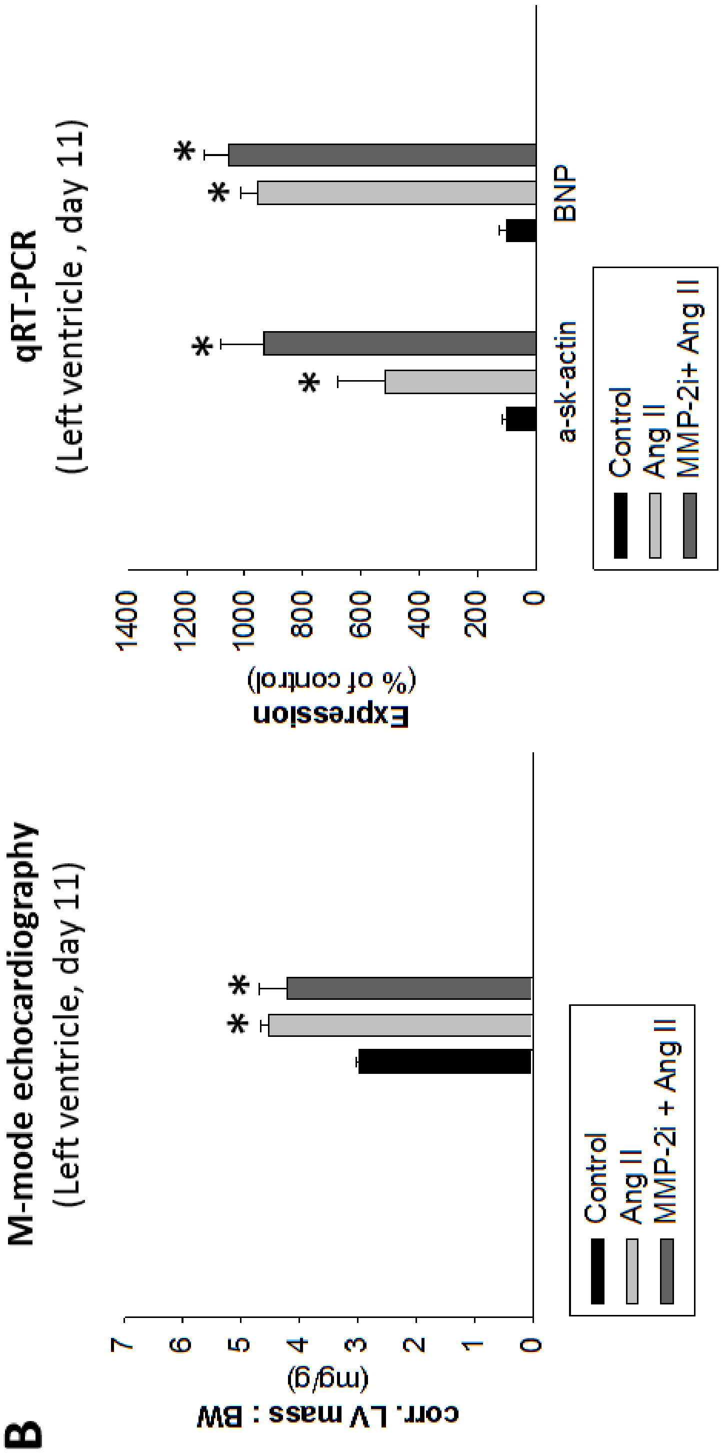
B
M-mode echocardiography
(Left ventricle, day 11)
corr. LV mass : BW
(mg/g)
0
1
2
3
4
5
6
7
*
*
Control
Ang II
MMP-2i + Ang II
qRT-PCR
(Left ventricle , day 11)
Expression
(% of control)
0
200
400
600
800
1000
1200
1400
*
*
*
*
a-sk-actin
BNP
Control
Ang II
MMP-2i+ Ang II

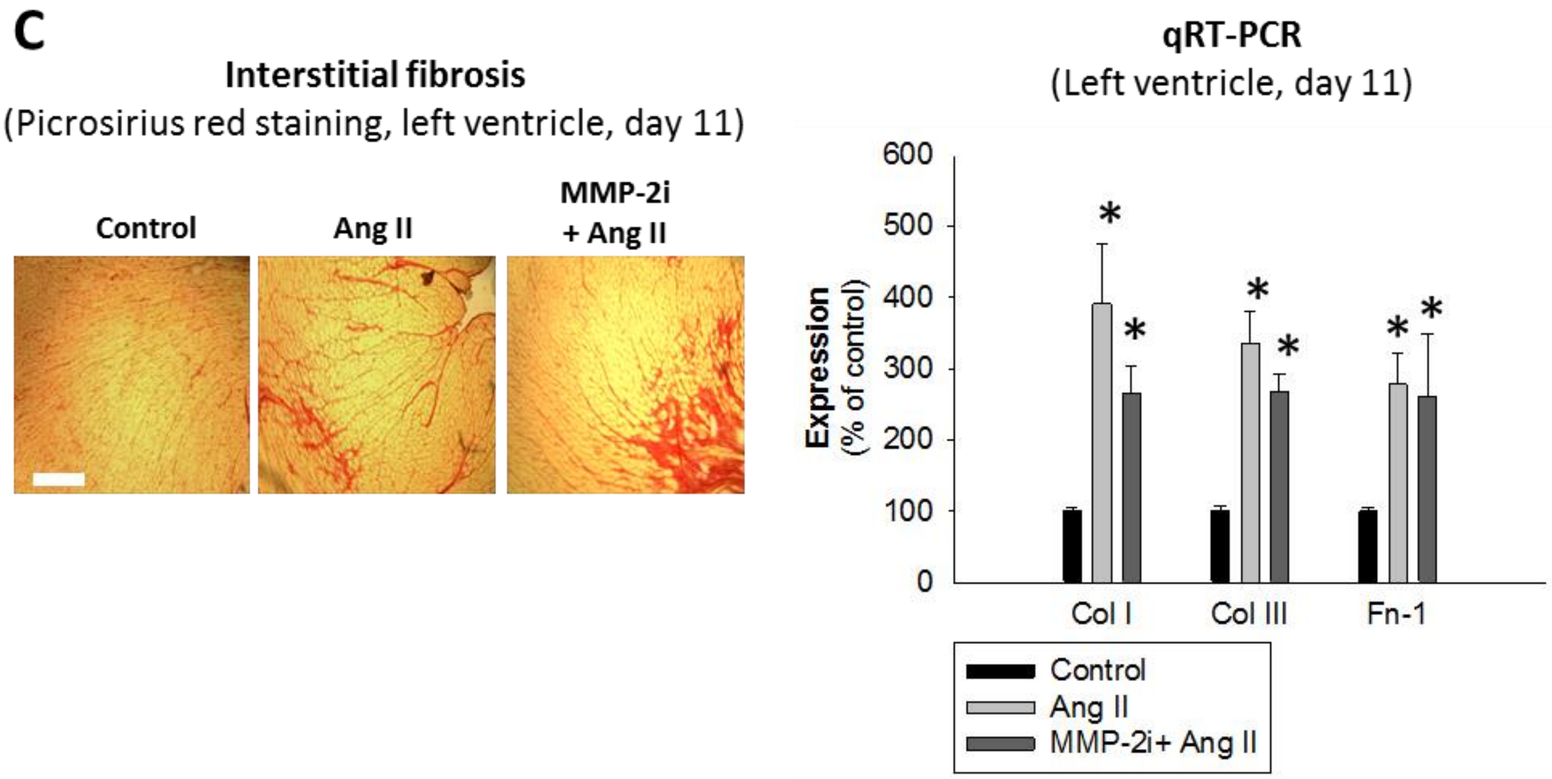

C

Interstitial fibrosis

(Picrosirius red staining, left ventricle, day 11)

qRT-PCR

(Left ventricle, day 11)

Figure 4-6 MMP-2 is not involved in the development of Ang II induced cardiac hypertrophy.

A) Heart weight to body weight ratios of mice treated with MMP-2 inhibitor I (40 mg/kg/d) beginning 1 day prior to Ang II infusion (1.4 mg/kg/d) for 12 days. **B)** Histological analysis of heart sections (10 μm) stained with WGA-FITC (upper panel) to quantify average cellular cross sectional area (lower panel). Scale bar indicates 100 μm. n=4 mice for each group. * indicates $p<0.05$ vs. control. ‡ Indicates $p<0.05$ vs Ang II.

(These data were obtained by Jeffrey Odenbach)

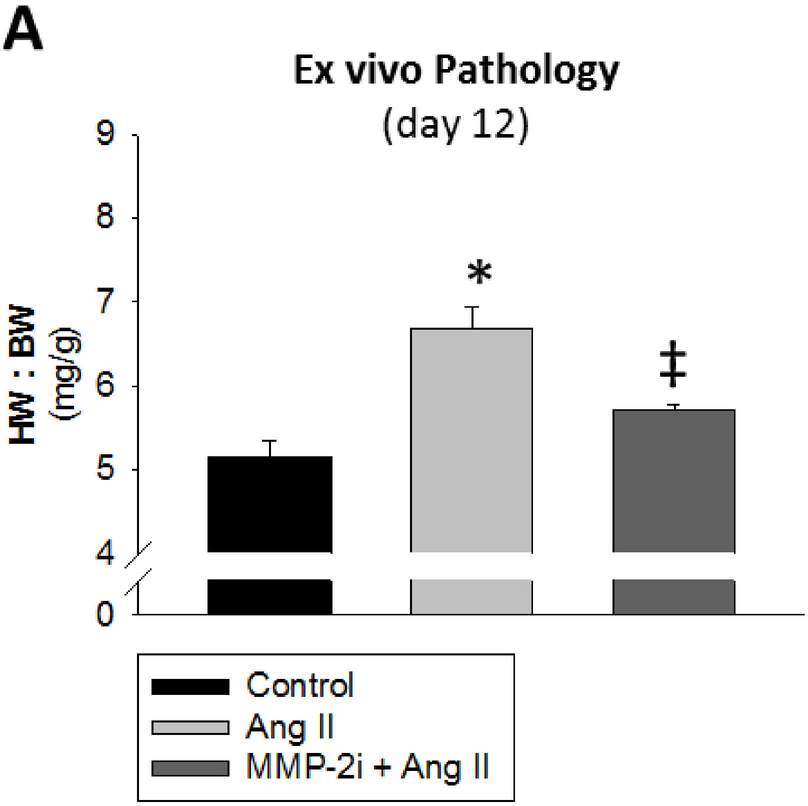

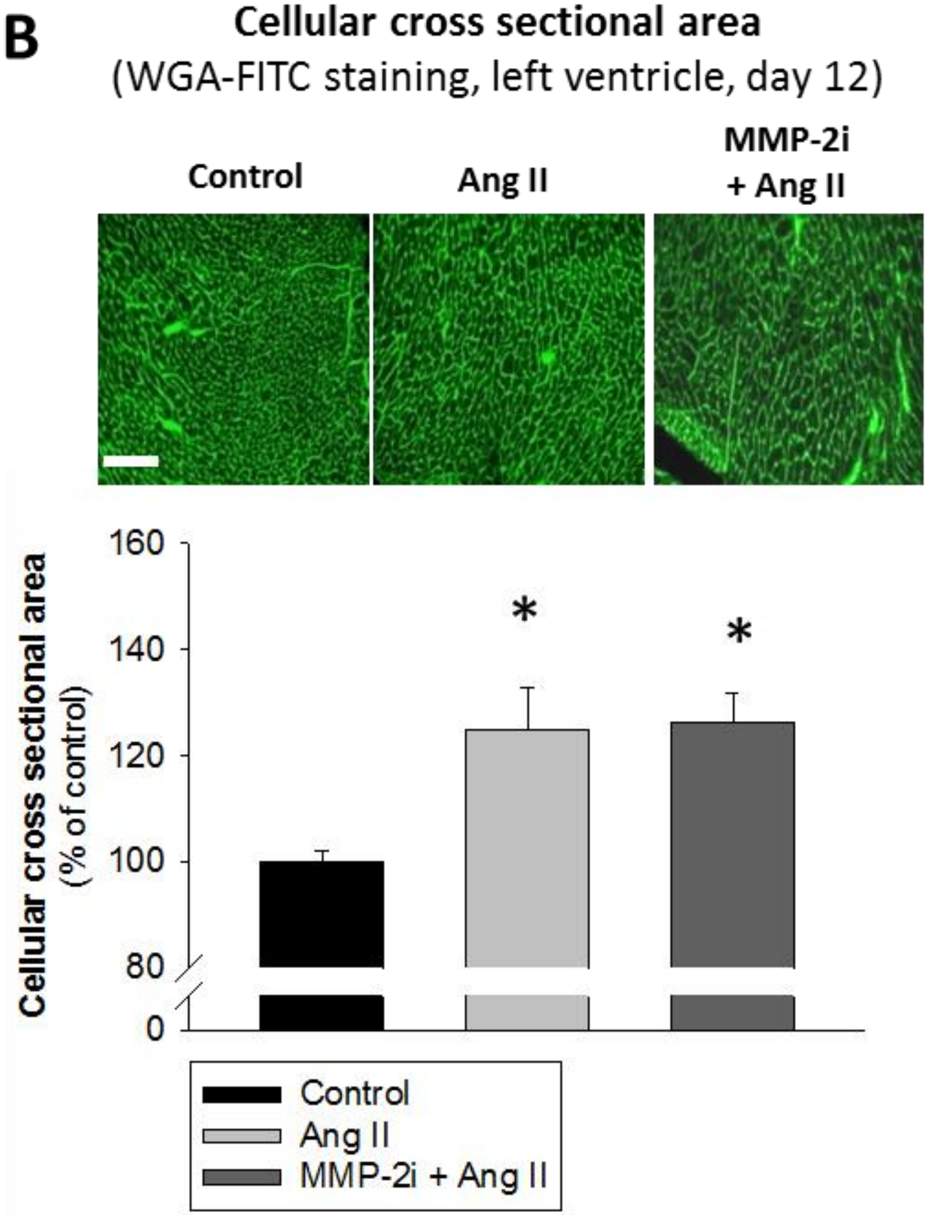
B
Cellular cross sectional area
(WGA-FITC staining, left ventricle, day 12)
Control
Ang II
MMP-2i
+ Ang II
Cellular cross sectional area
(% of control)
160
140
120
100
80
0
*
*
Control
Ang II
MMP-2i + Ang II

Figure 4-7 Validation of MMP-2 siRNA in cultured A7R5 cells.
Serum starved A7r5 cell were transfected with MMP-2 siRNA (100 nmol/L) using DharmaFECT-2 transfection reagent. Conditioned medium and cell lysate were collected 24 hours after transfection. Representative images of conditioned media (upper panel) and cell lysates (middle panel) subjected to gelatin zymography. Equal loading was confirmed by SDS-PAGE (lower panel). All experiments were performed in triplicate.

(These data were obtained by Jeffrey Odenbach)

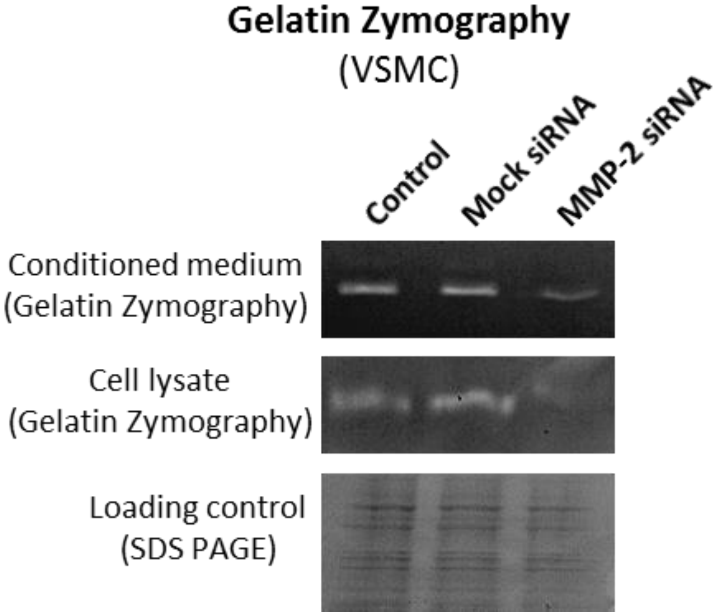
Gelatin Zymography
(VSMC)
Control
Mock siRNA
MMP-2 siRNA
Conditioned medium
(Gelatin Zymography)
Cell lysate
(Gelatin Zymography)
Loading control
(SDS PAGE)

Figure 4-8 MMP-2 siRNA attenuates Ang II-induced hypertension but not cardiac hypertrophy or fibrosis.

A-D) Upper panels-Treatment protocols of mice receiving MMP-2 siRNA (0.4 mg/kg/d) given either 5 days before (pre-treatment protocol, **A**) or after (rescue protocol, **B**) Ang II (1.4 mg/kg/d). lower panels- Representative images of aorta (**A, B**), heart(**A, B**), kidney (**C, D**) and liver (**C, D**) homogenates subjected to gelatin zymography. **E, F)** Tail cuff plethysmography analysis of systolic blood pressure of mice subjected to pre-treatment (**E**) or rescue (**F**) protocols. **G, H**) Echocardiographic analysis of left ventricle mass normalized to body weight (upper panels) and qRT-PCR analysis of hypertrophy markers (lower panels) in left ventricle samples of mice subjected to pre-treatment (**G**) or rescue (**H**) protocols. **I, J)** Heart weight to body weight ratios (upper panels) and histological analysis of heart sections (10 µm) stained with WGA-FITC to demonstrate cellular cross sectional area (lower panels) of mice subjected to to pre-treatment (**I**) or rescue (**J**) protocols. **K, L)** Collagen staining of heart sections (10 µm) stained with picrosirius red (upper panels) and qRT-PCR analysis of fibrosis markers (lower panels) in left ventricle samples of mice subjected to the pre-treatment (**K**) or rescue (**L**) protocols. Scale bar indicates 100 µm (WGA-FITC sections) or 250 µm (picrosirius red sections). n=3-4 mice for each group. * indicates $p<0.05$ vs. control. ‡ Indicates $p<0.05$ vs Ang II.

(These data were obtained by Jeffrey Odenbach)

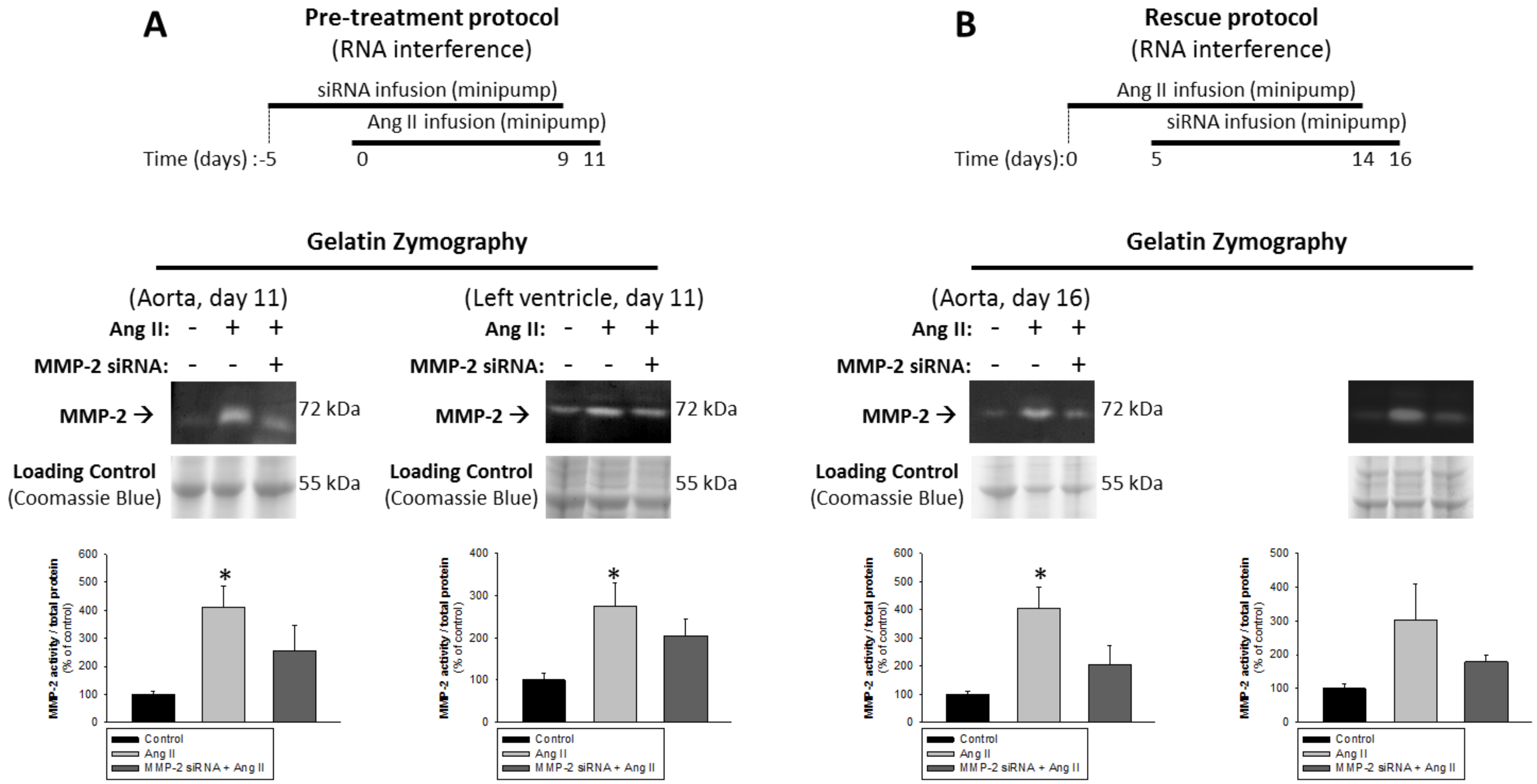
A
Pre-treatment protocol
(RNA interference)
siRNA infusion (minipump)
Ang II infusion (minipump)
Time (days) :-5
0
9
11
Gelatin Zymography
(Aorta, day 11)
(Left ventricle, day 11)
Ang II: - + +
MMP-2 siRNA: - - +
MMP-2 →
72 kDa
Loading Control
(Coomassie Blue)
55 kDa
MMP-2 activity / total protein
(% of control)
0
100
200
300
400
500
600
*
Control
Ang II
MMP-2 siRNA + Ang II
B
Rescue protocol
(RNA interference)
Ang II infusion (minipump)
siRNA infusion (minipump)
Time (days):0
5
14
16
Gelatin Zymography
(Aorta, day 16)
Ang II: - + +
MMP-2 siRNA: - - +
MMP-2 →
72 kDa
Loading Control
(Coomassie Blue)
55 kDa
MMP-2 activity / total protein
(% of control)
0
100
200
300
400
500
600
*
Control
Ang II
MMP-2 siRNA + Ang II

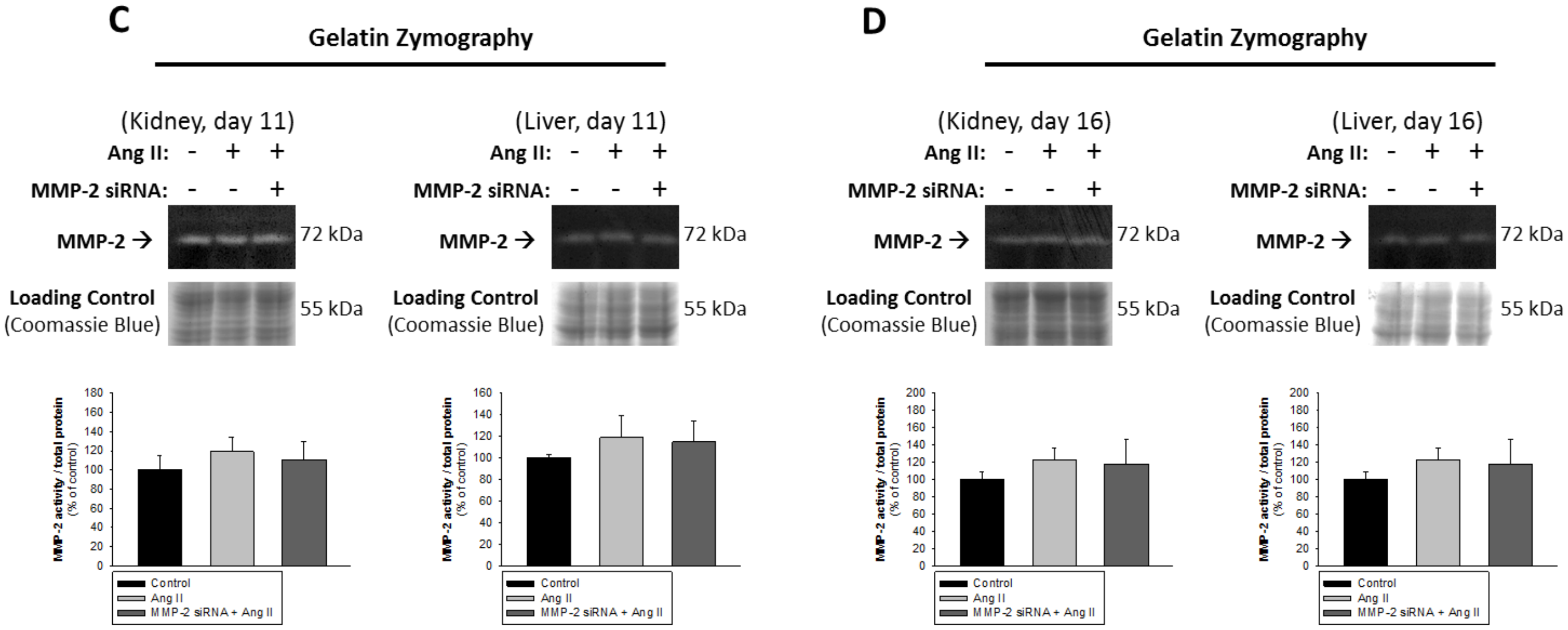
C
Gelatin Zymography
(Kidney, day 11)
(Liver, day 11)
Ang II: - + +
MMP-2 siRNA: - - +
MMP-2 →
72 kDa
Loading Control
(Coomassie Blue)
55 kDa
MMP-2 activity / total protein
(% of control)
0
20
40
60
80
100
120
140
160
180
Control
Ang II
MMP-2 siRNA + Ang II
D
Gelatin Zymography
(Kidney, day 16)
(Liver, day 16)
200

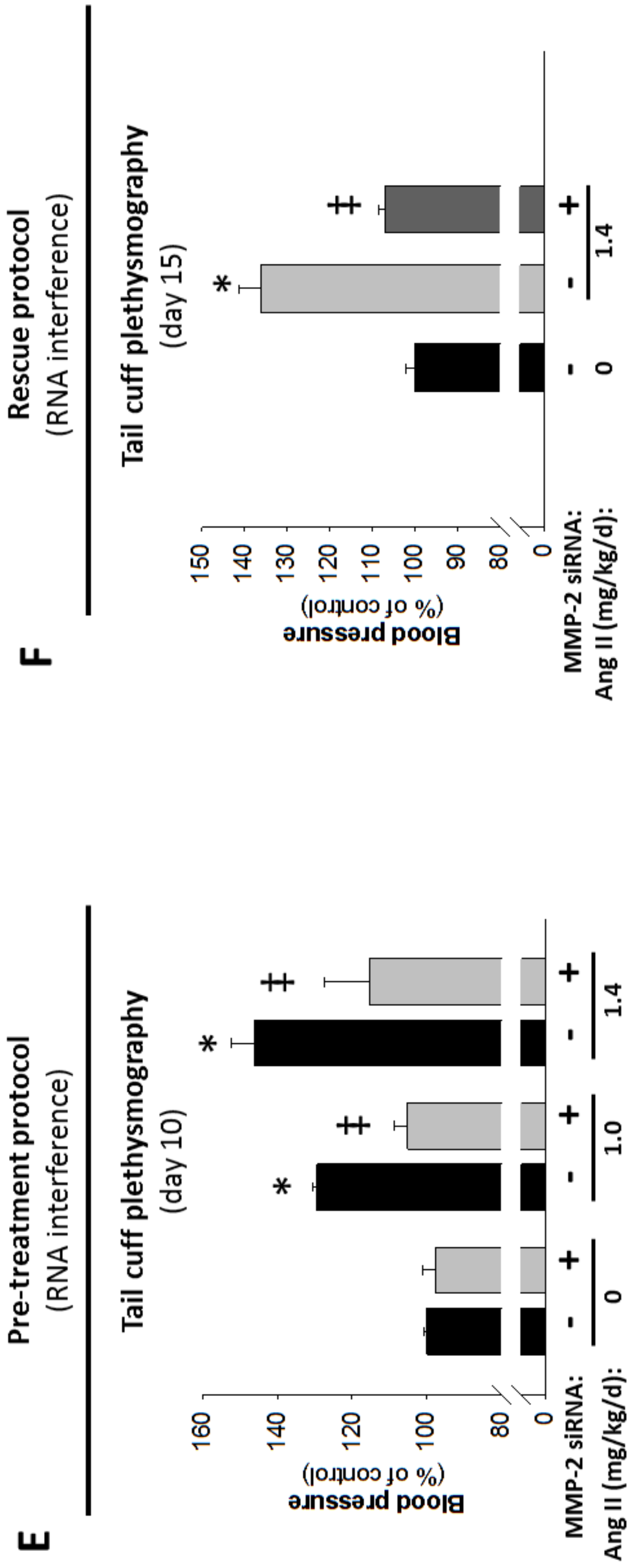
E
Pre-treatment protocol
(RNA interference)
Tail cuff plethysmography
(day 10)
Blood pressure
(% of control)
160
140
120
100
80
0
*
‡
*
‡
MMP-2 siRNA:
-
+
-
+
-
+
Ang II (mg/kg/d):
0
1.0
1.4
F
Rescue protocol
(RNA interference)
Tail cuff plethysmography
(day 15)
Blood pressure
(% of control)
150
140
130
120
110
100
90
80
0
*
‡
MMP-2 siRNA:
-
-
+
Ang II (mg/kg/d):
0
1.4

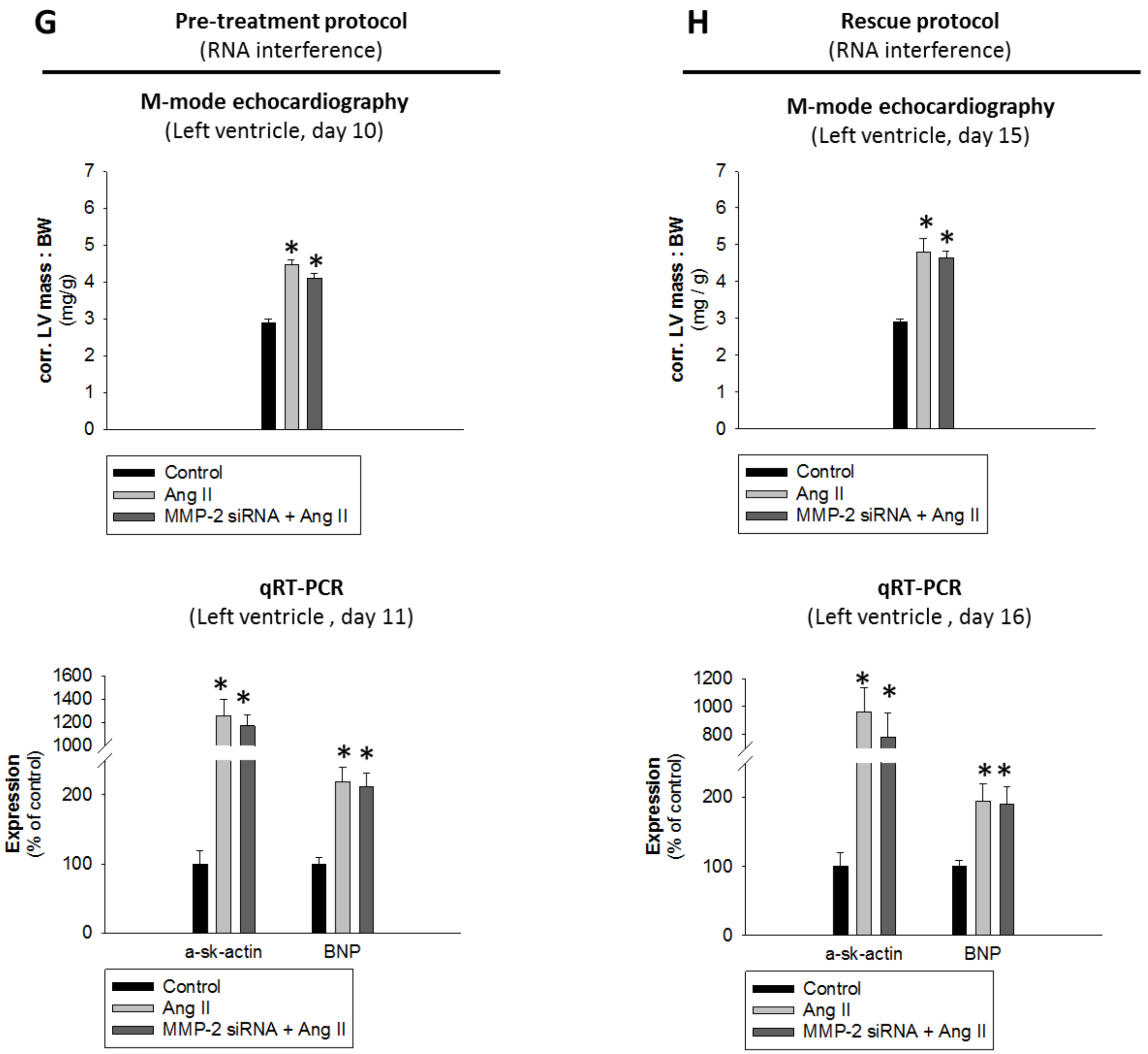
G
Pre-treatment protocol
(RNA interference)
M-mode echocardiography
(Left ventricle, day 10)
corr. LV mass : BW
(mg/g)
7
6
5
4
3
2
1
0
*
*
Control
Ang II
MMP-2 siRNA + Ang II
qRT-PCR
(Left ventricle , day 11)
Expression
(% of control)
1600
1400
1200
1000
200
100
0
*
*
*
*
a-sk-actin
BNP
Control
Ang II
MMP-2 siRNA + Ang II
H
Rescue protocol
(RNA interference)
M-mode echocardiography
(Left ventricle, day 15)
corr. LV mass : BW
(mg / g)
7
6
5
4
3
2
1
0
*
*
Control
Ang II
MMP-2 siRNA + Ang II
qRT-PCR
(Left ventricle , day 16)
Expression
(% of control)
1200
1000
800
200
100
0
*
*
*
*
a-sk-actin
BNP
Control
Ang II
MMP-2 siRNA + Ang II

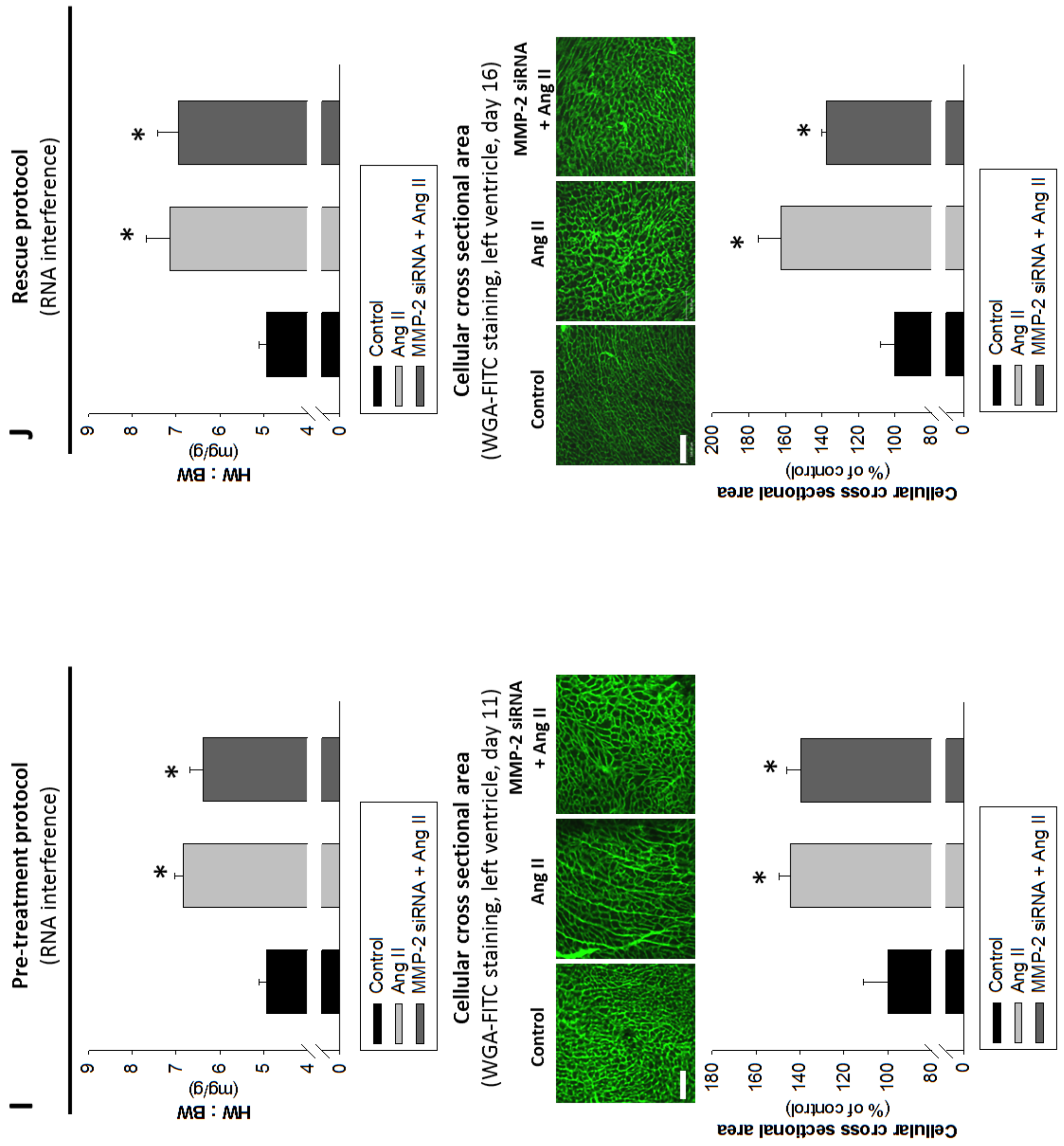
I
Pre-treatment protocol
(RNA interference)
HW : BW
(mg/g)
9
8
7
6
5
4
0
*
*
Control
Ang II
MMP-2 siRNA + Ang II
Cellular cross sectional area
(WGA-FITC staining, left ventricle, day 11)
Control
Ang II
MMP-2 siRNA
+ Ang II
Cellular cross sectional area
(% of control)
180
160
140
120
100
80
0
*
*
Control
Ang II
MMP-2 siRNA + Ang II
J
Rescue protocol
(RNA interference)
HW : BW
(mg/g)
9
8
7
6
5
4
0
*
*
Control
Ang II
MMP-2 siRNA + Ang II
Cellular cross sectional area
(WGA-FITC staining, left ventricle, day 16)
Control
Ang II
MMP-2 siRNA
+ Ang II
Cellular cross sectional area
(% of control)
200
180
160
140
120
100
80
0
*
*
Control
Ang II
MMP-2 siRNA + Ang II

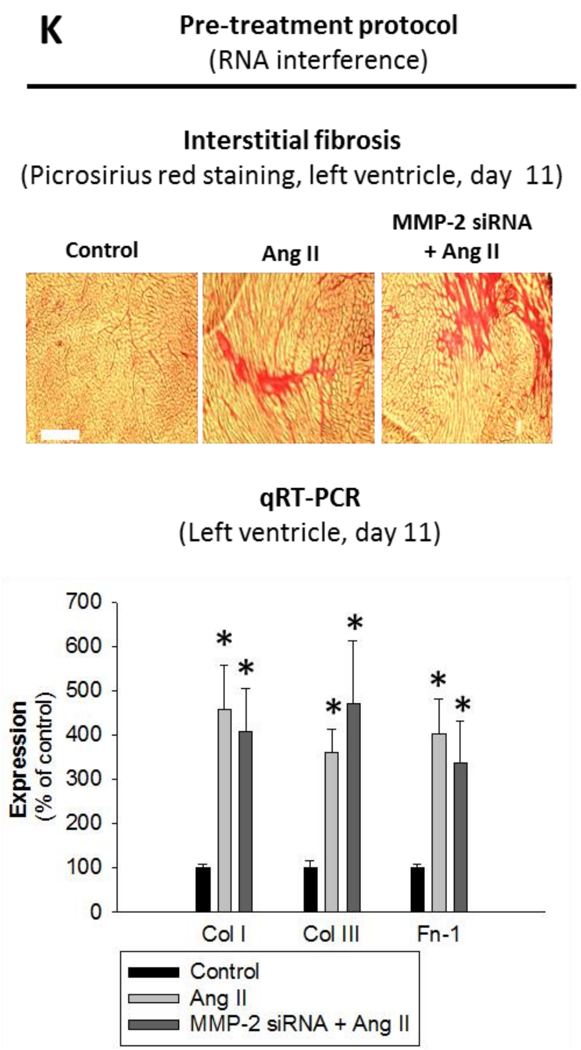
K
Pre-treatment protocol
(RNA interference)
Interstitial fibrosis
(Picrosirius red staining, left ventricle, day 11)
Control
Ang II
MMP-2 siRNA + Ang II
qRT-PCR
(Left ventricle, day 11)
Expression (% of control)
700
600
500
400
300
200
100
0
*
Col I
Col III
Fn-1
Control
Ang II
MMP-2 siRNA + Ang II

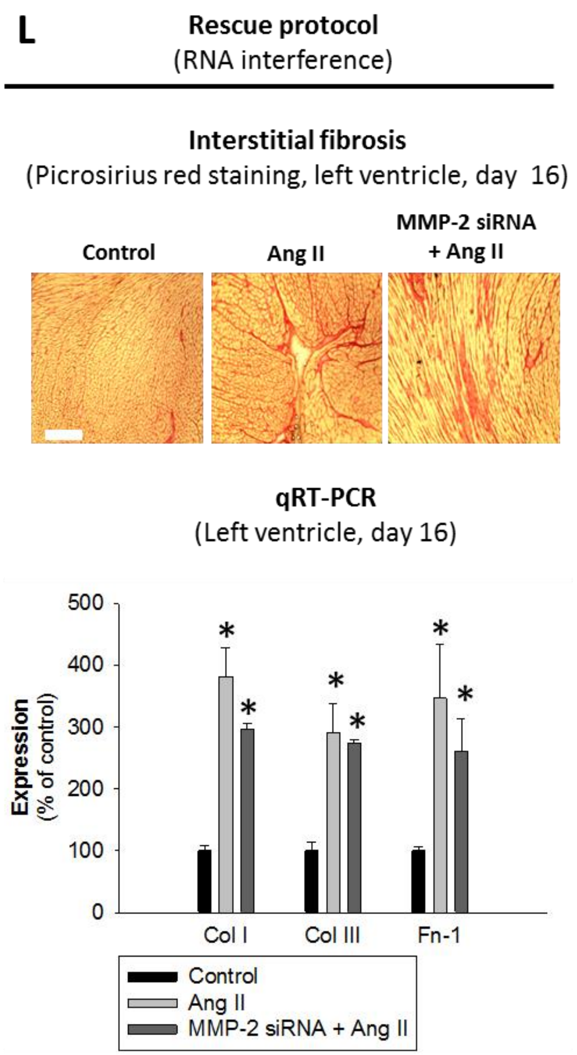
L
Rescue protocol
(RNA interference)
Interstitial fibrosis
(Picrosirius red staining, left ventricle, day 16)
Control
Ang II
MMP-2 siRNA + Ang II
qRT-PCR
(Left ventricle, day 16)
Expression (% of control)
500
400
300
200
100
0
*
Col I
Col III
Fn-1
Control
Ang II
MMP-2 siRNA + Ang II

Figure 4-9 Luciferase siRNA does not attenuate Ang II-induced hypertension, cardiac hypertrophy or fibrosis.

A) Experimental protocol for mice treated with Luciferase siRNA (0.4 mg/kg/d) and Ang II (1.4 mg/kg/d) by subcutaneous osmotic minipumps. **B)** Time course of systolic blood pressure in control mice, mice treated with Ang II or mice treated with Ang II and luciferase siRNA. **C)** Cardiac hypertrophy as assessed by echocardiographic analysis of left ventricle weight to body weight ratio (upper left panel), gross pathology of heart weight to body weight ratio (upper middle panel), qRT-PCR analysis of hypertrophy marker genes (upper right panel) and histological analysis of heart sections (10 µm) stained with WGA-FITC to quantify average cellular cross-sectional area (lower panels). **D**) Fibrosis was assessed by histological analysis of heart sections (10 µm) stained with picrosirius red to determine collagen deposition (left panel) and qRT-PCR analysis of fibrosis marker genes (right panel). **E**) qRT-PCR (left panel) and gelatin zymography (right panel) analysis of gelatinase expression and activity in cardiac homogenates. Scale bars indicate 100 µm (WGA-FITC micrographs) or 250 µm (Picrosirius red micrographs). n=4 mice for each group. * indicates $p<0.05$ vs. control group.

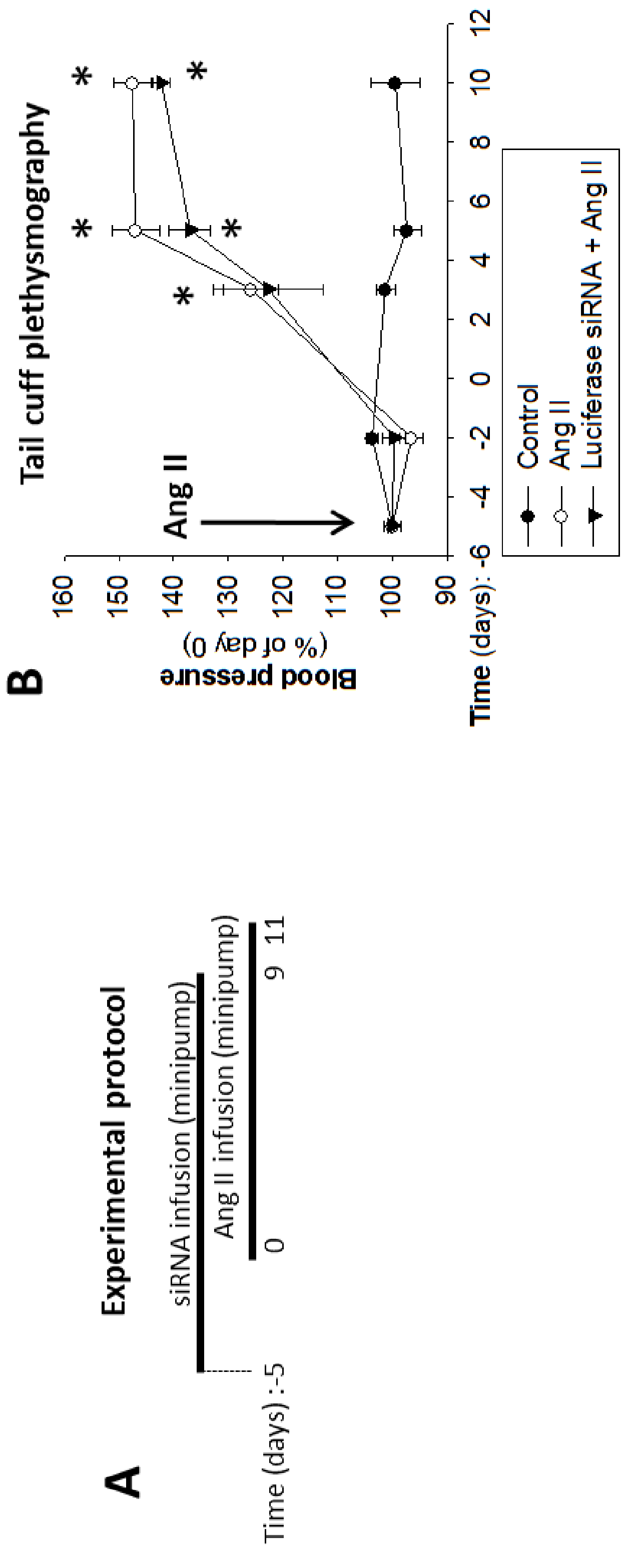
A
Experimental protocol
siRNA infusion (minipump)
Ang II infusion (minipump)
Time (days) : -5
0
9
11
B
Tail cuff plethysmography
Blood pressure (% of day 0)
160
150
140
130
120
110
100
90
Time (days): -6
-4
-2
0
2
4
6
8
10
12
Ang II
*
Control
Ang II
Luciferase siRNA + Ang II

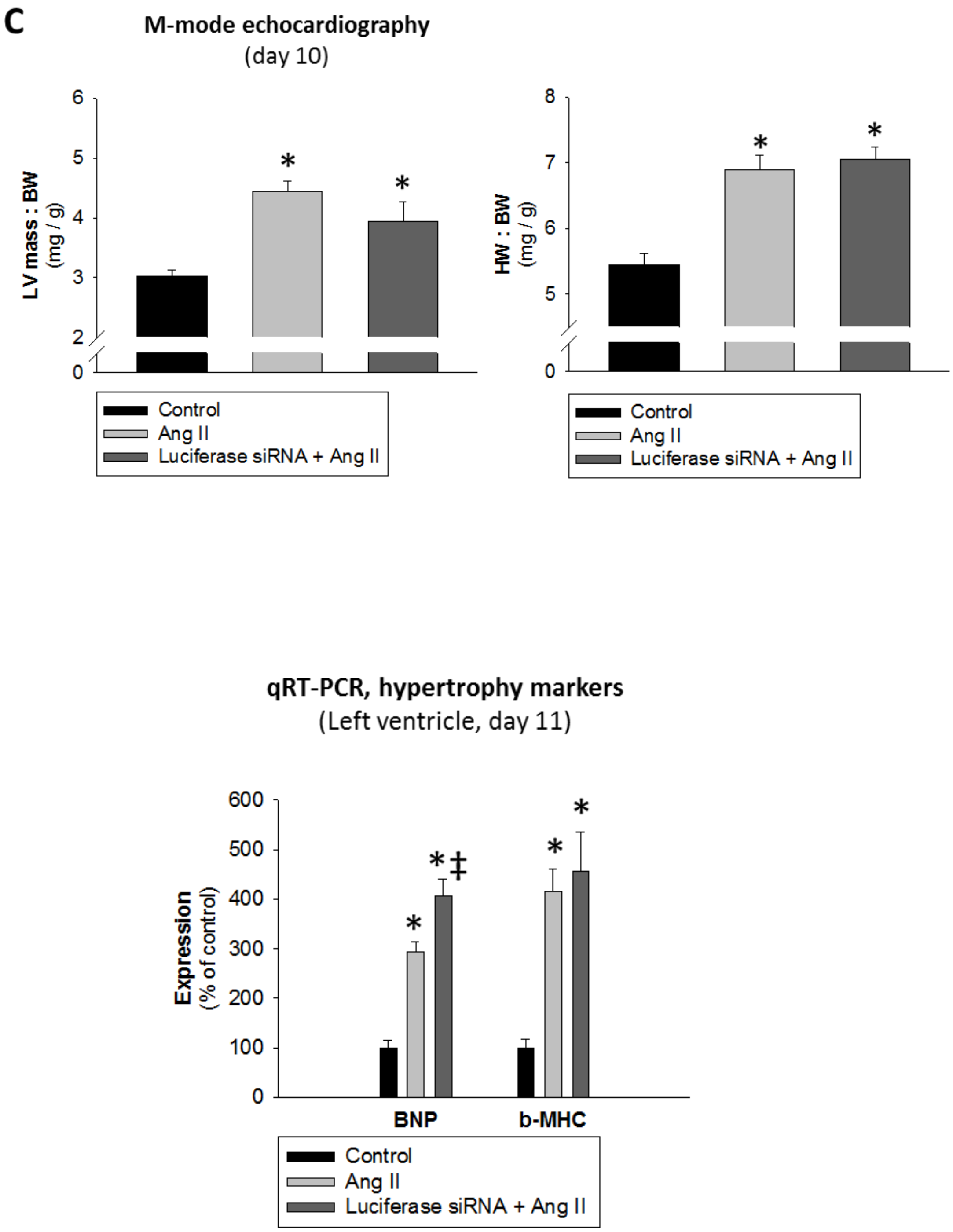
C
M-mode echocardiography
(day 10)
LV mass : BW
(mg / g)
6
5
4
3
2
0
*
*
Control
Ang II
Luciferase siRNA + Ang II
HW : BW
(mg / g)
8
7
6
5
0
*
*
Control
Ang II
Luciferase siRNA + Ang II
qRT-PCR, hypertrophy markers
(Left ventricle, day 11)
Expression
(% of control)
600
500
400
300
200
100
0
*
*‡
*
*
BNP
b-MHC
Control
Ang II
Luciferase siRNA + Ang II

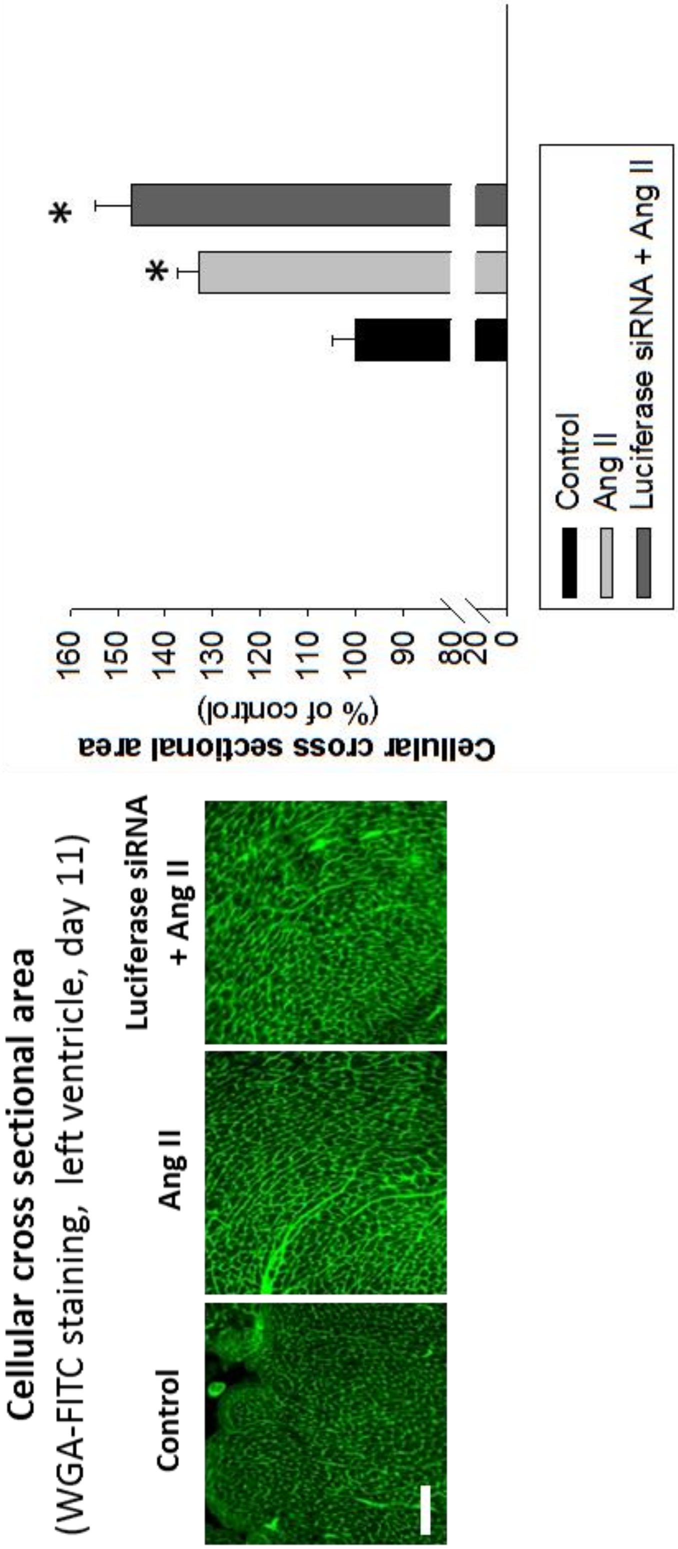
Cellular cross sectional area
(WGA-FITC staining, left ventricle, day 11)
Control
Ang II
Luciferase siRNA + Ang II
Cellular cross sectional area (% of control)
0
20
80
90
100
110
120
130
140
150
160
*
*
Control
Ang II
Luciferase siRNA + Ang II

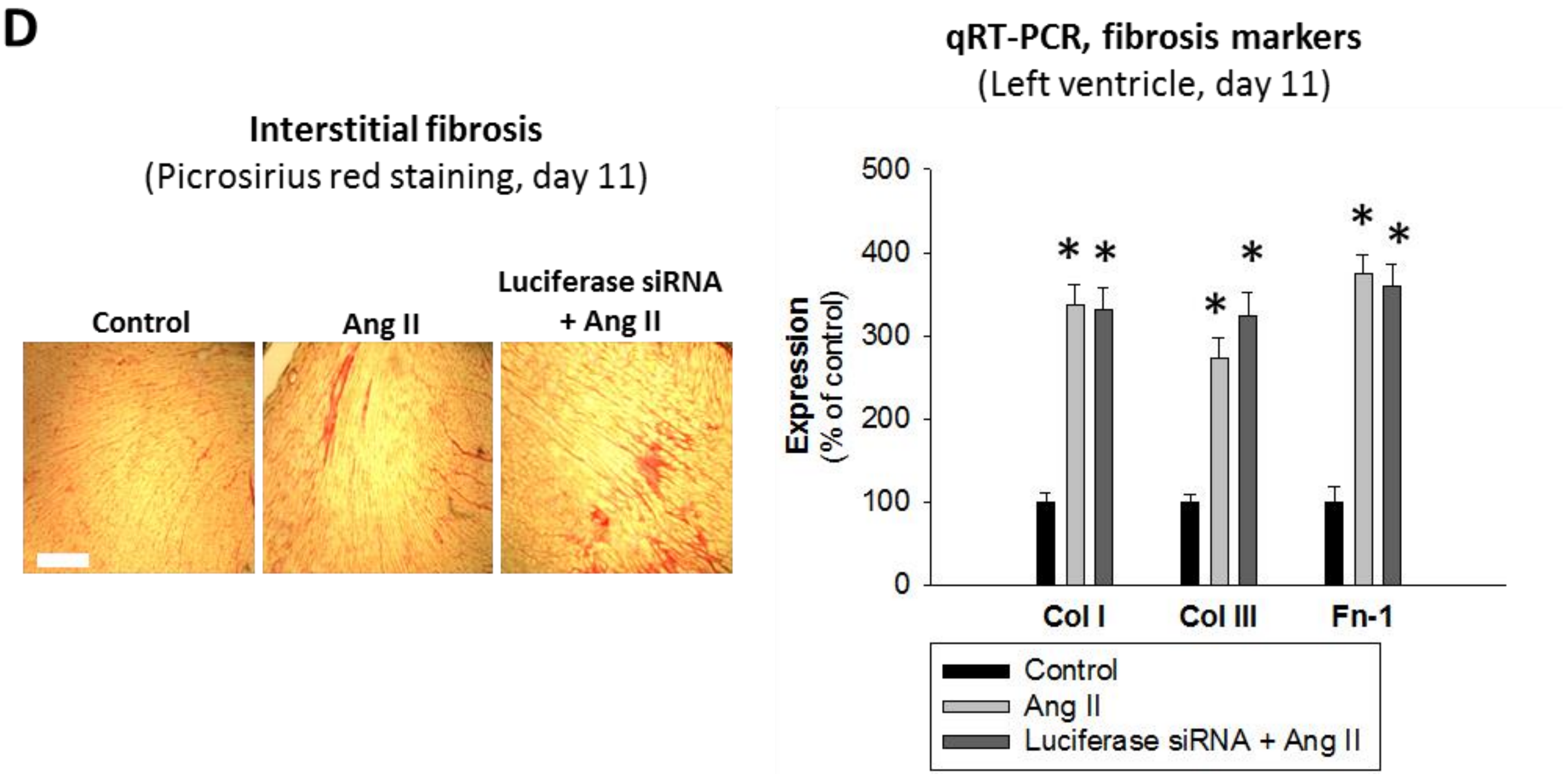
D
Interstitial fibrosis
(Picrosirius red staining, day 11)
Control
Ang II
Luciferase siRNA
+ Ang II
qRT-PCR, fibrosis markers
(Left ventricle, day 11)
Expression
(% of control)
500
400
300
200
100
0
*
*
*
*
*
*
Col I
Col III
Fn-1
Control
Ang II
Luciferase siRNA + Ang II

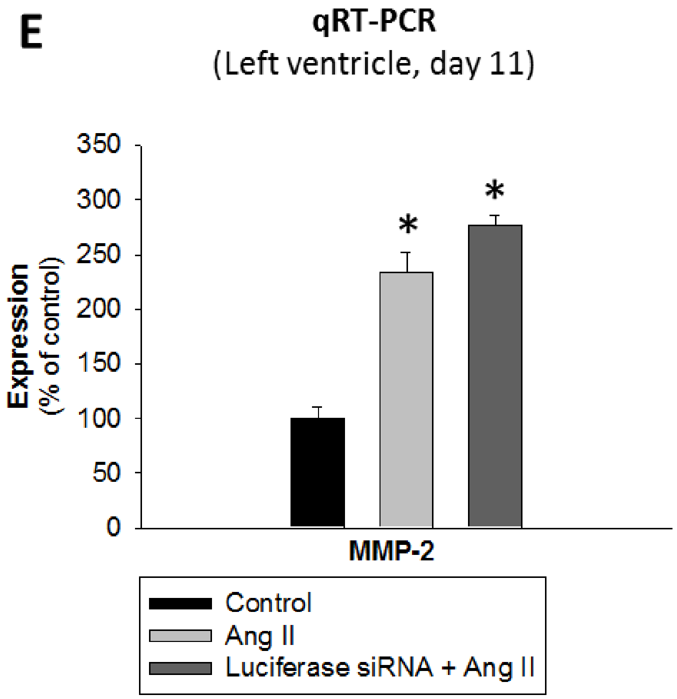
E
qRT-PCR
(Left ventricle, day 11)
Expression
(% of control)
350
300
250
200
150
100
50
0
*
*
MMP-2
Control
Ang II
Luciferase siRNA + Ang II

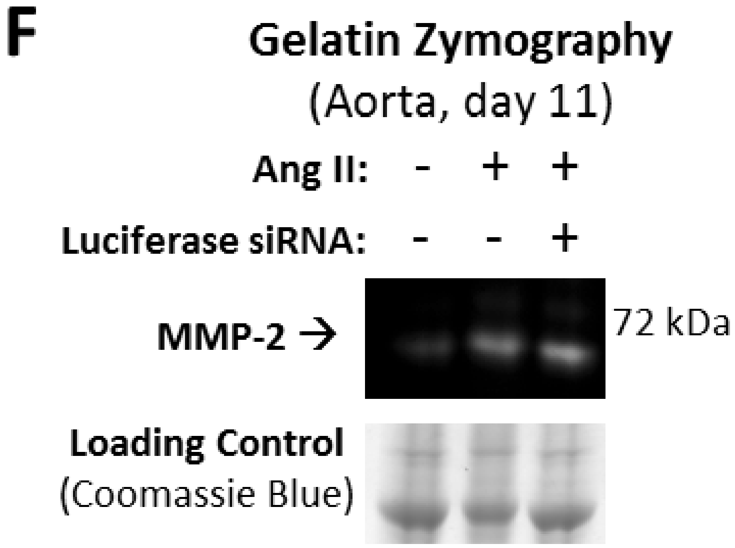
F
Gelatin Zymography
(Aorta, day 11)
Ang II: - + +
Luciferase siRNA: - - +
MMP-2 →
72 kDa
Loading Control
(Coomassie Blue)

Figure 4-10 MMP-7 and TACE mediate the upregulation of MMP-2 induced by Ang II.

A) Experimental protocol of mice treated with MMP-7 siRNA, TACE siRNA or both (0.4 mg/kg/d) 5 days prior to Ang II (1.4 mg/kg/d) by subcutaneous osmotic minipumps. **B)** qRT-PCR analysis of MMP-2 mRNA levels in left ventricle samples from mice treated as per experimental protocol. n=4 mice for each group. * indicates $p<0.05$ vs. control. ‡ Indicates $p<0.05$ vs Ang II.

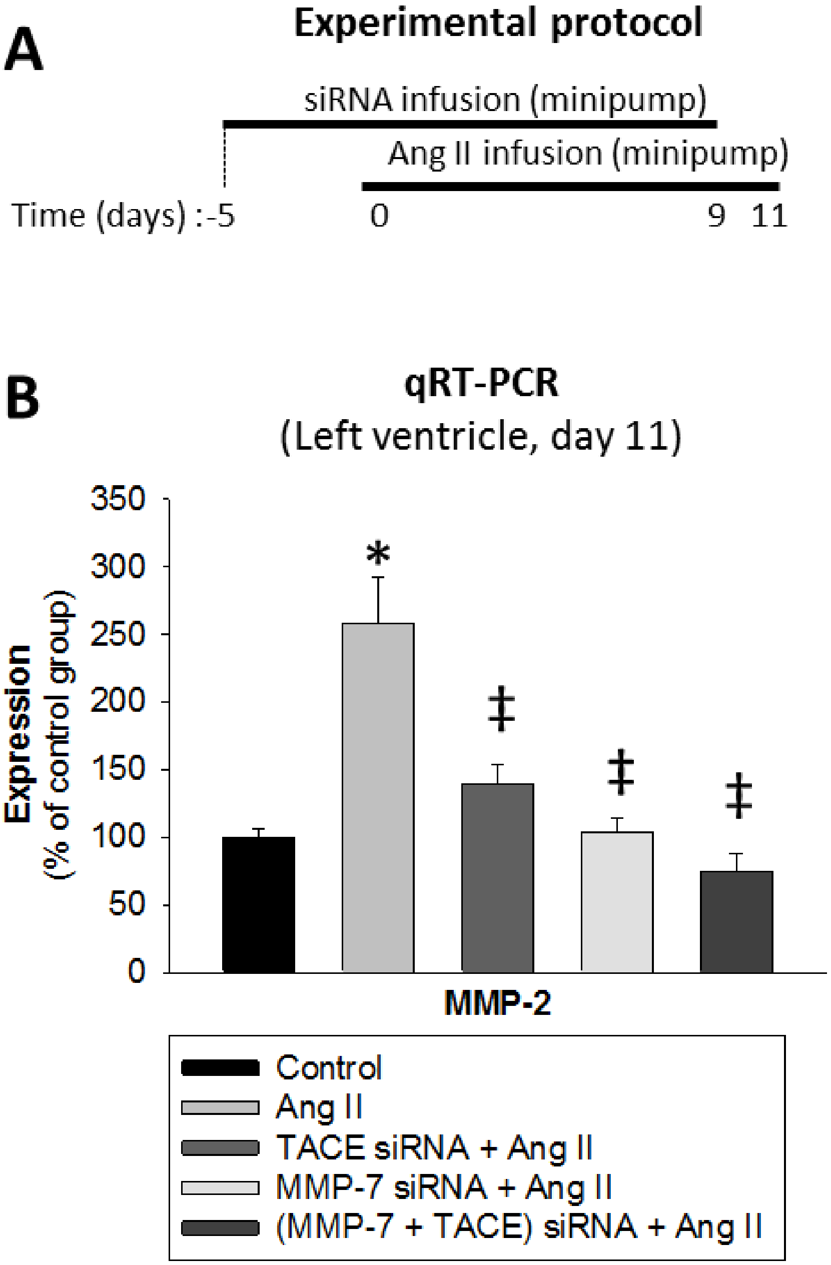

Figure 4-11 MMP-7 and TACE mediate Ang II-induced MMP-2 upregulation.

Gelatin zymography analysis of cardiac homogenates from mice treated with or without Ang II (1.4 mg/kg/d) or siRNAs against both MMP-7 and TACE (0.4 mg/kg/d). Images are representative of 4 mice from each group.

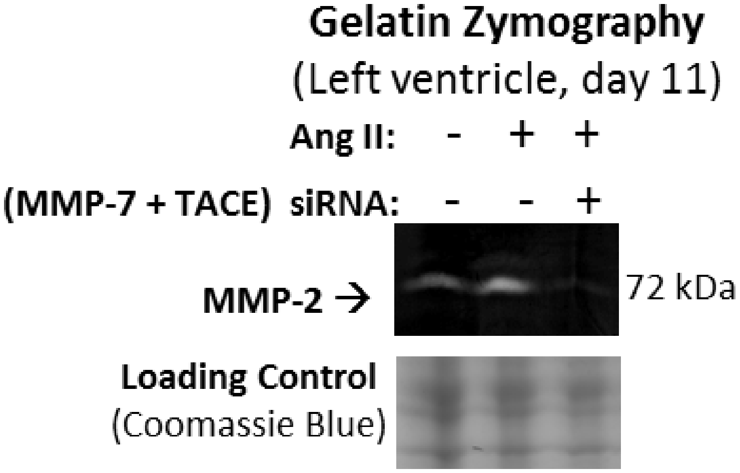
Gelatin Zymography
(Left ventricle, day 11)
Ang II: - + +
(MMP-7 + TACE) siRNA: - - +
MMP-2 →
72 kDa
Loading Control
(Coomassie Blue)

Figure 4-12 Simultaneous targeting of MMP-7 and TACE attenuates Ang II-induced hypertension, hypertrophy and fibrosis.

A) Experimental protocol of mice treated with MMP-7 siRNA, TACE siRNA or both (0.4 mg/kg/d) 5 days prior to Ang II (1.4 mg/kg/d) by subcutaneous osmotic minipump. B) Tail cuff plethysmography analysis of systolic blood pressure in mice subjected to the above protocol. Assessment of cardiac hypertrophy in mice subjected to the above protocol as measured by left ventricle mass to body weight ratio (M-mode echocardiography, **C**) and qRT-PCR analysis of hypertrophy marker genes (**D**). Assessment of cardiac fibrosis in mice subjected to the above protocol as measured by picrosirius red (collagen deposition, **E**) and qRT-PCR analysis of fibrosis marker genes (**F**). Scale bar indicates 250 µm. n=4 mice for each group. * indicates $p<0.05$ vs. control. ‡ Indicates $p<0.05$ vs Ang II.

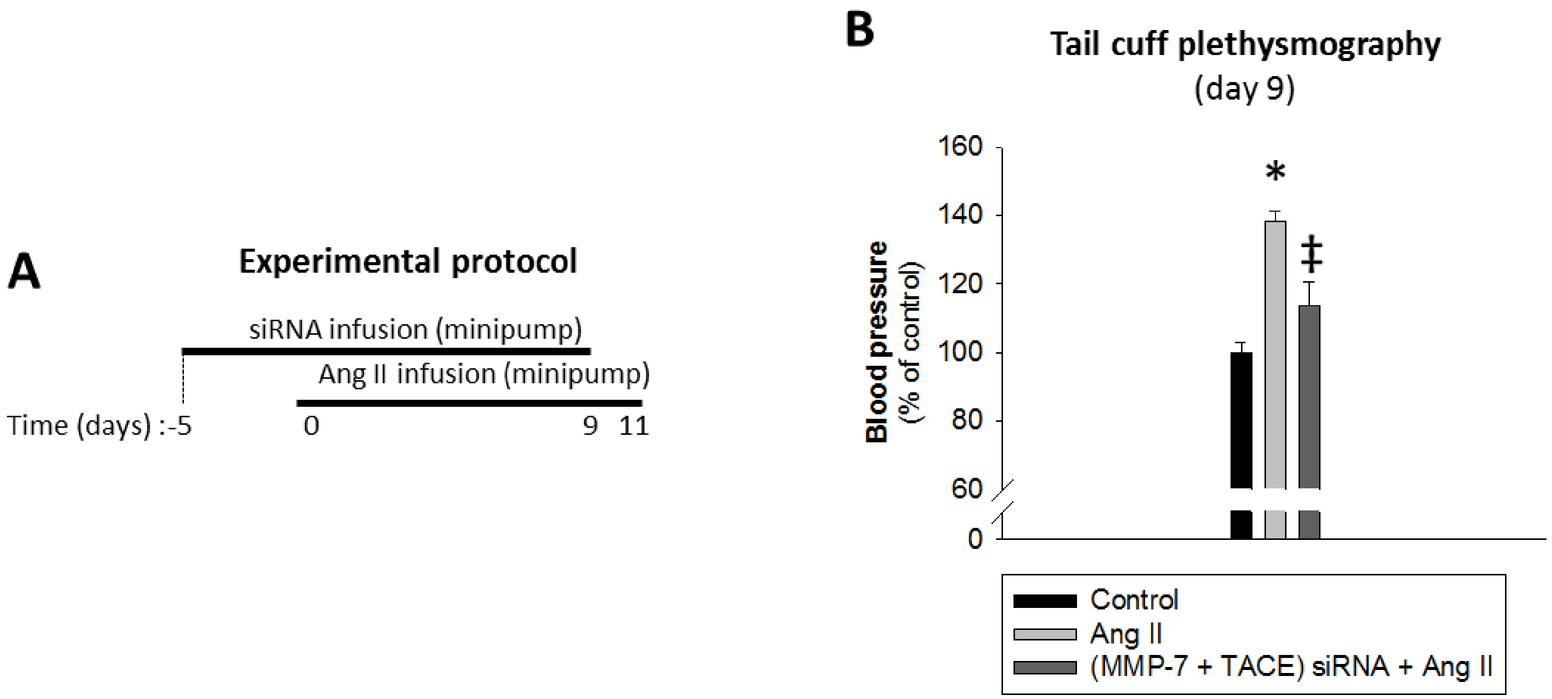
A
Experimental protocol
siRNA infusion (minipump)
Ang II infusion (minipump)
Time (days) :-5
0
9
11
B
Tail cuff plethysmography
(day 9)
Blood pressure
(% of control)
160
140
120
100
80
60
0
*
‡
Control
Ang II
(MMP-7 + TACE) siRNA + Ang II

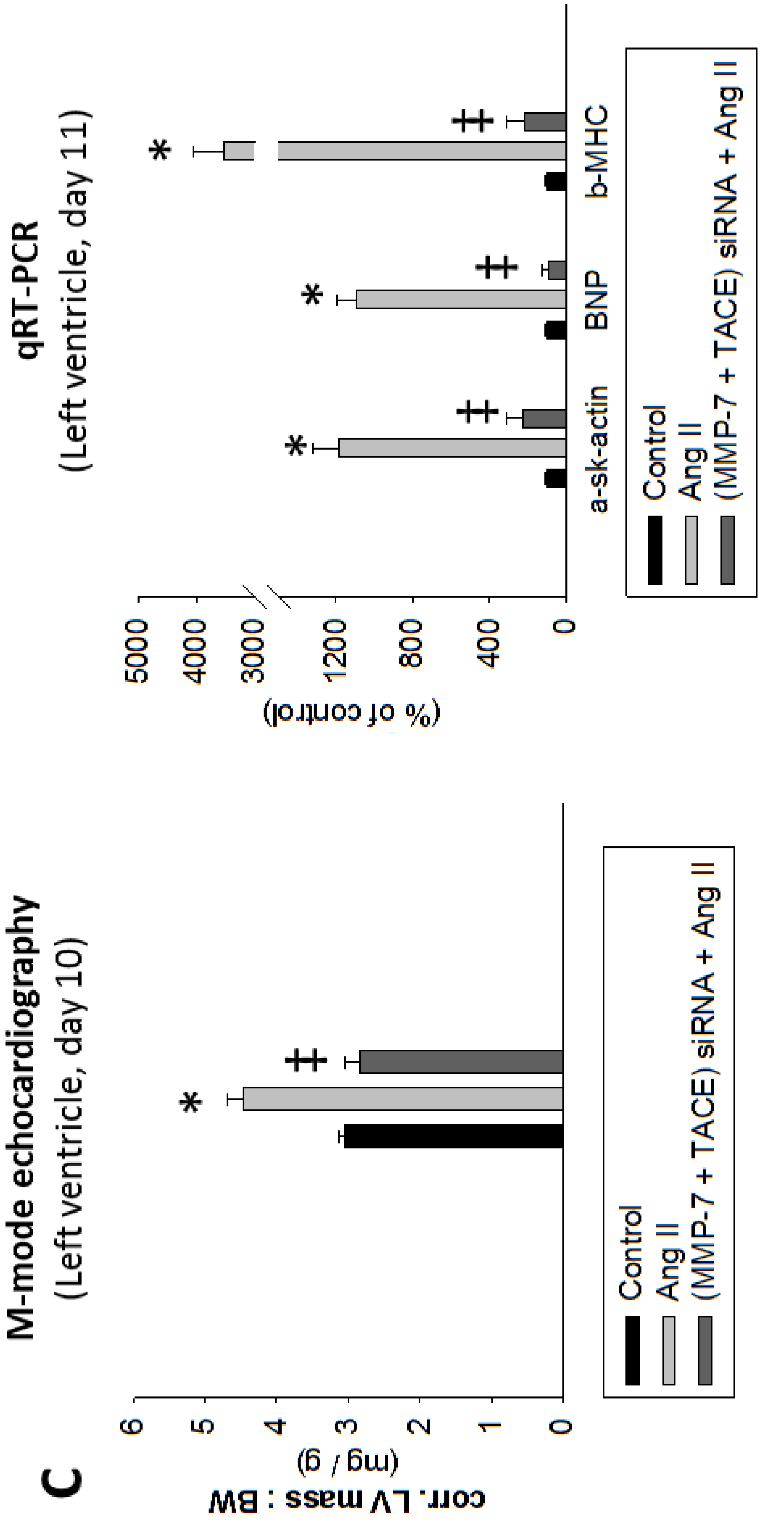
C
M-mode echocardiography
(Left ventricle, day 10)
corr. LV mass : BW
(mg / g)
0
1
2
3
4
5
6
*
‡
Control
Ang II
(MMP-7 + TACE) siRNA + Ang II
qRT-PCR
(Left ventricle, day 11)
(% of control)
0
400
800
1200
3000
4000
5000
a-sk-actin
BNP
b-MHC
*
‡
*
‡
*
‡
Control
Ang II
(MMP-7 + TACE) siRNA + Ang II

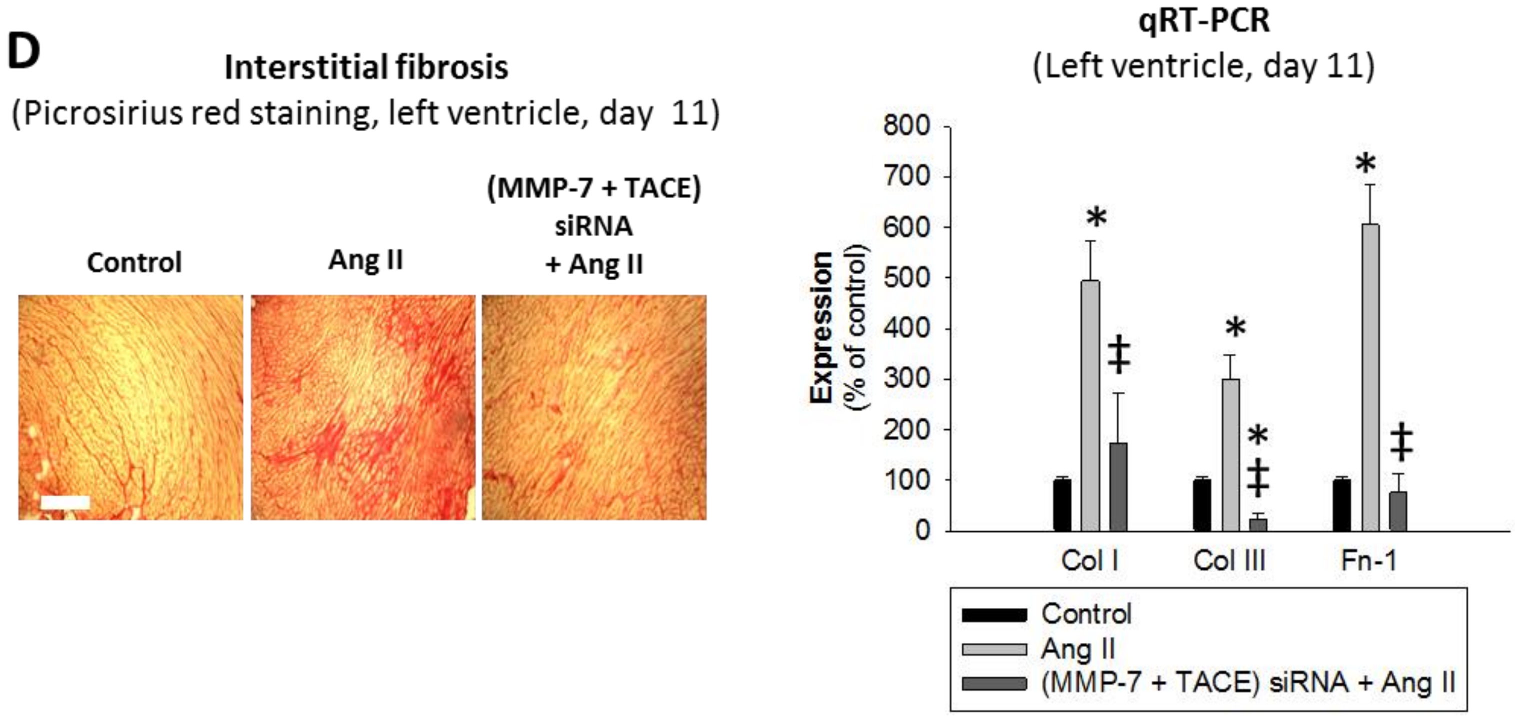
D
Interstitial fibrosis
(Picrosirius red staining, left ventricle, day 11)
Control
Ang II
(MMP-7 + TACE)
siRNA
+ Ang II
qRT-PCR
(Left ventricle, day 11)
Expression
(% of control)
800
700
600
500
400
300
200
100
0
*
‡
*
*
‡
*
‡
Col I
Col III
Fn-1
Control
Ang II
(MMP-7 + TACE) siRNA + Ang II

Figure 4-13 Proposed model of metalloproteinase signaling in Ang II-induced cardiovascular disease.

Ang II induces hypertension, cardiac and fibrosis which can be prevented by blockade of MMP-7 and TACE. A bifurcation in signaling exists downstream of MMP-7 and TACE where Ang II-induced hypertrophy and fibrosis occur independently of MMP-2 gene induction and the development of hypertension.

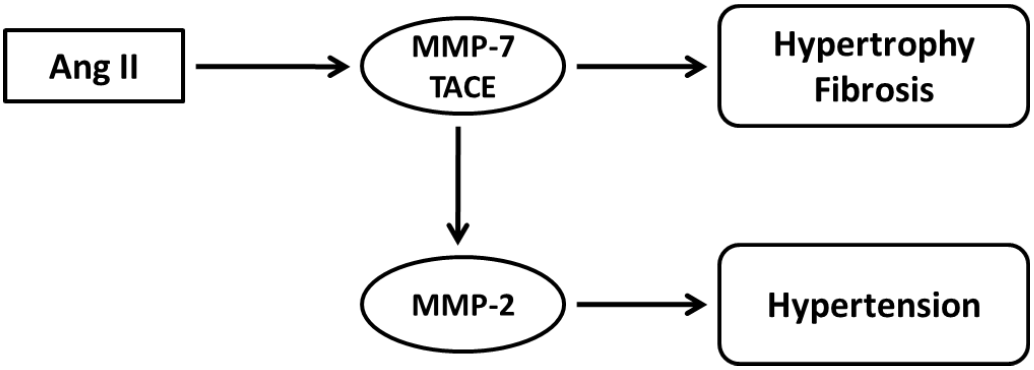
Ang II
MMP-7
TACE
Hypertrophy
Fibrosis
MMP-2
Hypertension

4.5 References

1. Lifton RP, Gharavi AG, Geller DS. Molecular mechanisms of human hypertension. *Cell*. 2001;104:545-556
2. Brilla CG, Maisch B, Weber KT. Myocardial collagen matrix remodelling in arterial hypertension. *Eur Heart J*. 1992;13 Suppl D:24-32
3. Diez J. Mechanisms of cardiac fibrosis in hypertension. *J Clin Hypertens (Greenwich)*. 2007;9:546-550
4. Weber KT, Clark WA, Janicki JS, Shroff SG. Physiologic versus pathologic hypertrophy and the pressure-overloaded myocardium. *J Cardiovasc Pharmacol*. 1987;10 Suppl 6:S37-50
5. Berk BC, Fujiwara K, Lehoux S. ECM remodeling in hypertensive heart disease. *J Clin Invest*. 2007;117:568-575
6. Prenzel N, Zwick E, Daub H, Leserer M, Abraham R, Wallasch C, Ullrich A. EGF receptor transactivation by G-protein-coupled receptors requires metalloproteinase cleavage of proHB-EGF. *Nature*. 1999;402:884-888
7. Asakura M, Kitakaze M, Takashima S, Liao Y, Ishikura F, Yoshinaka T, Ohmoto H, Node K, Yoshino K, Ishiguro H, Asanuma H, Sanada S, Matsumura Y, Takeda H, Beppu S, Tada M, Hori M, Higashiyama S. Cardiac hypertrophy is inhibited by antagonism of ADAM12 processing of HB-EGF: metalloproteinase inhibitors as a new therapy. *Nat Med*. 2002;8:35-40
8. Hao L, Du M, Lopez-Campistrous A, Fernandez-Patron C. Agonist-induced activation of matrix metalloproteinase-7 promotes vasoconstriction through the epidermal growth factor-receptor pathway. *Circ Res*. 2004;94:68-76
9. Lautrette A, Li S, Alili R, Sunnarborg SW, Burtin M, Lee DC, Friedlander G, Terzi F. Angiotensin II and EGF receptor cross-talk in chronic kidney diseases: a new therapeutic approach. *Nat Med*. 2005;11:867-874
10. Ohtsu H, Dempsey PJ, Frank GD, Brailoiu E, Higuchi S, Suzuki H, Nakashima H, Eguchi K, Eguchi S. ADAM17 mediates epidermal growth factor receptor transactivation and vascular smooth muscle cell hypertrophy induced by angiotensin II. *Arterioscler Thromb Vasc Biol*. 2006;26:e133-137
11. Fernandez-Patron C, Radomski MW, Davidge ST. Vascular matrix metalloproteinase-2 cleaves big endothelin-1 yielding a novel vasoconstrictor. *Circ Res*. 1999;85:906-911
12. Fernandez-Patron C, Stewart KG, Zhang Y, Koivunen E, Radomski MW, Davidge ST. Vascular matrix metalloproteinase-2-dependent cleavage of calcitonin gene-related peptide promotes vasoconstriction. *Circ Res*. 2000;87:670-676
13. Martinez A, Oh HR, Unsworth EJ, Bregonzio C, Saavedra JM,

Stetler-Stevenson WG, Cuttitta F. Matrix metalloproteinase-2 cleavage of adrenomedullin produces a vasoconstrictor out of a vasodilator. *Biochem J*. 2004;383:413-418

14. Wang X, Chow FL, Oka T, Hao L, Lopez-Campistrous A, Kelly S, Cooper S, Odenbach J, Finegan BA, Schulz R, Kassiri Z, Lopaschuk GD, Fernandez-Patron C. Matrix metalloproteinase-7 and ADAM-12 (a disintegrin and metalloproteinase-12) define a signaling axis in agonist-induced hypertension and cardiac hypertrophy. *Circulation*. 2009;119:2480-2489
15. Wang X, Oka T, Chow FL, Cooper SB, Odenbach J, Lopaschuk GD, Kassiri Z, Fernandez-Patron C. Tumor necrosis factor-alpha-converting enzyme is a key regulator of agonist-induced cardiac hypertrophy and fibrosis. *Hypertension*. 2009;54:575-582
16. Tran ED, DeLano FA, Schmid-Schonbein GW. Enhanced matrix metalloproteinase activity in the spontaneously hypertensive rat: VEGFR-2 cleavage, endothelial apoptosis, and capillary rarefaction. *J Vasc Res*. 2010;47:423-431
17. Delano FA, Chen AY, Wu KI, Tran ED, Rodrigues SF, Schmid-Schonbein GW. The Autodigestion Hypothesis and Receptor Cleavage in Diabetes and Hypertension. *Drug Discov Today Dis Models*. 2011;8:37-46
18. DeLano FA, Schmid-Schonbein GW. Proteinase activity and receptor cleavage: mechanism for insulin resistance in the spontaneously hypertensive rat. *Hypertension*. 2008;52:415-423
19. Kleinman ME, Yamada K, Takeda A, Chandrasekaran V, Nozaki M, Baffi JZ, Albuquerque RJ, Yamasaki S, Itaya M, Pan Y, Appukuttan B, Gibbs D, Yang Z, Kariko K, Ambati BK, Wilgus TA, DiPietro LA, Sakurai E, Zhang K, Smith JR, Taylor EW, Ambati J. Sequence- and target-independent angiogenesis suppression by siRNA via TLR3. *Nature*. 2008;452:591-597
20. Zhan M, Jin B, Chen SE, Reecy JM, Li YP. TACE release of TNF-alpha mediates mechanotransduction-induced activation of p38 MAPK and myogenesis. *J Cell Sci*. 2007;120:692-701
21. Kassiri Z, Oudit GY, Sanchez O, Dawood F, Mohammed FF, Nuttall RK, Edwards DR, Liu PP, Backx PH, Khokha R. Combination of tumor necrosis factor-alpha ablation and matrix metalloproteinase inhibition prevents heart failure after pressure overload in tissue inhibitor of metalloproteinase-3 knock-out mice. *Circ Res*. 2005;97:380-390
22. Castro MM, Rizzi E, Figueiredo-Lopes L, Fernandes K, Bendhack LM, Pitol DL, Gerlach RF, Tanus-Santos JE. Metalloproteinase inhibition ameliorates hypertension and prevents vascular dysfunction and remodeling in renovascular hypertensive rats. *Atherosclerosis*.

2008;198:320-331
23. Hao L, Nishimura T, Wo H, Fernandez-Patron C. Vascular responses to alpha1-adrenergic receptors in small rat mesenteric arteries depend on mitochondrial reactive oxygen species. *Arterioscler Thromb Vasc Biol*. 2006;26:819-825
24. Kagiyama S, Eguchi S, Frank GD, Inagami T, Zhang YC, Phillips MI. Angiotensin II-induced cardiac hypertrophy and hypertension are attenuated by epidermal growth factor receptor antisense. *Circulation*. 2002;106:909-912
25. Sen S, Petscher C, Ratliff N. A factor that initiates myocardial hypertrophy in hypertension. *Hypertension*. 1987;9:261-267
26. Pereira AH, Clemente CF, Cardoso AC, Theizen TH, Rocco SA, Judice CC, Guido MC, Pascoal VD, Lopes-Cendes I, Souza JR, Franchini KG. MEF2C silencing attenuates load-induced left ventricular hypertrophy by modulating mTOR/S6K pathway in mice. *PLoS One*. 2009;4:e8472
27. Muller P, Kazakov A, Jagoda P, Semenov A, Bohm M, Laufs U. ACE inhibition promotes upregulation of endothelial progenitor cells and neoangiogenesis in cardiac pressure overload. *Cardiovasc Res*. 2009;83:106-114
28. Rockman HA, Wachhorst SP, Mao L, Ross J, Jr. ANG II receptor blockade prevents ventricular hypertrophy and ANF gene expression with pressure overload in mice. *Am J Physiol*. 1994;266:H2468-2475
29. Yamazaki T, Komuro I, Zou Y, Kudoh S, Shiojima I, Hiroi Y, Mizuno T, Aikawa R, Takano H, Yazaki Y. Norepinephrine induces the raf-1 kinase/mitogen-activated protein kinase cascade through both alpha 1- and beta-adrenoceptors. *Circulation*. 1997;95:1260-1268
30. Lu Y, Yang S. Angiotensin II induces cardiomyocyte hypertrophy probably through histone deacetylases. *Tohoku J Exp Med*. 2009;219:17-23
31. Morganroth J, Maron BJ. The athlete's heart syndrome: a new perspective. *Ann N Y Acad Sci*. 1977;301:931-941
32. Zeisberg EM, Tarnavski O, Zeisberg M, Dorfman AL, McMullen JR, Gustafsson E, Chandraker A, Yuan X, Pu WT, Roberts AB, Neilson EG, Sayegh MH, Izumo S, Kalluri R. Endothelial-to-mesenchymal transition contributes to cardiac fibrosis. *Nat Med*. 2007;13:952-961
33. Crowley SD, Gurley SB, Herrera MJ, Ruiz P, Griffiths R, Kumar AP, Kim HS, Smithies O, Le TH, Coffman TM. Angiotensin II causes hypertension and cardiac hypertrophy through its receptors in the kidney. *Proc Natl Acad Sci U S A*. 2006;103:17985-17990
34. Jerez S, Peral de Bruno M, Coviello A. Cross talk between angiotensin II and alpha 1 adrenergic receptors in rabbit aorta: role of endothelium. *J*

Cardiovasc Pharmacol. 2004;43:402-409

35. Camp TM, Smiley LM, Hayden MR, Tyagi SC. Mechanism of matrix accumulation and glomerulosclerosis in spontaneously hypertensive rats. *J Hypertens*. 2003;21:1719-1727
36. Crabbe T, Smith B, O'Connell J, Docherty A. Human progelatinase A can be activated by matrilysin. *FEBS Lett*. 1994;345:14-16
37. Barille S, Bataille R, Rapp MJ, Harousseau JL, Amiot M. Production of metalloproteinase-7 (matrilysin) by human myeloma cells and its potential involvement in metalloproteinase-2 activation. *J Immunol*. 1999;163:5723-5728
38. Han YP, Tuan TL, Wu H, Hughes M, Garner WL. TNF-alpha stimulates activation of pro-MMP2 in human skin through NF-(kappa)B mediated induction of MT1-MMP. *J Cell Sci*. 2001;114:131-139
39. Yu WH, Woessner JF, Jr., McNeish JD, Stamenkovic I. CD44 anchors the assembly of matrilysin/MMP-7 with heparin-binding epidermal growth factor precursor and ErbB4 and regulates female reproductive organ remodeling. *Genes Dev*. 2002;16:307-323
40. Staun-Ram E, Goldman S, Shalev E. p53 Mediates epidermal growth factor (EGF) induction of MMP-2 transcription and trophoblast invasion. *Placenta*. 2009;30:1029-1036
41. Kumar B, Koul S, Petersen J, Khandrika L, Hwa JS, Meacham RB, Wilson S, Koul HK. p38 mitogen-activated protein kinase-driven MAPKAPK2 regulates invasion of bladder cancer by modulation of MMP-2 and MMP-9 activity. *Cancer Res*. 2010;70:832-841
42. Renkiewicz R, Qiu L, Lesch C, Sun X, Devalaraja R, Cody T, Kaldjian E, Welgus H, Baragi V. Broad-spectrum matrix metalloproteinase inhibitor marimastat-induced musculoskeletal side effects in rats. *Arthritis Rheum*. 2003;48:1742-1749
43. Bramhall SR, Hallissey MT, Whiting J, Scholefield J, Tierney G, Stuart RC, Hawkins RE, McCulloch P, Maughan T, Brown PD, Baillet M, Fielding JW. Marimastat as maintenance therapy for patients with advanced gastric cancer: a randomised trial. *Br J Cancer*. 2002;86:1864-1870

Chapter 5

Matrix metalloproteinase-2 is cardioprotective through a novel negative regulation of the SREBP-2 / HMGCR transcriptional pathway

Contribution: Adenovirus construction, conducted animal and cell culture studies, performed qRT-PCR, zymography and western immunoblotting assays, data analysis and data interpretation, contributed to the construction of the hypothesis, drafted the first version of the manuscript together with my supervisor and revised the manuscript.

5.1 Introduction

Hypertrophic cardiomyopathy is a major cause of morbidity and mortality in industrialized countries[1-3]. This condition can be caused by sustained hypertension as well as metabolic comorbidities such as diabetes, hyperlipidemia and hypercholesterolemia[1-3]. A common effector mechanism of these detrimental factors is a sustained elevation of the systemic levels of G protein-coupled receptor (GPCR) agonists including angiotensin (Ang) II[4,5]. These agonists elicit intracellular signaling of 'remodeling' (hypertrophy and fibrosis) processes in the heart, at least in part, through triggering an excessive transcriptional upregulation and activation of cardiac matrix metalloproteinases (MMPs).

Purportedly, MMPs act mainly through the proteolysis of substrates such as extracellular matrix proteins and growth factors to modulate the development of left ventricular (LV) hypertrophy and fibrosis. The ensuing LV remodeling can progress to cardiac dysfunction and, ultimately, heart failure[6,7]. Therefore, MMPs are attractive therapeutic targets to treat LV remodeling and dysfunction. However, understanding their precise mechanisms in animal models of human disease is crucial for the successful translation of MMP-targeted therapeutics to specific clinical contexts.

A major mechanism of LV remodeling and dysfunction depends on the activity of a ubiquitous enzyme, 3-hydroxy-3-methylglutaryl-coenzyme A (HMG-CoA) reductase (HMGCR)[8,9]. HMGCR catalyzes the conversion of HMG-CoA to mevalonate[10], which is the rate-limiting step in a series of enzymatic conversions that transform HMG-CoA to 5-carbon, 15-carbon and 20-carbon activated isoprenoids such as: isopentenyl pyrophosphate, farnesyl pyrophosphate and geranylgeranyl pyrophosphate. Both farnesyl pyrophosphate and geranylgeranyl pyrophosphate are used in protein prenylation that post-translationally modify intracellular signaling mediators with a CAAX motif

(C denotes cysteine, A denotes any aliphatic amino acid and X may be any amino acid) in their carboxyl terminus. Notable CAAX motif proteins include small GTPases of the Ras superfamily, which switch ‘on’ or ‘off’ intracellular signaling of hypertrophy, fibrosis and oxidative stress in response to GPCR agonists[11]. Alternatively, farnesyl pyrophosphate can be converted to molecules that support cellular growth such as dolichyl phosphate (used for N-glycosylation of growth factor receptors such as insulin-like growth factor receptor) and cholesterol (precursor of steroid hormones and cell membrane component).

HMGCR is strongly regulated at the transcriptional level by sterol-regulatory element binding protein (SREBP)-2[12]. In addition, SREBP-2 regulates the transcriptions of low-density lipoprotein (LDL) receptor (LDLR), which mediates LDL-cholesterol uptake[12], and pro-protein convertase subtilisin/kexin type 9 (PCSK9) [13,14]. Binding of PCSK9 to LDLR induces LDLR degradation, which limits LDL-cholesterol uptake[13,14].

The SREBP pathway is negatively regulated by intracellular sterols (both cholesterol and oxysterols)[15,16]. Insulin induced gene (Insig) proteins and SREBP cleavage activating protein (SCAP) are key elements of the feedback inhibition of the SREBP pathway triggered by sterols. Whereas cholesterol binds to SCAP and causes it to bind to Insigs, oxysterols bind to Insigs causing them to bind to SCAP. As a result, sterols prevent the activation of SREBPs to their nuclear form, thus inhibiting SREBP transcriptional activity and thereby cholesterol biosynthesis. Thus, the intracellular levels of sterols provide a negative feedback for the SREBP-2 pathway.

Here, we report novel cardioprotective actions of MMP-2 which are mediated through a negative regulation of the SREBP-2 pathway in the heart.

5.2 Materials and methods

Animal models Animal studies were conducted under the protocol approved by University of Alberta Animal Care and Use Committee. All animals were fed a regular chow and housed at the Animal Facility of the University of Alberta. Male C57BL/6 mice were purchased from Charles River (Wilmington, MA, USA). MMP-7 KO mice were purchased from The Jackson Laboratory (Bar Harbor, ME, USA). MMP-2 KO mice were bred and housed at the University of Alberta. The mice (11-14 week old) were anesthetised by 2.0% isoflurane inhalation and ALZET osmotic minipumps (DURECT Corporation, Cupertino, CA, USA) delivering either PBS or Ang II (0.14, 1.4 or 2.0 mg/kg/d, EMD Millipore, Billerica, MA, USA) were implanted subcutaneously on the posterior midsection. All mice were euthanized using sodium pentobarbital (65 mg/kg).

Recombinant adenovirus construct MMP-2-expressing adenovirus was generated using AdEasy™ system (Agilent Technology, Mississauga, Canada). pOTB7 plasmid containing human MMP-2 gene was obtained from ATCC (Manassas, VA, USA). The MMP-2 gene was excised from the plasmid by XhoI and EcoRI digestion, followed by mung bean nuclease digestion to generate blunt ends. The gene was inserted into adenoviral shuttle vector pAdTrack-CMV EcoRV site, and the orientation of the gene was confirmed by restriction endonuclease digestion. The generated pAdTack-CMV-MMP-2 plasmid was linearized by PmeI digestion and cotransformed into E. coli BJ5183 with adenoviral backbone plasmid, pAdEasy-1. pAdTack-CMV-MMP-2 can be integrated into pAdEasy-1 by homologous recombination. Recombinants were selected for kanamycin resistance and recombination was confirmed by restriction endonuclease analysis. Finally, the linearized recombinant plasmid (by PacI) was transfected into HEK293 cells to generate mature MMP-2 expressing adenovirus (AdMMP-2).

***In vivo* overexpression of MMP-2** MMP-2-expressing adenovirus (AdMMP-2, 10^8 pfu in 100 μL PBS) or control (green fluorescent protein (GFP)-expressing) adenovirus (AdGFP, 10^8 pfu in 100 μL PBS) were injected via tail vein. Ang II-delivering (0.14 mg/kg/d, 2 weeks) minipumps were implanted 3 days after adenovirus injection. Mice were euthanized 2 weeks after minipump implantation.

Cell Culture Mouse c1c7 hepatoma cells expressing LDLR (LDLR-positive) were cultured in α-modification Minimum Essential Medium (αMEM,Thermo Fisher Scientific, Nepean, ON) supplemented with 10% fetal bovine serum (FBS). To overexpress MMP-2, the cells were transduced with AdMMP-2 or control AdGFP (3 pfu/cell). To study how MMP-2 affected the time course of SREBP-2 and HMGCR expression, the cells were cultured in complete media and collected at 0, 24 48 or 72 hours after transduction with AdMMP-2 or AdGFP. To study the effects of MMP-2 overexpression on PCSK9-induced LDLR degradation, the cells transduced with AdMMP-2 or AdGFP were incubated in αMEM with 1% bovine serum albumin overnight before adding recombinant human (rh) PCSK9 (Creative Biomart, NY, USA) or vehicle. To study whether MMP-2 catalytic activity was required for protection, the cells were incubated with the 40 μmol/L MMP-2 inhibitor III (EMD Millipore) for 1 hour before adding rhPCSK9.

***In vitro* reactions** rhMMP-2 (EMD Millipore), PCSK9 and LDLR extracellular domain were incubated in enzyme assay buffer (25 mmol/L Tris, 5 mmol/L $CaCl_2$, 150 mmol/L NaCl, pH 7.4) at 37 ºC for 3 hours in the presence or absence of the MMP inhibitor, 1,10-phenanthroline (Sigma-Aldrich, Oakville, ON, Canada). Reactions were collected and subjected to SDS-PAGE, BN-PAGE, gelatin zymography and immunoblot.

Blood pressure measurement Systolic blood pressure was measured indirectly using a computerized tail cuff plethysmography system (Kent Scientific Corporation, Torrington, CT, USA). Conscious mice were maintained at 32-35ºC using a heating pad and restrained during measurements. Averages of 10 inflation/deflation cycles were conducted to obtain mean systolic blood pressure.

Echocardiography *In vivo* assessment of anatomical structures and hemodynamic function in mice was conducted by M-mode echocardiography. The animals were first anaesthetized with 2.0% isoflurane and their cardiac function was subsequently analyzed using a Vevo 770 high-resolution imaging system (Visualsonics, Toronto, ON, Canada). Analysis of the mitral valve annulus was performed using tissue Doppler imaging.

HMGCR inhibition using lovastatin Lovastatin (54 or 108 mg/kg/d, BioVision, San Francisco, CA, USA) or vehicle (soybean oil) was delivered daily by gavage feeding. Ang II-delivering (2.0 mg/kg/d for 2 weeks) minipumps were implanted 3 days after initiation of lovastatin administration. The mice were euthanized 2 weeks after minipump implantation for endpoint analysis.

Homogenization Heart and other organs were washed in isotonic saline buffer, rinsed and weighed. Protein extraction was done in 20 mmol/L Tris (pH 8.0), 150 mmol/L NaCl, 10% glycerol, 1% SDS, 0.1% Triton X-100 and protease inhibitor cocktail (Roche, Mannheim, Germany). To determine the protein content, homogenates were separated by 10% SDS-PAGE followed by densitometric analysis of Coomassie Brilliant Blue-stained bands. Equal protein quantities were loaded for subsequent gelatin zymography and immunoblotting.

Gelatin zymography MMP-2 enzymatic activity was determined using gelatin zymography. Organ homogenates, cell extracts or *in vitro* reactions were subjected to electrophoresis on SDS-PAGE or BN-PAGE gels co-polymerized with gelatin (2 mg/mL). Following electrophoresis, gels were washed three times with 2.5% Triton X-100 for 20 min. Enzymatic reaction was carried out for 16 hours at 37°C in enzyme assay buffer (25 mmol/L Tris, 5 mmol/L $CaCl_2$, 150 mmol/L NaCl, 0.5 mmol/L NaN_3, pH 7.4) and gels were stained with Coomassie Brilliant Blue.

Enzymatic activity was visualized as clear bands against a blue background in the gel.

Blue native (BN)-PAGE Gels were cast with equally-sized, discrete layers of 6% and 12% acrylamide. For gelatin zymography, gels were embedded with 2 mg/mL gelatin. Electrophoresis was performed at room temperature using Hoefer SE260 (Hoefer, Holliston, MA, USA) with a water cooling system. For immunoblotting, the BN-PAGE gel was incubated in SDS-PAGE running buffer supplemented with 1% 2-mercaptoethanol for 10 minutes before transfer to a nitrocellulose membrane.

Protein immunoblotting The expression of specific proteins was determined by immunoblotting (Western blot). Organ homogenates, cell extracts or *in vitro* reactions were separated by SDS-PAGE or BN-PAGE and transferred to a nitrocellulose membrane. The membrane was probed with primary antibodies against MMP-2 (EMD Millipore), HMGCR (Santa Cruz Biotechnology, Santa Cruz, CA, USA), SREBP-2, LDLR (Abcam, Cambridge, MA, USA) and GAPDH (Santa Cruz Biotechnology) and corresponding secondary antibodies (GE Healthcare, Buckinghamshire, UK), before being detected using ECL western blotting detection reagent (GE Healthcare).

In-gel microwave-assisted acid hydrolysis (MAAH) and its combination with liquid chromatography (LC)-electronspray ionization (ESI) MS/MS for PCSK9 sequence mapping The gel bands of rhPCSK9 prodomain and its cleavage fragment were cut out and washed twice with 1 mL of water for 5 min. Next, the gel bands were cut into small pieces and dehydrated using 500 µL of acetonitrile (ACN) for 5 min twice. Dry gel pieces were desiccated using Speedvac (Thermo Fisher Scientific, Nepean, ON) for 15 min. 120 µL of 12 mmol/L dithiotreitol (DTT) and 40 µL of trifluoroacetic acid (TFA) were added to the vial containing the dried gel pieces. The vial was immersed in a water bath and placed in a domestic 1200 W (2450 MHz) microwave oven. The irradiation time was 10 min. The generated peptide mixture was extracted using 300 µL of 85% ACN / 0.1% TFA solution twice, and desiccated using Speedvac. Reduction and alkylation of the peptide mixture was performed by using 20 µL of DTT (90 mmol/L) for 1 hour at 37 °C and 50 µL of iodoacetamide (200 mmol/L) for 1 hour at room temperature. The peptide mixture was then desalted. LC-MS/MS analysis of the peptide mixtures and database search were performed as described previously with minor changes[17].

RNA expression analysis by TaqMan qRT-PCR Total RNA was extracted from flash-frozen organs using Trizol reagent (Invitrogen, Burlington, ON, Canada) and cDNA was generated from 2 µg RNA using a random hexamer (Invitrogen). Expression analysis of the reported genes was performed by TaqMan qRT-PCR using ABI 7900 sequence detection system (Applied Biosystems, Carlsbad, CA, USA). Glyceraldehyde 3-phosphate dehydrogenase (GAPDH) was used as an internal standard.

Histological analysis Mice hearts were fixed in 10% neutral-buffered formalin overnight and embedded in paraffin. 4 µm-thick sections were cut and stained with a modified Lillie's variant of Masson's trichrome stain[18]. Briefly, sections were deparaffinised, mordanted overnight in Bouin's solution (Sigma-Aldrich), stained successively with fresh Weigert's hematoxylin, Biebrich scarlet-acid fuchsin (0.9% Biebrich scarlet, 0.1% acid fuchsin, 1% acetic acid), 2.5% phosphomolybdic – 2.5% phosphotungstic acid and aniline blue (2.4% aniline blue, 2% acetic acid) solutions (all from Sigma-Aldrich). Each staining step was performed for 5 minutes and followed by washes in running tap water and / or distilled water. After brief rinsing in 1% acetic acid (3 minutes), sections were dehydrated to xylene, mounted using Permount (Thermo Fisher Scientific) and visualized using a Leica microscope (Leica Microsystems Inc., Concord, ON).

Statistical analysis Results were analyzed using one-way ANOVA (between multiple groups) or t-test (between two groups) (Jandel SigmaPlot 11 software). All data are reported as means +/- SEM.

5.3 Results

MMP-2 expression correlates with Ang II-induced cardiac hypertrophy and diastolic dysfunction

As expected, in wild type (WT) mice, sustained Ang II (0-2.0 mg/kg/d) infusion caused a time- and dose-dependent systemic hypertension[19] and cardiac hypertrophy (as evidenced by the relative increase in the heart weight to either body weight or tibia length, **Figures 5-1A, B and 5-2**). These events were associated with upregulation of MMP-2 in the LV[19] (**Figure 5-3**). Cardiac fibrosis in this model was both interstitial and perivascular with significantly elevated markers of hypertrophy and fibrosis (**Figures 5-4, 5-5**). The hypertrophy and fibrosis induced by the maximum Ang II dose tested (2.0 mg/kg/d) were fully prevented by the HMGCR inhibitor lovastatin (**Figure 5-1B**). Overall, these data are consistent with previous research and confirm the mediator role of HMGCR in Ang II-induced cardiac disease[9,20-22].

MMP-2 and HMGCR are functionally linked in cardiac disease

We have also observed an early but transient increase in the levels of HMGCR mRNA (**Figure 5-8B**) and a more sustained elevation of MMP-2 (**Figure 5-3**) in response to Ang II. Moreover, we observed that, after MMP-2 levels peak, at week 2 on Ang II (**Figure 5-3**), there was no further increase in cardiac hypertrophy (**Figure 5-1A**).

These observations led us to test the hypothesis that MMP-2 and HMGCR are functionally related in the process of cardiac hypertrophy. To determine whether MMP-2 expression influences the time course and severity of Ang II-induced cardiac disease, we conducted studies with MMP-2 KO mice, which we compared with age-matched WT mice. Interestingly, MMP-2 KO predisposed to early onset of cardiac hypertrophy with perivascular fibrosis (**Figures 5-1A, C, 5-2, 5-4 and 5-5**). In MMP-2 KO mice, we also observed a marked decrease in the ratio between the mitral E’ and A’ waves (reflecting the peak velocity of the mitral valve annulus during early and late LV filling, respectively), indicating a higher propensity to diastolic dysfunction in MMP-2 KO mice (**Figure 5-6**).

Of note, MMP-2 KO mice had significantly increased baseline levels of cardiac SREBP-2 mRNA (**Figures 5-7A and 5-8A**) and protein (by 2.6 ± 0.12-fold *vs*. WT mice, n = 3-4 / group, $p<0.05$). In accordance, levels of HMGCR mRNA (**Figures 5-7B and 5-8B**) and protein (**Figure 5-7C**) were elevated as well. Isolated MMP-2 KO cardiomyocytes recapitulated this phenotype (**Figure 5-9**).

MMP-2-dependent negative regulation of HMGCR protects against pathological cardiac hypertrophy and fibrosis

Treatment with lovastatin dose-dependently prevented Ang II-induced cardiac hypertrophy in MMP-2 KO mice as well as in WT mice (**Figure 5-1B, C**), thus confirming the key contribution of HMGCR to Ang II-induced cardiac disease. However, MMP-2 KO mice required a two-fold higher dose for disease prevention, consistent with their higher HMGCR levels. At the molecular level, lovastatin attenuated the elevation of hypertrophy and fibrosis marker genes with the sole exception of fibronectin 1 (**Figure 5-5**).

To exclude the potential effect of hypertension in disease causation and mediation in MMP-2 KO mice, we examined mice under a subpressor Ang II regimen (0.14 mg/kg/d for 2 weeks). MMP-2 KO mice responded to the subpressor Ang II regimen with ~10% increase in heart weight**.** Contrary to MMP-2 gene KO, transduction of WT mice with adenovirus to overexpress MMP-2 resulted in decreased baseline expression of cardiac HMGCR and no increase in heart weight in response to Ang II (**Figure 5-10**).

MMP-2 and cholesterol in negative regulation of the SREBP-2 pathway.

Although cardiac SREBP-2 and HMGCR baseline levels were elevated in MMP-2 KO *vs.* WT mice, cardiac cholesterol levels were similar in both groups (**Figure 5-7**).

Infusing Ang II transiently elevated HMGCR immunoreactivity in MMP-2 KO mice, with HMGCR immunoreactivity peaking on week 2 (**Figure 5-7C**) as Ang II-induced hypertrophy was established (**Figure 5-1**). The elevation in HMGCR immunoreactivity induced by Ang II was associated with an increase in cardiac cholesterol (**Figures 5-7D, 5-8D**) and a corresponding mRNA decrease in SREBP-2, HMGCR, LDLR (**Figure 5-8**).

To determine whether MMP-2 deficiency affects the negative regulation of the cardiac SREBP-2 pathway by cholesterol, we examined the levels of SCAP, Insig 1 and 2 in MMP-2 KO mice whose diet was supplemented with 0.15% cholesterol (vs. 0.015% cholesterol in normal chow). High levels of Insig 1 and 2 in MMP-2 KO mice indicated an abundance of intracellular sterol sensors, although SCAP was no different in MMP-2 KO and WT mice (**Figure 5-11**). Feeding cholesterol strongly suppressed the otherwise high expression of SREBP-2, HMGCR and Insigs in MMP-2 KO mice (**Figure 5-11**). Therefore, MMP-2 KO mice can sense cholesterol as well as WT mice.

Therefore, MMP-2 deficiency induces the expression and activation of baseline cardiac SREBP-2 as well as downstream HMGCR transcription. However, hormonal stimulation by Ang II further facilitates the translation of HMGCR mRNA into protein, thereby, significantly increasing cardiac cholesterol levels (**Figures 5-7D, 5-8D**). This transient increase in cholesterol acts to inhibit the SREBP-2 pathway, which explains why the mRNA levels of SREBP-2 and its target genes are time-dependently decreased by Ang II (**Figure 5-8A-C**).

MMP-7 is not a negative regulator of the SREBP-2 / HMGCR pathway

We next examined whether the negative regulation of the SREBP-2 pathway exhibited by MMP-2 was shared by other MMPs. We studied if lack of MMP-7 (also known as matrilysin-1), a “prototypical” minimal-domain MMP, would upregulate the cardiac SREBP-2 / HMGCR pathway as well. In contrast to the characteristically high levels of cardiac SREBP-2 and HMGCR found in MMP-2 KO mice, MMP-7 KO mice had levels of both genes comparable to those of WT mice (**Figure 5-7A, B**). Therefore, negative regulation of the SREBP-2 pathway by MMP-2 is rather unique in that it is not shared at least by MMP-7.

Since MMP-7 is a minimal MMP that shares many substrates with MMP-2 and other MMPs[23], this finding suggested that MMP-2 acts through either a very unique substrate or a proteolysis independent mechanism.

Cardioprotection by MMP-2 results from inhibition of the SREBP-2 / HMGCR→ADAM-12 pathway of cardiac remodeling

This research shows that MMP-2 is cardioprotective and its absence promotes cardiac hypertrophy through the HMGCR pathway. We previously showed that MMP-7 is pro-hypertrophic through upregulation of an ‘a disintegrin and metalloproteinase-12’ (ADAM-12)-dependent hypertrophy pathway (**Figure 5-12A**). Interestingly, unlike MMP-7 KO mice, MMP-2 KO mice had significantly higher baseline and Ang II-induced levels of cardiac ADAM-12 *vs.* WT mice (**Figure 5-12B**). The elevation of ADAM-12 induced by Ang II was fully prevented by lovastatin. Therefore, the negative regulation of the SREBP-2 / HMGCR pathway by MMP-2 prevents ADAM-12-dependent pathway of pathological cardiac remodeling.

A molecular mechanism by which MMP-2 negatively regulates the SREBP-2 pathway

Intracellular sterols are major regulators of the SREBP-2 pathway. Thus, the upregulation of the SREBP-2 / HMGCR pathway in MMP-2 deficient mice could be due to decreased cholesterol synthesis or a defect in cholesterol uptake. We hypothesized that lack of MMP-2 inhibits normal cholesterol uptake.

Cultured c1c7 cells transduced with an adenoviral construct overexpressing MMP-2 had decreased mRNA expression of SREBP-2 and HMGCR (**Figure 5-13A-C**) confirming that MMP-2 negatively regulates the SREBP-2 pathway in cultured cells as well as in live mice.

A positive feedback for the SREBP-2 pathway depends on plasma PCSK9, a circulating LDLR ligand, which binds to the LDLR extracellular domain and re-routes the LDLR from the recycling pathway to lysosomes where the LDLR is degraded[13,14]. Interestingly, in cells that stably expressed LDLR, the overexpression of human MMP-2 inhibited PCSK9-induced degradation of the LDLR (**Figure 5-13D**).

rhMMP-2 concentration-dependently and readily cleaved the prodomain of PCSK9 at the Ala(14)/Leu(15) bond (**Figure 5-14A, B and Table 5-1**). SDS-PAGE band-shift studies using a chemical crosslinker BS3, a homobifunctional amine-to-amine crosslinker from the family of bis(sulfosuccinimidyl)suberates, suggested that MMP-2 may form a complex with PCSK9 (**Figure 5-14C**). These data suggested that human MMP-2 binds to human PCSK9 resulting in the release and cleavage of the prodomain of PCSK9 by MMP-2. Interestingly, cleavage of PCSK9 prodomain by MMP-2 did not affect PCSK9’s ability to induce LDLR degradation in cells (**Figure 5-15**). Further analysis of *in vitro* reaction mixtures by blue native (BN)-PAGE confirmed that PCSK9 indeed binds to MMP-2 as well as the LDLR extracellular domain (**Figure 5-13E**). Data from the chemical crosslinker and LDLR degradation assays suggested that MMP-2 binds to PCSK9 and may protect the LDLR even in the presence of a MMP-2 inhibitor (**Figure 5-16**). Therefore, protection of the LDLR by cellular MMP-2 may not require MMP-2 dependent proteolysis of substrates.

In vivo studies further supported the notion that MMP-2 expression protects the LDLR from degradation. In the LVs of both untreated and Ang II-treated MMP-2 KO mice, LDLR protein levels were decreased *vs*. WT (**Figure 5-13F**) even at baseline, where LDLR mRNA levels were elevated for MMP-2 KO mice (**Figure 5-4B**), and despite the similar plasma levels of PCSK9 in MMP-2 KO and WT mice as determined by ELISA (PCSK9 (WT) = 0.439 ± 0.23 ng/mL; PCSK9 (MMP-2 KO) = 0.453 ± 0.122 ng/mL, n = 3/group, p=0.96).

5.4 Discussion

We have identified novel cardioprotective actions of MMP-2 that are mediated by negative regulation of the SREBP-2 / HMGCR→ADAM-12 pathway in the heart. We further suggest that MMP-2 acts by protecting the LDLR from degradation via a non-proteolytic mechanism. The proposed pathways are illustrated in **Figure 5-17**.

Although MMPs have long been implicated in the modulation of cardiac remodeling, most studies including ours[19,24-27] have centered on the proteolytic cleavage of substrates such as extracellular matrix proteins, growth factors and receptors[28]. Upregulation of MMPs has often been considered a requirement for disease progression. However, here we observed that MMP-2 deficiency predisposes to cardiac hypertrophy, fibrosis and diastolic dysfunction. Moreover, we found that MMP-2 KO mice have surprisingly high baseline mRNA levels of cardiac SREBP-2, a major transcription factor for HMGCR and LDLR genes. These data functionally links MMP-2 to cholesterol synthesis and uptake. Therefore, MMP-2 is robustly upregulated during the first stages of Ang II-induced cardiac disease and protects the heart through a novel negative regulation of the cardiac SREBP-2 pathway. Given the ubiquitous expression of MMP-2 and the fundamental significance of the SREBP-2 pathway in normal physiology and the development of disease, our findings unmask a novel biological activity of MMP-2 with basic as well as clinical significance.

The combined results from our integrative physiology, cell biological and biochemical studies indicate that resident MMP-2 (but not MMP-2 in circulation) protects the plasma membrane-expressed LDLR from degradation. We propose that, by increasing LDLR bioavailability, MMP-2 facilitates LDL-cholesterol uptake which, in turn, inhibits the SREBP-2 pathway[12]. Indeed, MMP-2 KO (but not MMP-7 KO) mice had strongly elevated cardiac mRNA levels of SREBP-2 and downstream genes such as HMGCR, LDLR and Insigs (*vs.* WT mice). Thus, lack of MMP-2 results in a phenotype of, at least mild, cardiac cholesterol starvation when mice are fed normal chow (that contains 0.015% cholesterol). This phenotype, however, is reversed by cholesterol supplementation using a 10-fold enriched diet (i.e. 0.15% cholesterol).

Immunoreactivity for cardiac LDLR protein was dramatically weak in MMP-2 KO mice. Why were LDLR protein levels low in MMP-2 KO hearts? The cell biological studies revealed that MMP-2 can protect the LDLR from degradation induced by PCSK9. Interestingly, we found similar protection in the presence of MMP-2 inhibitors indicating that MMP-2 proteolytic activity is not required to protect the LDLR. Chemical cross-linking in combination with BN-PAGE for separation of protein complexes showed that MMP-2 binds PCSK9 and recombinant LDLR extracellular domain. We suggest that cell-surface expressed MMP-2 can recruit PCSK9 from the circulation to the plasma membrane and thus protects the LDLR from degradation (**Figure 5-17**). Whether other MMPs interact with PCSK9 in a similar fashion warrants investigation.

Our data suggest that pro-hypertrophic stimuli such as Ang II impact on cardiac SREBP-2 / HMGCR pathway. Ang II stimulates the translation of the relatively high HMGCR mRNA levels in MMP-2 KO into correspondingly high HMGCR protein levels. This increase in HMGCR protein causes an increase in cardiac cholesterol levels, which coincides with the establishment of cardiac hypertrophy. As cholesterol levels peak (ie., week 2 on Ang II infusion), the characteristically high mRNA levels of SREBP-2 and HMGCR in MMP-2 KO mice start to decline, confirming the SREBP-2 / HMGCR pathway in MMP-2 KO mice is still subject to negative feedback by one of its products: cholesterol. The pharmacological HMGCR inhibition by lovastatin prevented the induction of hypertrophy and fibrosis marker genes in both MMP-2 KO and WT mice. These data confirmed that active HMGCR is required for LV remodeling[9,20-22]. MMP-2 KO mice had reduced responsiveness to treatment with lovastatin as indicated by the HW/BW ratio and developed more cardiac hypertrophy. Therefore, HMGCR overexpression caused by MMP-2 deficiency predisposes to cardiac disease.

Excessive HMGCR expression and activity lead to increased synthesis of isoprenoids and cholesterol. Previous studies have demonstrated that Ang II induces the development of cardiac hypertrophy through isoprenylation of Rac1 and Rho, indicating the pro-hypertrophic potential of isoprenoids[9,22]. Rho regulates the hypertrophic process by activating downstream signaling molecules such as mitogen-activated protein kinases (MAPKs). Rac1 mediates cardiac hypertrophy through activation of nicotinamide adenine dinucleotide phosphate (NADPH) oxidase and superoxide production. However, in these studies, the involvement of cholesterol in cardiac hypertrophy was discarded on the basis that LDL-cholesterol levels were not decreased by statin treatment[9,22,29].

Although high levels of cholesterol in the circulation have long been appreciated as a risk factor for atherosclerosis and coronary artery disease, the role of cholesterol in the development of cardiac hypertrophy and fibrosis is not fully understood. In rat cardiomyocytes, cholesterol uptake by LDLR is low and HMGCR activity has been suggested to account for the intracellular cholesterol levels[30]. However, cardiomyocytes may acquire cholesterol from the circulation through LDLR-independent pathways[31]. Suggesting cholesterol is important in the development of cardiac hypertrophy, recent metabolites profile studies using mass spectrometry-based analysis combined with high-temperature gas chromatographic show an 7-fold increase in cholesterol levels in hypertrophic cardiac tissues[32]. Our study here shows that, in hypertrophic hearts, cholesterol to protein ratio was unchanged in wild type mice while it increased in MMP-2 KO mice. Supporting the notion that cholesterol is an essential component of the hypertrophy process, hypercholesterolemia in pig models is associated with expression of cardiac hypertrophy markers, which are upregulated downstream of cardiac mTOR[33]. Further, in cultured cardiomyocytes, exposure to cholesterol results in an increase in intracellular cholesterol levels and the development of hypertrophy due to the activation of PI3K-Akt pathway[34]. These studies, together with our results, suggest that cholesterol is indeed necessary for the development of cardiac hypertrophy.

Our data show MMP-2 negatively regulates the SREBP-2 / HMGCR pathways to prevent ADAM-12 signaling of pathological cardiac remodeling. We further show that cardioprotection by MMP-2 is not shared by MMP-7. Indeed, we confirmed that MMP-7 KO mice are less prone to cardiac remodeling when compared to MMP-2 KO or WT mice, in line with our earlier studies[24]. Unlike MMP-2 KO mice, MMP-7 KO mice had baseline levels of SREBP-2 and HMGCR comparable to those of WT mice. Therefore, the different actions of MMP-7 and MMP-2 in cardiac disease can be explained, at least in part, by their different regulation of HMGCR, and thereby, their different effects on the ADAM-12-dependent pathways of cardiac hypertrophy and fibrosis.

Clinical significance

An immediate clinical implication of our findings is that therapeutic agents targeting MMPs in the context of cardiovascular and non-cardiovascular conditions could be detrimental for heart function if these compounds were to decrease cardiac MMP-2 levels. This is important since MMPs remain attractive therapeutic targets in the context of cardiovascular conditions (e.g., atherosclerosis, ischemia reperfusion, hypertrophic heart disease in hypertension and post-myocardial infarction) as well as in non-cardiovascular disorders (cancer, rheumatoid arthritis and inflammation)[35-41].

Our findings can also help explain the results of human studies showing that MMP-2 expression is negatively correlated with the susceptibility to hypertensive heart disease. Functional genetic polymorphisms which increase MMP-2 gene expression protect against cardiac remodeling including increases in end-diastolic diameter and LV mass index in hypertensive subjects[42]. A rare panethnic genetic disease of deficiency in human MMP-2 enzyme activity affects some Saudi Arabian, Indian and Turkish families[43]. This condition presents with congenital heart disease including atrial and ventricular septal defects and gum hypertrophy, in addition to a syndrome of multicentric osteolysis with nodulosis and arthropathy. Recent human studies have also revealed that increased plasma MMP-2 levels, as part of a multibiomarkers' panel, can predict the presence of diastolic heart failure[44]. An imbalance in the ratio of MMPs to their tissue inhibitors in favor of decreased extracellular matrix degradation (such as decreased MMP-2 and MMP-13 or increased levels of tissue inhibitors of metalloproteinases (TIMPs)) is associated with LV hypertrophy and diastolic dysfunction in humans[45]. These observations support the notion of cardioprotection by MMP-2 with our findings providing a possible explanation.

In addition to regulating cardiac function, MMP-2 may have yet-unknown roles in lipid homeostasis. Supporting this notion, a single nucleotide polymorphism in the MMP-2 gene was linked to obesity in Korean population[46].

Conclusions

MMP-2 is cardioprotective by acting as a novel negative regulator of the SREBP-2 / HMGCR transcriptional pathway which, in turn, controls ADAM-12-dependent pathological cardiac remodeling. Given the pathophysiological importance and ubiquitous expression of both MMP-2 and the SREBP-2 pathway, we suggest that MMP-2 (and perhaps other metalloproteinases) could be playing important yet unknown roles in lipid homeostasis and cellular signaling in cardiac as well as non-cardiac tissues. Importantly, the data suggest that caution should be exercised before implementing therapeutic strategies targeting MMP-2, since MMP-2 deficiency could predispose to cardiac dysfunction.

Table 5-1 List of peptides identified by LC-MS/MS analysis of in-gel microwave-assisted acid hydrolysis products of PCSK9 prodomain cleavage fragment

Matched peptides shown in **Bold Red**

1 QEDEDGDYEE LVLA**LRSEED GLAEAPEHGT TATFHRCAKD PWRLPGTYVV**
51 **VLKEETHLSQ SERTARRLQA QAARRGYLTK ILHVFHGLLP GFLVKMSGDL**
101 **LELALKLPHV DYIEEDSSVF AQ**

Start - End	Observed	Mr(expt)	Mr(calc)	ppm	Miss	Sequence
15 - 27	708.3392	1414.6638	1414.6576	4	0	A.LRSEEDGLAEAPE.H (Ions score 46)
15 - 28	518.2374	1551.6904	1551.7165	-17	0	A.LRSEEDGLAEAPEH.G (Ions score 30)
15 - 29	805.3794	1608.7442	1608.7379	4	0	A.LRSEEDGLAEAPEHG.T (Ions score 34)
15 - 29	537.2596	1608.7570	1608.7379	12	0	A.LRSEEDGLAEAPEHG.T (Ions score 23)
15 - 32	628.3018	1881.8836	1881.8704	7	0	A.LRSEEDGLAEAPEHGTTA.T (Ions score 30)
15 - 38	664.5649	2654.2305	2654.2143	6	0	A.LRSEEDGLAEAPEHGTTATFHRCA.K (Ions score 15)
15 - 39	696.5886	2782.3253	2782.3093	6	0	A.LRSEEDGLAEAPEHGTTATFHRCAK.D (Ions score 36)
15 - 40	725.3466	2897.3573	2897.3362	7	0	A.LRSEEDGLAEAPEHGTTATFHRCAKD.P (Ions score 31)
15 - 40	725.3492	2897.3677	2897.3362	11	0	A.LRSEEDGLAEAPEHGTTATFHRCAKD.P (Ions score 25)
19 - 29	562.7459	1123.4772	1123.4782	-1	0	E.EDGLAEAPEHG.T (Ions score 15)
20 - 29	498.2356	994.4566	994.4356	21	0	E.DGLAEAPEHG.T (Ions score 20)
21 - 35	513.5804	1537.7194	1537.7161	2	0	D.GLAEAPEHGTTATFH.R (Ions score 13)
21 - 39	514.2590	2053.0069	2052.9799	13	0	D.GLAEAPEHGTTATFHRCAK.D (Ions score 19)
21 - 40	723.6776	2168.0110	2168.0069	2	0	D.GLAEAPEHGTTATFHRCAKD.P (Ions score 25)
41 - 45	334.6987	667.3828	667.3806	3	0	D.PWRLP.G (Ions score 18)
41 - 46	725.4178	724.4105	724.4020	12	0	D.PWRLPG.T (Ions score 14)
41 - 46	363.2128	724.4110	724.4020	12	0	D.PWRLPG.T (Ions score 21)
41 - 47	413.7353	825.4560	825.4497	8	0	D.PWRLPGT.Y (Ions score 15)
41 - 48	495.2643	988.5140	988.5130	1	0	D.PWRLPGTY.V (Ions score 18)
41 - 53	509.9779	1526.9119	1526.8973	10	0	D.PWRLPGTYVVVLK.E (Ions score 25)
43 - 53	622.8951	1243.7756	1243.7652	8	0	W.RLPGTYVVVLK.E (Ions score 24)
43 - 55	751.9345	1501.8544	1501.8504	3	0	W.RLPGTYVVVLKEE.T (Ions score 31)
44 - 55	673.8861	1345.7576	1345.7493	6	0	R.LPGTYVVVLKEE.T (Ions score 58)
45 - 52	847.4999	846.4926	846.4851	9	0	L.PGTYVVVL.K (Ions score 17)
45 - 55	617.3485	1232.6824	1232.6653	14	0	L.PGTYVVVLKEE.T (Ions score 39)
45 - 55	1233.7047	1232.6974	1232.6653	26	0	L.PGTYVVVLKEE.T (Ions score 24)
46 - 55	568.8229	1135.6312	1135.6125	17	0	P.GTYVVVLKEE.T (Ions score 36)
47 - 54	950.5647	949.5574	949.5484	9	0	G.TYVVVLKE.E (Ions score 24)
47 - 55	1079.5810	1078.5737	1078.5910	-16	0	G.TYVVVLKEE.T (Ions score 39)
47 - 55	540.3074	1078.6002	1078.5910	9	0	G.TYVVVLKEE.T (Ions score 14)
47 - 55	1079.6105	1078.6032	1078.5910	11	0	G.TYVVVLKEE.T (Ions score 18)
47 - 55	540.3099	1078.6052	1078.5910	13	0	G.TYVVVLKEE.T (Ions score 53)
47 - 56	1180.6616	1179.6543	1179.6387	13	0	G.TYVVVLKEET.H (Ions score 28)
47 - 57	659.3600	1316.7054	1316.6976	6	0	G.TYVVVLKEETH.L (Ions score 33)
47 - 57	439.9098	1316.7076	1316.6976	8	0	G.TYVVVLKEETH.L (Ions score 43)
47 - 58	715.9019	1429.7892	1429.7817	5	0	G.TYVVVLKEETHL.S (Ions score 56)
47 - 58	715.9032	1429.7918	1429.7817	7	0	G.TYVVVLKEETHL.S (Ions score 33)
47 - 58	477.6062	1429.7968	1429.7817	11	0	G.TYVVVLKEETHL.S (Ions score 38)
47 - 58	477.6089	1429.8049	1429.7817	16	0	G.TYVVVLKEETHL.S (Ions score 14)
47 - 59	759.4209	1516.8272	1516.8137	9	0	G.TYVVVLKEETHLS.Q (Ions score 28)
47 - 60	823.9393	1645.8640	1645.8563	5	0	G.TYVVVLKEETHLSQ.S Deamidated (NQ) (Ions score 34)
47 - 60	823.9457	1645.8768	1645.8563	12	0	G.TYVVVLKEETHLSQ.S Deamidated (NQ) (Ions score 36)
47 - 63	673.6873	2018.0401	2018.0320	4	0	G.TYVVVLKEETHLSQSER.T Deamidated (NQ) (Ions score 58)
59 - 76	512.0271	2044.0793	2044.0521	13	0	L.SQSERTARRLQAQAARRG.Y Deamidated (NQ) (Ions score 21)
77 - 85	567.3436	1132.6726	1132.6645	7	0	G.YLTKILHVF.H (Ions score 40)
77 - 85	378.5659	1132.6759	1132.6645	10	0	G.YLTKILHVF.H (Ions score 15)
77 - 86	635.8766	1269.7386	1269.7234	12	0	G.YLTKILHVFH.G (Ions score 68)
77 - 86	635.8767	1269.7388	1269.7234	12	0	G.YLTKILHVFH.G (Ions score 75)
77 - 87	664.3871	1326.7596	1326.7448	11	0	G.YLTKILHVFHG.L (Ions score 78)
77 - 87	664.3874	1326.7602	1326.7448	12	0	G.YLTKILHVFHG.L (Ions score 73)
77 - 87	664.3877	1326.7608	1326.7448	12	0	G.YLTKILHVFHG.L (Ions score 64)
79 - 86	332.1994	993.5764	993.5760	0	0	L.TKILHVFH.G (Ions score 17)
79 - 91	716.4277	1430.8408	1430.8398	1	0	L.TKILHVFHGLLPG.F (Ions score 22)
79 - 91	716.4278	1430.8410	1430.8398	1	0	L.TKILHVFHGLLPG.F (Ions score 29)

```
79 - 91     716.4278  1430.8410  1430.8398    1   0  L.TKILHVFHGLLPG.F  (Ions score 29)
81 - 91     601.8560  1201.6974  1201.6972    0   0  K.ILHVFHGLLPG.F  (Ions score 39)
86 - 95     540.8341  1079.6536  1079.6492    4   0  F.HGLLPGFLVK.M  (Ions score 43)
86 - 96     606.3616  1210.7086  1210.6896   16   0  F.HGLLPGFLVKM.S  (Ions score 27)
86 - 96     614.3541  1226.6936  1226.6846    7   0  F.HGLLPGFLVKM.S  Oxidation (M) (Ions score 50)
86 - 97     657.8685  1313.7224  1313.7166    4   0  F.HGLLPGFLVKMS.G  Oxidation (M) (Ions score 17)
86 - 98     686.3815  1370.7484  1370.7381    8   0  F.HGLLPGFLVKMSG.D  Oxidation (M) (Ions score 28)
87 - 96     545.8290  1089.6434  1089.6256   16   0  H.GLLPGFLVKM.S  Oxidation (M) (Ions score 35)
87 - 98     617.8545  1233.6944  1233.6791   12   0  H.GLLPGFLVKMSG.D  Oxidation (M) (Ions score 49)
87 - 98     617.8551  1233.6956  1233.6791   13   0  H.GLLPGFLVKMSG.D  Oxidation (M) (Ions score 48)
88 - 97     552.8310  1103.6474  1103.6413    6   0  G.LLPGFLVKMS.G  (Ions score 23)
88 - 98     589.3408  1176.6670  1176.6577    8   0  G.LLPGFLVKMSG.D  Oxidation (M) (Ions score 28)
89 - 95     773.5010   772.4937   772.4847   12   0  L.LPGFLVK.M  (Ions score 15)
89 - 96     452.7703   903.5260   903.5252    1   0  L.LPGFLVKM.S  (Ions score 27)
89 - 96     460.7707   919.5268   919.5201    7   0  L.LPGFLVKM.S  Oxidation (M) (Ions score 27)
89 - 97     496.2884   990.5622   990.5572    5   0  L.LPGFLVKMS.G  (Ions score 22)
89 - 98    1048.5946  1047.5873  1047.5787    8   0  L.LPGFLVKMSG.D  (Ions score 23)
89 - 98     524.8014  1047.5882  1047.5787    9   0  L.LPGFLVKMSG.D  (Ions score 36)
89 - 98     532.8002  1063.5858  1063.5736   12   0  L.LPGFLVKMSG.D  Oxidation (M) (Ions score 32)
90 - 95     660.4127   659.4054   659.4007    7   0  L.PGFLVK.M  (Ions score 20)
90 - 95     330.7106   659.4066   659.4007    9   0  L.PGFLVK.M  (Ions score 15)
90 - 95     660.4166   659.4093   659.4007   13   0  L.PGFLVK.M  (Ions score 22)
90 - 96     791.4514   790.4441   790.4411    4   0  L.PGFLVKM.S  (Ions score 15)
90 - 96     791.4560   790.4487   790.4411   10   0  L.PGFLVKM.S  (Ions score 17)
90 - 96     404.2278   806.4410   806.4361    6   0  L.PGFLVKM.S  Oxidation (M) (Ions score 19)
90 - 96     807.4555   806.4482   806.4361   15   0  L.PGFLVKM.S  Oxidation (M) (Ions score 16)
90 - 98     468.2598   934.5050   934.4946   11   0  L.PGFLVKMSG.D  (Ions score 17)
97 - 106   1058.6117  1057.6044  1057.6019    2   0  M.SGDLLELALK.L  (Ions score 40)
97 - 106    529.8137  1057.6128  1057.6019   10   0  M.SGDLLELALK.L  (Ions score 66)
98 - 106    486.2919   970.5692   970.5699   -1   0  S.GDLLELALK.L  (Ions score 18)
99 - 105    786.4677   785.4604   785.4534    9   0  G.DLLELAL.K  (Ions score 22)
99 - 106    457.7831   913.5516   913.5484    4   0  G.DLLELALK.L  (Ions score 32)

99 - 106    914.5659   913.5586   913.5484   11   0  G.DLLELALK.L  (Ions score 32)
100 - 106   400.2675   798.5204   798.5215   -1   0  D.LLELALK.L  (Ions score 32)
100 - 106   799.5364   798.5291   798.5215   10   0  D.LLELALK.L  (Ions score 27)
100 - 106   799.5389   798.5316   798.5215   13   0  D.LLELALK.L  (Ions score 16)
101 - 106   686.4523   685.4450   685.4374   11   0  L.LELALK.L  (Ions score 21)
101 - 111   624.3684  1246.7222  1246.7285   -5   0  L.LELALKLPHVD.Y  (Ions score 26)
102 - 116   892.4559  1782.8972  1782.9039   -4   0  L.ELALKLPHVDYIEED.S  (Ions score 16)
107 - 116   615.2934  1228.5722  1228.5612    9   0  K.LPHVDYIEED.S  (Ions score 36)
107 - 116  1229.5891  1228.5818  1228.5612   17   0  K.LPHVDYIEED.S  (Ions score 34)
107 - 117   658.8066  1315.5986  1315.5932    4   0  K.LPHVDYIEEDS.S  (Ions score 21)
108 - 116  1116.4860  1115.4787  1115.4771    1   0  L.PHVDYIEED.S  (Ions score 29)
108 - 116   558.7541  1115.4936  1115.4771   15   0  L.PHVDYIEED.S  (Ions score 18)
108 - 122   868.8883  1735.7620  1735.7577    3   0  L.PHVDYIEEDSSVFAQ.-  Deamidated (NQ) (Ions score 70)
```

Figure 5-1 MMP-2 deficiency exacerbates Ang II-induced cardiac hypertrophy in a time- and dose-dependent manner.

Differences in time course (**A**) and dose-dependence of cardiac hypertrophy induced by Ang II in WT (**B**) *vs*. MMP-2 KO mice (**C**), as determined by heart weight (HW) to body weight (BW) ratios.

HMGCR inhibition by lovastatin dose-dependently prevented the development of cardiac hypertrophy.

Lovastatin gavage was started 3 days before the Ang II minipumps were implanted. Dosage was based on a previous study[47].

Time axis refers to time on Ang II.

*: *p*<0.05 *vs*. WT day 0 or no treatment.

+: *p*<0.05 *vs*. MMP-2 KO day 0 or no treatment.

‡: *p*<0.05 *vs*. WT for the same day or treatment.

†: *p*<0.05 Ang II + Lovastatin *vs*. Ang II (2.0 mg/kg/d).

n=3-27 mice / group.

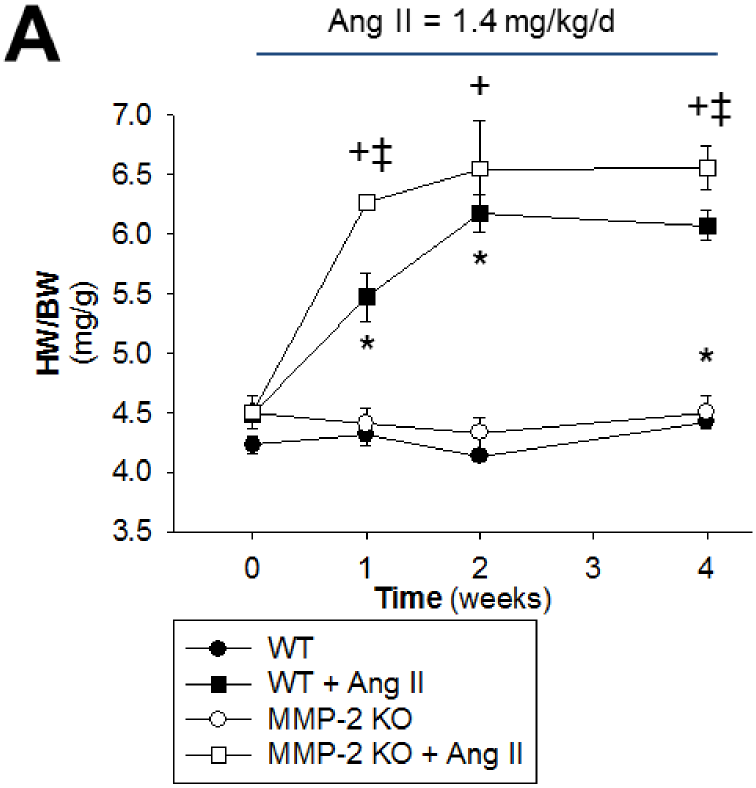

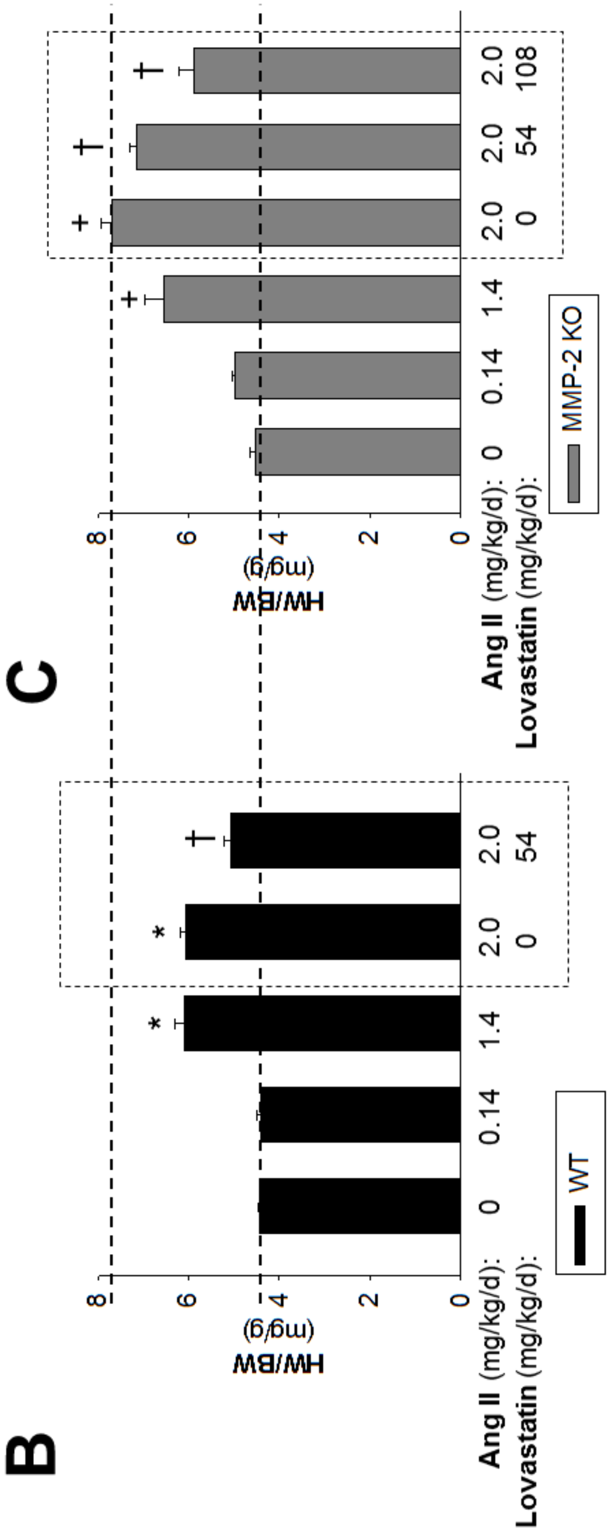
B
HW/BW (mg/g)
0
2
4
6
8
Ang II (mg/kg/d): 0 0.14 1.4 2.0 2.0
Lovastatin (mg/kg/d): 0 54
*
*
†
WT
C
HW/BW (mg/g)
0
2
4
6
8
Ang II (mg/kg/d): 0 0.14 1.4 2.0 2.0 2.0
Lovastatin (mg/kg/d): 0 54 108
+
+
†
†
MMP-2 KO

Figure 5-2 MMP-2 KO exacerbates Ang II-induced cardiac hypertrophy: heart weight to tibia length ratio.

Time course of Ang II-induced cardiac hypertrophy in MMP-2 KO *vs*. WT mice as determined by the heart weight to tibia length ratio (HW/TL).

*: *p*<0.05 *vs*. WT time 0.

+: *p* <0.05 *vs*. MMP-2 KO time 0.

‡: *p* <0.05 *vs*. WT for the same time point.

n=3-19 mice / group.

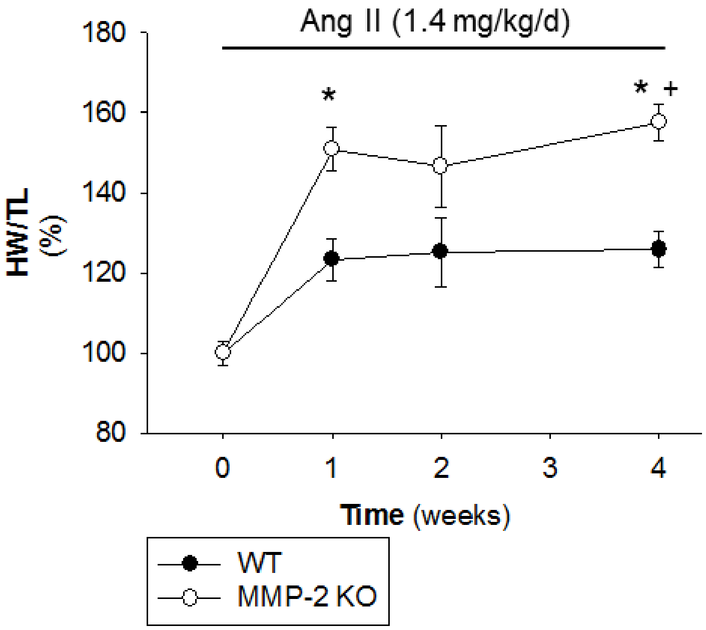

Figure 5-3 Time and dose-dependence of Ang II-induced LV MMP-2 expression in the mice.

Time- (**A**) and dose-dependent (**B**) elevation of MMP-2 mRNA levels induced by Ang II infusion (4 weeks at 1.4 mg/kg/d or 2 weeks at 0-2.0 mg/kg/d, respectively) in WT mice. HMGCR inhibition by lovastatin (54 mg/kg/d) prevented the increase in MMP-2 mRNA levels (**B**).

Lovastatin gavage was started 3 days before the Ang II minipumps were implanted.

Time axis refers to time on Ang II.

*: $p<0.05$ *vs*. WT day 0 or no treatment.

†: $p<0.05$ Ang II + Lovastatin vs. Ang II (2.0 mg/kg/d).

n=3-30 mice / group.

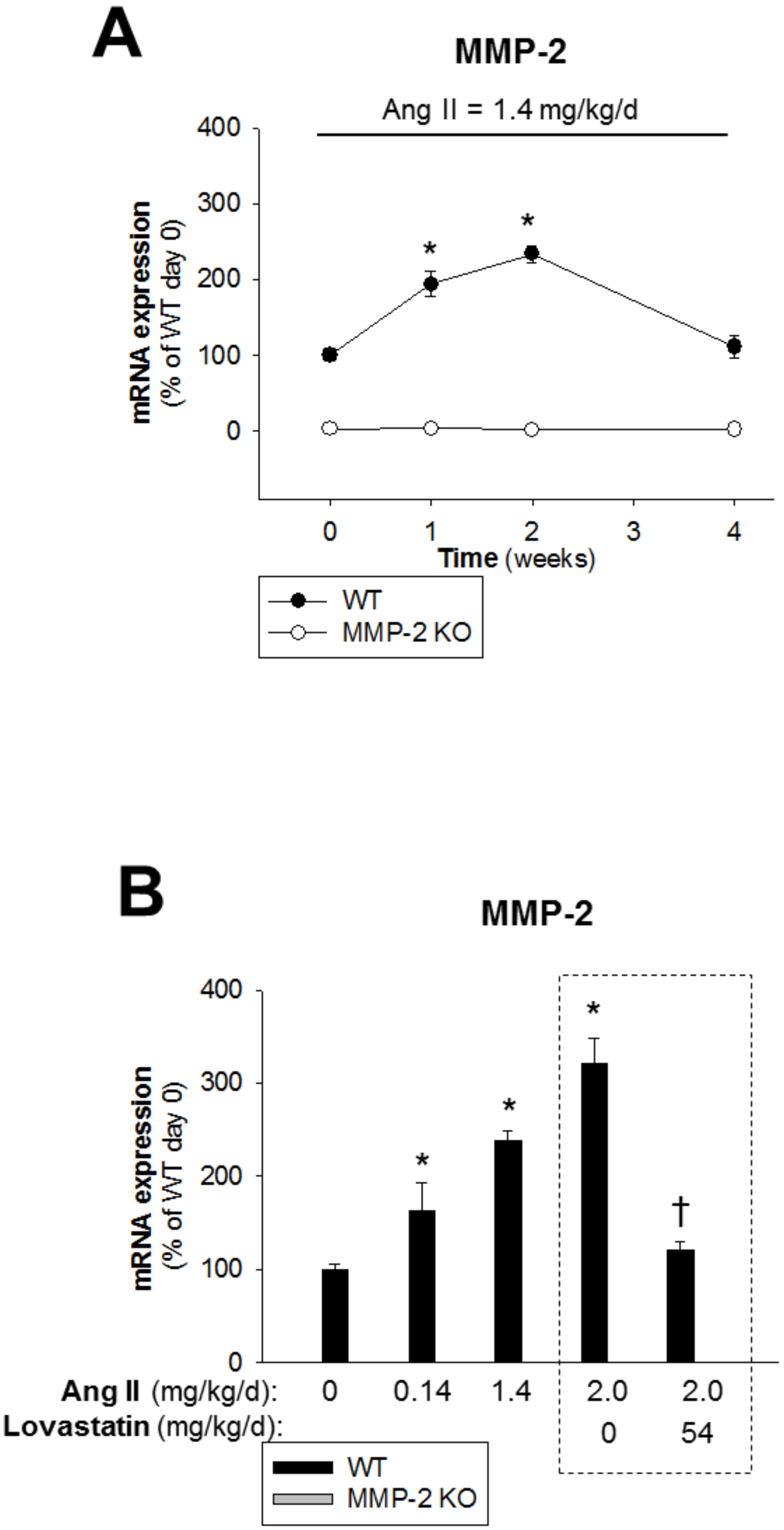
A
MMP-2
Ang II = 1.4 mg/kg/d
mRNA expression
(% of WT day 0)
400
300
200
100
0
*
*
0
1
2
3
4
Time (weeks)
WT
MMP-2 KO
B
MMP-2
mRNA expression
(% of WT day 0)
400
300
200
100
0
*
*
*
†
Ang II (mg/kg/d): 0 0.14 1.4 2.0 2.0
Lovastatin (mg/kg/d): 0 54
WT
MMP-2 KO

Figure 5-4 Analysis of Ang II-induced LV hypertrophy and fibrosis in MMP-2 KO *vs*. WT mice: Time-dependence.

A: Representative photomicrographs of Masson's trichrome-stained sections of hearts from experimental animals indicating Ang II (1.4 mg/kg/d, for 4 weeks)-induced interstitial and perivascular collagen deposition (red: muscle fibers; blue: collagen).

B-E: Time course of mRNA levels of hypertrophy markers (α-skeletal actin (**B**) and brain natriuretic peptide (BNP) (**C**)) and fibrosis markers (collagen III (**D**) and fibronectin 1 (**E**)) in WT *vs*. MMP-2 KO mice treated with Ang II (1.4 mg/kg/d).

*: $p<0.05$ *vs*. WT day 0.

+: $p<0.05$ *vs*. MMP-2 KO day 0.

‡: $p<0.05$ *vs*. WT for the same day.

n= 3-10 mice / group.

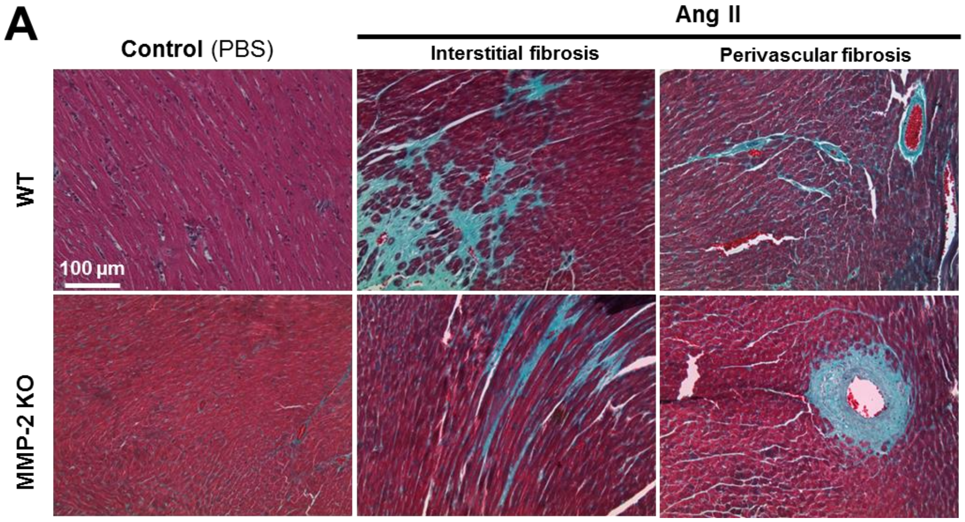
A
Ang II
Control (PBS)
Interstitial fibrosis
Perivascular fibrosis
WT
MMP-2 KO
100 µm

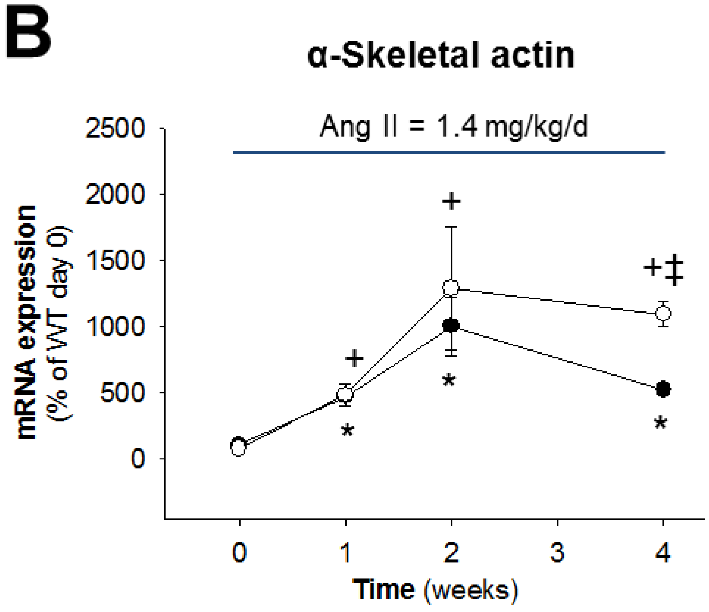
B
α-Skeletal actin
Ang II = 1.4 mg/kg/d
mRNA expression
(% of WT day 0)
2500
2000
1500
1000
500
0
+
+
+‡
*
*
*
0
1
2
3
4
Time (weeks)

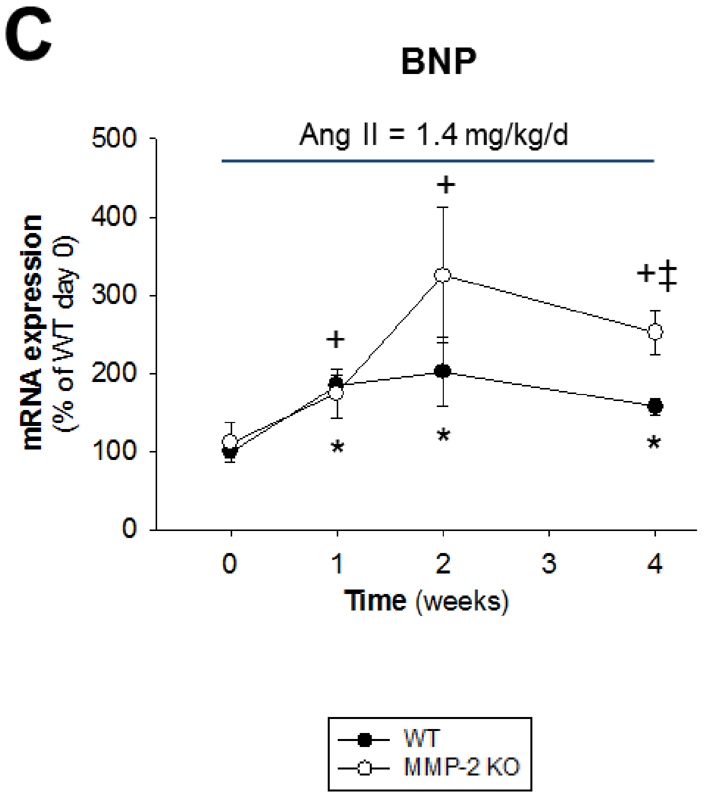
C
BNP
Ang II = 1.4 mg/kg/d
mRNA expression
(% of WT day 0)
500
400
300
200
100
0
+
+
+‡
*
*
*
0
1
2
3
4
Time (weeks)
WT
MMP-2 KO

D

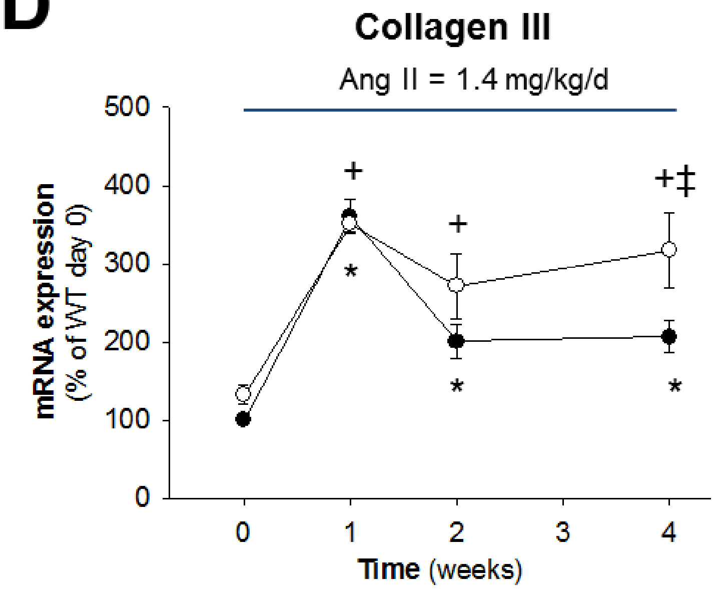
Collagen III
Ang II = 1.4 mg/kg/d
mRNA expression
(% of WT day 0)
500
400
300
200
100
0
0
1
2
3
4
Time (weeks)
+
*
+
*
+‡
*

E

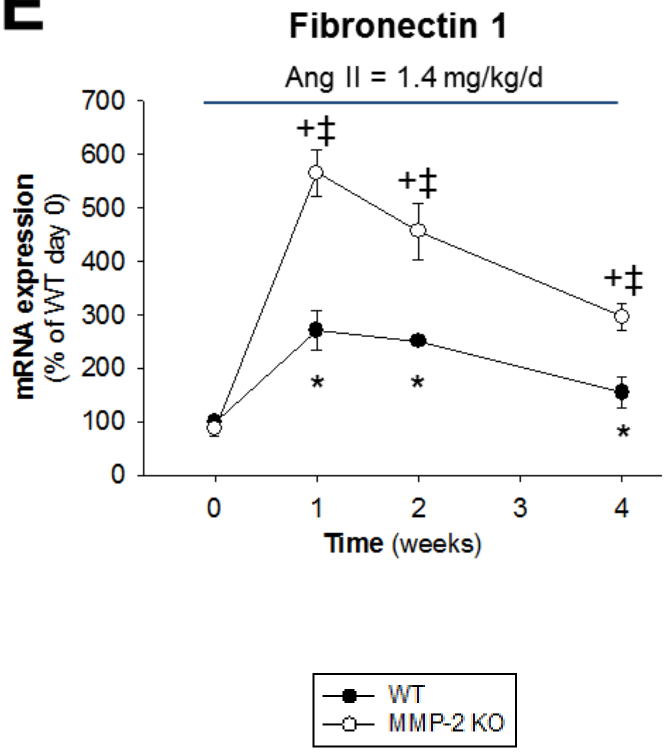
Fibronectin 1
Ang II = 1.4 mg/kg/d
mRNA expression
(% of WT day 0)
700
600
500
400
300
200
100
0
0
1
2
3
4
Time (weeks)
+‡
*
+‡
*
+‡
*
● WT
○ MMP-2 KO

Figure 5-5 Analysis of Ang II-induced LV hypertrophy and fibrosis in MMP-2 KO *vs*. WT mice: Dose-dependence.

A-D: Ang II dose-dependently increased mRNA levels of hypertrophy marker (α-skeletal actin (**A**)) and fibrosis markers (collagen I (**B**), collagen III (**C**) and fibronectin 1 (**D**)) in WT mice *vs*. MMP-2 KO mice treated with Ang II (0-2 mg/kg/d, for 2 weeks). HMGCR inhibition by lovastatin (54 mg/kg/d) prevented the Ang II-induced increases in marker mRNA levels.

*: $p<0.05$ *vs*. WT no treatment.

+: $p<0.05$ *vs*. MMP-2 KO no treatment.

‡: $p<0.05$ *vs*. WT for the same treatment.

†: $p<0.05$ Ang II + Lovastatin *vs*. Ang II (2.0 mg/kg/d).

n= 3-10 mice / group.

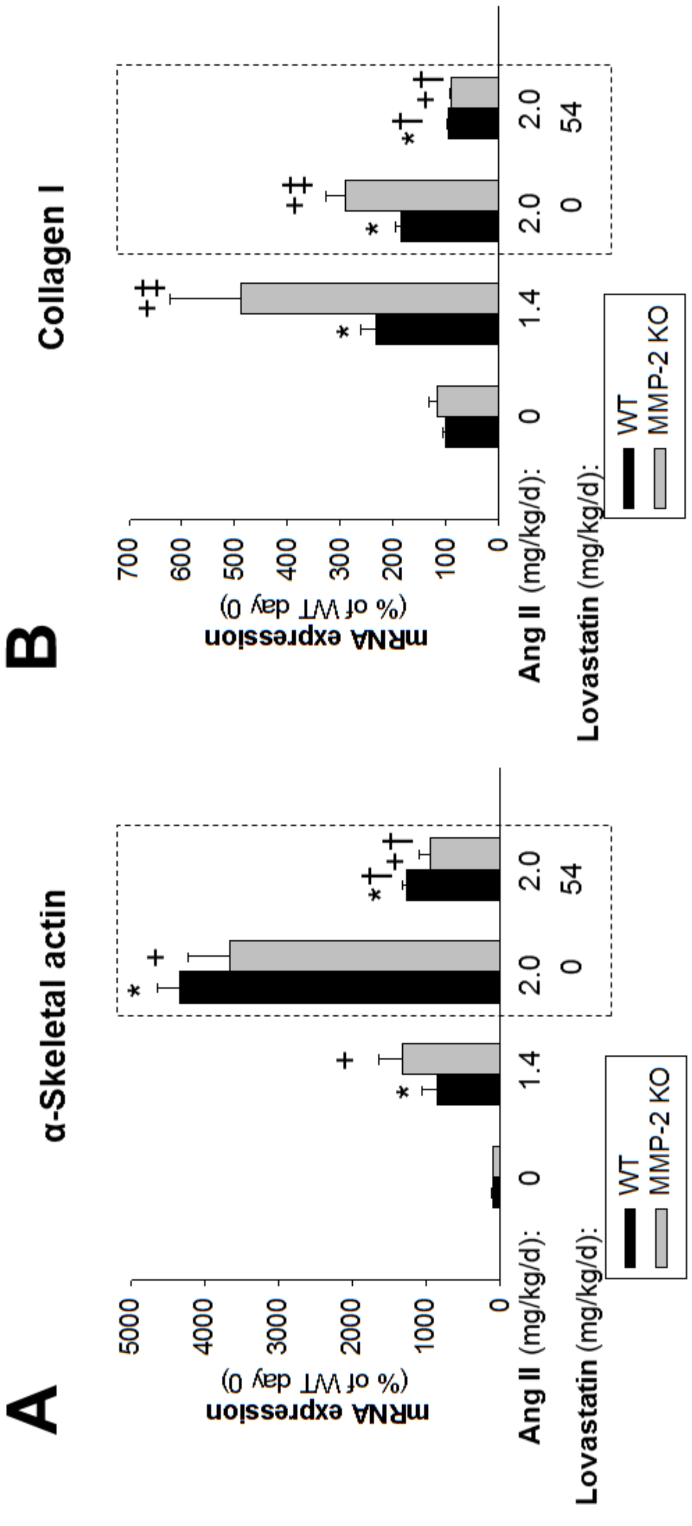
A
α-Skeletal actin
mRNA expression
(% of WT day 0)
0
1000
2000
3000
4000
5000
Ang II (mg/kg/d): 0 1.4 2.0 2.0
Lovastatin (mg/kg/d): 0 54
*
+
*
+
*†
+†
WT
MMP-2 KO
B
Collagen I
mRNA expression
(% of WT day 0)
0
100
200
300
400
500
600
700
Ang II (mg/kg/d): 0 1.4 2.0 2.0
Lovastatin (mg/kg/d): 0 54
*
+‡
*
+‡
*†
+†
WT
MMP-2 KO

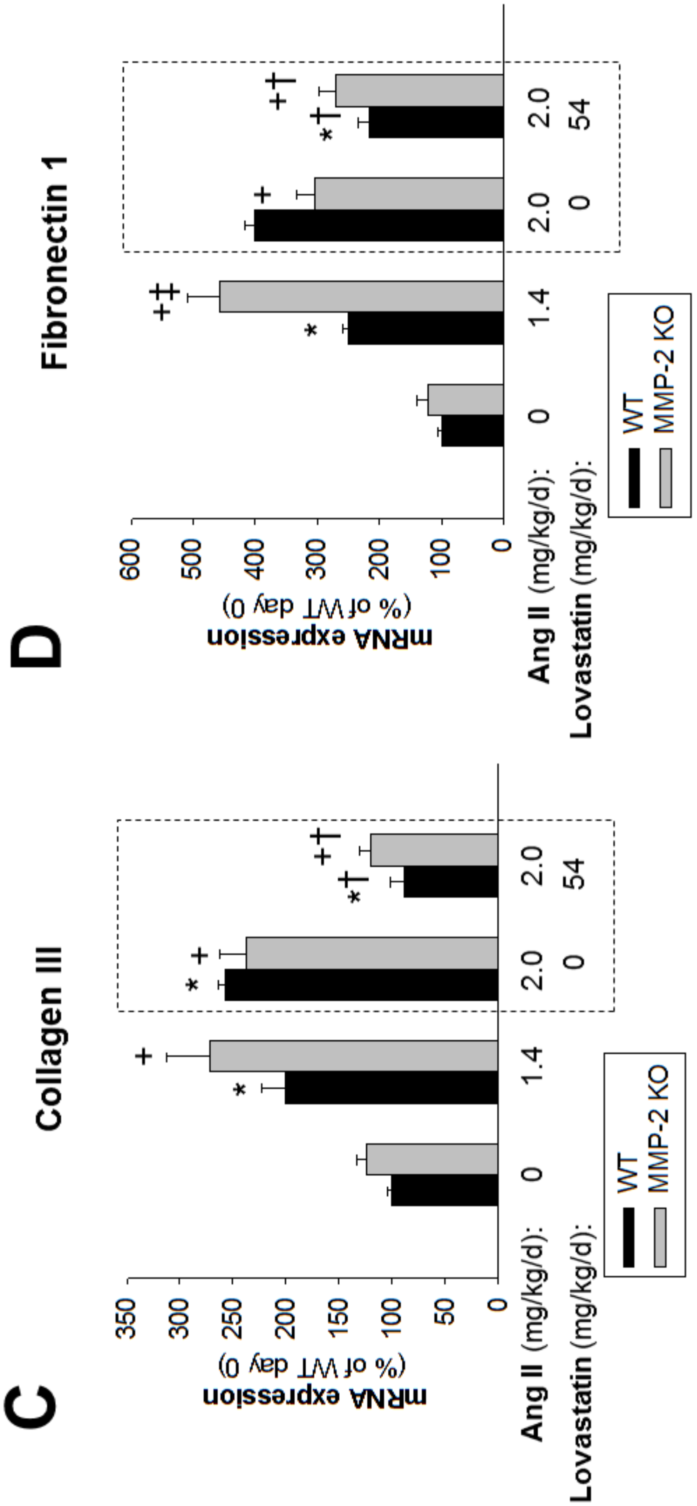
C
Collagen III
mRNA expression (% of WT day 0)
350
300
250
200
150
100
50
0
Ang II (mg/kg/d): 0 1.4 2.0 2.0
Lovastatin (mg/kg/d): 0 54
*
+
* +
*†
+†
WT
MMP-2 KO
D
Fibronectin 1
mRNA expression (% of WT day 0)
600
500
400
300
200
100
0
Ang II (mg/kg/d): 0 1.4 2.0 2.0
Lovastatin (mg/kg/d): 0 54
*
+‡
+
*†
+†
WT
MMP-2 KO

Figure 5-6 Echocardiographic analysis indicates a propensity to diastolic dysfunction in MMP-2 KO *vs*. WT mice.

Ang II administration (1.4 mg/kg/d for 4 weeks) induces a more pronounced decrease in the ratio between peak mitral valve tissue velocity during early (E' wave) and late (A' wave) LV filling.

*: $p < 0.05$ *vs*. WT no treatment.

+: $p < 0.05$ *vs*. MMP-2 KO no treatment.

n=3-19 mice / group.

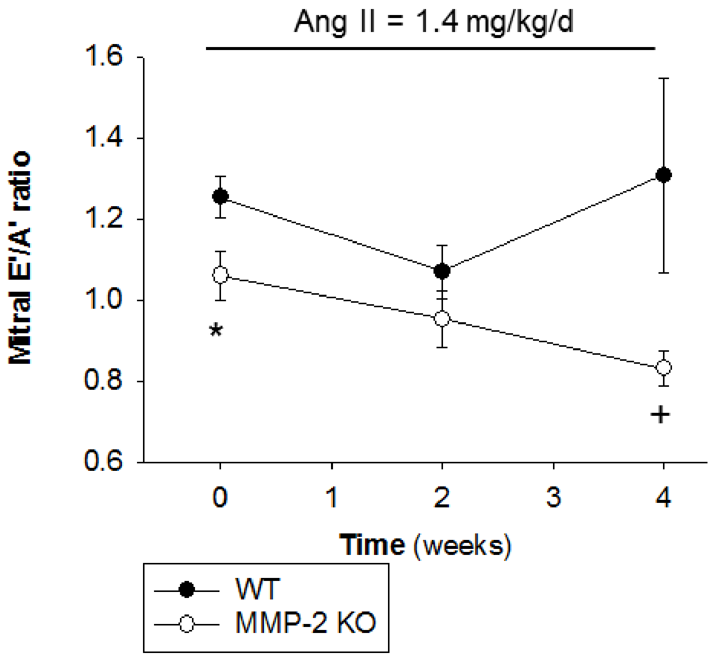

Figure 5-7 Negative regulation of the SREBP-2 / HMGCR pathway by MMP-2.

A, B: qRT-PCR analysis of baseline LV mRNA levels of SREBP-2 (**A**) and HMGCR (**B**) indicates that lack of MMP-2, but not MMP-7, upregulates the SREBP-2 / HMGCR pathway.

C: Western blot confirms increased protein levels of LV HMGCR in MMP-2 KO *vs*. WT mice with Ang II infusion (1.4 mg/kg/d, for 2 weeks).

D: Ang II (1.4 mg/kg/d, for 2 weeks) increased the levels of LV cholesterol, indicating elevated HMGCR activity, in MMP-2 KO *vs*. WT mice.

*: $p<0.05$ *vs*. WT no treatment.

+: $p<0.05$ *vs*. MMP-2 KO no treatment.

‡: $p<0.05$ *vs*. WT with Ang II.

n= 3-10 mice / group.

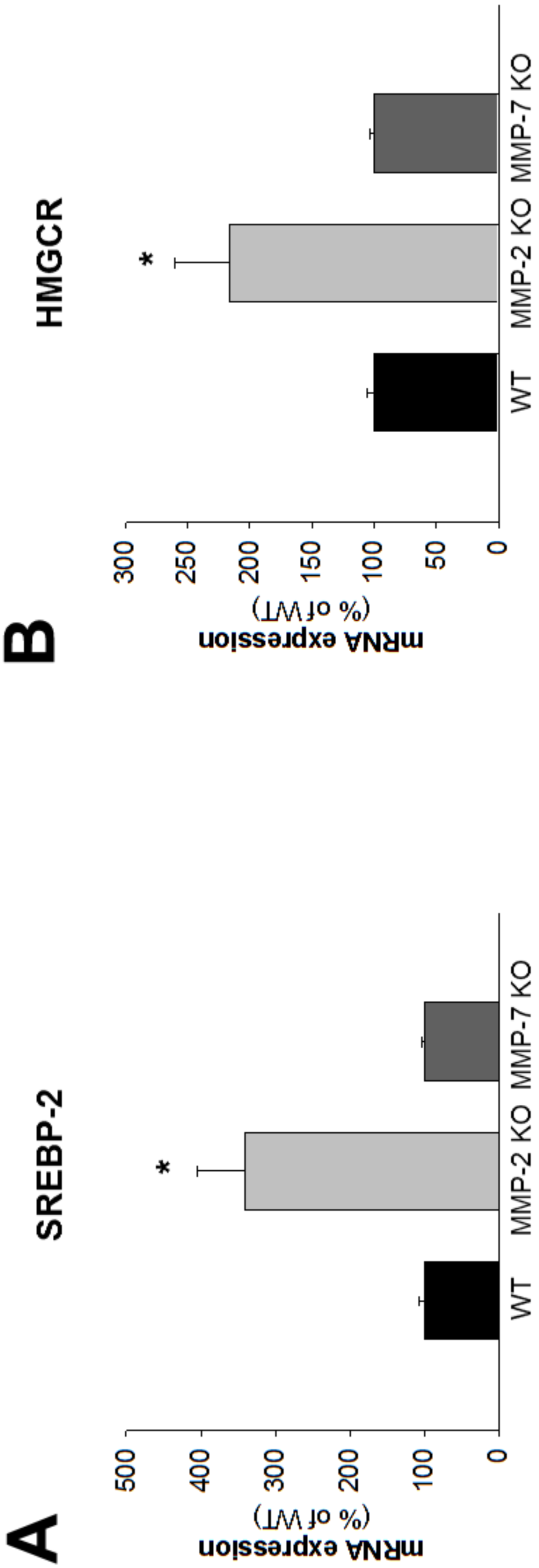
A
SREBP-2
mRNA expression (% of WT)
0
100
200
300
400
500
WT
MMP-2 KO
MMP-7 KO
*
B
HMGCR
mRNA expression (% of WT)
0
50
100
150
200
250
300
WT
MMP-2 KO
MMP-7 KO
*

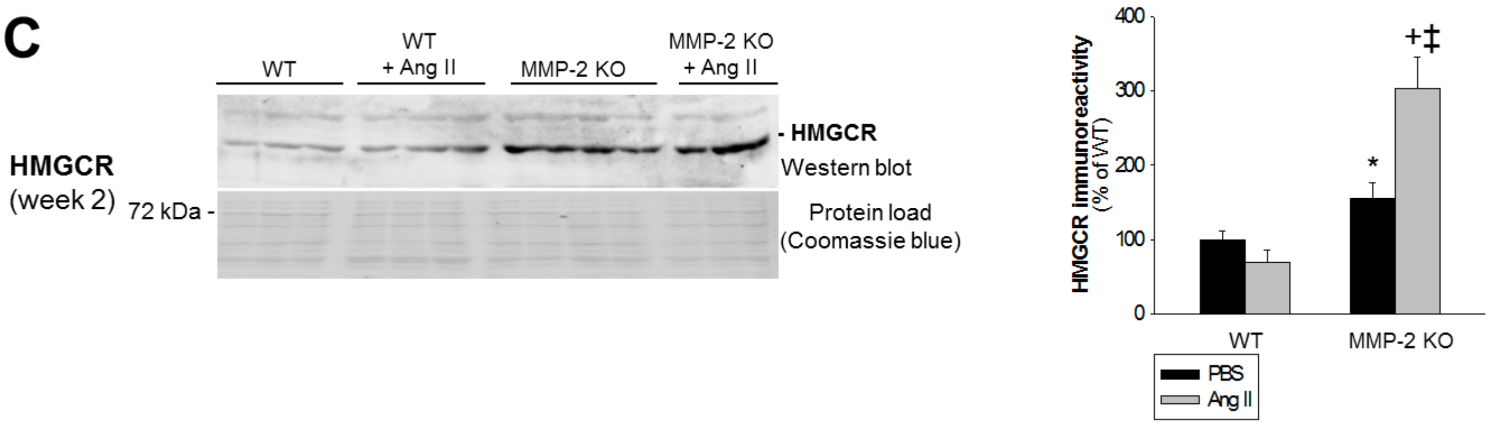
C
WT
WT
+ Ang II
MMP-2 KO
MMP-2 KO
+ Ang II
HMGCR
(week 2)
72 kDa -
- HMGCR
Western blot
Protein load
(Coomassie blue)
HMGCR immunoreactivity
(% of WT)
400
300
200
100
0
*
+‡
WT
MMP-2 KO
PBS
Ang II

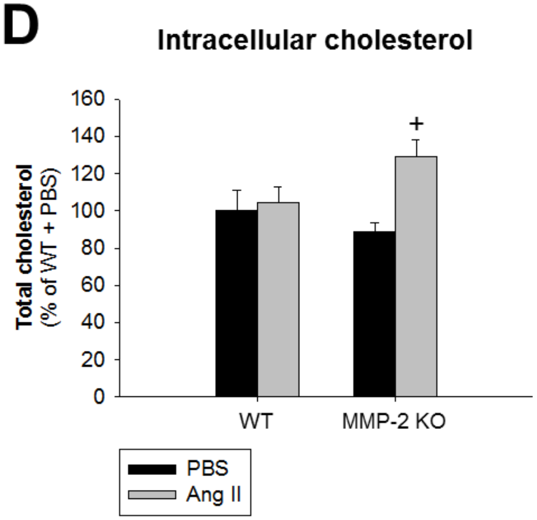
D
Intracellular cholesterol
Total cholesterol
(% of WT + PBS)
160
140
120
100
80
60
40
20
0
+
WT
MMP-2 KO
PBS
Ang II

Figure 5-8 Ang II induces changes in the cardiac SREBP-2 pathway.

A-C: Time course of mRNA levels of LV SREBP-2 (**A**), HMGCR (**B**) and LDLR (**C**) in WT *vs*. MMP-2 KO mice with Ang II infusion (1.4 mg/kg/d).

D: Time course of cardiac cholesterol levels in WT *vs*. MMP-2 KO mice with Ang II infusion (1.4 mg/kg/d).

*: $p<0.05$ *vs*. WT day 0.

+: $p<0.05$ *vs*. MMP-2 KO day 0.

‡: $p<0.05$ *vs*. WT for the same day.

n=3-10 mice / group.

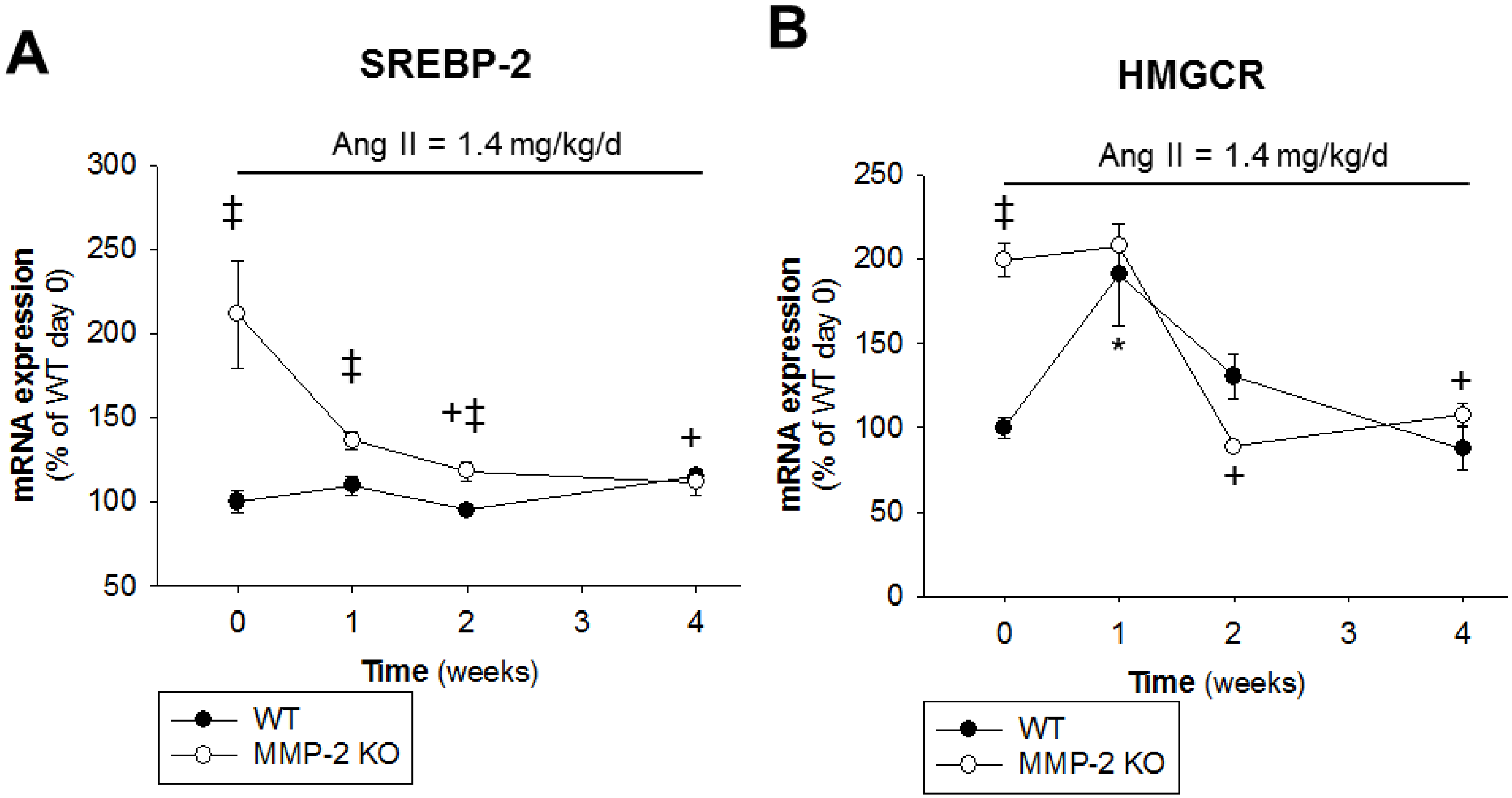
A
SREBP-2
Ang II = 1.4 mg/kg/d
mRNA expression
(% of WT day 0)
300
250
200
150
100
50
‡
‡
+‡
+
0
1
2
3
4
Time (weeks)
WT
MMP-2 KO
B
HMGCR
Ang II = 1.4 mg/kg/d
mRNA expression
(% of WT day 0)
250
200
150
100
50
0
‡
*
+
+
0
1
2
3
4
Time (weeks)
WT
MMP-2 KO

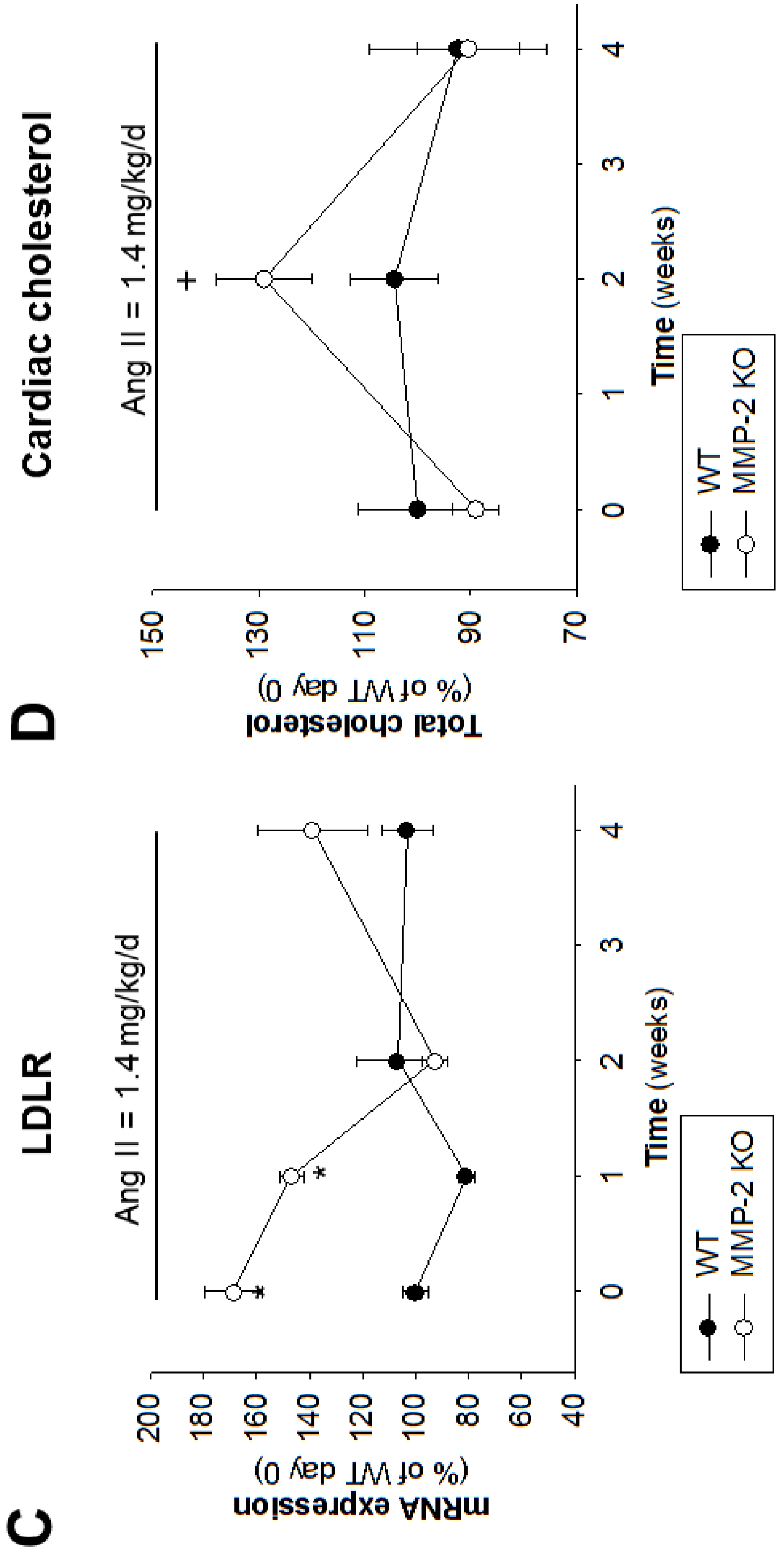
C
LDLR
Ang II = 1.4 mg/kg/d
mRNA expression
(% of WT day 0)
200
180
160
140
120
100
80
60
40
0
1
2
3
4
Time (weeks)
*
*
WT
MMP-2 KO
D
Cardiac cholesterol
Ang II = 1.4 mg/kg/d
Total cholesterol
(% of WT day 0)
150
130
110
90
70
0
1
2
3
4
Time (weeks)
+
WT
MMP-2 KO

Figure 5-9 Negative regulation of the SREBP-2 / HMGCR pathway by MMP-2 in mouse cardiomyocytes.

qRT-PCR analysis of mRNA levels of MMP-2, SREBP-2 , HMGCR and LDLR from primary LV cardiomyocytes indicates elevated expression of SREBP-2, HMGCR and LDLR in the absence of MMP-2.

*: $p < 0.05$ *vs*. WT.

n=3.

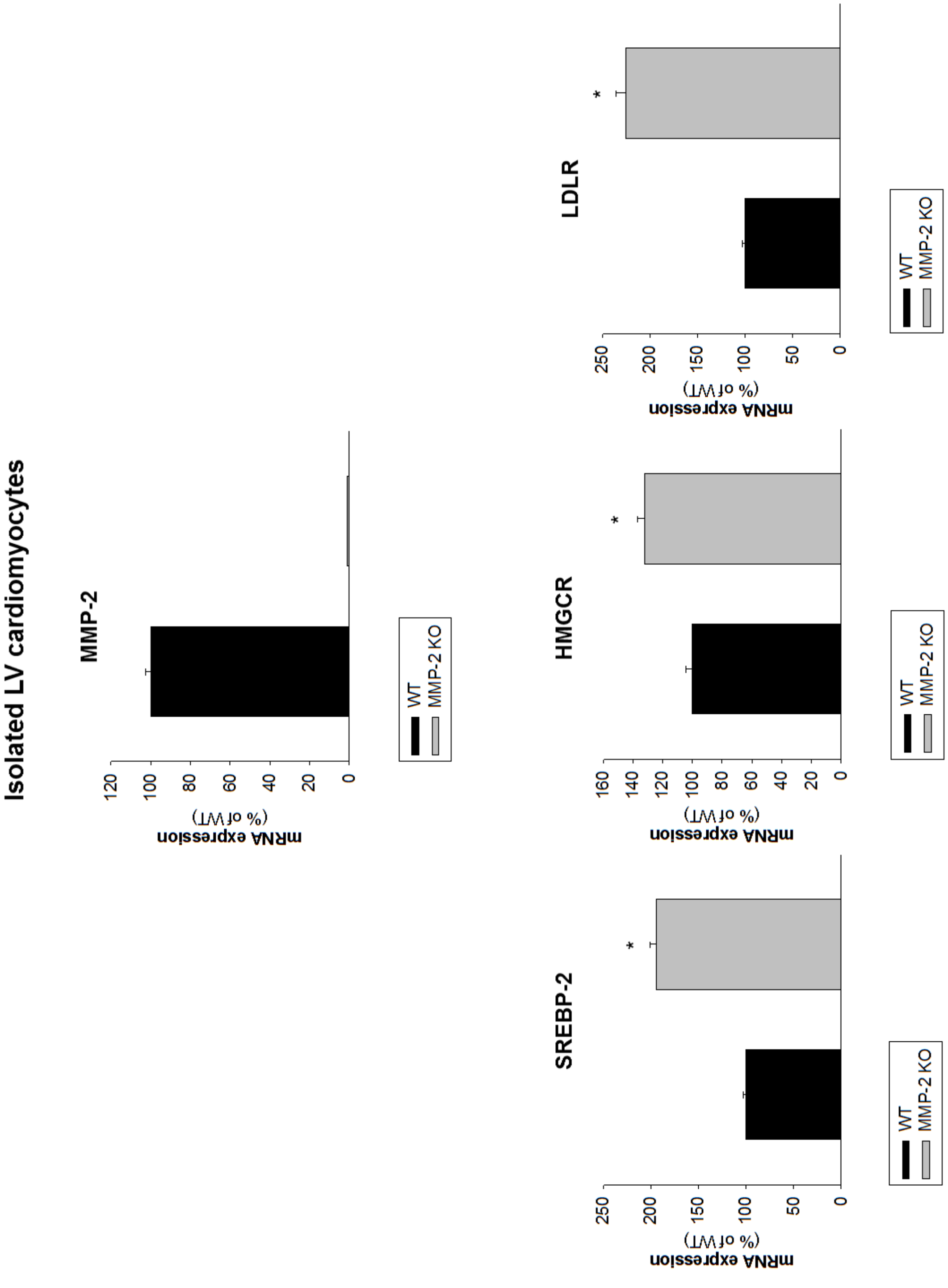
Isolated LV cardiomyocytes
MMP-2
mRNA expression (% of WT)
120
100
80
60
40
20
0
WT
MMP-2 KO
SREBP-2
250
200
150
100
50
0
*
HMGCR
160
140
120
100
80
60
40
20
0
*
LDLR
250
200
150
100
50
0
*

Figure 5-10 MMP-2 negatively regulates HMGCR and lack of MMP-2 predisposes to cardiac hypertrophy: Analysis of *in vivo* loss-of-function *vs*. gain-of-function models for a subpressor regimen of Ang II.

A: qRT-PCR analysis of LV HMGCR mRNA levels for WT *vs*. MMP-2 KO mice.

*: *p*<0.05 *vs*. WT.

Insets: Representative traces of cardiac MMP-2 as determined by gelatin zymography.

B: qRT-PCR analysis of LV HMGCR mRNA levels for WT mice transduced with MMP-2-overexpressing (AdMMP-2) *vs*. control (AdGFP) adenovirus.

*: *p*<0.05 *vs*. AdGFP.

Insets: Representative traces of cardiac MMP-2 as determined by gelatin zymography.

C: HW/BW for WT *vs*. MMP-2 KO mice and AdMMP-2 *vs*. AdGFP mice with or without infusion of a subpressor regimen of Ang II (0.14 mg/kg/d) for for 2 weeks.

*: *p*<0.05 *vs*. MMP-KO with no Ang II.

n= 3-4 mice / group.

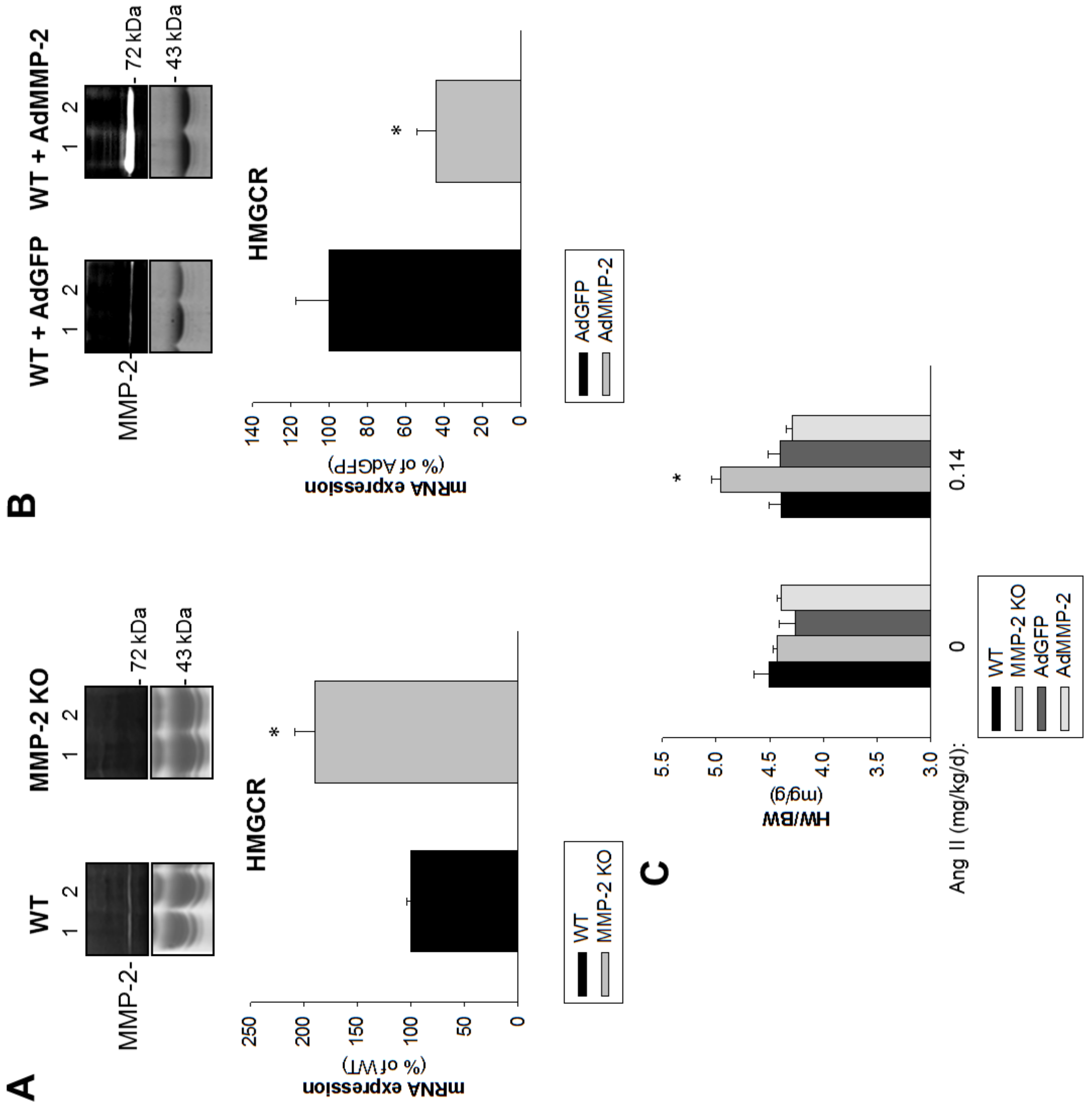
A
MMP-2-
WT
MMP-2 KO
1
2
1
2
72 kDa
43 kDa
HMGCR
mRNA expression
(% of WT)
250
200
150
100
50
0
*
WT
MMP-2 KO
B
WT + AdGFP
WT + AdMMP-2
MMP-2-
1
2
1
2
72 kDa
43 kDa
HMGCR
mRNA expression
(% of AdGFP)
140
120
100
80
60
40
20
0
*
AdGFP
AdMMP-2
C
HW/BW
(mg/g)
5.5
5.0
4.5
4.0
3.5
3.0
Ang II (mg/kg/d):
0
0.14
*
WT
MMP-2 KO
AdGFP
AdMMP-2

Figure 5-11 Negative regulation of the SREBP-2 / HMGCR pathway by cholesterol in MMP-2 KO and WT mice.

Mice were fed chow supplemented with 0.15% cholesterol for 2.5 days. qRT-PCR analysis of mRNA levels of SREBP-2, HMGCR, Insig 1, Insig 2 and SCAP indicates that inhibition of the SREBP-2 / HMGCR pathway by cholesterol is intact in MMP-2 KO mice.

*: *p*<0.05 *vs*. WT no treatment.

+: *p*<0.05 *vs*. MMP-2 KO no treatment.

‡: *p*<0.05 *vs*. WT with Ang II.

n= 3-10 mice / group.

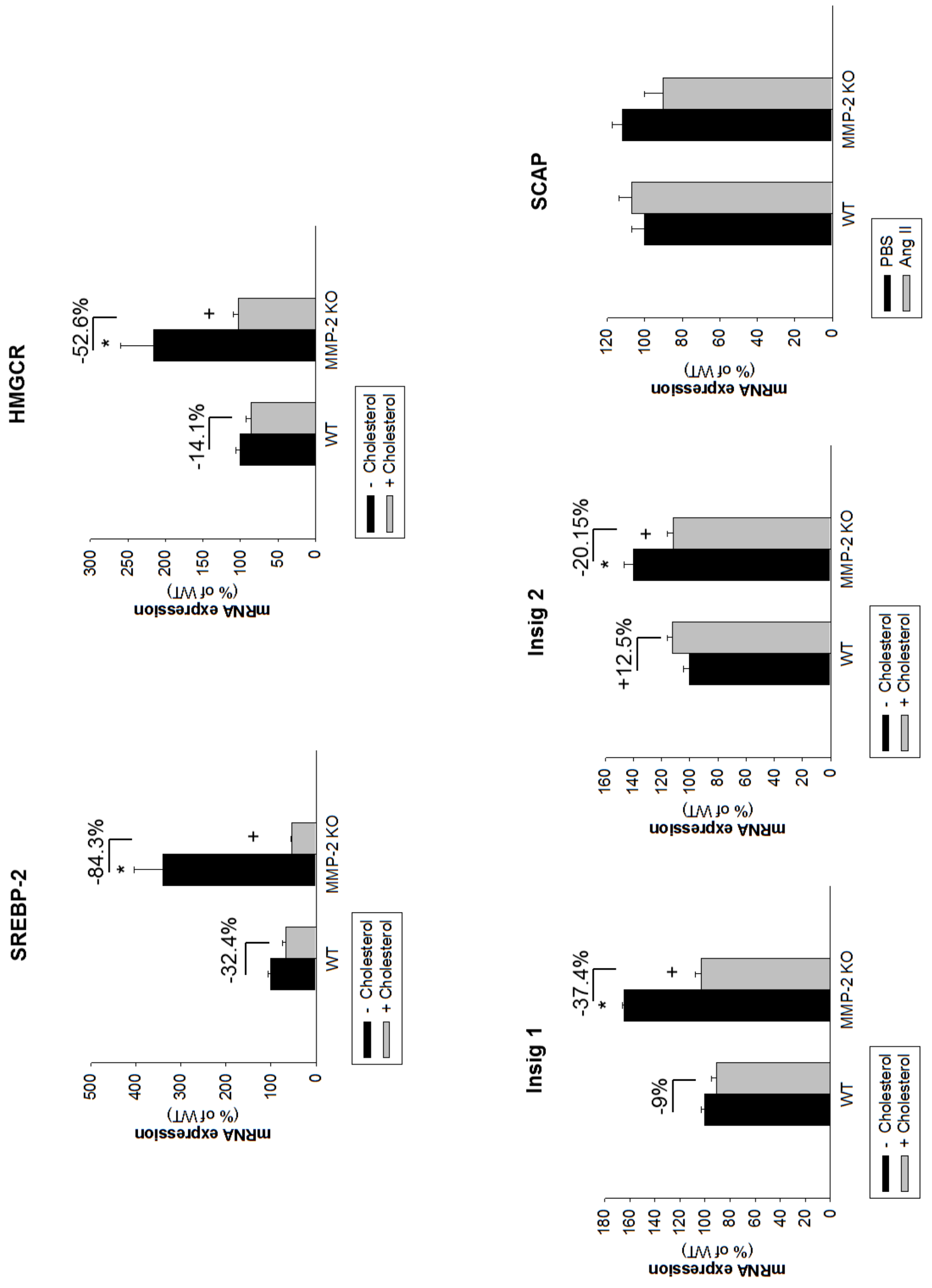
SREBP-2
mRNA expression (% of WT)
500
400
300
200
100
0
-32.4%
-84.3%
*
+
WT
MMP-2 KO
- Cholesterol
+ Cholesterol
HMGCR
mRNA expression (% of WT)
300
250
200
150
100
50
0
-14.1%
-52.6%
*
+
WT
MMP-2 KO
- Cholesterol
+ Cholesterol
Insig 1
mRNA expression (% of WT)
180
160
140
120
100
80
60
40
20
0
-9%
-37.4%
*
+
WT
MMP-2 KO
- Cholesterol
+ Cholesterol
Insig 2
mRNA expression (% of WT)
160
140
120
100
80
60
40
20
0
+12.5%
-20.15%
*
+
WT
MMP-2 KO
- Cholesterol
+ Cholesterol
SCAP
mRNA expression (% of WT)
120
100
80
60
40
20
0
WT
MMP-2 KO
PBS
Ang II

Figure 5-12 Contrasting effects of MMP-2 and MMP-7 in regulation of ADAM-12 in cardiac hypertrophy.

A: Cardiac hypertrophy induced by Ang II (1.4 mg/kg/d for 2 weeks) was exacerbated in MMP-2 KO mice, but less severe in MMP-7 KO mice *vs*. WT mice.

B: Cardiac ADAM-12 mRNA levels were increased in MMP-2 KO mice, but decreased in MMP-7 KO mice *vs*. WT mice with or without Ang II infusion (1.4 mg/kg/d for 2 weeks). HMGCR inhibition by lovastatin treatment (54 mg/kg/d) prevented the induction of cardiac ADAM-12 mRNA by Ang II, as determined by qRT-PCR.

*: $p<0.05$ *vs*. WT.

+: $p<0.05$ *vs*. MMP-2 KO.

‡: $p<0.05$ *vs*. WT + Ang II.

n=4-10 mice / group.

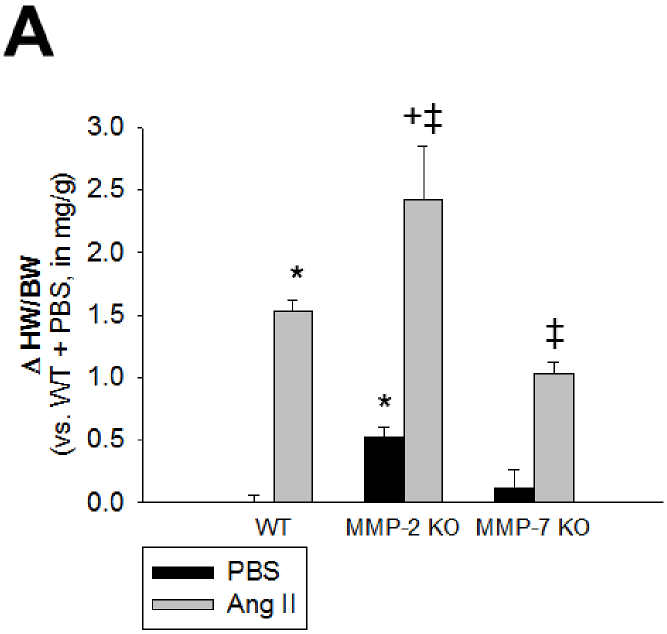
A
Δ HW/BW
(vs. WT + PBS, in mg/g)
3.0
2.5
2.0
1.5
1.0
0.5
0.0
*
+‡
*
‡
WT
MMP-2 KO
MMP-7 KO
PBS
Ang II

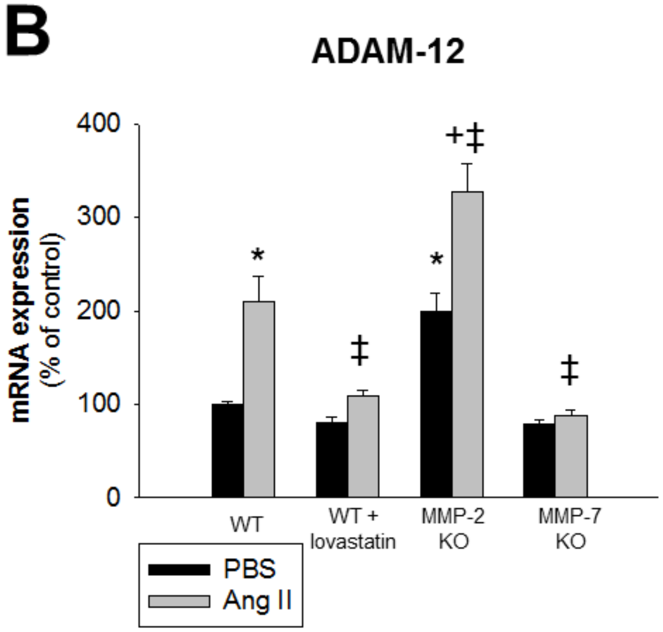
B
ADAM-12
mRNA expression
(% of control)
400
300
200
100
0
*
‡
*
+‡
‡
WT
WT +
lovastatin
MMP-2
KO
MMP-7
KO
PBS
Ang II

Figure 5-13 MMP-2 negatively regulates the SREBP-2 / HMGCR axis: Mechanistic studies in cultured cells, *in vitro* biochemical studies and *in vivo* validation.

A-C: MMP-2 controls the mRNA levels of SREBP-2 and HMGCR in LDLR-positive (c1c7) cells. LDLR-positive cells were seeded in complete medium with 10% FBS in 24-well plates. 70% confluent cells were transduced with either AdGFP or AdMMP-2 and collected at indicated time points. MMP-2 activity was measured by gelatin zymography(**A**). mRNA levels of MMP-2 (**B**), SREBP-2, HMGCR, LDLR, Insig 1 and Insig 2 (**C**) were measured by qRT-PCR.

*: $p<0.05$ *vs*. AdGFP (at time = 0 hours).

+: $p<0.05$ *vs*. AdGFP at the same time point.

n = 4 for each group and time point.

D: MMP-2 protects the LDLR from PCSK9-induced degradation. LDLR-positive cells were seeded in complete medium with 10% FBS in 24-well plates.70% confluent cells were transduced with either AdGFP or AdMMP-2. 24 hours later, the medium was replaced by serum-free medium. After overnight (16 hours) incubation, rhPCSK9 (3.5 µg/well) or vehicle (water) was added. 4 hours later, the cells were collected, lysed and lysates were subjected to Western blot with LDLR antibodies.

The LDLR Western blot traces are representative.

*: $p<0.05$ *vs*. AdGFP (vehicle).

n = 3-9 experiments for each PCSK9 amount.

E: ***Top***: BN-PAGE analysis indicates that rhMMP-2 forms protein complexes with rhPCSK9 and hLDLR extracellular domain (molar ratio 1:18:3). The proteins were incubated for 3 hours at 37°Cand reaction mixtures were resolved by BN-PAGE. Western blot analysis revealed complex-specific shifts in rhPCSK9 mobility *vs*. uncomplexed rhPCSK9. ***Middle***: BN-PAGE/gelatin zymography (to detect uncomplexed rhMMP-2) reveals inhibition of gelatinolytic activity when rhMMP-2 is in complex with rhPCSK9. ***Bottom***: SDS-PAGE/gelatin zymography shows total MMP-2 gelatinolytic activity. The streaks in the last two lanes of the SDS-PAGE gelatin zymography indicate a strong interaction between rhPCSK9 and rhMMP-2.

F: *In vivo* validation of LDLR protection by MMP-2. LDLR Western blot indicates decreased protein levels of LDLR in the LV of MMP-2 KO *vs*. WT mice.

Mice were infused with either PBS or Ang II (1.4 mg/kg/d) for 4 weeks.

*: $p<0.05$ *vs*. WT for the same day.

n= 3-10 mice / group.

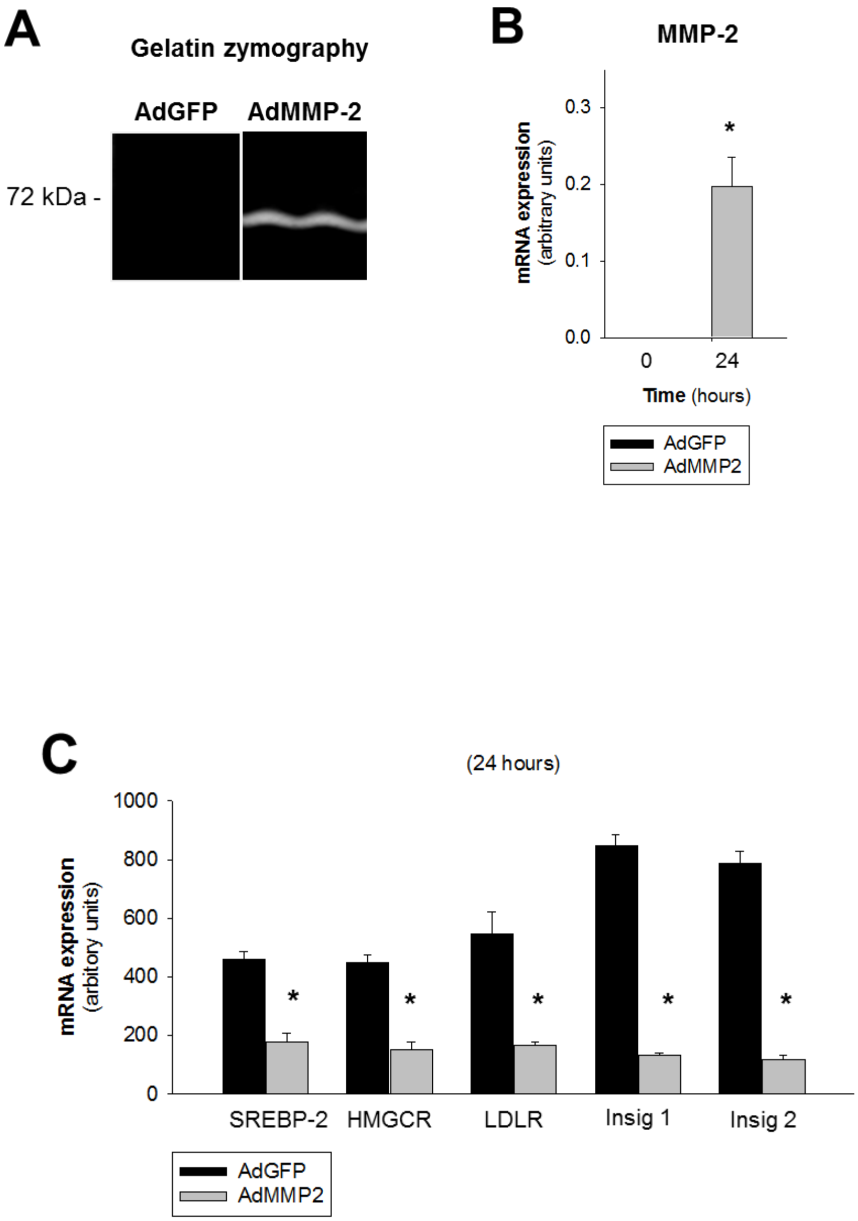
A
Gelatin zymography
AdGFP
AdMMP-2
72 kDa -
B
MMP-2
mRNA expression
(arbitrary units)
0.0
0.1
0.2
0.3
*
0
24
Time (hours)
AdGFP
AdMMP2
C
(24 hours)
mRNA expression
(arbitory units)
0
200
400
600
800
1000
*
*
*
*
*
SREBP-2
HMGCR
LDLR
Insig 1
Insig 2
AdGFP
AdMMP2

D

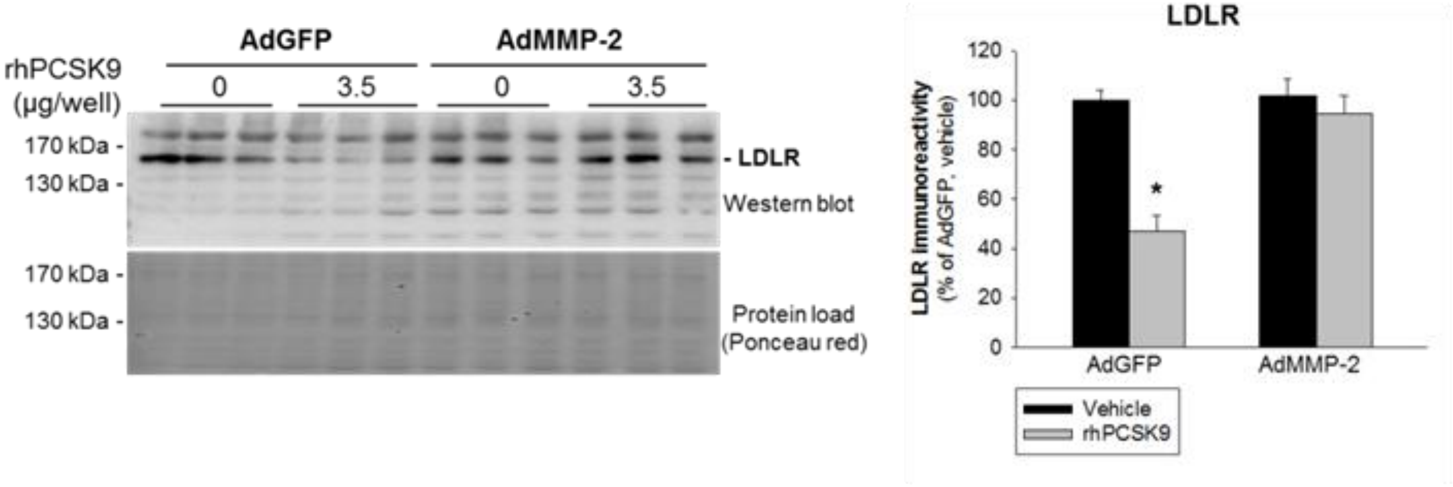
AdGFP
AdMMP-2
rhPCSK9
(µg/well)
0
3.5
0
3.5
170 kDa -
130 kDa -
- LDLR
Western blot
170 kDa -
130 kDa -
Protein load
(Ponceau red)
LDLR
LDLR immunoreactivity
(% of AdGFP, vehicle)
120
100
80
60
40
20
0
*
AdGFP
AdMMP-2
Vehicle
rhPCSK9

E

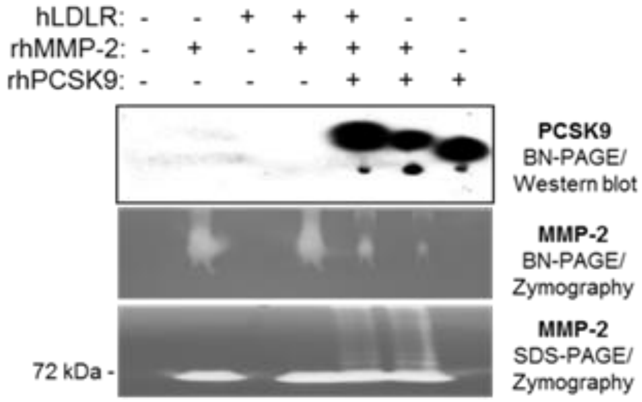
hLDLR: - - + + + - -
rhMMP-2: - + - + + + -
rhPCSK9: - - - - + + +
PCSK9
BN-PAGE/
Western blot
MMP-2
BN-PAGE/
Zymography
MMP-2
SDS-PAGE/
Zymography
72 kDa -

F

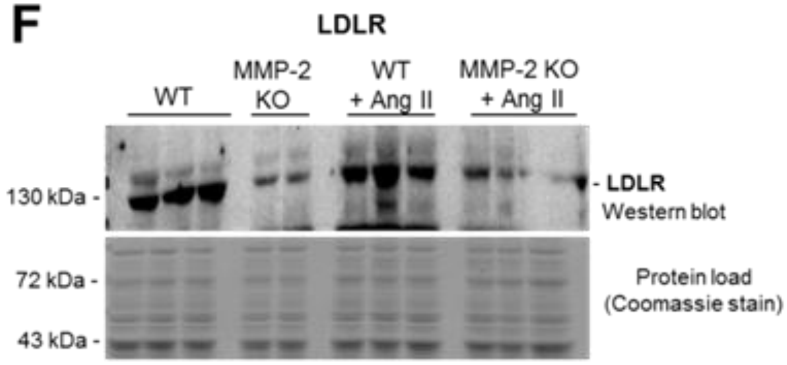
LDLR
WT
MMP-2
KO
WT
+ Ang II
MMP-2 KO
+ Ang II
130 kDa -
- LDLR
Western blot
72 kDa -
43 kDa -
Protein load
(Coomassie stain)

Figure 5-14 MMP-2 interacts with PCSK9 and cleaves PCSK9 prodomain.

A: rhMMP-2 and rhPCSK9 were incubated at indicated molar ratios with or without the MMP-2 inhibitor (1,10-phenanthroline, 100 μmol/L) for 3 hours. The reaction mixtures were resolved by SDS-PAGE.

B: The MMP-2 cleavage site of human PCSK9 prodomain was determined by in-gel MAAH combined with LC-ESI tandem mass spectrometric sequencing (**Table 5-1** shows peptide sequences).

C: rhPCSK9 (4 μg) was incubated with rhpro-MMP-2 or rhMMP-2 (PCSK9:pro-MMP-2 = 2 :1 or PCSK9:MMP-2 = 4:1; mol:mol) for 3 hours, with or without 1,10-phenanthroline. Each reaction mix was then divided into two halves, which received either chemical crosslinker BS3 (5mmol/L) or vehicle (water) for 30 min. The data suggest that MMP-2 binds to PCSK9 and releases as well as subsequently cleaves PCSK9's prodomain. Indeed, as shown in the figure, in native PCSK9, the PCSK9's prodomain is attached to PCSK9's catalytic domain. The prodomain can be resolved by denaturing SDS-PAGE and migrates at an apparent molecular weight of 18 kDa. As expected, this is prevented by addition of BS3 crosslinker. When either rhMMP-2 or rhpro-MMP-2 (which is partly active) was added to PCSK9, PCSK9's prodomain was cleaved but the crosslinker failed to prevent that PCSK9's prodomain and its cleavage fragment migrated at their expected molecular weights on SDS-PAGE. Therefore, a domain in MMP-2 interacts with PCSK9's catalytic domain as well as cleaves PCSK9's prodomain. However, the interaction between PCSK9 catalytic domain and MMP-2 persists in the presence of an MMP-2 inhibitor (that indeed prevented PCSK9's prodomain cleavage).

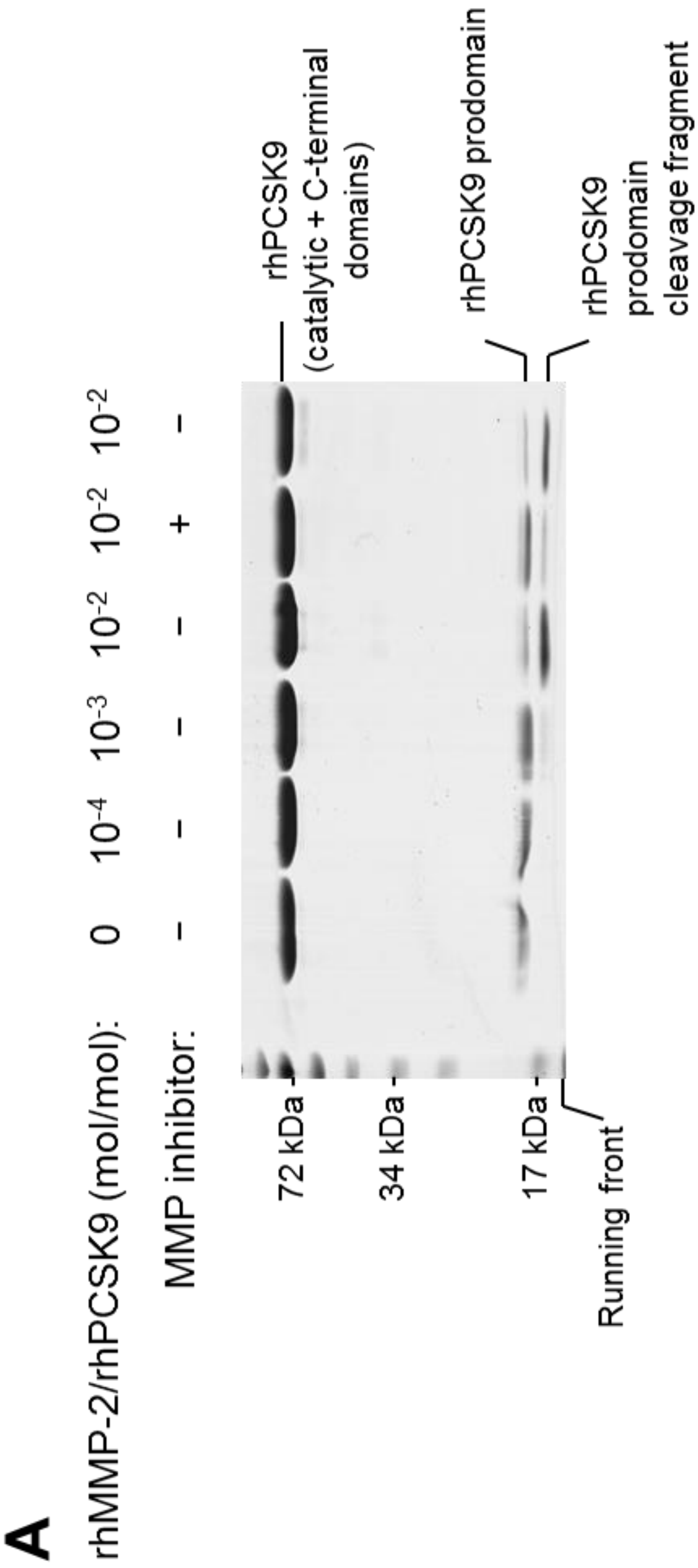
A
rhMMP-2/rhPCSK9 (mol/mol):
0
10^-4
10^-3
10^-2
10^-2
10^-2
MMP inhibitor:
–
–
–
–
+
–
72 kDa
34 kDa
17 kDa
Running front
rhPCSK9 (catalytic + C-terminal domains)
rhPCSK9 prodomain
rhPCSK9 prodomain cleavage fragment

B

hPCSK9 prodomain

Cleavage site ↓

```
  1 QEDEDGDYEE LVLALRSEED GLAEAPEHGT TATFHRCAKD PWRLPGTYVV
 51 VLKEETHLSQ SERTARRLQA QAARRGYLTK ILHVFHGLLP GFLVKMSGDL
101 LELALKLPHV DYIEEDSSVF AQ
```

C

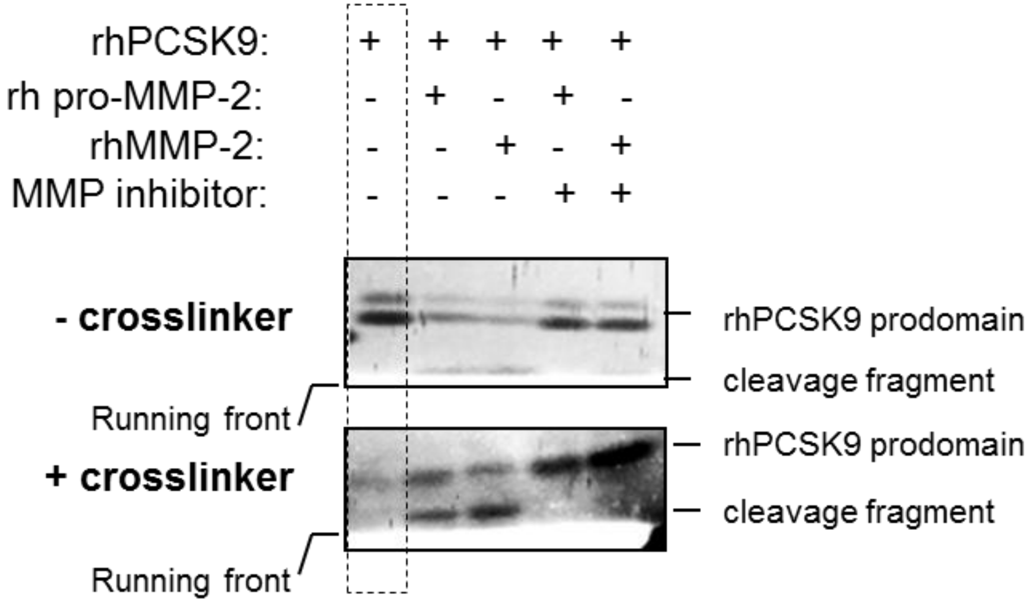
rhPCSK9: + + + + +
rh pro-MMP-2: - + - + -
rhMMP-2: - - + - +
MMP inhibitor: - - - + +
- crosslinker
Running front
+ crosslinker
Running front
rhPCSK9 prodomain
cleavage fragment
rhPCSK9 prodomain
cleavage fragment

Figure 5-15 The proteolytic action of MMP-2 alone does not affect the ability of PCSK9 to induce LDLR degradation.

A: The experiment was designed at a molar ratio (PCSK9:MMP-2 = 100:1; mol:mol) aiming to achieve >80% of PCSK9 prodomain cleavage with less than 1% of the PCSK9 catalytic domain being available for complex formation with MMP-2. Pre-incubation of rhPCSK9 with rhMMP-2 *in vitro* at 37 ºC for 5 hours selectively cleaved PCSK9 prodomain but not catalytic domain as confirmed by SDS-PAGE.

B: The reaction mixture was then added to cells transfected with either empty plasmid (LDLR-negative) or plasmid expressing LDLR (LDLR-positive). The cells were collected 4 hours later. LDLR protein was detected by Western blot.

A

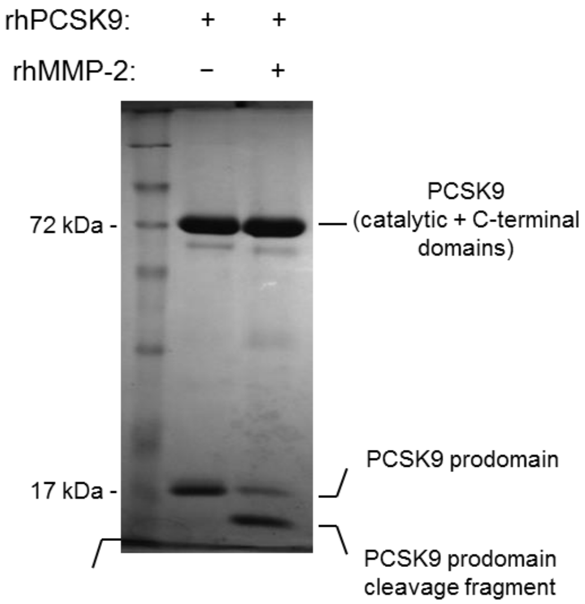
rhPCSK9: + +
rhMMP-2: − +
72 kDa -
17 kDa -
PCSK9 (catalytic + C-terminal domains)
PCSK9 prodomain
PCSK9 prodomain cleavage fragment

B

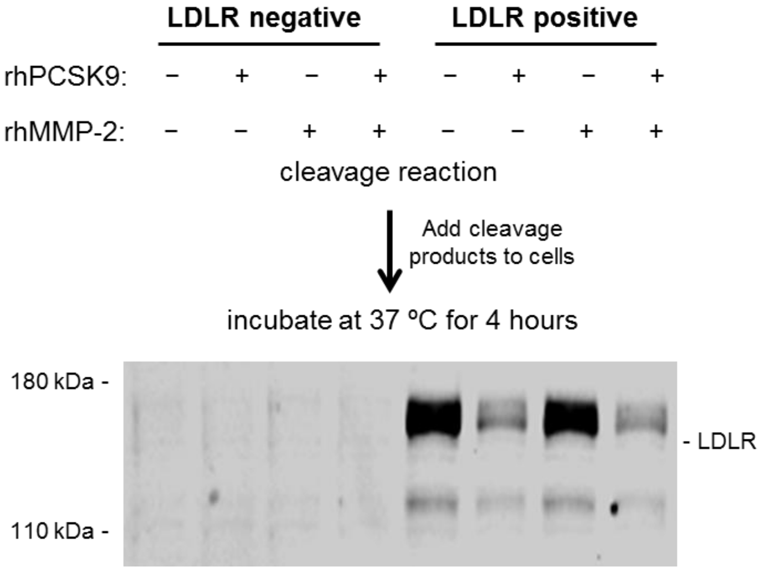
LDLR negative
LDLR positive
rhPCSK9: − + − + − + − +
rhMMP-2: − − + + − − + +
cleavage reaction
Add cleavage products to cells
incubate at 37 ºC for 4 hours
180 kDa -
110 kDa -
- LDLR

Figure 5-16 Functional evidence that a non-proteolytic action of MMP-2 protects LDLR from degradation.

LDLR positive cells were transduced with either AdGFP or AdMMP-2 to overexpress MMP-2. 24 hours later, the medium was replaced by media without serum. After overnight (16 hours) incubation, the pharmacological MMP-2 inhibitor III (40 µmol/L) or vehicle was added to the cells. 1 hour later, rhPCSK9 was added to the cells. 4 hours later, the cells were collected, lysed and lysates were subjected to western blot with LDLR antibodies. Similar levels of LDLR protection by MMP-2 were observed in the presence and absence of MMP-2 inhibitor III indicating that MMP-2 proteolytic activity is not required for LDLR protection by MMP-2.

*: $p < 0.05$ *vs*. AdGFP (vehicle).

n=3-4 / group

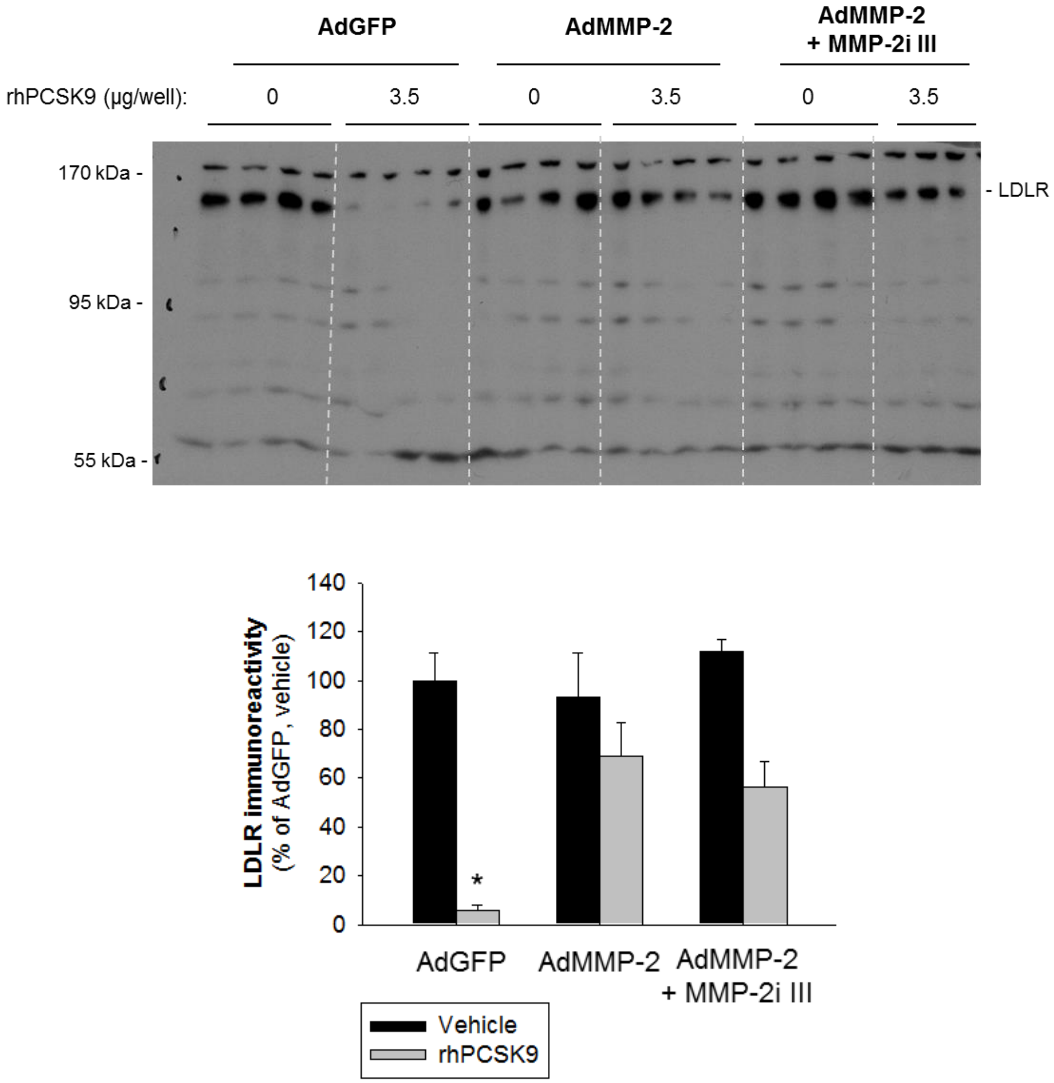

Figure 5-17 Proposed mechanism whereby MMP-2 negatively regulates the SREBP-2 / HMGCR pathway and protects against cardiac remodeling.
MMP-2 forms a multiprotein complex with PCSK9 and the LDLR extracellular domain at the plasma membrane. Complex formation prevents LDLR degradation. The resultant protection of LDLR promotes LDL-cholesterol uptake, which downregulates the SREBP-2 transcriptional pathway and HMGCR expression (**top**). Therefore, MMP-2 protects against HMGCR-dependent cardiac hypertrophy and fibrosis. Sustained stimulation with Ang II overrides the protection rendered by MMP-2 by increasing HMGCR protein levels. The elevated HMGCR activity produces more cholesterol and isoprenoids, which contribute to cardiac hypertrophy and fibrosis (**bottom**).

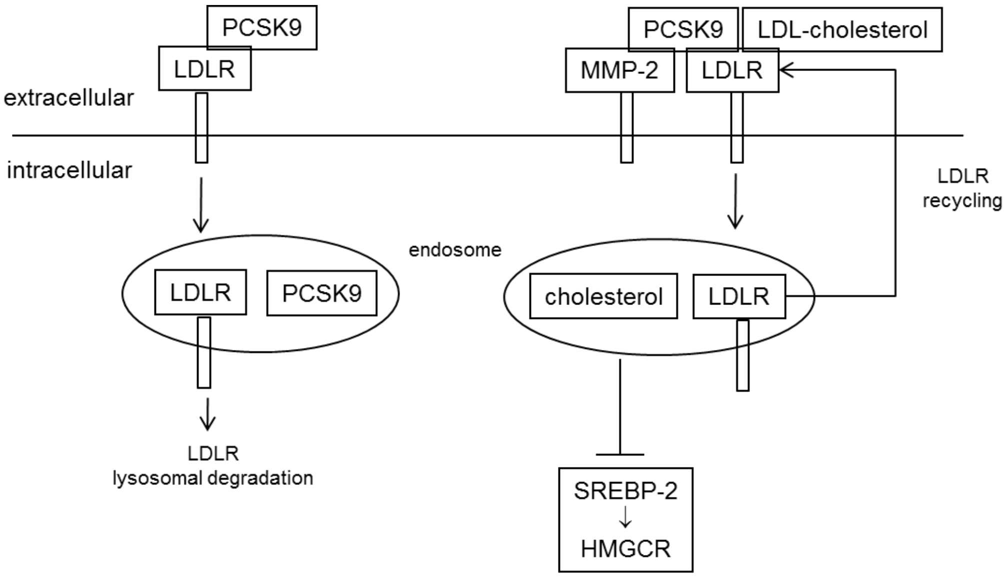
PCSK9
LDLR
extracellular
intracellular
LDLR
PCSK9
LDLR
lysosomal degradation
endosome
PCSK9
LDL-cholesterol
MMP-2
LDLR
LDLR
recycling
cholesterol
LDLR
SREBP-2
↓
HMGCR

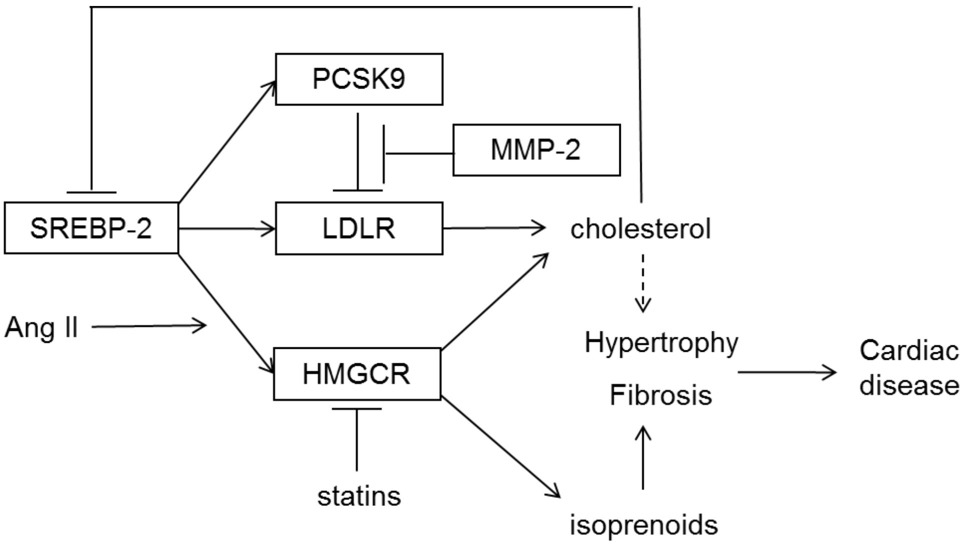
PCSK9
MMP-2
SREBP-2
LDLR
cholesterol
Ang II
HMGCR
Hypertrophy
Fibrosis
Cardiac
disease
statins
isoprenoids

5.5 References

1. Kearney PM, Whelton M, Reynolds K, Muntner P, Whelton PK, He J. Global burden of hypertension: analysis of worldwide data. *Lancet*. 2005;365:217-223
2. Lifton RP, Gharavi AG, Geller DS. Molecular mechanisms of human hypertension. *Cell*. 2001;104:545-556
3. Biaggioni I. Should we target the sympathetic nervous system in the treatment of obesity-associated hypertension? *Hypertension*. 2008;51:168-171
4. Rockman HA, Wachhorst SP, Mao L, Ross J, Jr. ANG II receptor blockade prevents ventricular hypertrophy and ANF gene expression with pressure overload in mice. *Am J Physiol*. 1994;266:H2468-2475
5. Muller P, Kazakov A, Jagoda P, Semenov A, Bohm M, Laufs U. ACE inhibition promotes upregulation of endothelial progenitor cells and neoangiogenesis in cardiac pressure overload. *Cardiovasc Res*. 2009;83:106-114
6. Delano FA, Chen AY, Wu KI, Tran ED, Rodrigues SF, Schmid-Schonbein GW. The Autodigestion Hypothesis and Receptor Cleavage in Diabetes and Hypertension. *Drug Discov Today Dis Models*. 2011;8:37-46
7. Fernandez-Patron C. Therapeutic potential of the epidermal growth factor receptor transactivation in hypertension: a convergent signaling pathway of vascular tone, oxidative stress, and hypertrophic growth downstream of vasoactive G-protein-coupled receptors? *Can J Physiol Pharmacol*. 2007;85:97-104
8. Liao Y, Zhao H, Ogai A, Kato H, Asakura M, Kim J, Asanuma H, Minamino T, Takashima S, Kitakaze M. Atorvastatin slows the progression of cardiac remodeling in mice with pressure overload and inhibits epidermal growth factor receptor activation. *Hypertens Res*. 2008;31:335-344
9. Liao JK. Statin therapy for cardiac hypertrophy and heart failure. *J Investig Med*. 2004;52:248-253
10. Brown MS, Goldstein JL. The LDL receptor and HMG-CoA reductase--two membrane molecules that regulate cholesterol homeostasis. *Curr Top Cell Regul*. 1985;26:3-15
11. Konstantinopoulos PA, Karamouzis MV, Papavassiliou AG. Post-translational modifications and regulation of the RAS superfamily of GTPases as anticancer targets. *Nat Rev Drug Discov*. 2007;6:541-555
12. Brown MS, Goldstein JL. The SREBP pathway: regulation of cholesterol metabolism by proteolysis of a membrane-bound transcription factor. *Cell*. 1997;89:331-340
13. Vogel RA. PCSK9 Inhibition: The Next Statin? *J Am Coll Cardiol*.

2012;59:2354-2355

14. Horton JD, Cohen JC, Hobbs HH. PCSK9: a convertase that coordinates LDL catabolism. *J Lipid Res*. 2009;50 Suppl:S172-177
15. Engelking LJ, Liang G, Hammer RE, Takaishi K, Kuriyama H, Evers BM, Li WP, Horton JD, Goldstein JL, Brown MS. Schoenheimer effect explained--feedback regulation of cholesterol synthesis in mice mediated by Insig proteins. *J Clin Invest*. 2005;115:2489-2498
16. Radhakrishnan A, Goldstein JL, McDonald JG, Brown MS. Switch-like control of SREBP-2 transport triggered by small changes in ER cholesterol: a delicate balance. *Cell Metab*. 2008;8:512-521
17. Wang N, Li L. Reproducible microwave-assisted acid hydrolysis of proteins using a household microwave oven and its combination with LC-ESI MS/MS for mapping protein sequences and modifications. *J Am Soc Mass Spectrom*. 2010;21:1573-1587
18. Lillie RD. Further Experiments with the Masson Trichrome Modification of Mallory's Connective Tissue Stain. *Biotechnic & Histochemistry*. 1940;15:17-22
19. Odenbach J, Wang X, Cooper S, Chow FL, Oka T, Lopaschuk G, Kassiri Z, Fernandez-Patron C. MMP-2 mediates angiotensin II-induced hypertension under the transcriptional control of MMP-7 and TACE. *Hypertension*. 2011;57:123-130
20. Yagi S, Aihara K, Ikeda Y, Sumitomo Y, Yoshida S, Ise T, Iwase T, Ishikawa K, Azuma H, Akaike M, Matsumoto T. Pitavastatin, an HMG-CoA reductase inhibitor, exerts eNOS-independent protective actions against angiotensin II induced cardiovascular remodeling and renal insufficiency. *Circ Res*. 2008;102:68-76
21. Zhou MS, Jaimes EA, Raij L. Atorvastatin prevents end-organ injury in salt-sensitive hypertension: role of eNOS and oxidant stress. *Hypertension*. 2004;44:186-190
22. Takemoto M, Node K, Nakagami H, Liao Y, Grimm M, Takemoto Y, Kitakaze M, Liao JK. Statins as antioxidant therapy for preventing cardiac myocyte hypertrophy. *J Clin Invest*. 2001;108:1429-1437
23. Wilson CL, Heppner KJ, Labosky PA, Hogan BL, Matrisian LM. Intestinal tumorigenesis is suppressed in mice lacking the metalloproteinase matrilysin. *Proc Natl Acad Sci U S A*. 1997;94:1402-1407
24. Wang X, Chow FL, Oka T, Hao L, Lopez-Campistrous A, Kelly S, Cooper S, Odenbach J, Finegan BA, Schulz R, Kassiri Z, Lopaschuk GD, Fernandez-Patron C. Matrix metalloproteinase-7 and ADAM-12 (a disintegrin and metalloproteinase-12) define a signaling axis in agonist-induced hypertension and cardiac hypertrophy. *Circulation*.

2009;119:2480-2489

25. Berry E, Bosonea AM, Wang X, Fernandez-Patron C. Insights into the activity, differential expression, mutual regulation, and functions of matrix metalloproteinases and a disintegrin and metalloproteinases in hypertension and cardiac disease. *J Vasc Res*. 2013;50:52-68
26. Wang X, Oka T, Chow FL, Cooper SB, Odenbach J, Lopaschuk GD, Kassiri Z, Fernandez-Patron C. Tumor necrosis factor-alpha-converting enzyme is a key regulator of agonist-induced cardiac hypertrophy and fibrosis. *Hypertension*. 2009;54:575-582
27. Hao L, Du M, Lopez-Campistrous A, Fernandez-Patron C. Agonist-induced activation of matrix metalloproteinase-7 promotes vasoconstriction through the epidermal growth factor-receptor pathway. *Circ Res*. 2004;94:68-76
28. Spinale FG. Myocardial matrix remodeling and the matrix metalloproteinases: influence on cardiac form and function. *Physiol Rev*. 2007;87:1285-1342
29. Zhou Q, Liao JK. Statins and cardiovascular diseases: from cholesterol lowering to pleiotropy. *Curr Pharm Des*. 2009;15:467-478
30. Shmeeda H, Petkova D, Barenholz Y. Cholesterol homeostasis in cultures of rat heart myocytes: relationship to cellular hypertrophy. *Am J Physiol*. 1994;267:H1689-1697
31. Yokoyama M, Seo T, Park T, Yagyu H, Hu Y, Son NH, Augustus AS, Vikramadithyan RK, Ramakrishnan R, Pulawa LK, Eckel RH, Goldberg IJ. Effects of lipoprotein lipase and statins on cholesterol uptake into heart and skeletal muscle. *J Lipid Res*. 2007;48:646-655
32. Jung HJ, Lee WY, Yoo YS, Chung BC, Choi MH. Database-dependent metabolite profiling focused on steroid and fatty acid derivatives using high-temperature gas chromatography-mass spectrometry. *Clin Chim Acta*. 2010;411:818-824
33. Glazer HP, Osipov RM, Clements RT, Sellke FW, Bianchi C. Hypercholesterolemia is associated with hyperactive cardiac mTORC1 and mTORC2 signaling. *Cell Cycle*. 2009;8:1738-1746
34. Lee H, Yoo YS, Lee D, Song EJ. Cholesterol induces cardiac hypertrophy by activating the AKT pathway. *J Steroid Biochem Mol Biol*. 2013;138C:307-313
35. Rodriguez D, Morrison CJ, Overall CM. Matrix metalloproteinases: what do they not do? New substrates and biological roles identified by murine models and proteomics. *Biochim Biophys Acta*. 2010;1803:39-54
36. Morrison CJ, Butler GS, Rodriguez D, Overall CM. Matrix metalloproteinase proteomics: substrates, targets, and therapy. *Curr Opin Cell Biol*. 2009;21:645-653

37. Newby AC. Matrix metalloproteinase inhibition therapy for vascular diseases. *Vascul Pharmacol*. 2012;56:232-244
38. Schmid-Schonbein GW. An emerging role of degrading proteinases in hypertension and the metabolic syndrome: autodigestion and receptor cleavage. *Curr Hypertens Rep*. 2012;14:88-96
39. Santos-Martinez MJ, Medina C, Jurasz P, Radomski MW. Role of metalloproteinases in platelet function. *Thromb Res*. 2008;121:535-542
40. Burrage PS, Brinckerhoff CE. Molecular targets in osteoarthritis: metalloproteinases and their inhibitors. *Curr Drug Targets*. 2007;8:293-303
41. Spinale FG, Coker ML, Krombach SR, Mukherjee R, Hallak H, Houck WV, Clair MJ, Kribbs SB, Johnson LL, Peterson JT, Zile MR. Matrix metalloproteinase inhibition during the development of congestive heart failure : effects on left ventricular dimensions and function. *Circ Res*. 1999;85:364-376
42. Lacchini R, Jacob-Ferreira AL, Luizon MR, Gasparini S, Ferreira-Sae MC, Schreiber R, Nadruz W, Jr., Tanus-Santos JE. Common matrix metalloproteinase 2 gene haplotypes may modulate left ventricular remodelling in hypertensive patients. *J Hum Hypertens*. 2012;26:171-177
43. Tuysuz B, Mosig R, Altun G, Sancak S, Glucksman MJ, Martignetti JA. A novel matrix metalloproteinase 2 (MMP2) terminal hemopexin domain mutation in a family with multicentric osteolysis with nodulosis and arthritis with cardiac defects. *Eur J Hum Genet*. 2009;17:565-572
44. Zile MR, Desantis SM, Baicu CF, Stroud RE, Thompson SB, McClure CD, Mehurg SM, Spinale FG. Plasma biomarkers that reflect determinants of matrix composition identify the presence of left ventricular hypertrophy and diastolic heart failure. *Circ Heart Fail*. 2011;4:246-256
45. Ahmed SH, Clark LL, Pennington WR, Webb CS, Bonnema DD, Leonardi AH, McClure CD, Spinale FG, Zile MR. Matrix metalloproteinases/tissue inhibitors of metalloproteinases: relationship between changes in proteolytic determinants of matrix composition and structural, functional, and clinical manifestations of hypertensive heart disease. *Circulation*. 2006;113:2089-2096
46. Han DH, Kim SK, Kang S, Choe BK, Kim KS, Chung JH. Matrix Metallopeptidase 2 Gene Polymorphism is Associated with Obesity in Korean Population. *Korean J Physiol Pharmacol*. 2008;12:125-129
47. Kita T, Brown MS, Goldstein JL. Feedback regulation of 3-hydroxy-3-methylglutaryl coenzyme A reductase in livers of mice treated with mevinolin, a competitive inhibitor of the reductase. *J Clin Invest*. 1980;66:1094-1100

Chapter 6

Discussion and Conclusions

Our studies have discovered previously unknown mechanisms by which metalloproteinases contribute to the development and progression of hypertensive cardiac disease, a major disorder that predisposes to heart failure and death.

In humans, hypertrophic cardiac disease presents with a multifactorial etiology, which makes the elucidation of the disease pathways challenging. Interestingly, many factors involved in causation of hypertrophic heart disease (stress, obesity, diabetes, renal dysfunction) are linked to the production of pathologically high levels of vasoconstrictive GPCR agonists such as Ang II and catecholamines (e.g., norepinephrine)[1-6]. Moreover, these GPCR agonists signal through highly overlapping pathways. Therefore, the identification and functional characterization of common signaling events downstream of multiple GPCR agonists should enhance our understanding and clinical management of hypertensive cardiac disease even when the etiology is complex or unknown.

Here, we used Ang II and adrenoceptor ligands as prototypes of GPCR agonist to gain insight into mechanisms of hypertensive cardiac disease in rodent models. In line with the reports of other investigators[5,7,8], we show that metalloproteinases are common downstream mediators of GPCR agonists.

The notion that hypertensive cardiac disease is mediated by GPCR agonist-activated metalloproteinases is still relatively novel and its recognition has only grown in importance over the past decade. For instance, there are attempts to develop personalized therapeutic approaches for hypertensive cardiac disease patients through targeting specific metalloproteinases directly in the heart of the patient[9].

These developments, which are centered on targeting metalloproteinases, contrast with and complement current therapeutic approaches which were derived from the notion that cardiovascular signaling was “Ca^{2+}-centric”.

In fact, for many years, the cardiovascular effects of GPCR agonists were interpreted as a direct consequence of Ca^{2+} release from intracellular stores and Ca^{2+} uptake from the extracellular milieu. Induction of Ca^{2+} signaling by agonists can successfully explain how agonists evoke contractile responses in the cardiovascular system.

However, as shown in papers from our group, to explain the maintenance of contraction over prolonged periods of agonist stimulation or the mitogenic effects induced by agonists, it is necessary to consider additional pathways such as those mediated by GPCR agonist-activated metalloproteinases[6,10]. These metalloproteinases include the members of the MMP and ADAM families studied in this thesis (i.e. MMP-2, MMP-7, ADAM12 and ADAM-17).

Originally thought to only degrade components of the ECM during the long-term process of tissue remodeling, MMP and ADAM family members also cleave and regulate many non-ECM substrates in an acute fashion. Excessive GPCR signaling thus translates into pathological metalloproteinase cleavage of ECM and non-ECM substrates, including cell surface receptors and ligands of receptors[11-13].

Previous studies from our lab demonstrated that, MMP-7 is important in GPCR agonist-induced vasoconstriction[6]. MMP-7 can shed ligands of the EGFR such as HB-EGF which next transactivate EGFR-dependent intracellular signaling of vascular tone and cardiovascular hypertrophy. Indeed, studies described in this thesis have, for the first time, found that MMP-7 is a mediator in the development of GPCR agonist-induced hypertension and cardiac hypertrophy.

Previous research revealed that two disintegrin metalloproteinases, ADAM-12 and ADAM-17, are also involved in signaling of hypertrophy in cardiaomyocytes and vascular smooth muscle cells through the transactivation of the EGFR[7,8]. However, there has been a paucity of *in vivo* studies on ADAM-17. Our studies demonstrate, for the first time *in vivo*, that GPCR agonist-induced cardiac remodeling is signaled through ADAM-17. We further show that ADAM-17 acts, at least in part, by upregulating the expression of ADAM-12, a major effector metalloproteinases[7].

Although MMP-2 was shown to cleave vasoactive peptides such as big endothelin-1[14], its role in hypertension and cardiac hypertrophy was never defined. Our studies show that MMP-2 mediates GPCR-induced vasoconstriction and hypertension. Our studies also indicate that GPCR agonists upregulate MMP-2 expression in the heart as a cardioprotective mechanism against hypertensive cardiac remodeling effects. This is clearly evidenced by our observation that the MMP-2 gene knockout mice are predisposed to Ang II-induced pathological cardiac remodeling. Moreover, we have found that MMP-2 protects the heart against hypertensive cardiac remodeling through a novel mechanism involving the inhibition of hypertrophy signaling by SREBP-2 and HMGCR, the rate-limiting enzyme in the cholesterol biosynthesis pathway. Mice lacking MMP-2 express high levels of SREBP-2 mRNA and HMGCR mRNA which, in response to Ang II, are translated into correspondingly high levels of HMGCR protein. The consequent increase in HMGCR activity causes a transient but significant increase in cardiac cholesterol and intensifies the development of Ang II-induced cardiac hypertrophy.

Our studies further expose the integration and mutual regulation of metalloproteinase-dependent pathways in signaling of cardiovascular disease. We show that GPCR agonists signal through both MMP-7 and ADAM-17 to induce: 1) hypertension (which is mediated by MMP-2 under transcriptional control of

MMP-7 and ADAM-17) and, 2) cardiac remodeling (which is mediated by ADAM-12 and opposed by MMP-2) (**Figure 6-1**).

6.1 Mutual regulation of metalloproteinases in the development of hypertension and cardiac remodeling

In the mouse model of Ang II-induced hypertension and cardiac remodeling, early activation of MMP-7 and ADAM-17 appears to be necessary for subsequent upregulation of MMP-2 and ADAM-12 transcription. Indeed, partial inhibition of the expression of MMP-7 and ADAM-17 individually or together prevents the upregulation of MMP-2 by Ang II in terms of both mRNA levels and enzymatic activity. This in turn attenuates the severity of Ang II-induced hypertension, a process mediated by MMP-7 (in its early stages) and MMP-2 (once hypertension is established).

Ang II induces an upregulation of ADAM-12 that mediates hypertrophic processes in the heart. Inhibition of MMP-7 and ADAM-17 in mice (by gene knock-out, siRNA or pharmacological inhibition), prevent Ang II-induced ADAM-12 overexpression as well as cardiac hypertrophy. Therefore, agonist activation of constitutively expressed metalloproteinases such as MMP-7 and ADAM-17 induces transcription of metalloproteinases, such as MMP-2 and ADAM-12, probably through EGFR transactivation and MAPK signaling[15]. The resulting feed-forward loop allows constitutively expressed metalloproteinases to mediate *de novo* production of metalloproteinases.

The interaction and regulation between metalloproteinases has been observed in previous studies. For example, MMP-3 can cleave and activate MMP-1, MMP-7, MMP-8 MMP-9 and MMP-13[16,17]. MMP-7 proteolytically activates MMP-8 (alone with MMP-1, MMP-2 and MMP-9) but not MMP-13[18]. Pro-MMP-8 accumulation in the absence of MMP-7 leads to decreased pro-MMP-13 levels, perhaps to maintain baseline collagenolytic levels. This interaction between MMP-8 and MMP-13 does not induce the remodeling of mouse left ventricle, suggesting MMP-8 and MMP-13 may play redundant roles[18]. In addition to activation, metalloproteinases can also cleave and inactivate other metalloproteinases. For instance, MT1-MMP has recently been reported to proteolytically cleave ADAM-9 and ADAM15 and lead to their inactivation[19,20]. Therefore, metalloproteinases do not act independent from each other. Rather, they interact and regulate each other to mediate various physiological and pathological processes, including the development of hypertension and cardiac hypertrophy.

6.2 Differential metalloproteinase expression leads to varying physiological roles in hypertensive cardiac remodeling and other conditions

The roles played by metalloproteinases in hypertension and cardiac remodeling are an area of intense investigation and the scientific literature still contains some inconsistencies. There are reports of increased, decreased or no differences in levels of plasma MMP-9 in human hypertension[21-24]. There are discrepancies about the levels of MMP-2 in hypertension[21,25]. Our studies here suggest that different metalloproteinases are differentially expressed at different stages of hypertension and cardiac remodeling.

MMP-7 is ubiquitously expressed, albeit in small quantities, in various systems including the immune system and the cardiovascular system. These features may help MMP-7 act as a signaling mediator downstream of many agonists. However, its role might be limited to strict time windows, such as the early stages of agonist signaling. Indeed, following the administration of Ang II to mice, vascular (aortic) MMP-7 (but not MMP-2) is acutely activated (within one hour). Lack of acute detectable activation of MMP-2 indicates that basal MMP-2 may be engaged in agonist-induced processes. We also show that broad spectrum blockade of MMPs (using doxycycline) as well as a biphenylsulfonamido-hydroxamate inhibitor selective for MMP-2 (MMP-2 inhibitor III, Calbiochem) relaxes phenylephrine pre-constricted small mesenteric arteries. Therefore, agonist-induced vasoconstriction may depend at least in part on MMP-7 acute activation as well as on MMP-2 basal activity. Interestingly, previous studies using MMP-9 knock-out mouse models indicate that MMP-9 plays a key role in the early stages of hypertensive vascular disease[26]. The onset of Ang II-induced hypertension was found to be accompanied by increased MMP-9 activity in conductance vessels. The absence of MMP-9 activity resulted in vessel stiffness and increased pulse pressure. Therefore, MMP-9 activity is associated with a beneficial role early on in hypertension by preserving vessel compliance and alleviating blood pressure increase.

We have found that several days after Ang II infusion, cardiac MMP-7 and MMP-9 mRNA levels tend to decrease. By contrast, the cardiac mRNA levels of MMP-2 and ADAM-12 are strongly upregulated. MMP-2 activity is also elevated in arteries. These processes probably amplify as well as sustain GPCR agonist-induced signaling over time.

In the setting of established hypertension, the regulation of MMP promoter activity is likely to depend on both mechanical and hormonal stimuli. Recent work suggests that vascular (aortic) metalloproteinase promoters may be differently responsive to single and collective mechanical (wall tension, up to 100 mmHg) and hormonal (Ang II) stimuli[27]. Increased tension was found to enhance MT1-MMP promoter activity, but did not have an additional effect on Ang II-induced MT1-MMP promoter activation. Elevated tension plus Ang II administration had an additive effect on MMP-2 promoter activation, while MMP-9 promoter activity decreased. Therefore, exposure to a biological stimulus such as Ang II in the presence of high vessel-wall tension can modulate MMP promoter activation. *In vivo*, the combined action of mechanical and hormonal stimuli likely regulates the activity of individual metalloproteianases which, in turn, regulate the expression and activity of (as well as being subject to mutual regulation by) other metalloproteinases.

Varying physiological and pathological roles of metalloproteinases been reported in other conditions and diseases. Differential upregulation of MMP-2 and MMP-9 may have both pathogenic and protective effects during the development and progression of Alport syndrome, a progressive hereditary kidney disease leading to glomeruli damage and kidney failure[28]. Preservation of the integrity of the glomerular basement membrane and the extracellular matrix by inhibiting MMP-2 and MMP-9 before the onset of proteinuria leads to significant disease protection. However, if this window of opportunity is missed, MMP-inhibition in later stages of Alport disease causes accelerated glomerular and interstitial fibrosis. In addition, the expression patterns of MMP-2, MMP-3 and MMP-9 in the kidney glomerulus are linked in a compensatory manner, as shown by studies of genetic knock-out mouse models. Similarly, differential actions and expression profiles of MMP-2 and MMP-9 have been implicated in platelet aggregation as well as in the response to injury in the carotid artery[29,30].

As expected, complex interactions characterize the biology of metalloproteinases in cardiovascular as well as non-cardiovascular settings including the nervous system and immune system. In the setting of neuropathic pain, a condition of constant pain in the absence of a stimulus resulting from damage to the nervous system[31], MMP-9 is both necessary and sufficient for producing the neuropathic pain syndrome whereas MMP-2 expression is necessary to maintain neuropathic pain[32]. Even though MMP-9 is active in the early stages with MMP-2 activity increasing at later time points, both MMP-9 and

MMP-2 act through cleavage of interleukin-1b. Similarly, MMP-2 and MMP-9 play complex and multiphasic roles after acute stroke and brain damage[33]. Although these MMPs mediate neurovascular injury, they have also been involved in neuroplasticity and stroke recovery. As in other models that involve MMPs, spatial and temporal regulation remains to be defined so as to allow targeting of acute MMPs to ameliorate neurovascular pathophysiology without interfering with brain tissue repair[33].

Emerging evidence links immune system responses induced by pathogens to MMP gene expression. For instance, acute *Pseudomonas aeruginosa* pulmonary infection results in the induction of both MMP-7 and MMP-10[34]. Analysis of gene expression changes in *Pseudomonas aeruginosa* infected tracheal epithelial cell cultures identified 2091 MMP-7-dependent and 1628 MMP-10-dependent genes that were differentially expressed. MMPs control distinct gene expression programs (as shown through key node analysis) involved in proliferation, cell death, immune responses and signal transduction, among other host defense processes. Because MMP-7 functions to promote inflammation, and MMP-10 acts to restrain inflammation, it appears that MMPs could play unique roles in epithelial responses to *Pseudomonas aeruginosa* infection[34]. These data from a non-cardiovascular disease model further suggest that the expression and activity of single metalloproteinases can have profound effects on the expression of many other genes.

6.3 Opposite roles of MMP-2 and ADAM-12 in cardiac remodeling

Although cardiac MMP-2 and ADAM-12 are both upregulated downstream of MMP-7 and ADAM-17 in agonist-induced cardiac remodeling, they may have opposite roles in the development of the disease. ADAM-12 mediates the development of cardiac remodeling via its ability to shed HB-EGF and transactivate EGFR. Inhibition of ADAM-12 can block the development of cardiac remodeling[7]. ADAM-12 has also been reported to interact with TGF-β receptor and facilitate the downstream Smad signaling, the main pathway mediating cardiac fibrosis[35].

In contrast to ADAM-12, partial inhibition of MMP-2, by a selective pharmacological inhibitor or RNA interference, has little effects on the development of cardiac remodeling, despite attenuating the severity of GPCR agonist-induced hypertension. However, complete knockout of MMP-2 predispose to severe Ang II-induced cardiac remodeling in mice. Therefore, MMP-2 can be pro-hypertensive, and yet also cardioprotective.

The role of MMP-2 in cardiac remodeling is still unclear. Acute expression and release of MMP-2 during reperfusion after ischemia have been suggested to contribute to cardiac mechanical dysfunction and inhibition of MMP-2 improves the recovery of mechanical function during reperfusion[36]. In cardiomyocytes, MMP-2 has also been reported to cleave contractile proteins such as troponin I and Titin and thus contribute to the development of cardiac dysfunction and heart failure[37,38]. Cardiac overexpression of MMP-2 induces cardiac contractile dysfunction[39]. Meanwhile, increased level of circulating MMP-2 is suggested to be the marker of heart failure and MMP-2 values above the mean serum level are associated with poor prognosis for mortality of patients with chronic heart failure[40]. Targeted deletion of MMP-2 ameliorates pressure overload-induced cardiac hypertrophy and attenuates cardiac remodeling after myocardiac infarction[41].

However, MMP-2 deletion has been reported to reduce survival and exacerbate cardiac dysfunction in cytokine-induced cardiomyopathy[42]. Genetic polymorphisms which increase MMP-2 gene expression protect against cardiac remodeling including increases in end-diastolic diameter and LV mass index in hypertensive subjects[43]. Decreased levels of MMP-2 and MMP-13 have also been reported to associate with the development of hypertensive cardiac hypertrophy[44].

Our studies, for the first time, suggest that MMP-2 negatively regulates the SREBP-2 / HMGCR pathway in the heart and thus protects from GPCR agonist-induced cardiac remodeling. Therefore, MMP-2 has multiple roles the development of hypertensive cardiac remodeling: 1) It functions as ECM protease to modify ECM composition and structure; 2) It transactivates extracellular receptors to mediate cardiac hypertrophy and fibrosis; 3) It inhibits the SREBP-2 / HMGCR pathway which promotes cardiac remodeling.

6.4 Limitations and future directions

Our studies used animal models to demonstrate the significance of MMP-2, MMP-7, ADAM-12 and ADAM-17 in the development of GPCR agonist-induced hypertension and cardiac remodeling. We demonstrate that MMP-2 mediates GPCR agonist-induced vasoconstriction and hypertension. MMP-2 can cleave and activate vasoactive peptides such as big endothelin-1 and adrenomedullin, contributing to the development of hypertension[14,45]. Further studies are required to establish the contribution of these mechanisms to the development of hypertension.

We also show that MMP-7 and ADAM-17 are upstream regulators of the expression and activity of MMP-2 and ADAM-12. One likely mechanism is the proteolytic shedding of the proinflammatory cytokine TNF-α[46,47]. MMP-7 and ADAM-17 can also shed growth factors such as EGF, which induces MMP-2 transcription[48]. However, the specific pathways linking MMP-7, ADAM-17 and MMP-2, ADAM-12 in hypertensive cardiac remodeling require elucidation. Studies are also needed to further dissect the metalloproteinase networks that operate in various models of hypertension and cardiac remodeling and in different stages of the disease.

We show that MMP-2 expression negatively regulates the SREBP-2 / HMGCR pathway to protect from GPCR agonist-induced cardiac remodeling and suggest that MMP-2 acts by complexing with PCSK9 to protect the LDLR from PCSK9-induced degradation. However, MMP-2 has a broad spectrum of substrates and binding partners. Future studies should clarify whether other mechanisms are involved in the regulation of the SREBP-2 / HMGCR pathway by MMP-2 and whether other metalloproteinases can also regulate this pathway.

HMGCR mediates the development of cardiac hypertrophy through 1) increasing cholesterol synthesis and 2) activation NADPH oxidase and MAPKs via isoprenoid-mediated activation of small GTPases. In our model of agonist-induced cardiac remodeling in MMP-2 KO mice, we do not examine which mechanism is essential for the development of agonist-induced cardiac remodeling. Determination of isoprenoids and isoprenylated GTPases would help us better define the mechanisms of MMP-2 and HMGCR in hypertension and cardiac remodeling.

Due to the significance of GPCR agonists in the development of hypertensive cardiac remodeling, our studies used GPCR agonist-induced hypertensive cardiac remodeling animal models. To confirm the general validity of our findings, in some studies, we further used spontaneously hypertensive rats, which are a genetic model where hypertension is characterized by upregulation of catecholamines (i.e. sympathetic nervous system activity) and Ang II, in addition to oxidative stress[49]. A limitation of the current studies is that we did not examine other factors (e.g., obesity, diabetes, high salt diet or renal dysfunction) which are well known to cause hypertensive cardiac disease. In the future, this limitation could be addressed by extending the characterization of metalloproteinases to other animal models such as the deoxycorticosterone acetate-salt induced hypertension model, 2-kidney 1-clip model, obesity-induced hypertension model and transaortic constriction-induced cardiac remodeling model[50-53].

Gene function can be studied by gain-of-function and/or loss-of-function approaches, two independent but complimentary ways, to determine the role of an individual gene in biological processes[54]. Our studies mainly utilized loss-of-function studies, including gene knockout, RNA interference and inhibition of activity by pharmacological means, to investigate the role of MMPs and ADAMs in the development of hypertensive cardiac remodeling. Further, each of these approaches has disadvantages. For instance, gene knockout effect can be compromised by compensatory gene expression; RNA interference and pharmacological inhibitors can both cause unintended off-target effects. Future studies involving gain-of-function approaches should further our current understanding of the biology of metalloproteinases in hypertensive cardiac disease.

To knockdown the expression of target metalloproteinases including MMP-2, MMP-7 and TACE, we used the tools of antisense oligodeoxynucleotides and siRNA. The antisense oligodeoxynucleotides are single-strand oligodeoxynucleotides (normally 15-20 nucleotides in length) which can bind to target mRNAs through Watson-Crick base pairing. This interaction induces RNase H-dependent degradation, translational arrest or alternative splicing of the target mRNA[55,56]. The siRNA are double-stranded oligoribonucleotides composed of a sense (passenger) strand and an antisense (guide) strand. For effective gene silencing by siRNA, there is a requirement for the siRNA strands to be at least 21 nucleotides in length[57]. When the siRNA molecule interacts with the Argonaute protein in the RNA-induced silencing complex, the sense strand is degraded. The antisense strand is used to guide the degradation of target mRNA sequences complementary to the seed region (nucleotides 2-7) of the antisense strand[58,59].

Both antisense oligodeoxynucleotides and siRNA are large polyanionic molecules and cannot efficiently cross the plasma membranes. *In vitro*, antisense oligodeoxynucleotides and siRNA are normally delivered by electroporation or lipophilic transfection reagent. *In vivo*, siRNA are often delivered using nanoparticles, liposomes, peptides and cholesterols to increase the efficiency of delivery[60,61]. However, intravenous injection of naked siRNA to mice can effectively deliver siRNA to the heart, lung and kidney and inhibit the expression of target genes[53,62,63].

Delivery of antisense oligodeoxynucleotides and siRNA can induce off-target effects. Antisense oligodeoxynucleotides and siRNA can activate Toll-like receptors on immune cells (such as monocytes), triggering the induction of cytokines, such as interferons and interleukins, to downregulate gene expression[58,64,65]. siRNA also lead to inhibition of non-target genes through the imperfect binding between the seed region of siRNA and non-target mRNA, leading to the degradation or translational arrest of these non-target mRNA[58].

In our studies, we delivered antisense oligodeoxynucleotides and siRNA by subcutaneously-implanted osmotic minipump or intravenous injection. The dosage of siRNA has been shown to effectively downregulate the cardiac expression of target genes[53]. The sequence of the antisense oligodeoxynucleotides and siRNA against MMP-7 and TACE have been validated by previous studies[66,67]. 2’-O-metheylation was used to increase the stability of siRNA[68]. We also used scrambled oligodeoxynucleotides and siRNA against luciferase, which have no target mRNA in mammalian animals, as negative controls. The antisense oligodeoxynucleotides and siRNA against MMP-2, MMP-7 and TACE, but not the scrambled oligodeoxynucleotides or luciferase siRNA, inhibited the expression of target genes in the heart and aorta. The siRNA did not change the expression of non-target genes (such as MMP-9 and TIMPs) and did not induce an increase of interferon-γ, suggesting the off-target effects of siRNA are not induced.

The efficiency of siRNA-based gene silencing *in vivo* is variable and the available techniques are insuficiently robust for clinical application[69]. Naked siRNA has also been shown to successfully downregulate target gene expression *in vivo*[53,70]. Indeed, in our animal experiments, siRNAs were delivered without transfection agent and inhibition of target gene expression was demonstrated. It is possible that factors such as arterial pressure and contractile movement in the cardiovascular system increases the flux of siRNAs across membranes into cells. We speculate that, once in the circulation, naked siRNAs might complex with components of the circulation such as lipids which would then act as transmembrane carriers. Because of the potential for clinical translation, understanding how naked siRNAs enter cells *in vivo* and the development of robust delivery systems remain areas of intensive research worldwide[60,71].

However, in our *in vivo* studies, we did not determine whether these oligodeoxynucleotides and siRNA were delivered into cardiomyocytes or any other cells. Rather, we limited our studies to measuring changes in cardiac gene expression in response to the specific siRNA. These studies could have been supplemented with the use of siRNA with a fluorescent label that could be used to indicate both: i) the targeted organ and cells and ii) the efficiency of siRNA delivery. Other control oligonucleotides such as C911 siRNA (which is the same siRNA except that bases 9 through 11 are the complement of the original siRNA) would be complementary to scrambled oligodeoxynucleotides and luciferase siRNA as the negative controls[72]. In addition, our studies did not cover the entirety of possible off-target effects of oligodeoxynucleotides and siRNA. Broad-spectrum examination of cytokine levels and non-target gene expression could help establish the targeted knockdown of MMP-7, TACE and MMP-2 by the chosen siRNA sequences as opposed to resulting from off-target effects.

6.5 Conclusions

In conclusion, we studied the different roles of metalloproteinases, including MMP-2, MMP-7, ADAM-12 and ADAM-17, in the development of hypertension and cardiac remodeling. Our studies showed that:

1. MMP-7 mediates GPCR agonist-induced hypertensive cardiac remodeling. MMP-7 inhibition by pharmacological blockade, RNA interference or genetic knockout protects against hypertensive cardiac remodeling.

2. Acting in parallel to MMP-7, ADAM-17 contributes to GPCR agonist-induced cardiac hypertrophy and fibrosis. These effects of ADAM-17 are signaled, at least in part, by ADAM-12, a major effector metalloproteinases in cardiac hypertrophy signaling.

3. MMP-2 contributes to the development of agonist-induced hypertension such that partial blockade of MMP-2 by pharmacological means and RNA interference attenuates Ang II-induced hypertension.

4. Complete lack of MMP-2 predisposes to GPCR agonist-induced cardiac remodeling, as observed in MMP-2 knockout mice. MMP-2 is cardiopretective against hypertensive cardiac remodeling by negatively regulating the SREBP-2 / HMGCR pathway, which signals cardiac remodeling.

These findings are a major contribution to our current understanding of the cardiovascular biology of metalloproteinases and show the diversity of the roles metalloproteinases play in the cardiovascular system. Metalloproteinases remain attractive therapeutic targets in the context of cardiovascular conditions (e.g., atherosclerosis, ischemia reperfusion, hypertrophic heart disease in hypertension and post-myocardial infarction) as well as in non-cardiovascular disorders (cancer, arthritis and inflammation)[73-78]. Since metalloproteinases have different functions in different stages of disease development and progression, caution should be exercised when designing therapeutic strategies targeting metalloproteinases for the treatment of cardiovascular and non-cardiovascular diseases.

Figure 6-1 Postulated model of metalloproteinase signaling in GPCR agonist-induced hypertension and cardiac remodeling.

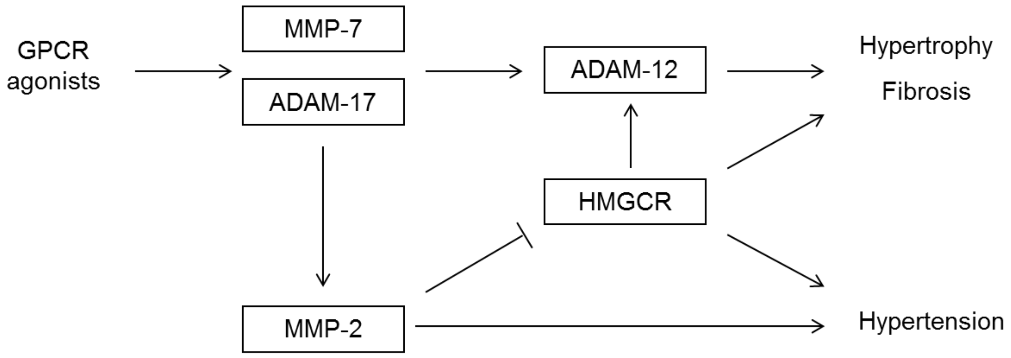
GPCR agonists
MMP-7
ADAM-17
ADAM-12
Hypertrophy
Fibrosis
HMGCR
MMP-2
Hypertension

6.6 References

1. Rockman HA, Wachhorst SP, Mao L, Ross J, Jr. ANG II receptor blockade prevents ventricular hypertrophy and ANF gene expression with pressure overload in mice. *Am J Physiol*. 1994;266:H2468-2475
2. Muller P, Kazakov A, Jagoda P, Semenov A, Bohm M, Laufs U. ACE inhibition promotes upregulation of endothelial progenitor cells and neoangiogenesis in cardiac pressure overload. *Cardiovasc Res*. 2009;83:106-114
3. Berk BC, Vekshtein V, Gordon HM, Tsuda T. Angiotensin II-stimulated protein synthesis in cultured vascular smooth muscle cells. *Hypertension*. 1989;13:305-314
4. Geisterfer AA, Peach MJ, Owens GK. Angiotensin II induces hypertrophy, not hyperplasia, of cultured rat aortic smooth muscle cells. *Circ Res*. 1988;62:749-756
5. Prenzel N, Zwick E, Daub H, Leserer M, Abraham R, Wallasch C, Ullrich A. EGF receptor transactivation by G-protein-coupled receptors requires metalloproteinase cleavage of proHB-EGF. *Nature*. 1999;402:884-888
6. Hao L, Du M, Lopez-Campistrous A, Fernandez-Patron C. Agonist-induced activation of matrix metalloproteinase-7 promotes vasoconstriction through the epidermal growth factor-receptor pathway. *Circ Res*. 2004;94:68-76
7. Asakura M, Kitakaze M, Takashima S, Liao Y, Ishikura F, Yoshinaka T, Ohmoto H, Node K, Yoshino K, Ishiguro H, Asanuma H, Sanada S, Matsumura Y, Takeda H, Beppu S, Tada M, Hori M, Higashiyama S. Cardiac hypertrophy is inhibited by antagonism of ADAM12 processing of HB-EGF: metalloproteinase inhibitors as a new therapy. *Nat Med*. 2002;8:35-40
8. Ohtsu H, Dempsey PJ, Frank GD, Brailoiu E, Higuchi S, Suzuki H, Nakashima H, Eguchi K, Eguchi S. ADAM17 mediates epidermal growth factor receptor transactivation and vascular smooth muscle cell hypertrophy induced by angiotensin II. *Arterioscler Thromb Vasc Biol*. 2006;26:e133-137
9. Spinale FG. Myocardial matrix remodeling and the matrix metalloproteinases: influence on cardiac form and function. *Physiol Rev*. 2007;87:1285-1342
10. Hao L, Nishimura T, Wo H, Fernandez-Patron C. Vascular responses to alpha1-adrenergic receptors in small rat mesenteric arteries depend on mitochondrial reactive oxygen species. *Arterioscler Thromb Vasc Biol*. 2006;26:819-825
11. Daub H, Weiss FU, Wallasch C, Ullrich A. Role of transactivation of the EGF receptor in signalling by G-protein-coupled receptors. *Nature*.

1996;379:557-560

12. Rodrigues SF, Tran ED, Fortes ZB, Schmid-Schonbein GW. Matrix metalloproteinases cleave the beta2-adrenergic receptor in spontaneously hypertensive rats. *Am J Physiol Heart Circ Physiol*. 2010;299:H25-35
13. Tran ED, DeLano FA, Schmid-Schonbein GW. Enhanced matrix metalloproteinase activity in the spontaneously hypertensive rat: VEGFR-2 cleavage, endothelial apoptosis, and capillary rarefaction. *J Vasc Res*. 2010;47:423-431
14. Fernandez-Patron C, Radomski MW, Davidge ST. Vascular matrix metalloproteinase-2 cleaves big endothelin-1 yielding a novel vasoconstrictor. *Circ Res*. 1999;85:906-911
15. Xiao LJ, Lin P, Lin F, Liu X, Qin W, Zou HF, Guo L, Liu W, Wang SJ, Yu XG. ADAM17 targets MMP-2 and MMP-9 via EGFR-MEK-ERK pathway activation to promote prostate cancer cell invasion. *Int J Oncol*. 2012;40:1714-1724
16. Beklen A, Tuter G, Sorsa T, Hanemaaijer R, Virtanen I, Tervahartiala T, Konttinen YT. Gingival tissue and crevicular fluid co-operation in adult periodontitis. *J Dent Res*. 2006;85:59-63
17. Salo J, Mackiewicz Z, Indahl A, Konttinen YT, Holm AK, Sukura A, Holm S. Plasmin-matrix metalloproteinase cascades in spinal response to an experimental disc lesion in pig. *Spine (Phila Pa 1976)*. 2008;33:839-844
18. Dozier S, Escobar GP, Lindsey ML. Matrix metalloproteinase (MMP)-7 activates MMP-8 but not MMP-13. *Med Chem*. 2006;2:523-526
19. Chan KM, Wong HL, Jin G, Liu B, Cao R, Cao Y, Lehti K, Tryggvason K, Zhou Z. MT1-MMP inactivates ADAM9 to regulate FGFR2 signaling and calvarial osteogenesis. *Dev Cell*. 2012;22:1176-1190
20. Wong HL, Cao R, Jin G, Chan KM, Cao Y, Zhou Z. When MT1-MMP meets ADAMs. *Cell Cycle*. 2012;11:2793-2798
21. Zervoudaki A, Economou E, Stefanadis C, Pitsavos C, Tsioufis K, Aggeli C, Vasiliadou K, Toutouza M, Toutouzas P. Plasma levels of active extracellular matrix metalloproteinases 2 and 9 in patients with essential hypertension before and after antihypertensive treatment. *J Hum Hypertens*. 2003;17:119-124
22. Onal IK, Altun B, Onal ED, Kirkpantur A, Gul Oz S, Turgan C. Serum levels of MMP-9 and TIMP-1 in primary hypertension and effect of antihypertensive treatment. *Eur J Intern Med*. 2009;20:369-372
23. Tayebjee MH, Nadar S, Blann AD, Gareth Beevers D, MacFadyen RJ, Lip GY. Matrix metalloproteinase-9 and tissue inhibitor of metalloproteinase-1 in hypertension and their relationship to cardiovascular risk and treatment: a substudy of the Anglo-Scandinavian Cardiac Outcomes Trial (ASCOT).

Am J Hypertens. 2004;17:764-769

24. Li-Saw-Hee FL, Edmunds E, Blann AD, Beevers DG, Lip GY. Matrix metalloproteinase-9 and tissue inhibitor metalloproteinase-1 levels in essential hypertension. Relationship to left ventricular mass and anti-hypertensive therapy. *Int J Cardiol*. 2000;75:43-47
25. Friese RS, Rao F, Khandrika S, Thomas B, Ziegler MG, Schmid-Schonbein GW, O'Connor DT. Matrix metalloproteinases: discrete elevations in essential hypertension and hypertensive end-stage renal disease. *Clin Exp Hypertens*. 2009;31:521-533
26. Flamant M, Placier S, Dubroca C, Esposito B, Lopes I, Chatziantoniou C, Tedgui A, Dussaule JC, Lehoux S. Role of matrix metalloproteinases in early hypertensive vascular remodeling. *Hypertension*. 2007;50:212-218
27. Ruddy JM, Jones JA, Stroud RE, Mukherjee R, Spinale FG, Ikonomidis JS. Differential effects of mechanical and biological stimuli on matrix metalloproteinase promoter activation in the thoracic aorta. *Circulation*. 2009;120:S262-268
28. Zeisberg M, Khurana M, Rao VH, Cosgrove D, Rougier JP, Werner MC, Shield CF, 3rd, Werb Z, Kalluri R. Stage-specific action of matrix metalloproteinases influences progressive hereditary kidney disease. *PLoS Med*. 2006;3:e100
29. Fernandez-Patron C, Martinez-Cuesta MA, Salas E, Sawicki G, Wozniak M, Radomski MW, Davidge ST. Differential regulation of platelet aggregation by matrix metalloproteinases-9 and -2. *Thromb Haemost*. 1999;82:1730-1735
30. Zempo N, Kenagy RD, Au YP, Bendeck M, Clowes MM, Reidy MA, Clowes AW. Matrix metalloproteinases of vascular wall cells are increased in balloon-injured rat carotid artery. *J Vasc Surg*. 1994;20:209-217
31. Treede RD, Jensen TS, Campbell JN, Cruccu G, Dostrovsky JO, Griffin JW, Hansson P, Hughes R, Nurmikko T, Serra J. Neuropathic pain: redefinition and a grading system for clinical and research purposes. *Neurology*. 2008;70:1630-1635
32. Kawasaki Y, Xu ZZ, Wang X, Park JY, Zhuang ZY, Tan PH, Gao YJ, Roy K, Corfas G, Lo EH, Ji RR. Distinct roles of matrix metalloproteases in the early- and late-phase development of neuropathic pain. *Nat Med*. 2008;14:331-336
33. Rosell A, Lo EH. Multiphasic roles for matrix metalloproteinases after stroke. *Curr Opin Pharmacol*. 2008;8:82-89
34. Kassim SY, Gharib SA, Mecham BH, Birkland TP, Parks WC, McGuire JK. Individual matrix metalloproteinases control distinct transcriptional responses in airway epithelial cells infected with Pseudomonas aeruginosa. *Infect Immun*. 2007;75:5640-5650

35. Atfi A, Dumont E, Colland F, Bonnier D, L'Helgoualc'h A, Prunier C, Ferrand N, Clement B, Wewer UM, Theret N. The disintegrin and metalloproteinase ADAM12 contributes to TGF-beta signaling through interaction with the type II receptor. *J Cell Biol*. 2007;178:201-208
36. Cheung PY, Sawicki G, Wozniak M, Wang W, Radomski MW, Schulz R. Matrix metalloproteinase-2 contributes to ischemia-reperfusion injury in the heart. *Circulation*. 2000;101:1833-1839
37. Ali MA, Cho WJ, Hudson B, Kassiri Z, Granzier H, Schulz R. Titin is a target of matrix metalloproteinase-2: implications in myocardial ischemia/reperfusion injury. *Circulation*. 2010;122:2039-2047
38. Wang W, Schulze CJ, Suarez-Pinzon WL, Dyck JR, Sawicki G, Schulz R. Intracellular action of matrix metalloproteinase-2 accounts for acute myocardial ischemia and reperfusion injury. *Circulation*. 2002;106:1543-1549
39. Wang GY, Bergman MR, Nguyen AP, Turcato S, Swigart PM, Rodrigo MC, Simpson PC, Karliner JS, Lovett DH, Baker AJ. Cardiac transgenic matrix metalloproteinase-2 expression directly induces impaired contractility. *Cardiovasc Res*. 2006;69:688-696
40. Zile MR, Desantis SM, Baicu CF, Stroud RE, Thompson SB, McClure CD, Mehurg SM, Spinale FG. Plasma biomarkers that reflect determinants of matrix composition identify the presence of left ventricular hypertrophy and diastolic heart failure. *Circ Heart Fail*. 2011;4:246-256
41. Matsusaka H, Ide T, Matsushima S, Ikeuchi M, Kubota T, Sunagawa K, Kinugawa S, Tsutsui H. Targeted deletion of matrix metalloproteinase 2 ameliorates myocardial remodeling in mice with chronic pressure overload. *Hypertension*. 2006;47:711-717
42. Matsusaka H, Ikeuchi M, Matsushima S, Ide T, Kubota T, Feldman AM, Takeshita A, Sunagawa K, Tsutsui H. Selective disruption of MMP-2 gene exacerbates myocardial inflammation and dysfunction in mice with cytokine-induced cardiomyopathy. *Am J Physiol Heart Circ Physiol*. 2005;289:H1858-1864
43. Lacchini R, Jacob-Ferreira AL, Luizon MR, Gasparini S, Ferreira-Sae MC, Schreiber R, Nadruz W, Jr., Tanus-Santos JE. Common matrix metalloproteinase 2 gene haplotypes may modulate left ventricular remodelling in hypertensive patients. *J Hum Hypertens*. 2012;26:171-177
44. Ahmed SH, Clark LL, Pennington WR, Webb CS, Bonnema DD, Leonardi AH, McClure CD, Spinale FG, Zile MR. Matrix metalloproteinases/tissue inhibitors of metalloproteinases: relationship between changes in proteolytic determinants of matrix composition and structural, functional, and clinical manifestations of hypertensive heart disease. *Circulation*. 2006;113:2089-2096

45. Martinez A, Oh HR, Unsworth EJ, Bregonzio C, Saavedra JM, Stetler-Stevenson WG, Cuttitta F. Matrix metalloproteinase-2 cleavage of adrenomedullin produces a vasoconstrictor out of a vasodilator. *Biochem J*. 2004;383:413-418
46. Seguin CA, Pilliar RM, Madri JA, Kandel RA. TNF-alpha induces MMP2 gelatinase activity and MT1-MMP expression in an in vitro model of nucleus pulposus tissue degeneration. *Spine (Phila Pa 1976)*. 2008;33:356-365
47. Baertling F, Kokozidou M, Pufe T, Clarner T, Windoffer R, Wruck CJ, Brandenburg LO, Beyer C, Kipp M. ADAM12 is expressed by astrocytes during experimental demyelination. *Brain Res*. 2010;1326:1-14
48. Staun-Ram E, Goldman S, Shalev E. p53 Mediates epidermal growth factor (EGF) induction of MMP-2 transcription and trophoblast invasion. *Placenta*. 2009;30:1029-1036
49. Suzuki H, Swei A, Zweifach BW, Schmid-Schonbein GW. In vivo evidence for microvascular oxidative stress in spontaneously hypertensive rats. Hydroethidine microfluorography. *Hypertension*. 1995;25:1083-1089
50. Sarikonda KV, Watson RE, Opara OC, Dipette DJ. Experimental animal models of hypertension. *J Am Soc Hypertens*. 2009;3:158-165
51. Lerman LO, Chade AR, Sica V, Napoli C. Animal models of hypertension: an overview. *J Lab Clin Med*. 2005;146:160-173
52. Takemoto M, Node K, Nakagami H, Liao Y, Grimm M, Takemoto Y, Kitakaze M, Liao JK. Statins as antioxidant therapy for preventing cardiac myocyte hypertrophy. *J Clin Invest*. 2001;108:1429-1437
53. Clemente CF, Tornatore TF, Theizen TH, Deckmann AC, Pereira TC, Lopes-Cendes I, Souza JR, Franchini KG. Targeting focal adhesion kinase with small interfering RNA prevents and reverses load-induced cardiac hypertrophy in mice. *Circ Res*. 2007;101:1339-1348
54. Prelich G. Gene overexpression: uses, mechanisms, and interpretation. *Genetics*. 2012;190:841-854
55. Dias N, Stein CA. Antisense oligonucleotides: basic concepts and mechanisms. *Mol Cancer Ther*. 2002;1:347-355
56. Bennett CF, Swayze EE. RNA targeting therapeutics: molecular mechanisms of antisense oligonucleotides as a therapeutic platform. *Annu Rev Pharmacol Toxicol*. 2010;50:259-293
57. Elbashir SM, Martinez J, Patkaniowska A, Lendeckel W, Tuschl T. Functional anatomy of siRNAs for mediating efficient RNAi in Drosophila melanogaster embryo lysate. *Embo J*. 2001;20:6877-6888
58. Jackson AL, Linsley PS. Recognizing and avoiding siRNA off-target effects for target identification and therapeutic application. *Nat Rev Drug Discov*. 2010;9:57-67

59. Anderson EM, Birmingham A, Baskerville S, Reynolds A, Maksimova E, Leake D, Fedorov Y, Karpilow J, Khvorova A. Experimental validation of the importance of seed complement frequency to siRNA specificity. *RNA*. 2008;14:853-861
60. Whitehead KA, Langer R, Anderson DG. Knocking down barriers: advances in siRNA delivery. *Nat Rev Drug Discov*. 2009;8:129-138
61. Yu B, Zhao X, Lee LJ, Lee RJ. Targeted delivery systems for oligonucleotide therapeutics. *AAPS J*. 2009;11:195-203
62. Marin TM, Clemente CF, Santos AM, Picardi PK, Pascoal VD, Lopes-Cendes I, Saad MJ, Franchini KG. Shp2 negatively regulates growth in cardiomyocytes by controlling focal adhesion kinase/Src and mTOR pathways. *Circ Res*. 2008;103:813-824
63. Guido MC, Clemente CF, Moretti AI, Barbeiro HV, Debbas V, Caldini EG, Franchini KG, Soriano FG. Small interfering RNA targeting focal adhesion kinase prevents cardiac dysfunction in endotoxemia. *Shock*. 2012;37:77-84
64. Kleinman ME, Yamada K, Takeda A, Chandrasekaran V, Nozaki M, Baffi JZ, Albuquerque RJ, Yamasaki S, Itaya M, Pan Y, Appukuttan B, Gibbs D, Yang Z, Kariko K, Ambati BK, Wilgus TA, DiPietro LA, Sakurai E, Zhang K, Smith JR, Taylor EW, Ambati J. Sequence- and target-independent angiogenesis suppression by siRNA via TLR3. *Nature*. 2008;452:591-597
65. Senn JJ, Burel S, Henry SP. Non-CpG-containing antisense 2'-methoxyethyl oligonucleotides activate a proinflammatory response independent of Toll-like receptor 9 or myeloid differentiation factor 88. *J Pharmacol Exp Ther*. 2005;314:972-979
66. Hasegawa S, Koshikawa N, Momiyama N, Moriyama K, Ichikawa Y, Ishikawa T, Mitsuhashi M, Shimada H, Miyazaki K. Matrilysin-specific antisense oligonucleotide inhibits liver metastasis of human colon cancer cells in a nude mouse model. *Int J Cancer*. 1998;76:812-816
67. Zhan M, Jin B, Chen SE, Reecy JM, Li YP. TACE release of TNF-alpha mediates mechanotransduction-induced activation of p38 MAPK and myogenesis. *J Cell Sci*. 2007;120:692-701
68. Ji L, Chen X. Regulation of small RNA stability: methylation and beyond. *Cell Res*. 2012;22:624-636
69. Shim MS, Kwon YJ. Efficient and targeted delivery of siRNA in vivo. *FEBS J*. 2010;277:4814-4827
70. Pereira AH, Clemente CF, Cardoso AC, Theizen TH, Rocco SA, Judice CC, Guido MC, Pascoal VD, Lopes-Cendes I, Souza JR, Franchini KG. MEF2C silencing attenuates load-induced left ventricular hypertrophy by modulating mTOR/S6K pathway in mice. *PLoS One*. 2009;4:e8472
71. Gooding M, Browne LP, Quinteiro FM, Selwood DL. siRNA delivery:

from lipids to cell-penetrating peptides and their mimics. *Chem Biol Drug Des*. 2012;80:787-809

72. Buehler E, Chen YC, Martin S. C911: A bench-level control for sequence specific siRNA off-target effects. *PLoS One*. 2012;7:e51942
73. Rodriguez D, Morrison CJ, Overall CM. Matrix metalloproteinases: what do they not do? New substrates and biological roles identified by murine models and proteomics. *Biochim Biophys Acta*. 2010;1803:39-54
74. Morrison CJ, Butler GS, Rodriguez D, Overall CM. Matrix metalloproteinase proteomics: substrates, targets, and therapy. *Curr Opin Cell Biol*. 2009;21:645-653
75. Newby AC. Matrix metalloproteinase inhibition therapy for vascular diseases. *Vascul Pharmacol*. 2012;56:232-244
76. Schmid-Schonbein GW. An emerging role of degrading proteinases in hypertension and the metabolic syndrome: autodigestion and receptor cleavage. *Curr Hypertens Rep*. 2012;14:88-96
77. Santos-Martinez MJ, Medina C, Jurasz P, Radomski MW. Role of metalloproteinases in platelet function. *Thromb Res*. 2008;121:535-542
78. Burrage PS, Brinckerhoff CE. Molecular targets in osteoarthritis: metalloproteinases and their inhibitors. *Curr Drug Targets*. 2007;8:293-303